THE UNIVERSITY OF HULL

Managed realignment in the Humber estuary: factors influencing sedimentation

being a Thesis submitted for the Degree of
Doctor of Philosophy
in the University of Hull

by

Jennifer Clapp, BSc (Hons)

March 2009

Abstract

In September 2003 a managed realignment site was breached on the north bank of the Humber estuary at Paull Holme Strays (PHS). The site was breached as part of the Environment Agency Humber Flood Risk Management Strategy, with the main aims to create intertidal habitat to replace that which has been lost in other areas of the estuary and to alleviate increasing flood-risk associated with climate change induced sea level rise. Managed realignment is a relatively new method of flood defence that has gained in popularity with flood managers over the last 20 years. At PHS, the accretion rates predicted by modelling of the site prior to breaching were an order of magnitude slower than those recorded immediately post-breach.

This thesis outlines the monitoring programme followed that investigates the reasons for the fast accretion rates at PHS, researches the sediment properties, calculates a sediment budget and produces a conceptual model for fast accreting managed realignment sites. Results have shown that the initial fast accretion rates continued on the site to the end of the monitoring period five years post-breach, particularly on the NW sector of the site. Net sediment deposition within the site compared favourably with the amount of sediment measured as accreting on the site. A number of sediment properties that were measured did not correlate significantly with accretion rates. The main factors influencing the fast accretion were the elevation of the site and thus the tidal inundation time, and the design of the site. A flume based study of the erosion of sediment cores taken from the site highlighted differences between the SE and NW sector of PHS, again related to elevation and tidal inundation, but not between sites with differing sediment properties. The conceptual model indicates that these types of fast-accreting managed realignment sites will quickly progress to becoming mainly saltmarsh habitat within ten years, aiding flood managers in the design and monitoring of similar sites.

Table of Contents

List of Figures

List of Tables

List of Abbreviations

ABP   Associated British Ports

ABS   acoustic backscatter

ADP   acoustic Doppler profiler

ADV   acoustic Doppler velocimeter

BGS   British Geological Survey

BIOTA   Biological Influences On interTidal Areas

BP   before present

CEH   Centre for Ecology and Hydrology

CET   critical erosion threshold

CSM   cohesive strength meter

DEM   digital elevation map

DGPS   differential global positioning system

EA   Environment Agency

EAP   Environmental Action Plan

ENU   east-north-up

EPS   extracellular polymeric substances

EQPC   equivalent projection area of a circle

EU   European Union

GIS   Geographical Information System

GMT   Greenwich Mean Time

HFRMS   Humber Flood Risk Management Strategy

HRLD   high resolution laser diffraction

IDW   inverse distance weighed

INSEEV   *in situ* settling velocity

IPCC   Intergovernmental Panel on Climate Change

KGD   King George Dock

LIDAR   light detecting and ranging

LOI	loss on ignition
LOIS	Land-Ocean Interaction Study
MHWN	mean high water neap
MHWS	mean high water spring
MLWS	mean low water spring
NE	north east
NERC	Natural Environmental Research Council
NW	north west
OBS	optical backscatter sensor
ODN	Ordnance Datum Newlyn
PEEP	photo-electronic erosion pin
PHS	Paull Holme Strays
PPS	Planning Policy Statement
SAC	Special Area of Conservation
SET	sediment erosion table
SSC	suspended sediment concentration
SE	south east
SNR	signal to noise ratio
SPA	Special Protection Area
SPM	suspended particulate matter
SSSI	Site of Special Scientific Interest
TIN	triangular irregular networks
UKCIP	United Kingdom Climate Impacts Programme
UK	United Kingdom
US	United States

List of symbols and units

cm	centimetres
cma^{-1}	centimetres per annum
cms^{-1}	centimetres per second
dB	decibels
gcm^{-3}	grams per cubic centimetre
Hz	Hertz
ha	hectares
km	kilometres
km^2	square kilometres
kt	kilo tonnes
l	litres
ln	natural log
Nm^{-2}	Newton's per metre squared
m	metres
m^2	square metres
MHz	mega Hertz
mgl^{-1}	milligrams per litre
ml	millilitres
mm	millimetres
μm	micrometres
mms^{-1}	millimetres per second
mma^{-1}	millimetres per annum
m^3s^{-1}	cubic metres per second
ppt	parts per thousand
t	tonnes
ta^{-1}	tonnes per annum
t/tide	tonnes per tide
º	degrees
ºC	degrees Celsius
%	percent

Chapter 1 : Introduction

1.1 Focus of research

The present study focuses on a 'managed realignment' site located on the north bank of the Humber estuary, UK, hereafter called Paull Holme Strays (PHS). PHS is one of a small number of managed realignment sites that have been created in the UK; their main purposes being to compensate for habitat loss in other areas of the estuary and to alleviate increasing flood risk due to relative sea level rise. A numerical model of the site created prior to breaching by the Environment Agency (EA) in 2003 indicates slower rates of accretion (by an order of magnitude) than those recorded on the site during the first two years of monitoring. Failure of prediction means that results from the modelling carried out prior to breaching of the site are unreliable. Faster rates of accretion on a managed realignment site affects the floodwater storage potential of the site and the types and range of colonisation by plants, the two main aims of creating the site at PHS.

Due to the relatively recent introduction of managed realignment sites (they date back just over 20 years), there are a lack of data available on the relationship between breaching of the flood-banks on a site and the accretion rates on the newly created intertidal land. There is also a lack of understanding of the controls on sedimentation patterns across a managed realignment site as most current sites are small and published results are not detailed, generally stating a mean yearly accretion rate across the whole site. Studies of the controls on the accretion rates at newly created managed realignment sites are few (Chang, *et al.*, 2001; Cundy, *et al.*, 2002; French, 2006; Pontee, *et al.*, 2006; Watts, *et al.*, 2003; Wolters, *et al.*, 2005). It is recognised in the literature that there is a strong link between accretion and elevation of the site and a further link between elevation and colonisation of saltmarsh species on intertidal sites (e.g. Boorman, 2003; Boorman, *et al.*, 2001; Crooks, *et al.*, 2002; Garbutt, *et al.*, 2006; Morgan, *et al.*, 2002; Pasternack, *et al.*, 1998; Pontee, 2003). These relationships however, have not been widely studied at a newly created intertidal area such as the managed realignment site at PHS. Other controls on accretion include the properties of the sediment such as size, water content and bulk density. Studies have been carried out on these sediment properties in natural intertidal mudflat and saltmarsh sites (e.g. Aberle, *et al.*, 2004; Black, *et al.*, 2002; Black, 199; Christie, *et al.*, 2000; Defew, *et al.*,

2002; Flemming, *et al.*, 2000; Friend, *et al.*, 2003; Huntley, *et al.*, 2001; Quaresma, *et al.*, 2004; Uncles, 2002), however there is no comprehensive study of these properties when considering the broad changes taking place at a managed realignment site.

Managed realignment is increasingly being used as a soft engineering flood defence option in the United Kingdom (UK) and north-west (NW) Europe, and plays a large part in the EA future management proposals for the Humber estuary (Environment Agency, 2008). The creation of new intertidal habitat to meet European Union (EU) Habitat Regulations and the use of land as flood storage areas becomes more crucial with the anticipated rise in sea levels and increased storminess likely to result from climate change (Yorkshire Futures Regional Intelligence Network, 2002). The present research provides an opportunity to study the development of an intertidal area and to inform flood managers for future developments of managed realignment sites.

1.2 Aims of research

Main aim:

To identify the main factors leading to the fast rates of sediment accreted (compared to the numerical model) on PHS managed realignment site following breaching in 2003.

Subsidiary aims:

To understand the relationship between sediment flux over a tidal cycle and the spatially distributed accretion rates.

To analyse the spatial variability of sediment characteristics and vegetation found across PHS and their relationship to the accretion rates.

1.3 Objectives of research

To undertake a full monitoring programme across PHS, investigating the accretion rates and sediment properties at strategic sites.

To investigate the relationships between the physical and biological factors and the patterns of sedimentation.

To produce a sediment budget for the site showing the amount of sediment entering and leaving PHS during an annual tidal cycle.

To study the critical erosion properties of sediment from areas of PHS with differing accretion rates in a laboratory flume.

To produce a conceptual model of managed realignment site development based on the results of this study that can be used to predict development in similar sites.

1.4 Overview of thesis

Chapter 2 reviews the literature on managed realignment, factors influencing sedimentation, the Humber estuary and the research to date on PHS produced on behalf of the EA.

Chapter 3 presents the methodology used in collecting the data needed to answer the research aims and meet the objectives. This is split between field methods used to carry out a monitoring programme, and laboratory methods used to analyse sediment properties and to run a flume study.

Chapter 4 presents spatial and temporal results from the accretion/ erosion monitoring and the relationship between these rates and the site elevation.

Chapter 5 presents a sediment budget for the site calculated from hydrodynamic data and compares it with the sediment load calculated using the accretion rates. Also presented are tidal inundation data related to the site elevation.

Chapter 6 presents the results from analysis of the sediment properties monitored on PHS, again looking at spatial and temporal patterns and the interaction between properties to establish any influences on sedimentation.

Chapter 7 presents the results from the flume based erosion study.

Chapter 8 discusses the findings and presents a conceptual model of site development across PHS.

Chapter 9 puts forward conclusions to the current research and recommendations for future work.

Chapter 2 : Literature Review

2.1 Managed Realignment

Managed realignment is a soft engineering flood defence option that flood managers are increasingly turning to since initial experiments were carried out on sites in the Blackwater estuary, Essex, UK during the early 1990s. The process involves realigning flood embankments in certain areas along an estuary or coastline to a more inland position and then the original embankment is breached. Managed realignment is the current name for this process however others such as "managed retreat" and "setback" are also found in the literature. Managed realignment can essentially be seen as flood managers mimicking the way a marsh habitat reacts to rising sea-levels (French, 2006). The growing popularity of using this method of management for estuary flood defences is due in part to economic pressures and enhancement of the environment, as well as addressing the impacts of climate change.

2.1.1 Reasons for creating a managed realignment site and desirable outcomes

The benefits of managed realignment to a flood defence strategy:

- creating a site that will store floodwater, which in turn can lower the peak water levels in the estuary;
- reducing flood risk at other locations within the estuary;
- improving the functioning of the hydrodynamic and sedimentary system;

The benefits of managed realignment to the environment:

- allowing rollover and alleviating coastal squeeze (see section 2.1.1.1 for description);
- creating new intertidal habitats;
- compensating for the loss of intertidal habitat elsewhere in the estuary;
- complying with EU Habitats Directive (transposed into law by the Conservation (Natural Habitats & c.) Regulations 1994);
- increasing the burial of some contaminant metals;

The economic benefit of managed realignment:

- reducing economic costs of flood defence (Environment Agency, 2008; Andrews, *et al.*, 2006; Leggett, *et al.*, 2004; Rupp & Nicholls, 2002; Shepherd, *et al.*, 2007; Townend, *et al.*, 2002).

2.1.1.1 Rollover and coastal squeeze

The concept of rollover is as follows: as the sea-level rises within an estuary, so the estuary will adjust to maintain its form, and in doing this it migrates towards the land (see Figure 2.1) (Townend, *et al.*, 2002). Migration occurs in two stages, firstly with the horizontal erosion of the seaward margins of saltmarshes and secondly the upper mudflats stabilising by vertical accretion of sediments on their surfaces so that the landward margin can creep forward.
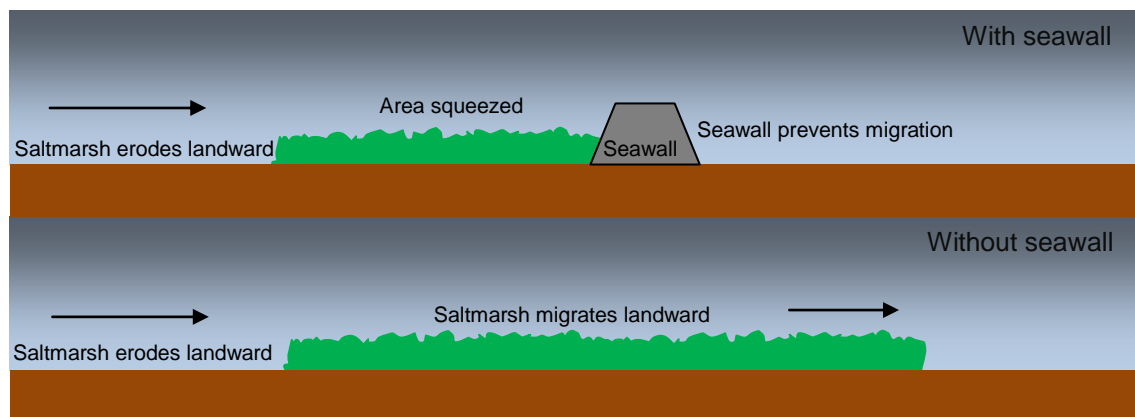
Figure 2.1:Coastal squeeze and rollover (adapted from Rupp & Nicholls, 2002)

A sediment balance can be achieved if the system continues to move landward by an amount proportional to sea-level rise (Townend, *et al.*, 2002). Modelling of the predicted vertical migration rate of marshes on the Humber estuary (Pethick, 2001) has been shown to keep pace with the horizontal erosion rate observed of 1-2 mm over the past 20 years. However, with the placement of flood defences along estuaries, natural features, and the use of reclaimed land for industry, many estuaries are not able to transgress landwards under rollover. This can lead to the problem of coastal squeeze- as low and middle marsh zones steadily progress landwards, the high marsh is lost. This contributes to a current loss of 100 ha each year of saltmarshes in England (Townend, *et al.*, 2002).

2.1.1.2 The impacts of climate change

The Fourth Assessment Report (Bernstein, *et al.*, 2007) from the Intergovernmental Panel on Climate Change (IPCC) published in 2007 concluded that the warming of the climate system is unmistakeable. Increased warming of the atmosphere caused by the rise in greenhouse gases has led to thermal expansion of water and the melting of glaciers, ice sheets and ice caps. This has caused a global rise in sea levels of 1.8 mm (range 1.3-2.3 mm) per year from 1961 to 2003 (Bernstein, *et al.*, 2007). Even with an immediate reduction in greenhouse gas emissions, the thermal expansion of the oceans and ice melting is set to continue for many centuries and thus sea levels will continue to rise during this period (Bernstein, *et al.*, 2007).

The rise in sea levels in an estuary puts added pressure on flood defences. Embankments will provide less protection as sea levels rise, thus increasing the economic burden of raising the defences. In areas that have to be protected, such as urban and industrial, there is no choice other than to increase embankment heights, however in areas of less importance, such as low-grade agricultural land, managed realignment of the defences could take place. This increase in intertidal land within an estuary can reduce the water level and remove pressure from other flood defences. The creation of new habitat also compensates for the loss of land in other locations from the rising sea levels.

2.1.2 Design considerations when planning a managed realignment site

Careful consideration of the design of the managed realignment site is essential. The physical, geographical and topographical designs are all important factors in the resultant functioning of the sedimentary and biological systems. Each design aspect can affect the type, duration and pattern of the sediment on a managed realignment site.

2.1.2.1 Geographical setting

To successfully locate a managed realignment site the present land-use of the area, infrastructure available to carry out works, historical context of the site and intertidal habitats near to the proposed site need to be taken into account. Locating the managed realignment site close to intertidal habitats such as saltmarshes provides the new site with a source of species for colonisation, hopefully accelerating saltmarsh creation. To realign flood defences within urban areas or industrial complexes is not usually

considered for economic and social reasons; land that is of low-grade agricultural value or is situated apart from urban areas is more suited for managed realignment.

To find the optimum location within an estuary, the sites are modelled to predict development under different scenarios. All proposed sites in an estuary can be modelled and the results used to predict the ideal locations for managed realignment.

A further constraint on the locating of managed realignment sites is the cost and ease of purchase of the land. Some landowners are either not willing to sell or may place conditions on the sale as happened during the planning of Hesketh Out Marsh West managed realignment site in the Ribble estuary, Lancashire and Merseyside, UK (Pontee, *et al.*, 2007). In this case the issues were resolved and the scheme continued, however delays were incurred.

The geographical location of the site is not the only consideration when assessing whether managed realignment is viable, of equal importance are the physical properties of the site, such as elevation and shape.

2.1.2.2 Height of the proposed managed realignment site

In the UK especially the main criterion for the success of a managed realignment site relates to the frequency and duration of tidal inundation after breaching, as determined by the height of the land (French, 2006). This directly determines both the type of habitat created and rates of sedimentation. To recreate saltmarsh at a managed realignment site in the UK, the height needs to be between mean high water neap (MHWN) tides and mean high water spring (MHWS) tides, this equates to the site being inundated 450-500 times every year (Pontee, 2003). For the creation of other habitats this range is altered to accommodate more or less saltmarsh. A review of literature on managed realignment sites (French, 2006) showed that the most common reason for site failure historically is the artificial adjustment of the site elevation and as such, it is imperative for the chosen location to be at the right height for the desired outcome prior to breaching.

2.1.2.3 Site size and shape

A study by Wolters, *et al.* (2005) concluded, after examining data from 70 different managed realignment sites in Europe, that the site should be in excess of 30 ha in area to sustain at least 50% of the target species for a saltmarsh habitat. Data from the US also indicate that small, narrow sites are unsuccessful and must have a minimum

threshold width of 6 to 10 m (Pontee, 2003). Maximising size is desirable for creating new habitat and to store the greatest volume of flood-water, but is frequently curtailed by economic factors.

2.1.2.4 The type of breach: size and design

There are three types of breach design used in the UK:

1. Removal of a section of the old flood embankment (can be at a number of locations along the embankment) to allow inundation by the tide
2. Regulation of tidal exchange using tidal flaps, valves and weirs/spillways
3. Total removal of the old flood embankment so that the new intertidal land is completely exposed to the tide. (Leggett, *et al.*, 2004; Pontee, *et al.*, 2006; Pontee, 2007; Townend, 2008a).

Some sites may employ a combination of 1 and 2, for example at Abbotts Hall in the Blackwater estuary, UK. This can give a better control over tidal inundation during the initial post-breach period (Pontee, 2007).

However, in the UK, option 1 is the most frequently adopted, but it is unclear from the literature whether this is because it has distinct advantages over the other options or merely because it is popular and therefore perceived to be the best. Debate in the literature centres on the pros and cons of options 1 and 3 (Anisfeld, *et al.*, 1999; French, 1999; Garbutt, *et al.*, 2006; Pethick, 2002; Pontee, 2007). Some authors are concerned that breaching the site in two locations could lead to the tide entering through one breach then leaving through the other creating a high energy channel through the site (French, 1999). A further concern for small-scale breaching is the increasing of the estuary accommodation space without increasing the cross section of the estuarine channel in compensation. The increased flow could lead to erosion around the estuary to increase the cross section, resulting in a loss of saltmarshes (Pontee, 2007; Townend, *et al.*, 2002).

Numerical models to calculate the optimum breach width for a particular site are found in the literature (see e.g. Pethick, 2002; Townend, 2008a; Townend, 2008b). For example, Pethick (2002) proposed a minimum breach width related to tidal range and intertidal surface elevation in order to allow sufficient tidal flow to promote accretion and provide tidal drainage.

Removing all the old flood embankment in front of the managed realignment site has led to sites having no protection from the fast estuarine tidal flows and to the drowning of the marsh (Anisfeld, *et al.*, 1999). However, a site at Welwick in the Humber estuary, UK, due to be breached in 2009 is one of the first in the UK to remove all of the old flood embankments. Fast accretion rates are undesirable on Welwick as elevations are already suitable to create saltmarsh and so the greater exposure to wave energy provided by the total removal of the old flood embankment should maintain the current height (Pontee, *et al.*, 2006).

2.1.2.5 The creation of artificial creeks

A final design element is artificially created creeks. This is of particular relevance in sites where the main aim is to create marsh habitat, or to link the new site with an existing marsh system. Creeks will help the water flow in and drain out of the site quickly so that waterlogging does not occur, which may be desirable in some managed realignment sites depending on what habitat is to be created (Garbutt, *et al.*, 2006; Wolters, *et al.*, 2005). Tidal creeks have been shown to transfer sediment further into a marsh than might occur by flooding alone. A study by Reed, *et al.* (1999) found that on a local scale tidal creeks at Scolt Head Island, Norfolk, UK, controlled sediment deposition with a decline of an order of magnitude within 20 m of the creeks.

A study of a site at Freiston Shore, UK, investigated the use of an artificial creek system created to link existing marshes to newly created intertidal habitat. The new creeks quickly incised headward for the first two years, probably due to the difference in bed level between the new managed realignment site and the adjacent marsh; in the third year the creeks silted up to return to the stable conditions present before breaching (Symonds, *et al.*, 2007). Again, the need for careful numerical modelling and design of the site is demonstrated, as is the importance of continuous data collection.

Hesketh Out Marsh West site was due to be breached in 2008. Design of this site has made extensive use of Geographic Information Systems (GIS) and a 2 dimensional depth averaged hydrodynamic model system (DAWN, Halcrow). Using a digital elevation map (DEM) created for the site from aerial photographs, the former creek patterns have been modelled and this allowed the design of a sustainable creek network. The whole design could then be tested using the 2-D numerical model under various regimes to predict the development of saltmarsh vegetation on Hesketh Out Marsh West (Pontee, *et al.*, 2007).

Andrews, *et al.*, (2006) neatly summarised the criteria discussed in the previous section 2.2.2 used to select sites for managed realignment (Table 2.1 below).

Table 2.1: Criteria used to determine the feasibility of realigning sea defences/flooding land modified from Andrews, *et al.*, (2006)

Area below the high spring tide level: maximise area of potential intertidal habitat
Present land use: undeveloped land most suitable as easiest to engineer and economical, designated land e.g. SSSI, SAC may not be suitable (Reed, *et al.*, 1999)
Infrastructure: presence of urban areas, roads railway etc
Historical context: land reclaimed recently, therefore easier to revert; presence of archaeological sites that need preserving
Spatial context of area: *Size*- realignment not cost effective on very small areas (less than 5 ha) (Pilcher, *et al.*, 2002)   *Shape*- trade-off between a wide intertidal area that will maximise benefits and length of realigned defences (Pilcher, *et al.*, 2002)   *Elevation*- maximise the potential of habitat development on the site or use higher ground that will act as a natural defence to minimise maintenance costs of defences   *Proximity to existing intertidal habitats*- facilitates movement of species between habitats and colonisation by plants (Begon, *et al.*, 1996).
Sediment supply: limits the amount and type of intertidal land that can be created/ sustained post-breach.

2.1.3 Role of sediment on intertidal areas when planning a managed realignment site

Sediment has a very important role to play in the success of a managed realignment site. If, for example, success is measured by the colonisation of halophytic species to form a saltmarsh, then the site will need to accrete and then maintain a certain height above MHWN. The site must therefore promote transport of sediment, drainage to prevent waterlogging, settling of suspended sediment and entrainment, and finally consolidation of sediment to prevent erosion. The following is a discussion of sediment properties and their importance in producing a successful managed realignment site.

2.1.3.1 Controls on accretion/erosion and influences on sediment stability

The important controls on accretion/erosion of sediment on a managed realignment site are summarised in Table 2.2 below.

Table 2.2: Controls on the accretion and erosion of sediment on an intertidal area

Accretion Control	Erosion control
Elevation (high areas likely to accrete more slowly than low areas, linked to the inundation time of the water listed below).	
Tidal inundation time (areas that are inundated for longer mean that the SPM has a longer residence time on the site and are likely to accrete more sediment).	
Net sediment flux (positive flux into the site implies sediment accreting).	**Net sediment flux** (positive flux out of site implies sediment eroding).
Vegetation cover (areas with greater vegetation likely to trap and build up sediment, however this is also linked to elevated areas and may indicate slower rather than faster accretion).	
Organic matter content (similar to vegetation cover as implies greater amount of vegetation trapping sediment, can also be linked with amount of biofilms and macroinvertebrates that stabilise sediment).	**Organic matter content** (may be linked to bioturbators that destabilise sediment leading to erosion).
	Critical erosion threshold (the higher the threshold the less erosion occurs, this is governed by other factors: velocity, bulk density, grain size, biological controls).
	Flow velocity (faster flows lead to more erosion, this can be inferred from the analysis of particle size).
Bulk density (a high bulk density implies consolidated material less likely to erode, however a low bulk density can indicate rapid accretion of sediment as well as unconsolidated sediment more susceptible to erosion).	**Bulk density** (a high bulk density implies consolidated material less likely to erode, however a low bulk density can indicate high accretion of sediment as well as unconsolidated sediment more susceptible to erosion).
Particle size (larger particles may be deposited when water velocity falls, indicated an area of greater accretion, ratios of mud to sand influence erosion potential).	**Particle size** (larger particles may be deposited when water velocity falls, indicated an area of faster accretion, ratios of mud to sand influence erosion potential).
Water content (high water content may imply areas that are inundated frequently and thus areas of fast accretion).	**Water content** (high water content can indicate areas of unconsolidated mud and thus an area more susceptible to erosion).

Sediment size

Sediments can be sub-divided into a number of different size classes ranging from very large boulders to small clays. However, when investigating grain sizes in an estuary, sediments are generally fine and usually fall into two categories. Larger sediments from 63 μm to 2mm in diameter are termed sand and are free to behave individually. Anything smaller than this is classed as mud and can be further categorised as either silt (63 μm-2 μm) or clay (less than 2 μm). The smaller grain sizes tend to be cohesive and behave very differently from larger ones. The small-scale processes controlling the movement of sediment are:

1. Transport of sediment in the bedload or suspended load via momentum transfer from the fluid to the sediment.
2. Entrainment of sediment into the flow via stresses and forces acting on the seabed.
3. Settling and deposition of sediment to the bed due to gravity (Masselink, *et al.*, 2003).

The type of sediment, whether cohesive, non-cohesive or a mixture of both, will influence the settling rate, consolidation and entrainment into the flow on a managed realignment site. One important difference is the creation of flocs or microaggregates in clays- particularly when they meet salt water. This process is discussed below.

Flocculation of sediment

The flocculation process occurs when microscopic clay particles join to form aggregates; clay sized particle surfaces have ionic charges that cause the particles to interact electrostatically. The degree of attraction rises in proportion to the proportion of clay in the sediment and becomes significant when it contains more than 5-10 % of clay by weight (Dyer, 1986). An individual floc may comprise up to ten million particles (Manning, *et al.*, 1999), and is much less dense than its constituent components. The size, settling velocity and density of the flocs and the salinity of the fluid are important characteristics which influence floc behaviour (Manning, *et al.*, 2002; Manning, *et al.*, 1999). The effects of these characteristics are as follows:

- Smaller particles have a larger relative surface area and will flocculate more readily although they are more likely to interact with particles bigger than themselves. This in turn leads to flocculation continuously removing the finer particles from suspension.

- Flocculation tends to very quickly reach an equilibrium situation at moderately low salinities, providing the particle concentration is high.
- As temperature increases the thermal motions of the ions increase in magnitude and this leads to increased repulsion. Consequently, flocculation is less effective as the temperature rises.
- Organic material on the sediment particles, such as mucal films, carry positive charges and significantly enhance flocculation (Dyer, 1986).
- Low SPM concentrations and low shear stresses appear to promote flocculation whereas high SPM concentrations and high shear stresses promote floc breakdown (Dyer, *et al.*, 1999).

An experiment using a video camera based instrument called INSEEV (Manning, *et al.*, 2002) (*in situ* settling velocity, University of Plymouth) on the Tamar Estuary, Devon and Cornwall, UK, found that lower SPM concentration neap tides produced mixed sizes of flocs, and during the most floc-productive conditions, the macroflocs approached 0.75 mm in length with settling velocities of 4-5 mms^{-1}. During spring tides the combination of conditions allowing optimum flocculation altered 95% of the SPM concentration into large, fast settling, rounded, cluster type macroflocs. A number of the smaller macroflocs had their settling characteristics significantly improved by becoming interlinked with organic matter to form strings (Manning, *et al.*, 1999).

On a managed realignment site, sediment characteristics will play an important role in defining the type of intertidal area created. For example, it is unlikely that a very sandy substrate will produce the diverse mudflat and saltmarsh for which such sites are often designed.

Settling and consolidation of sediment

The rate of settling of sediments is related to sediment grain size, shape (roundness and sphericity), density, and the viscosity and density of water. Sediment deposition involves the settling of grains from either the bedload or suspended load towards the bed. In the case of suspended load, the grains must settle a considerable distance through the fluid before coming to rest (Dyer, 1986; Masselink, *et al.*, 2003).
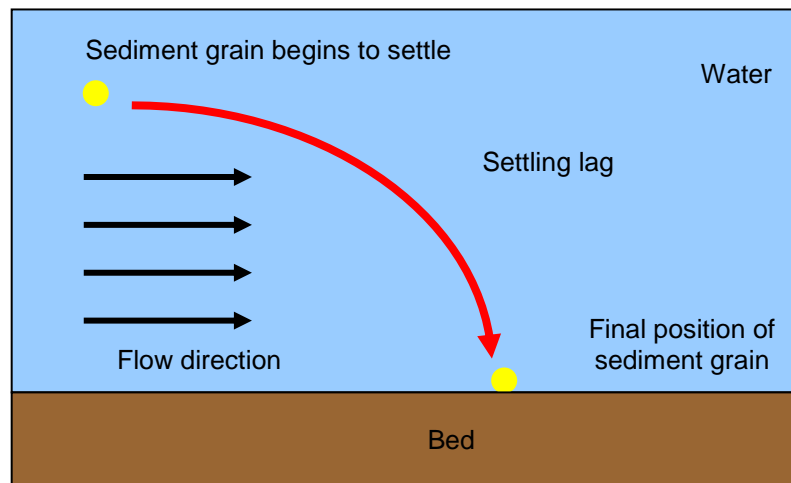
Figure 2.2: Settling lag of a sediment grain.

The settling lag of a particle (see Figure 2.2) is an important variable in an estuarine system where flows are tidal. It influences the final position in which a particle settles on the flood tide and the re-suspension on the ebb tide. The basic premise of the settling lag is thus: the suspended particle takes a finite time to settle and so is carried landwards on the flood tide, the flow velocity on the ebb tide will now be lower and will be unable to re-entrain the particle leading to accretion of sediment (Pritchard, 2005; Pritchard, *et al.*, 2003).

The formation of a cohesive sediment bed requires the combined processes of settling and consolidation. Suspended sediments are deposited onto the bed at low bed shear stress. Throughout consolidation, the sediment flocs and aggregates rearrange themselves to form a denser structure and force out the pore water. The presence of sand in the initial suspension has a large impact on the bed formation processes and the settling rates of the mud/sand suspension increase with increasing sand content (Mitchener, *et al.*, 1996). On a managed realignment site, the optimum conditions to facilitate settling and consolidation are required so that a sediment bed can be formed on top of the original pre-breach surface.

Sediment budget

The net flux of sediment into and out of a managed realignment site will depend on the amount of sediment in suspension in the estuary, the transport rate into the site, settling and consolidation within the site and the potential for re-erosion. Even with high concentrations of sediment entering the site, if there is rapid erosion, consolidation will not occur and sediments will not accrete.

Primarily, geomorphology and the physical forces of wind, tides and wave action along with biological processes determine the extent and stability of intertidal areas (Brown, *et al.*, 1998). The erosive potential for cohesive and intertidal mudflats depends on a balance between the physical and biological processes of stabilisation and destabilisation (Uncles, 2002; Widdows, *et al.*, 2002).

Factors affecting erosion of sediment

Much research has been carried out into the erosion of sediments within an estuary (e.g. Aberle, *et al.*, 2004; Andersen, *et al.*, 2005; Friend, *et al.*, 2005; Widdows, *et al.*, 2002). Generally this has focused on mud, sand, and mixtures of the two sediments. The erodability of cohesionless sediments depends on factors such as the shape and density of individual grains, and grain size distribution (e.g. Aberle, *et al.*, 2004; van Ledden, *et al.*, 2004). However the erosion of cohesive sediments is much more complex and requires consideration of many additional factors including mineral composition and organic content, biological processes, salinity, structure of pore water and other eroding fluids, and the consolidation and time related histories of the bed.

The critical erosion threshold (CET) of the sediment

When water is flowing over a bed, there will be a certain velocity at which the combined drag and lift forces on the surface particle layer will be sufficient to move individual or groups of particles from their stable positions. This velocity is known as the critical or threshold velocity and related to this threshold velocity is a critical or threshold shear stress (Dyer, 1986). The critical erosion shear stress (the shear stress at which sediment moves) increases with depth into a cohesive sediment bed. To study the CET of cohesive sediment requires the derivation of the point at which erosion commences. This is difficult to determine within a controlled flume environment and even more so *in situ* as there is always some sediment in suspension above the bed, movement of which can obscure the view of the bed and also be mistaken for the onset of erosion.

Mitchener, *et al.*, (1996) carried out experiments into the change in critical erosion shear stress when sand is added to a muddy bed and mud added to a sandy bed. The critical shear stress for erosion of a sandy bed increases when a cohesive material such as mud is added. The addition of 30% mud to a sandy bed can increase the critical shear stress for erosion by a factor of 10, the erosion rate once erosion has begun is also significantly reduced and the mode of erosion is also changed. The physical roughness

15

of the bed alters with the mud and sand content. The composition of a mixed sediment bed, and deposition and consolidation history of the bed can significantly affect the bulk properties and thus the erosion resistance of the resulting deposit.

Correlations between bulk properties and critical erosion shear stress have been found in various studies. Bulk density in particular has been found to correlate positively with critical erosion shear stress (Amos, *et al.*, 2004; Bale, *et al.*, 2006; Quaresma, *et al.*, 2004; Riethmuller, *et al.*, 2000; Tolhurst, *et al.*, 2000). Studies by both Bale, *et al.* (2006) and Friend, *et al.* (2003) found that the CET and critical erosion shear stress correlated positively with bulk density and negatively with moisture and silt content. The CET and critical erosion shear stress are related properties.

Erosion parameters such as critical erosion shear stress, CET, and erosion rate are measured on mudflats *in situ* and by creating artificial conditions in a flume. Studies undertaken on mudflats measuring critical erosion shear stress, commonly use a cohesive strength meter (CSM) which is put in place over an area of mudflat and erodes the surface using jets of water (Defew, *et al.*, 2002; Friend, *et al.*, 2005; Friend, *et al.*, 2003; Tolhurst, *et al.*, 2000). Flume studies are conducted using both running track (Schaaff, et al., 2006) and annular flumes (Cloutier, *et al.*, 2006; Lau, *et al.*, 2000; Manning, *et al.*, 2007; Neumeier, *et al.*, 2006; Pope, *et al.*, 2006), depending on the study parameters, mud is either transported and placed in the flume or mud is mixed and settled.

Biotic effects on erosion potential

Plants on a mudflat can stabilise the sediment and increase the rate of accretion once vegetation cover has been established on a site (Boorman, 2003). The vegetation traps the sediment flowing over the site and reduces the re-suspension of sediment. The vegetation also acts as a buffer to wave propagation influencing calmer tidal conditions that increase the settling of sediment and reducing erosion. As a saltmarsh colonises, islands of vegetation develop initially that will join to form swards of vegetation; this accelerates the accretion of sediment and causes rapid elevation of the mudflat surface (Armstrong, 1988). Organic matter is also increased from the breaking down of dead plants leading to further sediment accumulation.

A study by Boorman, *et al.*, (2001) investigated the effects of rapid sedimentation rates on pioneer saltmarsh species, *Salicornia europaea* and *Aster tripolium,* the former of

which has a lower threshold elevation for colonisation. Both species responded well to the addition of large quantities of sediment, in general developing better when subjected to these fast accretion rates. This indicates that once saltmarsh has developed on a mudflat, continuing accretion will facilitate further saltmarsh growth in turn enhancing accretion.

Biological activity can either bind or destabilise sediments. The following mechanisms that affect sediment stability have been identified:

1. Alteration of fluid momentum impinging on the bed by changing the near bed flow or bed roughness.
2. Alteration of particle exposure to the flow, by burrowing or bioturbation.
3. Adhesion between particles produced by mucus and biofilms.
4. Alteration of particle momentum by filter feeding or ejection of pseudo-faeces.

It is generally reported that bacteria and microphytobenthos tend to be sediment stabilisers and benthic fauna destabilisers despite some exceptions (Black, *et al.*, 2002). Experiments led to the suggestion that stable beds persist despite the destabilising effect of the animal tubes because of mucus films. Microbial growth and the grazing of benthic fauna produces mucus films that can bind the sediment, in particularly benthic diatoms are known to secrete large amounts of extracellular polymeric substances (EPS) that act as mucus films (de Brouwer, *et al.*, 2000; Dyer, 1986). Many *in situ* studies have demonstrated that erosion thresholds generally increase significantly when epipelic diatoms are present in large concentrations in fine grained sediments. Macrozoobenthos on the other hand generally destabilise the sediment surface by bioturbation, creation of surface tracks and by forming sediment into pellets (Andersen, *et al.*, 2005).

Various field and flume studies have been done looking at the significant factors that enhance or limit erosion of cohesive sediments. A study by Quaresma, *et al.* (2004) investigated the effects of biological activity and bed consolidation time on erosion resistance. The study used mud collected from Hythe, Hampshire, UK, and an annular flume. The bed was found to become more stable with increasing consolidation time and the erosion threshold was positively correlated with wet bulk density. Biological activity can lower the wet bulk density, however the critical erosion threshold was still kept high due to microbiological activity and a surface biofilm. A further study using sediment from the same area by Neumeier, *et al.* (2006) focused on the erosion patterns of bed sediment with biofilm present, again using an annular flume. They found that

only minor variations in key factors could affect the bed and that bioconsolidation significantly increased the erosion threshold. A recent study by Bale, *et al.* (2006) looked at the erodibility of sediments in the Tamar estuary, Devon and Cornwall, UK, using a mini-annular flume that could take measurements either *in situ* or be used with cores taken from the study site. This study found no correlation with the biological markers chlorophyll *a* or colloidal carbohydrate but did find significant correlations with wet bulk density similar to the study of Quaresma, *et al.* (2004).

In this section the many controls on sediment accretion and erosion have been discussed. Referring back to Table 2.2, a number of sediment properties can have an effect on both the erosion and accretion at a managed realignment site. These factors will all influence accretion and erosion rates to a greater or lesser degree and will interact with each other. To evaluate the possible effects of these controls, a discussion of the findings from managed realignment sites follows below.

2.1.4 Research to date on managed realignment sites

In the UK there have been a number of managed realignment sites created in the last 20 years and a number that are planned as part of the estuary management plans of the EA. The main purposes of these managed realignment sites are to provide either flood storage or intertidal habitat. The success or failure of these sites in relation to sedimentation rates and properties, creation of intertidal habitat, creek formation and the impact on surrounding intertidal areas will inform the current research on the variety of sedimentation patterns which may develop in a newly created intertidal habitat.

2.1.4.1 Recorded accretion rates and types of sedimentation

In the Blackwater estuary, Essex, UK, four managed realignment sites were created to compensate for the loss of intertidal habitat and to create more sustainable flood defences (Blott, *et al.*, 2004; Crooks, *et al.*, 2002; Townend, *et al.*, 2002). The locations of each site are shown in Figure 2.3 below.
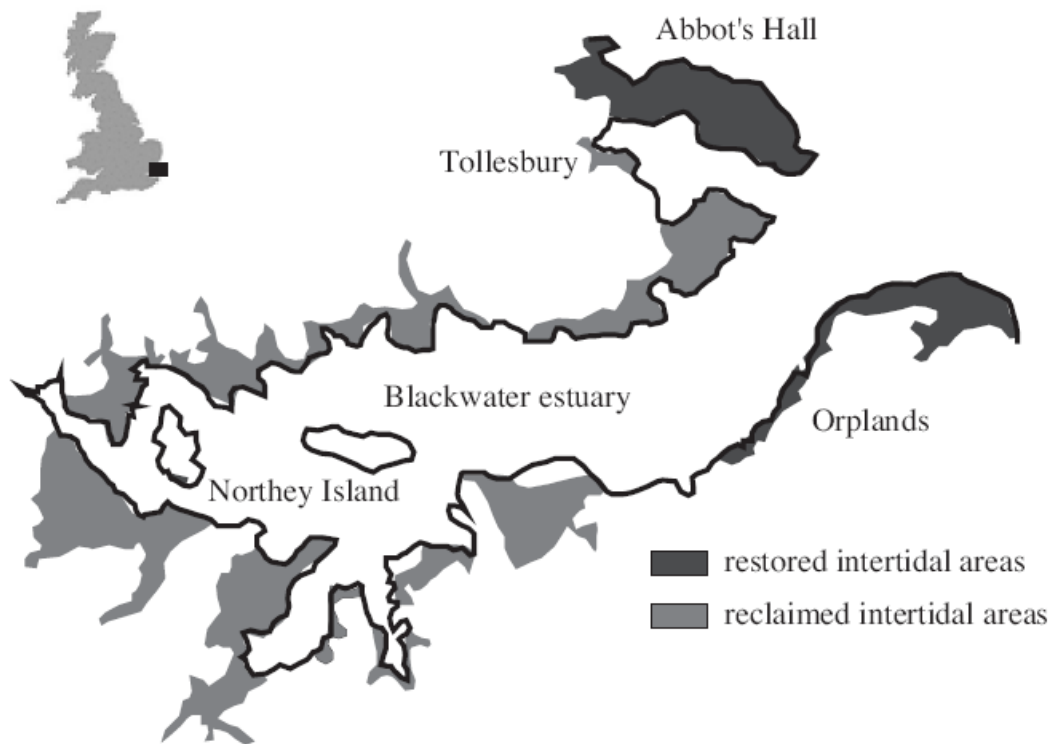
Figure 2.3: The locations of the managed realignment trials on the Blackwater estuary, Essex (Townend & Pethick, 2002).

The sites at Orplands, Northey Island and Tollesbury did not accrete sediment until colonisation by vegetation enhanced deposition. The site at Tollesbury was located lower in the tidal frame and took longer for accretion to accelerate than the site at Orplands (Pethick, 2002), which accumulated nearly 50 mm of sediment in two years (French, 2006). The site at Tollesbury is mentioned in various studies of accretion rates, habitat development, sediments post-breach, and bird communities (Atkinson, *et al.*, 2004; Boorman, *et al.*, 2001; Chang, *et al.*, 2001; Cundy, *et al.*, 2002; French, 2006; Garbutt, *et al.*, 2006; Hazelden, *et al.*, 2001; Pontee, *et al.*, 2006; Watts, *et al.*, 2003). There are some discrepancies between the various published rates of accretion for this site. This may be due to reports coming from different periods of the site's development. However most agree that the rates were fast, especially in the areas of low elevation, ranging from rates of 40 mm per year to between 100 and 300 mm per year (Cundy, *et al.*, 2002; French, 2006; Pontee, *et al.*, 2006).

The sites discussed above are all in the one estuary. The only other mention of precise accretion rates is the 40 mm of sediment accretion per year at Lantern Marsh, Suffolk, UK (Pontee, *et al.*, 2006). This site is also on the east of the UK.

A study of the sediment at Tollesbury managed realignment site has identified its enhanced resistance to erosion. The authors used a Cohesive Strength Meter (CSM) to deduce the *in situ* strength and stability of sediments on the site. Investigations found that after six years of regular tidal inundation, the initial surface appeared strong and very resistant to erosion. Where sediment accretion was greatest, below the MHWN level, both strength and resistance to erosion were lowest (Watts, *et al.*, 2003). A study that looked at the sediments on the site found that they usually coarsened and became better sorted and more positively skewed from the sea walls toward the central part of the site. The dominant factors affecting sediment deposition and transport within the site are topography and tidal flow. Overall, the grain size patterns reveal that coarser material predominates at the centre of the site, suggesting redistribution of finer material around the site on the incoming tides and the influence of a settling lag at high tide (Chang, *et al.*, 2001).

A study by Wolters, *et al.*, (2005) compared over 70 sites across Europe (including the UK) where land had been returned to intertidal habitat and found that on all sites elevation increased rapidly in the first few years after breaching. The sites in the study are a combination of managed realignment and historical seawall failure. Few sites have published accretion rates: apart from the Blackwater estuary sites, two sites in the Netherlands declared sedimentation rates of 5 to 20 mm per year. A similar study by Morgan, *et al.* (2002) found that the fastest rates of accretion (no figures given) were found on the more recent sites as opposed to the older ones. Table 2.3 collates together all the sediment accretion rates from managed realignment, historic breach failure, natural saltmarsh and mudflat sites.

Table 2.3: Yearly accretion rates at PHS, other managed realignment sites and natural saltmarshes**.**

	Location		Accretion Rate (mma^{-1})
Managed realignment	Blackwater Estuary, Essex, UK	Tollesbury	40 at low elevations 3-5 at high elevations (Cundy, *et al.*, 2002; French, 2006) 100-300 initially (Pontee, *et al.*, 2006)
		Abbot's Hall	0 for 1st 3 years Starting to accrete when vegetated (Pethick, 2002)
	Lantern Marsh, Suffolk, UK		40 (Pontee, *et al.*, 2006)
Historic breach failure	Pagham Harbour, West Sussex, UK		5 (from cores) (Cundy, *et al.*, 2002)
Natural saltmarsh	UK		2-20 (Pontee, 2003)
Mudflat	Spurn Bight, Humber estuary, UK		Few mm during calm conditions (Christie, *et al.*, 1999)

In general, the literature points to fast rates of accretion for newly breached managed realignment sites when compared with natural saltmarshes (see Table 2.3). At some sites this accretion has slowed when an elevation for the site has been reached that reduces inundation of the mudflat.

2.1.4.2 Intertidal habitat creation

Increasingly, the main aim of managed realignment is to create intertidal habitat to meet the EU Habitats Directive and to compensate for the loss of habitat through development (mainly port schemes) and predicted future losses from sea level rise.

Saltmarsh habitat creation was one of the main aims of the Blackwater estuary scheme. Saltmarsh along the Essex coastline has decreased by 12% since the 1970s, with a further decline of up to 40% by 2050 due to sea level rise (Blott, *et al.*, 2004; Crooks, *et al.*, 2002; O'Riordan, *et al.*, 2000).

Northey Island had full saltmarsh cover after just two years, however the site is very small (less than 1 ha). At the other sites, accretion only began once vegetation had become established, starting with the colonisation of *Salicornia* (Pethick, 2002). After accretion rates had increased, the site at Tollesbury quickly reached a soil salinity level suitable for colonisation by halophytic plants (Boorman, *et al.*, 2001; Hazelden, *et al.*, 2001). The deposition of sediment means the site has successfully met the aims of protecting the coast from erosion and creating habitat (Watts, *et al.*, 2003).

At Tollesbury an experiment was carried out to find if pre-treatment of sediment plots could improve the rate of development of saltmarsh habitat. Five different pre-treatments were investigated: saltmarsh seeds at low density, saltmarsh seeds at high density, plug plants, turfs of vegetation and an untreated control. The treatments were set up six months after breaching by which time there was 10 mm of accretion over the sediment plot areas. The study found that none of the pre-treatments proved effective in promoting the development of saltmarsh species. Waterlogging was a major factor in the mortality of plug plants and the turf, however the natural succession of saltmarsh plants occurred across certain areas of the site. The role of creeks in dewatering newly accreted sediments within realignment sites is thus important to vegetation development (Garbutt, *et al.*, 2006).

The study by Wolters, *et al.*, (2005) evaluating the success of the 70 sites across Europe (including the UK), used a saturation index where the presence of all target plant species was expressed as a percentage of the total regional target species pool of the region. The percentage of target species at the different sites ranged from 18% to 64%. Findings suggested that UK sites were the worst with the majority of sites only restoring less than 30% of the total species list. The most common species were typical pioneer saltmarsh species such as *Salicornia*, *Suaeda maritima*, *Aster tripolium* and *Puccinellia maritima*. Best results were found for sites larger than 100 ha.

In the United States (US) a number of saltmarsh restorations have taken place throughout the coastal areas of the country. These have been undertaken purely to replace lost and reclaimed marsh habitat. One such area is in San Francisco Bay where 940 ha of former saltmarsh have been restored. Within 4-20 years 9 out of 15 of the sites studied had returned to more than 50% cover, driven by fast accretion rates in the lowest parts of the sites (Defew, *et al.*, 2002; Williams, *et al.*, 2002).

In general, natural and engineered coastal flooding sites appear to have developed saltmarsh habitat. This relies heavily on the height of the site and the salination of the soil. The success across all sites probably indicates that any prior numerical modelling carried out to locate managed realignment schemes, e.g. in the Blackwater estuary, was successful.

2.1.5 Conclusions on the role of managed realignment

Managed realignment is increasingly used to create intertidal habitat as compensation for losses in other parts of an estuary, to counteract rising sea levels and to increase the accommodation space of the estuary thus reducing flood risk. For a site to be successful many design aspects need to be considered such as the size, shape and method of breaching to best optimise the outcome of the site. The role of sediment properties in controlling the accretion rates and habitat development is important. Managed realignment sites to date have shown the success of various options and the expectations for sites in the planning stage with regards to accretion rates and habitat creation. They have also demonstrated the importance of prior numerical modelling to create conditions that best fulfils initial aims and objectives. There is, however, incomplete understanding of the sedimentary processes occurring in such a site.

A major scheme is now taking place within the UK on the Humber estuary to create an integrated shoreline management plan that maintains flood protection as well as creates new intertidal habitat. This scheme makes use of a number of managed realignment sites to achieve these aims.

2.2 The Humber estuary

The Humber estuary is one the principal estuaries of the North Sea. It is located on the east coast of the UK, flowing into the North Sea between Spurn Point and Cleethorpes (see Figure 2.4).
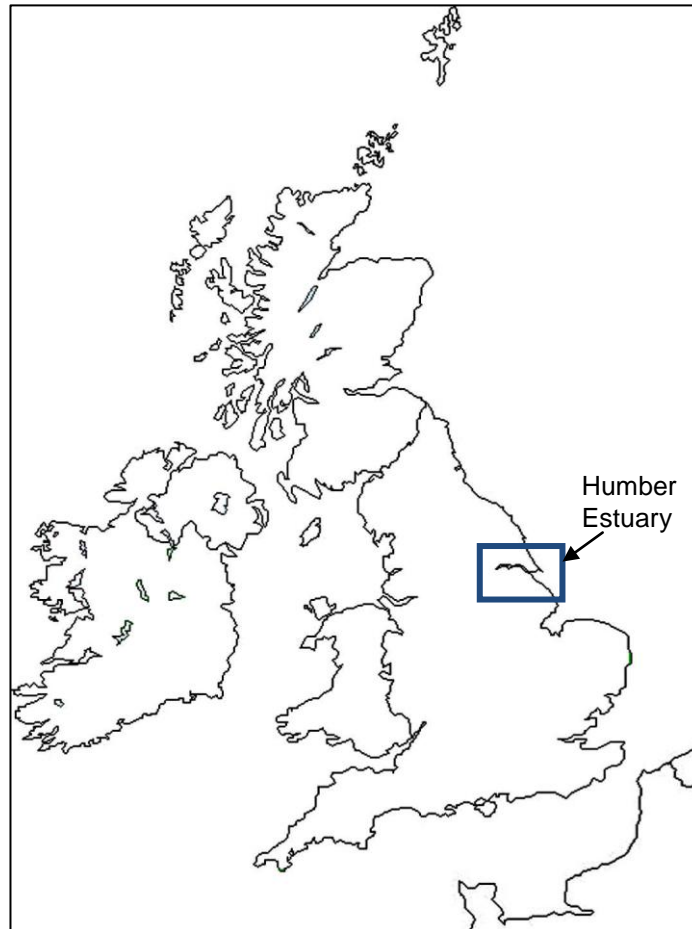
Figure 2.4: Location of the Humber estuary within the UK.

2.2.1. Estuary catchment

The catchment of the Humber estuary drains an area of 24 472 km^2; this is 20% of the area of England and is inhabited by 10.5 million people based on 2001 census (see Figure 2.5 below).
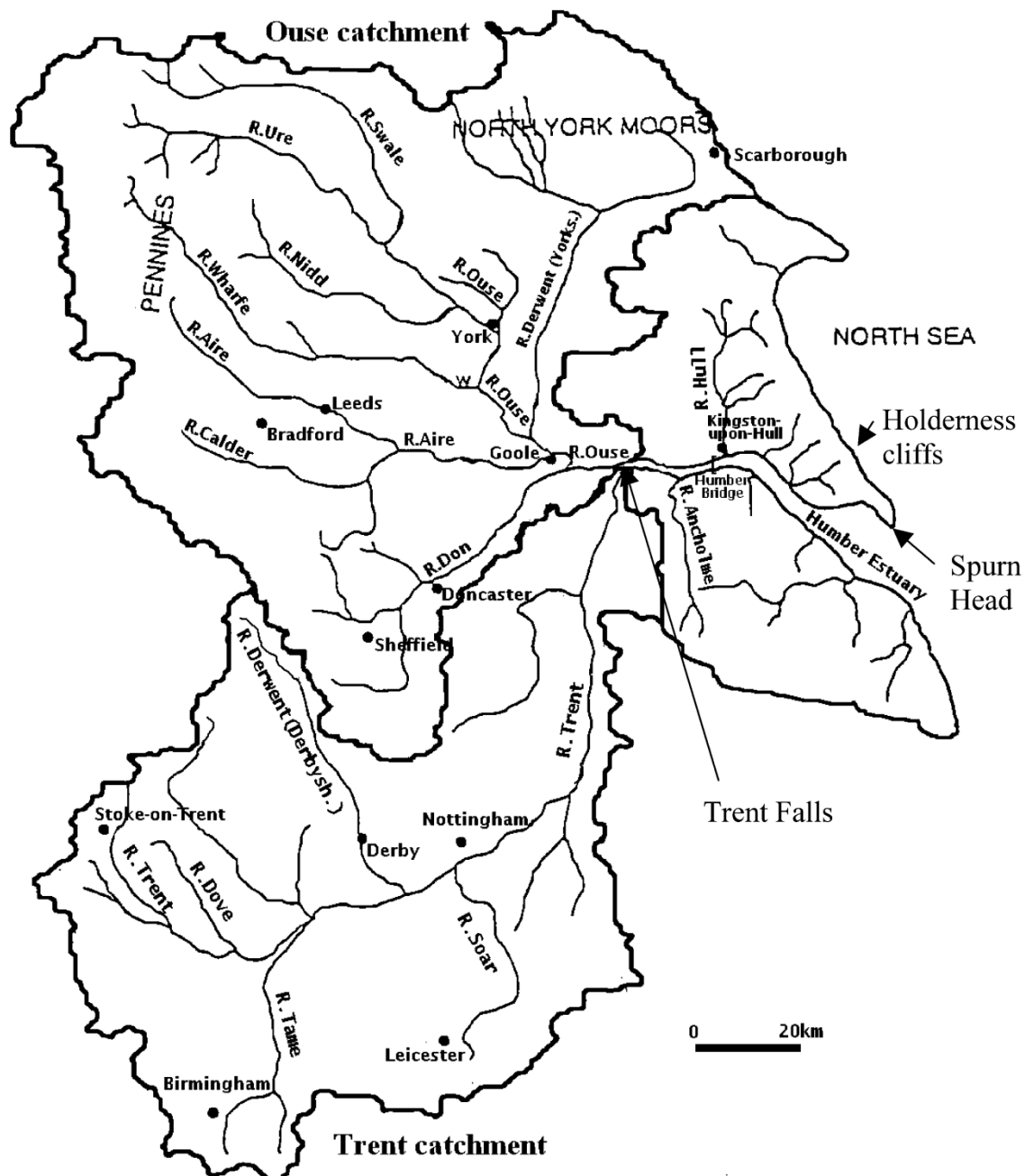
Figure 2.5: The Humber estuary catchment showing major tributaries (Cave, *et al.*, 2003)

The ports of Goole, Hull, Grimsby and Immingham lie on the Humber estuary, which assumes this name below the confluence of the rivers Trent and Ouse, at a point called the Trent Falls (see Figure 2.5). There is an average annual freshwater input of 244 cumecs, with discharges ranging between 165 and 320 cumecs. The convergence at Trent Falls is 60 km west of where the Humber estuary meets the North Sea at Spurn Point (Law, *et al.*, 1997). The length of the tidal estuary is 317 km, and it varies in width from 13 km at the mouth to 1.5 km further upstream, with a tidal plain covering an area of 90,000 ha (Cave, *et al.*, 2005; Pethick, 1988; Winn, 2004). The Humber

estuary is the largest single input of freshwater from Britain into the North Sea and has a large tidal range of 7.2 m. It is therefore classed as macrotidal (Winn, 2004).

Figure 2.6: The Humber estuary showing locations of major cities and the different sections of the estuary (Winn, 2004).

From morphological studies, the Humber estuary can be naturally divided into three main areas based on the nature of the processes taking place, and/or the impact of these processes on the rest of the estuary. The outer estuary covers Spurn Head to Grimsby and Hawkins Point and acts more as a coastal inlet than an estuary, the middle estuary stretches to the Humber Bridge and marks the start of more typical estuary processes, and the inner estuary is the final section to Trent Falls (see Figure 2.6) (Winn, 2004).

2.2.2. Geological history

The changes to the Humber catchment during the Quaternary period were important in terms of deposition and evolution of river basins. Between 18 000 and 13 000 years BP (before present) ice approached the Humber basin from the north and north east blocking the northern end near the Vale of York and the eastern end of the Humber blocking drainage and creating a lake. Clays started to accumulate over the lake bed and as the lake began to dry up, streams and rivers in the clay were formed (Jarvie, *et al.*, 1997; Pethick, 1988). River flows continued to scour at the Hull sill (waterfall) whilst sea-levels rose. Eventually, the overflow of freshwater at the Hull sill became a tidal channel, with complete saline conditions establishing in the inner part of the basin around 6000 years BP. Overall the estuary has been transgressing landward under the influence of a rising sea-level (ABP mer, 2004b; Jarvie, *et al.*, 1997; Winn, 2004).

2.2.3 Importance of Humber estuary for industry and conservation

The Humber estuary is of economic as well as environmental importance both in the UK and internationally.

2.2.3.1 Industry

The estuary sustains the UK's largest port complex run by Associated British Ports (ABP) which handles 14% of the UK's international trade (Environment Agency, 2008; Manning, 2006) its banks also house a variety of industries including oil refineries, power stations and chemical works. The main city of Kingston-upon-Hull and smaller towns of Goole, Grimsby and Scunthorpe lying on the Humber estuary all contribute to the economy of the region and the UK. Much of the remaining floodplain area (85%) consists of farmland, both arable and grazing.

2.2.3.2 Conservation

The entire Humber estuary is proposed as a European marine site comprising the Humber estuary Special Area of Conservation (SAC), the Humber estuary Special Protection Area (SPA) and the Humber estuary Ramsar site. The SPA and SAC status denotes European importance and the Ramsar site status is of international significance. The habitats protected by these designations are saltmarsh, mudflat, sand dunes, samphire beds, reed beds and lagoons (Manning, 2006). These support a variety of species in an ecosystem dominated by flooding. Table 2.4 lists some of the protected species found in the Humber estuary.

Table 2.4: Internationally important species found within the Humber estuary ecosystem collated from (Manning, 2006).

Type	Species	Designation
Fish	River Lamprey, Sea Lamprey	European marine site
Birds- Breeding	Avocet, Little tern, Marsh harrier	Annex 1
Wintering	Bar-tailed godwit, Bittern, Golden plover, Hen harrier	Annex 1
Migratory	Redshank, Ringed plover, Sanderling, Dunlin, Grey plover, Knot, Lapwing, Shelduck	Internationally important
Waterfowl	Black-tailed godwit, Curlew, Dark-bellied brent geese, Goldeneye, Mallard, Oystercatcher, Pochard, Scaup, Wigeon	Internationally important
Invertebrates	Ground beetle, Lagoon sand shrimp, Muscid fly, Scarce pug moth	Internationally important (threatened)
Animals	Grey seals	rare

Provision of habitats within the Humber estuary and thus the continued use of the estuary by internationally important species, is driven largely by the movement of water and sediment within the estuary and the greater North Sea area.

2.2.4 Importance of sediment movement in estuaries

The sediment within estuaries creates intertidal areas which in turn support the vast wealth of ecological habitats that are the hallmark of an estuary. Without the mudflat, sandflat and marshland there is no substrate for invertebrates to live in, for the plant species to colonise and for the infauna to feed, over winter and breed on. The flux of sediment is key to the extent and character of intertidal areas, itself influenced by the tidal flows and topography of the estuary.

Sediment deposition on intertidal areas increases the height and/or the area of mudflat or marsh. However, this is balanced by a net flux of sediment into the estuary from both fluvial and marine sources, which together determine the overall sediment load. The majority of this is held in suspension, or deposited and re-suspended on the subsequent tide (Townend, *et al.*, 2003).

2.2.4.1 Sediment movement in the Humber estuary

The movement of sediment in the Humber estuary was studied as part of the Land-Ocean Interaction Study (LOIS) funded by the Natural Environmental Research Council (NERC). The period of research lasted from 1992 to 1998 and was followed by a three year modelling phase (Huntley, *et al.*, 2001).

Townend and Whitehead (Townend, *et al.*, 2003) produced a net sediment budget for the Humber estuary and a report by the British Geological Survey (BGS) (Balson, *et al.*, 2004) suggested the sources, sinks and pathways for sediment at its mouth. They showed that there is a net flux of sediment into the estuary on the southern bank and a net flux of sediment out of the estuary on the northern bank. The eroding cliffs of the Holderness Coast produce the majority of sediment, with major sinks including Spurn Head, the Binks, and the infilling of the Sand Hole. Donna Nook and Haile Sand Flat are also major areas of sand deposition (see Figure 2.7 below).

Figure 2.7: Location of sediment source and sink areas on the Humber estuary (Edwards, *et al.*, 2006).

Figure 2.8 shows diagrammatically the amounts of sediment entering and leaving the estuary as well as the sources and sinks of that sediment during each tide. The average tidal flux is 1.2×10^6 tonnes per tide, 200 tonnes are deposited to the intertidal bed and 11 tonnes to saltmarshes (Townend & Whitehead, 2003).
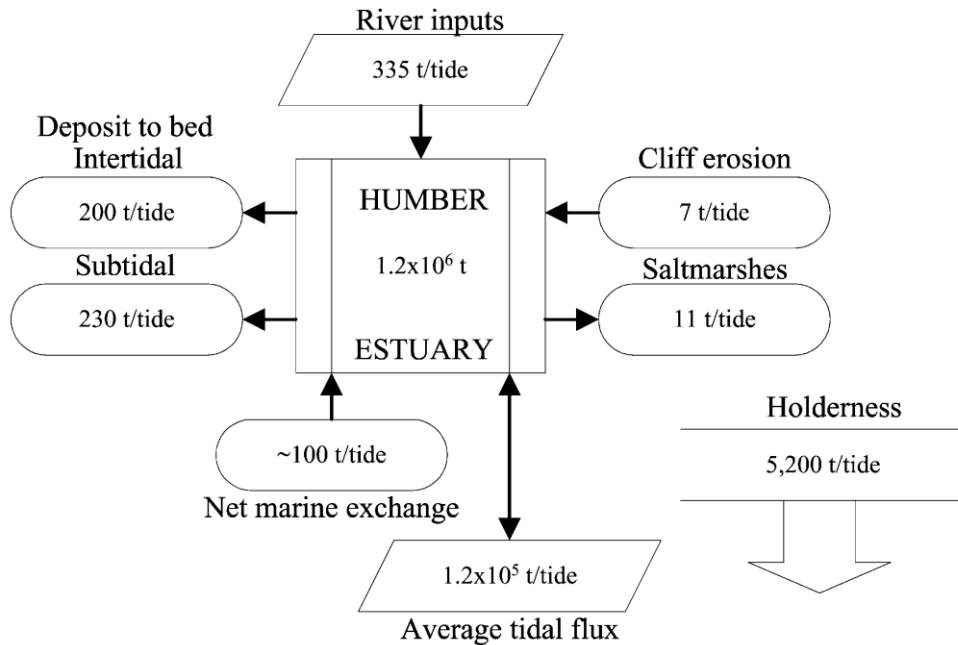
Figure 2.8: The tidal budget for the Humber estuary showing values for sediment from major sources and sinks (Townend & Whitehead, 2003).

Between November 1994 and October 1997 large annual variations in SPM net flux were recorded (as part of the LOIS study): 373 kt in first year, 95 kt in second year and 232 kt in third year. The fluxes tended to be highest from November to January. The Humber estuary has a net storage capacity of approximately 300 000 ta^{-1} of sediment (Cave, *et al.*, 2005). The range of suspended sediment concentration (SSC) quoted in the literature can be from 20 to 3,200 mgl^{-1} (Pontee, *et al.*, 2006).

The marine inputs to the system generally exceed the fluvial inputs by an order of magnitude (see the river inputs compared to the input from the Holderness cliffs in Figure 2.8). Looking at the movement of different grain sizes, the sand generally moved towards the mouth of estuary during the winter months and returned towards the head during the summer and autumn (Huntley, *et al.*, 2001).

2.2.4.2 Sediment movement on intertidal areas in the Humber estuary

Approximately 30% of the outer area of the Humber estuary is intertidal. Strong tidal asymmetry in macrotidal estuaries leads to high vertical suspended sediment concentration gradients (Mitchell, *et al.*, 2003). Over short timescales, such as those of semi-diurnal tidal cycles, the transport and re-suspension of material by tidal currents can cause changes in suspended sediment concentration in the Humber estuary of around 360 mgl^{-1} (Pontee, *et al.*, 2004).

Much research on sediment movement has been undertaken at various sites on the Humber estuary (Black, 1998; Brown, *et al.*, 1998; Christie, *et al.*, 1999; Christie, *et al.*, 2000; Mitchell, *et al.*, 2003; Paterson, *et al.*, 2000; Pontee, *et al.*, 2004; Robinson, *et al.*, 1998; Widdows, *et al.*, 2000; Wood, *et al.*, 2002; Wood, *et al.*, 2003; Wu, *et al.*, 1998), most notably on the Skeffling mudflat and Spurn Bight close to the mouth of the estuary (see Figure 2.9 for location). Studies have looked at a variety of sediment properties including the transport, accretion and erosion of mudflat as well as biotic effects. They provide data on the general conditions on mudflats within the Humber estuary and act as a background to the current research.

Figure 2.9: Location of Spurn Bight and Skeffling mudflats on the Humber estuary (Christie, *et al.*, 2000)

Accretion rates and sediment flux on Humber mudflats

Brown, *et al.* (1998) looked at the eastern end of the Humber estuary as part of the Biological Influences On interTidal Areas (BIOTA) programme from 1993 to 1997. The authors found that accretion was fastest in the middle and lower zones of continuous vegetation dominated by *P.maritima*, but lower at the edge of the marsh. The net accretion at this marsh edge was also lower than on the bare mudflat in front of

31

the marsh. Periodic episodes of accretion at the marsh front were recorded on these marshes during the time of the study. Long-term vertical marsh accretion was influenced by a variety of factors including relative sea-level, compaction, marsh age and frequency of reclamation, and the contribution of *in situ* organic matter and accumulated surface litter.

In the paper by Christie, *et al.* (1999), detailed analysis of the annual variations in suspended sediment flux and bed level were reported for Spurn Bight. The authors found that shoreward flux and gradual accretion were typical of calm hydrodynamic conditions; whereas large waves caused the erosion of several centimetres of sediment and prevented any deposition over slack water. The height of the mudflat was continually moving; net seasonal changes in bed height were a few millimetres.

At the upstream end of the Humber estuary, near to Trent Falls, research has been carried out on sediment flux at Blacktoft (Mitchell, *et al.*, 2003). The research used both photo-electronic and manual pins on an intertidal bank to measure the rates of accretion and erosion. They showed a correlation between sedimentation and tidal range, freshwater flow and wind speed. Both biological activity and consolidation of mudflats modified the processes of sediment exchange. The authors concluded that deposition and erosion occurred over periods of time on all intertidal banks within the study area.

Influences on sediment stability on Humber mudflats

A paper by Paterson, *et al.* (2000) details the use of a CSM to investigate sediment stability on the Skeffling mudflat. The authors suggest that the photosynthetic biomass (mainly diatoms) is the significant factor in controlling sediment stability. The diatom biomass in the top 2 mm appears to be a major control on the sediment surface and their influence on sediment properties decreases with depth. Christie, *et al.* (1999) also found evidence of biofilms stabilising the mudflat at Spurn Bight during their study discussed in the previous section.

Black, (1998) looked at the sediment dynamics across the mudflat at Spurn Bight as part of the LOIS programme with particular attention to the higher mudflat regions. The experiments took place during a spring neap tide cycle on Spurn Bight. The author concluded that the high intertidal region of the mudflats acts as a sink for SPM and that some of this SPM was being eroded from the middle marsh zone.

A paper by Wood, *et al.* (2002) modelled biotic (biota density) and abiotic (tidal height and SSC) effects on intertidal sediment transport based on laboratory and field experiments from Spurn Bight. The numerical model combined a simple one-dimensional onshore-offshore model of water movement with a semi empirical model of cohesive sediment erosion and deposition. The authors found that the pattern of intertidal erosion is sensitive to the bathymetry, with greatest erosion occurring over flatter sections of shore. They also showed that biota can have a significant effect on sediment redistribution within the intertidal zone and that this is important for the morphological evolution of intertidal areas. The same model set-up was used by Wood, *et al.* (2003) to investigate the effects of climate change on intertidal sediment transport.

Investigations of the sediment movement, accretion, and erosion in the Humber estuary reveal a dynamic system with many factors contributing to the development of intertidal habitat and the continued functioning of the estuarine system.

2.2.5 Humber flood risk management strategy

The inhabitants and industry within the Humber floodplain are vulnerable to the risks of flooding from the North Sea. The storm surge that took place during January 1953 caused devastation along the East coast of England and along the North Sea coastline of Europe (Environment Agency, 2008). If there were no flood defences on the Humber estuary, 90 000 ha of land could be flooded by a storm surge from the North Sea (see Figure 2.10). Flood defences were improved after 1953 to prevent flooding; an example of the measures taken along the Humber estuary is the tidal barrier in place at the point where the River Hull flows into the Humber estuary to protect the inhabitants of Hull.

More recently the EA have developed a long-term integrated management strategy published in March 2008 (Environment Agency, 2008). This has been developed specifically to adapt the current flood management options to the problem of rising sea levels thought to be a consequence of climate change (Bernstein, *et al.*, 2007).
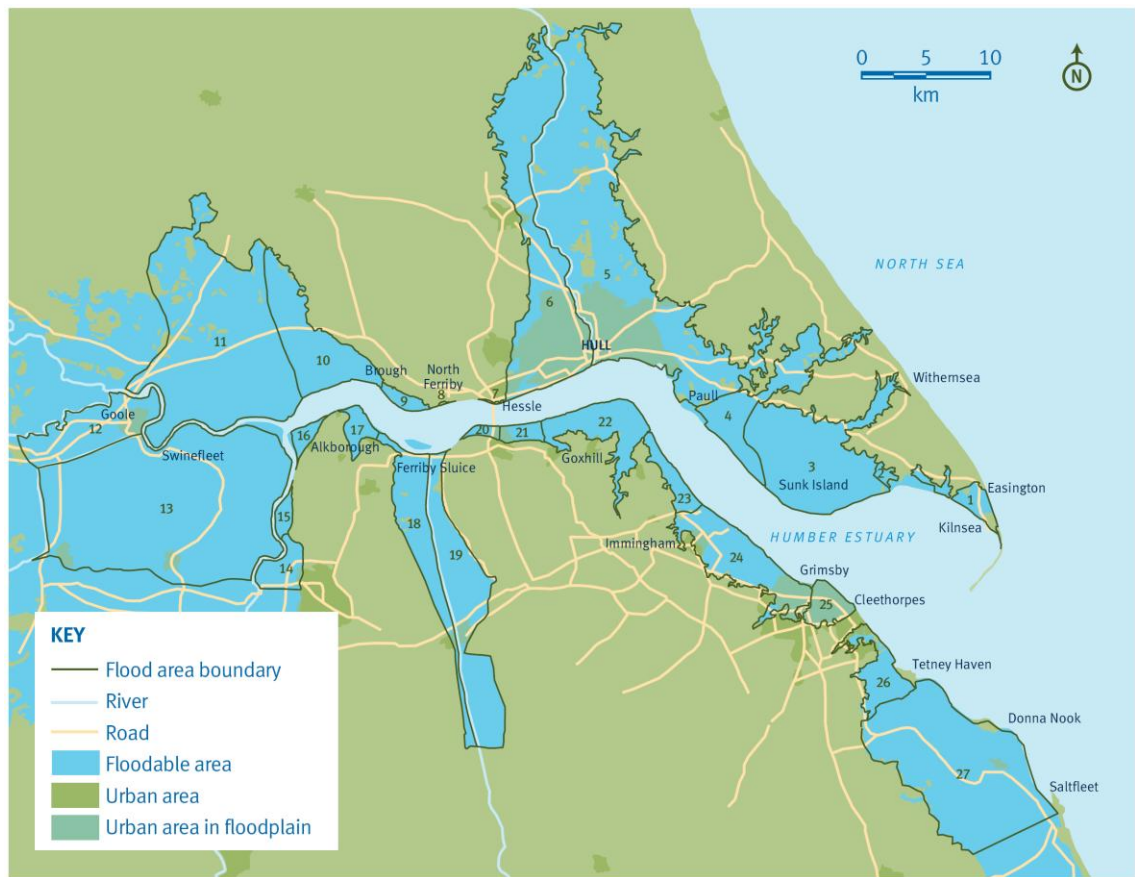
Figure 2.10: The floodplain of the Humber estuary. Numbers refer to EA flood areas (Environment Agency, 2008).

The Humber estuary has been divided for management purposes so that each area can be viewed independently as well as integrated into the overall scheme. Defences in areas that protect residential and industrial land will continue to be maintained, however along some stretches of the shoreline the EA is proposing to abandon defences that are uneconomic and to do so would not impact significantly on housing and industry. The management strategy requires inter-agency working to ensure the majority of the Humber estuary is protected from flooding for the foreseeable future.

2.2.5.1 Sea level rise in the Humber estuary

For the past 80 years mean sea levels have risen at between 1.5 and 3.6 mm per year (Figure 2.11) (Yorkshire Futures Regional Intelligence Network, 2002). The rate of isostatic change for the Humber estuary is estimated at -0.86 mmyr^{-1} for the inner estuary and -0.78 mmyr^{-1} for the outer estuary (Shennan & Horton, 2002). As the Humber estuary has been dropping due to isostatic change, this would have increased the sea level relative to the land. Over the last 80 years the Humber estuary will have dropped between about 70 and 60 mm (inner and outer estuary), increasing the tidal prism of the estuary and decreasing intertidal land.
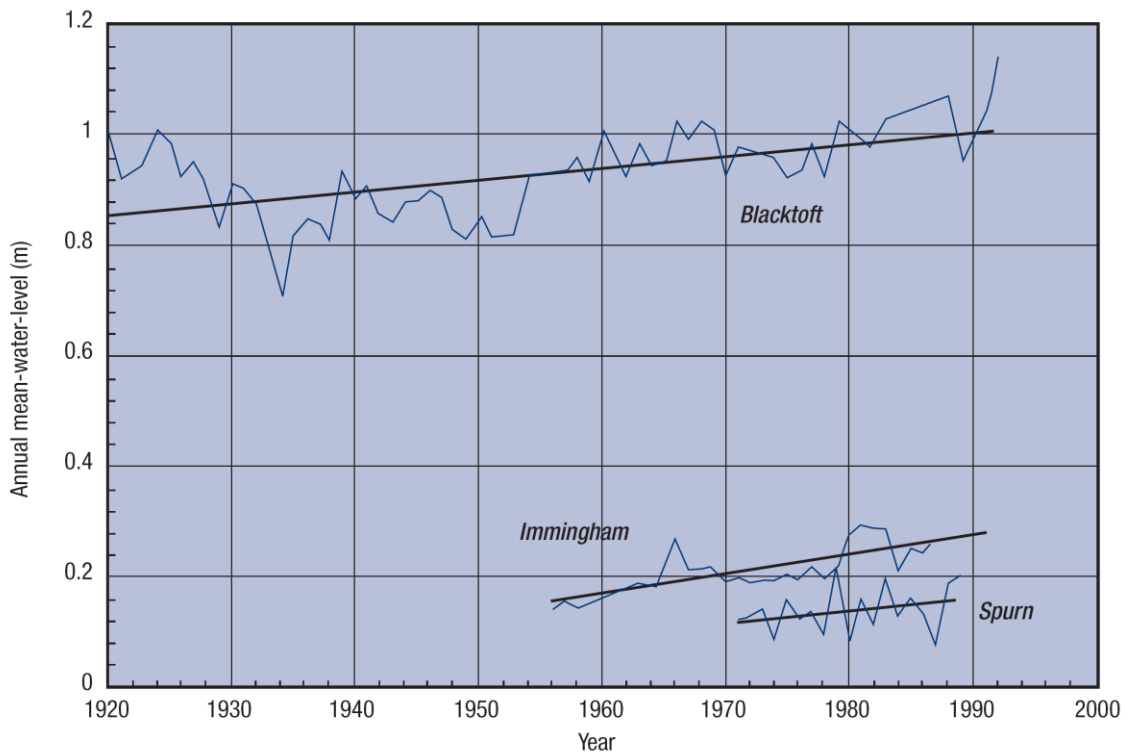
Figure 2.11: Rising sea levels at three sites on the Humber estuary (Yorkshire Futures Regional Intelligence Network, 2002)

The data in Figure 2.11 are extracted from the UK Climate Impacts Programme (UKCIP), which was set up to translate the advice of the IPCC into UK specific predictions. The findings have been incorporated into the government's Planning Policy Statement 25 (PPS 25) first published in 2006 (Communities and Local Government, 2006). This gives the following recommended allowances for net sea level rise (mma^{-1}) in areas south of Flamborough Head:

- 1990 to 2025: 4.0
- 2025 to 2055: 8.5
- 2055 to 2085: 12.0
- 2085 to 2115: 15.0

In addition, national recommendations for various other factors likely to impact on the Humber estuary are given in Table 2.5, below.

Table 2.5: Recommended national precautionary sensitivity ranges for peak rainfall intensities, peak river flows, offshore wind speeds and wave heights (Communities and Local Government, 2006).

Parameter	1990 to 2025	2025 to 2055	2055 to 2085	2085 to 2115
Peak rainfall intensity	+ 5%	+ 10%	+ 20%	+ 30%
Peak river flow	+ 10%		+ 20%	
Offshore wind speed	+ 5%		+ 10%	
Extreme wave height	+ 5%		+ 10%	

This combination of factors indicates that the Humber estuary needs to be carefully managed to protect homes and industry as well as compensate for the loss of intertidal habitat.

2.2.5.2 Loss of intertidal habitat

Saltmarshes within the Humber estuary are scattered from Spurn Point and Donna Nook to a westerly point of the Trent Falls (Armstrong, 1988) (see Figure 2.7). Studies undertaken by the EA have indicated that the net loss of intertidal habitat in the Humber estuary over the last 50 years is about 85 ha, however if sea-levels rise at the rates predicted above, this could lead to a loss of 460 ha over the next 50 years, particularly in the middle estuary. Coupled with the loss from sea-level rise is the threat from pollutants, as previously mentioned the Humber estuary is an international port complex and a location for major industry (Armstrong, 1988). To counteract this loss of habitat the EA are hoping to create between 650 ha and 850 ha of 'new' habitat to meet its responsibilities as set out in the Habitats Directive (Environment Agency, 2008).

2.2.5.3. Locations of existing and planned managed realignment sites

The Humber Flood Risk Management Strategy identifies the locations of two existing managed realignment sites plus a further five sites that may be completed between 2010 to 2050, (depending on the needs for more intertidal land), and two flood storage areas (see Figure 2.12 below).

Figure 2.12: Location of existing and proposed managed realignment sites (Environment Agency, 2008).

To predict the effects of these locations on the functioning of the Humber estuary and investigate the prime locations for habitat creation and water storage, a number of numerical models have been constructed during planning.

2.2.5.4 Modelling of sites prior to breaching

The aims of the modelling are fourfold:

1. to predict the quantity of intertidal area likely to be lost as a result of sea-level rise in the next 50 years;
2. to predict the quantity and location of managed realignment sites that are required to counteract this loss;
3. to predict the possible impacts of the managed realignment sites on the range and quantity of habitats; and
4. to predict the impact on flows and flooding in the Humber estuary.

Pethick, (2002) used *top down* regime models. The approach hypothesises that the estuary system will reduce stresses applied by tidal flows and waves by increasing bed area until such stresses lie below a particular threshold level. The two main assumptions

underlying the regime theory are: the estuary will achieve some form of dynamic equilibrium and there is a characteristic function that describes the equilibrium relation.

Three different sea-level rise scenarios are investigated using the regime model:

1. The current rate of sea-level rise (1.8 mm per year) would continue for the next 50 years.
2. The rate of sea-level rise would be 6 mm per year as predicted due to global warming.
3. The rate would rise to a worst case scenario of 10 mm per year.

Two assumptions are made for the modelling of sea-level rise:

1. The increase in sea-level is not associated with changes in tidal range.
2. The elevation of the tidal frame will keep pace with sea-level rise.

Under the worst case scenario, the model predicted that the potential loss of saltmarsh in the Humber estuary over the next 50 years will be between 200 ha and 550 ha. The EA's target of creating between 650 ha and 850 ha of intertidal area through managed realignment schemes will thus provide ample equivalent habitat for the highest sea-level rise predicted. The model is run to show the impact of the proposed realignment sites; this is done on an individual and group basis covering a variety of different permutations depending on the combinations of sites that may actually be created. Realignment of all groups and sites produces net saltmarsh gain if sea-level remains static. All groups also yield saltmarsh gains with present rates of sea-level rise extrapolated for 50 years. Analysis demonstrated that the critical factor for determining the impact of a managed realignment site on the estuary was the location of the site within the estuary. Those sites in the upper estuary are mainly providing flood storage apart from Alkborough- see Figure 2.12, which provides both flood storage and habitat creation potential. The remaining sites that fall into the middle and lower estuary mainly provide habitat creation opportunities.

Further modelling undertaken by ABP (ABP mer, 2004c) for the EA using a new hydrodynamic model of the Humber estuary designed by Delft (WL Delft Hydraulics, The Netherlands) 3D modelling. This model examines the short-term changes in the Humber estuary water levels and morphology due to managed realignment of sites. The baseline for the hydrodynamic model came from the 2000 bathymetric survey of the Humber estuary. The model was first used to simulate surge high water levels and to assess the impact of managed realignment sites on these levels, and second to drive a

morphodynamic model that would predict the evolution of the estuary for several years assuming the estuary comprised only sandy sediment, and then only of muddy sediment.

The baseline for the modelling of the proposed realignment schemes included PHS as this had already been breached when the model was running. Two sites, at Alkborough and Whitton Ness (see Figure 2.12), which are located upstream of the Humber Bridge caused significantly larger reductions in spring high water levels than the other proposed sites. With the predicted sea-level rise of 6 mm a year, a reduction of 90 mm in maximum level would counteract sea-level rise for 15 years, the maximum reductions of around 210 mm predicted when all sites are developed could delay the works required to cope with sea-level rise by around 35 years. In conclusion, the authors found the managed realignment sites upstream of the Humber Bridge caused much larger local changes than those further downstream.

Additional modelling by ABP (ABP mer, 2004a) on behalf of the EA used the Estmorph *hybrid* model as well as a *form* model to predict the impacts of the proposed managed realignment sites on the Humber estuary. Estmorph does not require the assumption that the estuary is in equilibrium and allows the tidal conditions in the estuary to respond to changes in cross-section shape and volume. The modelling was firstly used to hindcast conditions in the Humber estuary that can be verified against historical data; this confirmed that the model was able to reproduce enough of the changes previously observed to be acceptable.

Estmorph was subsequently used to test the impact of the proposed managed realignment sites. The baseline situation (before including the proposed managed realignment sites in different groups) for these tests once again included the managed realignment site at PHS. The model predicted that after 50 years running of the baseline situation intertidal area of the estuary will decrease by just 4 ha, less than the 445 ha loss reported for the reference case excluding the baseline developments.

Delft (WL Delft Hydraulics, The Netherlands) 3D modelling of the historic bathymetries along with the geometric properties of the Humber estuary derived from the previous ABP report (ABP mer, 2004c) were analysed to develop a *form* model.

The form model was used to predict future changes in the Humber estuary's intertidal area for sea-level rise rates of both 1.8 mm (the current trend) and 6 mm (the predicted

trend under sea-level rise) per year. These predictions have suggested a loss of 125 ha over the next 50 years if sea-levels continue to rise at 1.8 mm year, increasing to 325 ha if sea-levels rise at 6 mm a year. These losses are closer to the anticipated value used by the EA in their planning for new managed realignment sites. Related to the overall loss of intertidal area is a further prediction of loss of intertidal areas due to coastal squeeze for the next 50 years based on the current line of flood defences. Results show 150 ± 50 ha for a 1.8 mm rise per year rise, 450 ± 150 ha for a 6 mm rise per year rise and 730 ± 240 ha for a 10 mm rise per year.

2.2.6 Conclusions on the Humber estuary

The Humber estuary is important nationally and internationally for both economic and environmental reasons. The large area of intertidal habitat supports a wealth of important species and the floodplain supports a large number of inhabitants and industries. To protect these an integrated flood management plan was developed by the EA and published in 2008, which details the levels of flood protection for all sectors of the estuary and takes into account the future increasing flood risk linked with climate change. As part of this plan, the Humber estuary is a key location for creating managed realignment sites so that intertidal habitat can be replaced in compensation for that lost via industrial expansion or coastal squeeze. One of only two existing managed realignment sites created by the EA on the Humber estuary is at Paull Holme Strays.

2.3 Paull Holme Strays

The current research was undertaken at a breached managed realignment site on the Humber estuary at a location known as Paull Holme Strays, (Figure 2.13). The site is located behind the extensive Paull Holme Sands mudflat that is included within the Humber Flats, Marshes and Coast SPA, Ramsar and SAC European Marine Site. Paull Holme Sands mudflat is also part of the larger area of mudflats called Cherry Cobb and Foulholme Sands.

Figure 2.13: Location of PHS within the Humber estuary.

2.3.1 Reasons for creating the managed realignment site at PHS

An area of 80 ha was breached by the EA on the 7th September 2003 after a two year construction period, prior to this the site had been used for arable farming mainly of cereals and oilseed. The anticipated benefits of this were:

- Creating compensatory habitat (a legal requirement) for losses brought about by other current flood defence schemes in the middle estuary in particular on the south bank of the estuary at Pyewipe where encroachment was taking place into the SPA.

41

- Creating additional intertidal habitat for future urgent works thus creating "habitat in the bank".

- Addressing the potential loss of intertidal habitat from the expected sea-level rise of 6 mm per year over the next 50 years (Boyes, *et al.*, 2004).

The qualitative targets set out in the Environmental Action Plan (EAP) for PHS were:

- to create mudflat that would support an invertebrate assemblage of similar species, population abundance and biomass to reference sites in the middle estuary;

- to develop saltmarsh habitat that should support a range of species representative of middle and lower estuary communities in the area;

- to support at least 30 species of feeding wintering waterbirds including specific species such as Redshank (*Tringa totanus*) and Dunlin (*Calidris alpina*) and at least 12 species of roosting wintering waterbirds (Golden Plover *Pluvialis apricaria*) (Environment Agency, 2007).

2.3.2 Summary of previous monitoring by EA

Monitoring of the site for accretion rates, vegetation cover, invertebrates and birds started as soon as the site was breached in 2003. Details on precise locations of these sampling stations and results from this monitoring are discussed in the following sections. Full details can be found in these references: Boyes, *et al.*, 2004; Brown, *et al.*, 2004; Brown, *et al.*, 2005; Brown, *et al.*, 2006; Brown, *et al.*, 2008.

In summary, accretion rates were found to be particularly fast in the north-western area of the site, closest to the bottom of the photo in Figure 2.14.
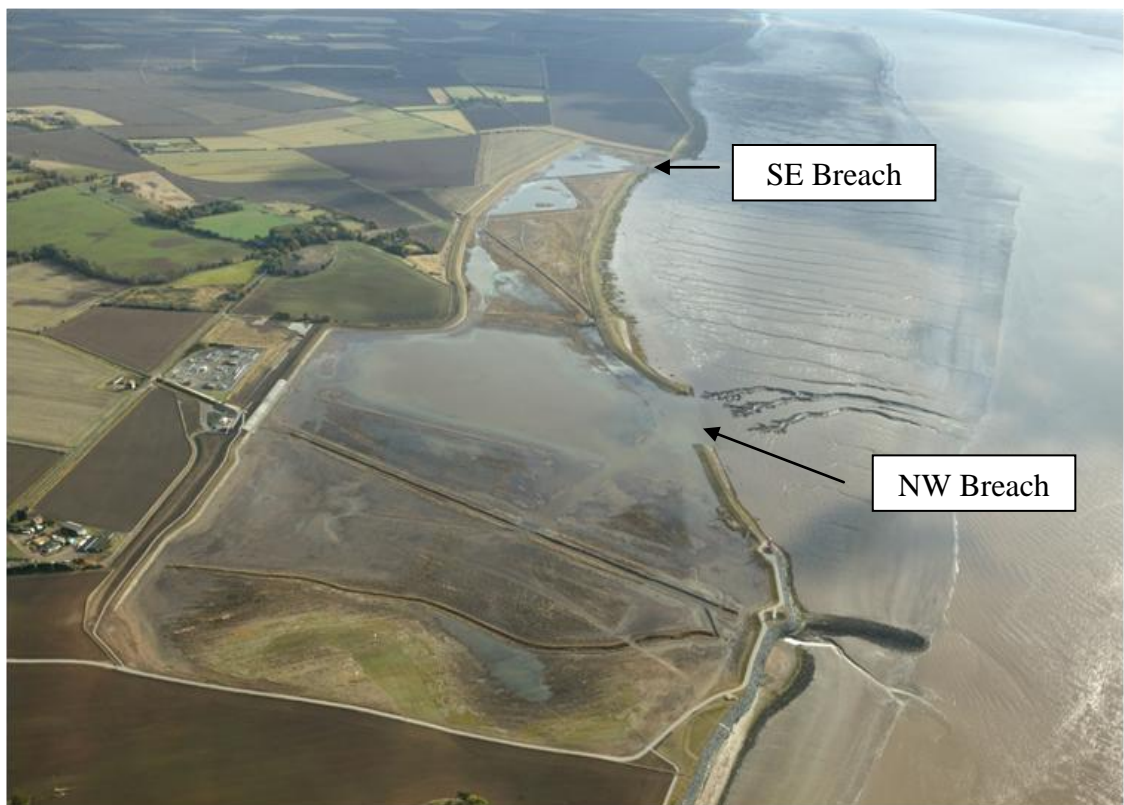
Figure 2.14: An aerial photo of PHS with the north-western end of the site at the base of the picture, taken October 2003 (Environment Agency).

2.3.2.1 Bed level changes at PHS since 2003
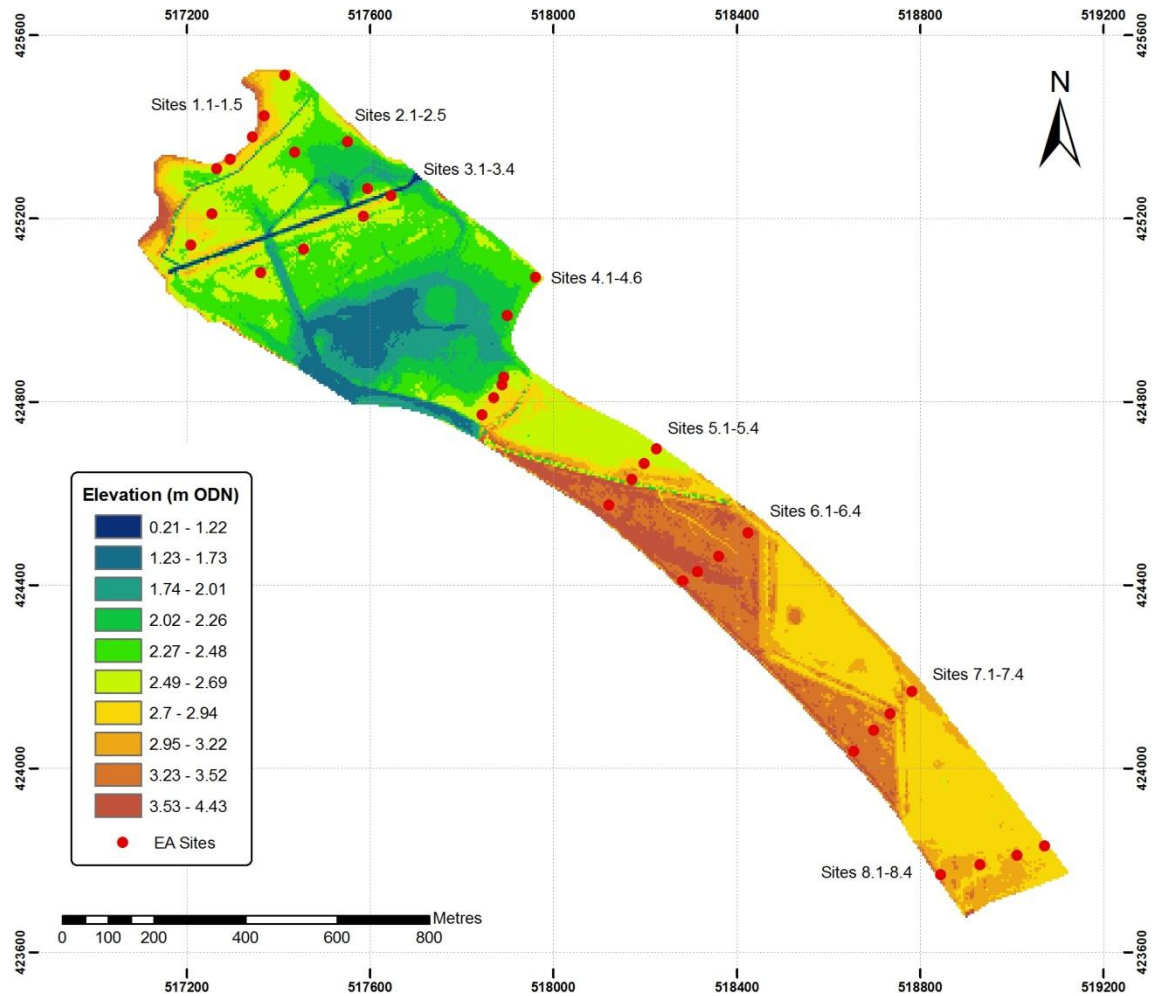
Figure 2.15: Location of Environment Agency monitoring sites.

The northern sector of PHS has experienced a mean total accretion of 285 mm (range 34-544 mm), estimating to the time of breaching (details given in Brown, *et al.* (2008)) i.e. a total vertical change of is 405 mm. In the southern sector the mean total accretion is 45 mm (range 7-134 mm) and using back calculations this rises to 55 mm. The cumulative accretion can be seen for each site in Figure 2.16 (for sampling site locations see Figure 2.15 above).
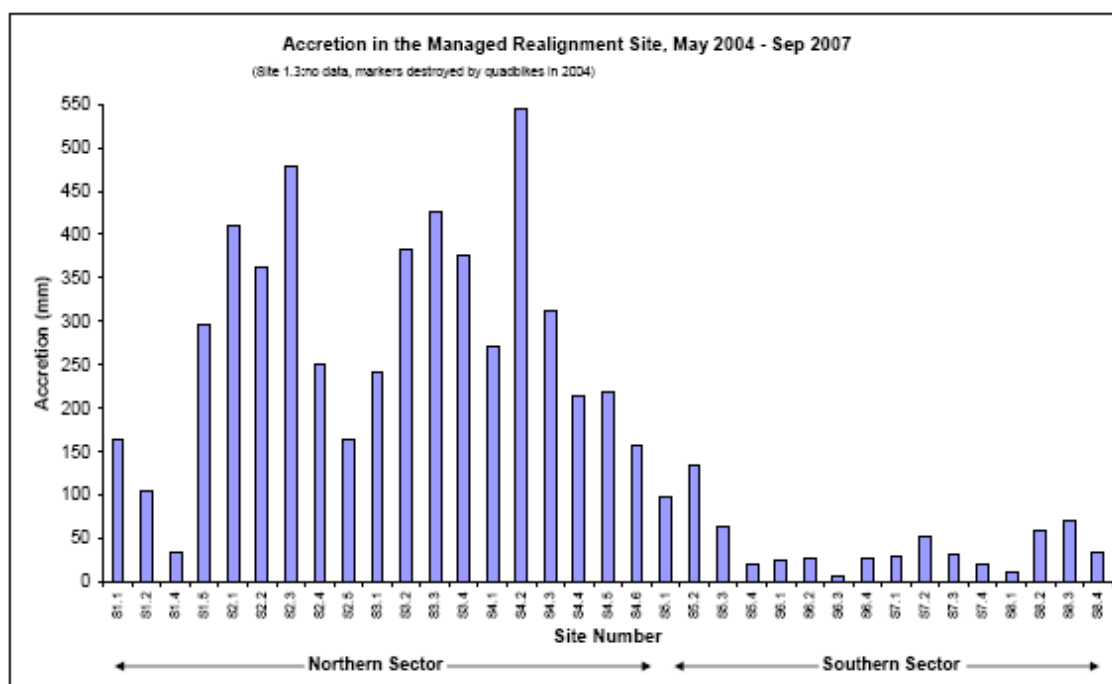
Figure 2.16: Total accretion over PHS from EA monitoring data (**Brown, et al., 2008**)

Accretion measurements have been made by the Centre for Ecology and Hydrology (CEH) outside the realignment site on both saltmarsh and mudflat locations. These sites have experienced continuous accretion over the measurement period, however both have experienced a lower rate than the equivalent areas inside PHS, marshes: 40 mm compared to 82 mm inside PHS, mudflats: 87 mm, compared with 354 mm in PHS.

2.3.2.2 Vegetation changes at PHS since 2004

This section discusses the measurements of vegetation cover taken on behalf of the EA by the CEH during a monitoring period of three years from 2004 until 2007. Measurement of vegetation was not taken during the present research as the EA results provide a large spatial coverage of the site, are very comprehensive in their detail including percentage cover data, species numbers and links to the elevation of the site, and the monitoring period coincided with the present research.

The percentage vegetation cover has been monitored yearly by the EA since 2004 (see Figure 2.17). In the NW sector more than half the sampling site quadrats (12 out of 20) contained less than 1% vegetation cover during the full monitoring period (for locations see Figure 2.15). By 2007, however, only seven of the sites remained with no vegetation cover. The most coverage was at site 1.4, increasing from 56 to 115% (percentages over 100 are because the amount for each plant species was estimated separately then summed to give the total percentage cover). Site 1.3 had the second most cover (75%)

45

for 2004 before the canes marking the site were vandalised. Sites 1.1, 1.2 and 4.1 all had coverage from 2006 and site 4.4 had coverage from 2005. The sites with less coverage during 2007 were 1.5, 2.1, 2.5, 3.4, 4.3, 4.5 and 4.6.

Across the SE sector vegetation cover was more complete. This sector had remnants of the field vegetation during the first years post-breach, most of this has now gone and been colonised by saltmarsh species. Sites 5.1, 5.2 and 8.2 were the only ones without vegetation cover during 2004, sites 5.2 and 8.2 also had no vegetation cover during 2005. At half of the sites vegetation cover increased year on year, the other half of the sites the vegetation cover decreased from 2006 to 2007. The highest vegetation cover of 120% was recorded at site 8.1.
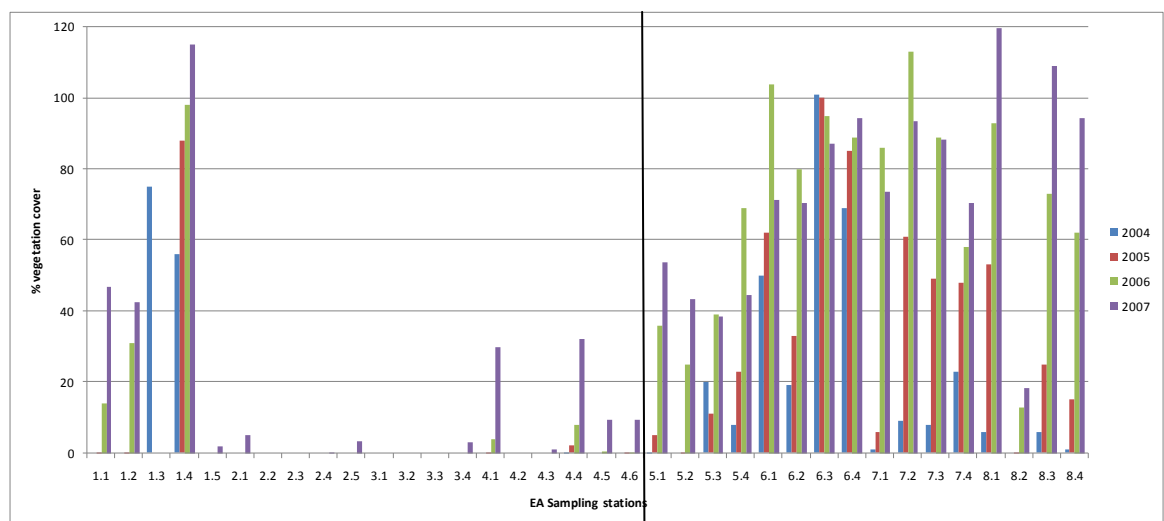
Figure 2.17: Total vegetation cover in the $25m^2$ quadrats from 2004 to 2007 from the EA monitoring data on PHS. Station 1.3 was abandoned after 2004. Black line represents the break between the NW and SE sectors of the site.

Across the NW sector, the pattern of total number of vegetation species was similar to total vegetation cover (see Figure 2.18). At seven sites, only one plant species was recorded during the four years of monitoring and at a further three sites only two species were recorded. The highest number of species recorded was at site 1.4 ranging from 4 to 14 plants over the full period, this was the highest number of species recorded on the whole site. Sites 4.5 and 4.6 registered four species by 2007 and sites 1.1 and 1.2 registered eight and seven species, respectively.

The SE sector had higher numbers of vegetation species present at all sites than on the NW sector. All sites apart from 7.1 had at least two plant species present. Even though vegetation cover dropped at half the sites between 2006 and 2007, at only two sites (8.3

and 8.4) did the amount of species also drop. This indicates that in the SE sector, the vegetation was becoming more diverse as the site aged.
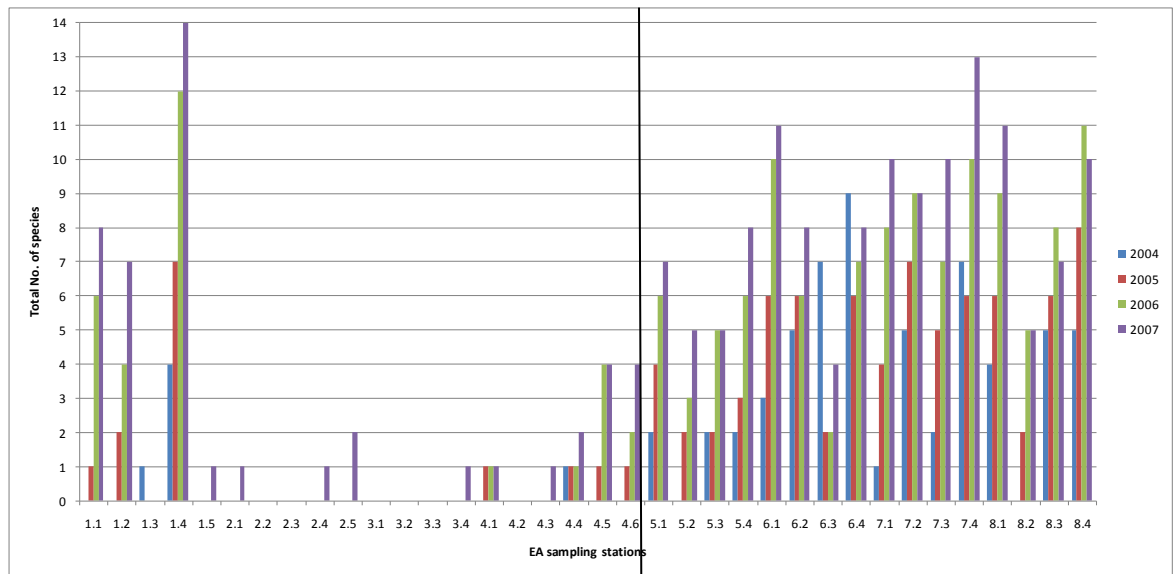
Figure 2.18: Total number of species in the 25m^2 quadrats from 2004 to 2007 from the EA monitoring data on PHS. Station 1.3 was abandoned after 2004. Black line represents the break between the NW and SE sectors of the site.

Vegetation species

For the first two years of monitoring post-breach only two sites on the NW sector had any vegetation present. At site 1.3 (which was subsequently vandalised) coverage of *Atriplex portulacoides* was recorded during the first year as at site 1.4. *Atriplex maritima* was then recorded at the latter site during the second year of monitoring. Both these species are associated with a lower marsh community, the location of the sites was very close to the transitional vegetation zone to the north of the site and an area of low inundation.

Five sites on the NW sector recorded saltmarsh species by 2006. As well as *A. Prostrata* present at sites 1.1, 1.2 and 1.4, *Spartina anglica* (1.1, 1.2, 4.1, 4.4), *Elytrigia atherica* (1.4) and *Spergularia marina* (1.4) had established on the mudflat. *S. anglica* is typical of pioneer saltmarsh communities in this part of England, and indicates the beginnings of a community becoming established. From personal experience of the site, the vegetation cover on the NW sector has spread from just a few clumps of *S. anglica* along the edges of the new flood embankment, (especially to the north and in the corners), towards the middle of the site (see Figure 2.19, below). This was particularly noticeable during the summer months of 2007 when the longer periods of warmer

weather led to a larger proportion of the NW sector than ever before being covered with vegetation.

Figure 2.19: Clumps of Spartina across the NW sector, looking from the old embankment towards the northern corner of the site, taken on 12/09/2006.

By 2007 another three sites on the NW sector were colonised with saltmarsh species. In addition to the species already mentioned above, *Aster tripolium* (1.1, 1.2, 1.4), *Puccinellia spp.* (1.1, 1.4), *Suaeda maritima* (1.2), *Parapholis strigosa* (1.4) and *Salicornia europaea* (4.6) were recorded. Most of these species are representative of a pioneer or lower marsh community, indicating the start of saltmarsh colonisation across the NW sector.

Across the SE sector, all the monitoring sites had some established vegetation by 2006. Sites without vegetation during the first two years post-breach (5.1, 5.2, 8.2) were located near to drainage channels where the presence of water makes colonisation by vegetation harder. Over this sector, terrestrial species were present originally as relics from the arable crops farmed on the land prior to breaching. By the time of the last survey in 2007, only a very small section contained these species as saltmarsh plants had colonised the bulk of the SE sector.

During 2006 and 2007 the majority of the SE sector was covered with *A. tripolium,* a lower marsh species. A number of sites contain species associated with mid and high marsh communities including *Plantago maritima*, *Elytrigia atherica* and *Festuca rubra*.

A full list of plant species by site can be found in Appendix 1.

Vegetation cover by elevation range

Elevation is a key indicator of the types of saltmarsh communities that can be sustained on a mudflat. Table 2.6 below, shows the increasing mean percentage cover of vegetation as elevation increases on the whole site. It should be noted that the elevation range is from the start of the monitoring programme in 2004 and so many sites in fast accreting areas may have moved out of these ranges by 2007, however the ranges are still applied so that a comparison can be made between the same sites.

Table 2.6: Mean percentage cover and range from $25m^2$ quadrats for different elevation ranges across the whole of PHS (modified from CEH 2008)

Elevation range (m ODN)	Sites	Mean				Range			
		2004	2005	2006	2007	2004	2005	2006	2007
2.0 – 2.3	6	0.00	0.00	0.00	0.83	0	0	0	0-5
> 2.3 – 2.6	10	0.01	0.13	1.26	9.07	0-0.1	0-1	0-8	0-32.2
> 2.6 – 3.0	11	3.84	14.65	44.09	57.27	0-20	0-55	13-78	18-97
> 3.0 – 3.5	8	40.88	55.00	74.38	67.5	8-98	20-95	55-95	30-85

Of the six sites in the lowest elevation range (2.0 to 2.3 m ODN), only during 2007 was there any vegetation cover (mean 0.83%). The ten sites in the second lowest elevation range (greater than 2.3 to 2.6 m ODN) have very low (0.01%) vegetation cover from the start of monitoring that gradually increases each year to just under 10% coverage by 2007. The eleven sites in the second highest elevation range (greater than 2.6 to 3.0 m ODN) had vegetation cover from 3.84% during 2004 to 57.27% during 2007. The eight sites in the highest elevation range (greater than 3.0 to 3.5 m ODN) had considerably higher vegetation cover during 2004 (40.88%), some of this due to remnant pre-breach vegetation, however discounting this, the percentage cover would still be greater than that found at the lower elevation ranges. The cover thereafter stays relatively constant, increasing to a high of 74.38% during 2006 and then dropping again to 67.5% by 2007.

In summary, the vegetation cover over the whole of PHS has increased since breaching. Over the SE sector, almost full saltmarsh coverage has been attained apart from directly behind the SE breach and near to the drainage channel separating the two sectors. This coverage has increased year on year, as has the number of species sustained on the

sector. On the NW sector, coverage by saltmarsh species has also increased year on year since the site was breached. Clumps of *Spartina* have spread from the corners and behind the embankments towards the centre of the sector. Most species recorded on the site are pioneer or lower marsh species, as expected in a newly created saltmarsh habitat, however some sites in the SE sector have recorded mid to high marsh species indicating that the marsh is becoming more established.

2.3.3 Reasons for studying PHS

The fast rates of accretion found on PHS during the monitoring by the EA have led to the current research. The site was modelled prior to breaching to predict the accretion rates and final elevation of the site. The fast rates of accretion in the north-west are an order of magnitude higher than predicted. The intertidal habitat at PHS is now expected to be dominated by saltmarsh with only some smaller areas retained as mudflat. This may impact on the use of the site by waterfowl and also on the ability of the site to store flood water and increase the accommodation space of the estuary thus reducing the flood risk in other areas of the Humber estuary.

The growing importance of managed realignment sites to create habitat and store floodwater within the Humber estuary and other UK estuaries means that the reasons for the failure of the model to predict the accretion rates on PHS must be identified. Accurate predictions of accretion rates and the type of habitat being created by managed realignment depend on studies such as this one at PHS.

2.3.3.1 Ability of site to answer research aims

The main aim of the present research is to identify the reasons for the rapid sediment accretion on a managed realignment site on the Humber estuary. The site at PHS has experienced fast rates of accretion ever since breaching in 2003. The secondary aims are to explain the relationship between sediment entering and leaving a managed realignment site and the accretion rates. Flood banks at PHS have been breached in two places, at the NW end and the SE end. The longer of the two breaches at the NW of the site appears to provide (from previous monitoring results) the bulk of the sediment flux into the site. This gives a good opportunity to monitor the sediment flux of the site at this location and produce a sediment budget for a managed realignment site and to provide valuable comparisons to other planned and current managed realignment sites. The sediments on PHS are all cohesive and the behaviour of such materials is poorly

understood especially when looking at a newly formed intertidal area (e.g. Andersen, *et al.*, 2005; Black, *et al.*, 2002; Chang, *et al.*, 2001; Defew, *et al.*, 2002; Garbutt, *et al.*, 2006). This site thus gives an opportunity to study these sediments under fairly controlled conditions. The formation of habitat on a new intertidal area is reliant on the accretion of sediment and the elevation of the site, again PHS is a prime example of changing accretion rates and elevations providing a study of the effects of these on habitat creation.

To facilitate this study and answer the research aims and objectives set in section 1.2, a monitoring programme of both field and laboratory work needed to be undertaken. This programme is outlined in the following chapter.

Chapter 3 : Methodology

3.1 Sampling Strategy

To answer the aims and objectives set out in section 1.2, a field sampling strategy that provides data on accretion rates, sediment properties and the hydrodynamics and sediment transport into the site was required. The method for measuring sediment accretion/erosion is outlined in section 3.2.1, the collection of soil samples and the analysis of soil properties is outlined in sections 3.2.3 and 3.3, and the methods to measure the hydrodynamics and sediment transport is set out in sections 3.2.4 to 3.2.8.

Field sampling surveys on PHS took place over a period of 19 months from February 2006 until September 2007. The main survey of sediment accretion/erosion took place once a month throughout this time. This covers a period when the EA monitoring programme was taking place and allows direct comparison between the two data sets. Two surveys of sediment characteristics were undertaken in the summer of 2006 and the winter of 2006/2007 to give a spatial and temporal understanding of sediment properties. A number of hydrodynamic surveys took place throughout this period to cover a full range of tidal conditions experienced at the site. During the summer of 2007 cores for use in the flume experiments were also collected from the site.

3.2 Sampling Methods

3.2.1 Sediment Accretion/Erosion

The most important variable for this study is the sediment accretion/erosion on the site. The controls on the accretion rate are studied in later chapters. To measure accretion/erosion researchers have used a variety of different techniques that measure both discontinuous and continuous change over different spatial and temporal scales (Thomas, *et al*., 2004) (see Table 3.1 below for discussion of different methods).

Table 3.1: Methods used for measuring sediment accretion and erosion on an intertidal area.

Method	Description of method	Advantages	Disadvantages
Marker horizon/ metal plate (Cahoon, *et al.*, 1989)	Layer of feldspar, clay, brick dust, sand or sediment with rare element spread over area of sediment. Cores taken at intervals to measure amount of sediment accumulation above layer. Metal plates can be buried and then sediment accumulated on top measured. Resolution of $\pm$ 1mm.	- Inexpensive - Simple - Measurements can be made over large area - Provides wide scope for comparison and repeat measurements - Cores can be collected on different temporal scales	- Marker may sink through sediment if denser - Large quantity needed for easy identification of layer - May affect hydrology and life forms - Disturbance by biofilms - Smearing while coring - Marker may be washed away - Only measures accretion of sediment
Anchored tile (Pasternack, *et al.*, 1998)/ filter paper method (Reed, 1989)	Rod sunk into sediment and topped with a detachable tile flush with the surface. Material on top of tile at low tide collected at intervals, dried and weighed. An alternative is the placing of pre-weighed filter papers that are then collected, dried and weighed. Potential resolution of 0.001-0.002 μm depending on sediment collection and processing.	- High vertical resolution - Inexpensive - Multiple measurements can be obtained	- High potential for disturbance of surrounding environment - Limited collection interval - Filter papers may be washed away - Only measures accretion of sediment
Stakes/ graduated pegs	Stakes sunk into the sediment that are either graduated and the changing level of the sediment can be recorded, or are placed in pairs and the distance to the sediment from a mid-point can be recorded. Resolution of $\pm$ 1 mm	- Inexpensive - Simple - Robust - Measurements can be made over large area - Measures accretion and erosion	- Restricted potential for time variability analysis - Disturbance caused around base of peg/ stake can affect measurement
Sediment erosion table (SET) (Boumans, *et al.*, 1993)	The table is placed into a pre-installed pipe that is permanently cemented into the sediment. Pins from the SET are lowered from the table to the ground surface. The length of each pin above the SET is directly related to the distance between the table and the	- Relatively low-cost (not in comparison to stakes) - Large sample size of 36-75 measurements - Measures accretion and erosion	- Complicated set-up and measurement procedure - High accuracy of set-up required - Number of site measurements limited

	ground. Resolution of ± 1.4 to ± 2 mm		• Subsidence of seat pipes • Requires permanent structure • Interference with sediment
Short-term radionuclides (Alvisi, *et al.*, 2001)	Sediment cores sampled then analysed for presence of short-term radionuclides to quantify the amount of time the sediment has been present on the bed.	• Temporal resolution of days possible, usually resolved for months	• Limited by restricted abundance of natural radionuclides • Constraints on the release of artificial nuclides • Expensive due to cost of processing samples
Sedimeter (developed by Erlingsson (Erlingsson, 1991))	Array of sideways pointing infrared transmitters and optical backscatter sensors (OBS) in transparent rod. Rod sunk into ground, as sediment level changes more or fewer sensors receive signals, this is recorded on a data logger. Resolution of 100 μm achieved in laboratory	• Rapid changes over very small temporal scale detectable • Measures accretion and erosion	• Interference with water flow • Each instrument expensive so to cover large spatial scale very costly
Photo-electronic erosion pin (PEEP) (Mitchell, *et al.*, 2003)	Works in similar way to the sedimeter, uses connected photosensitive cells in a transparent rod. Resolution of approximately 2 mm	• Measures accretion and erosion • Allows comparison of elevation changes with tidal and wind forcings	• Resolution too high for small-scale measurements • Scouring around instrument • Long deployments limited by fouling of sensors • Relatively high cost of instrument so spatial coverage limited by funds

After considering the advantages and disadvantages of each method; during this study vertical stakes were used due to the practical advantages of ease of carrying out measurements, low cost, high spatial coverage and comparability with measurements already undertaken on the site for the EA (also using this method).
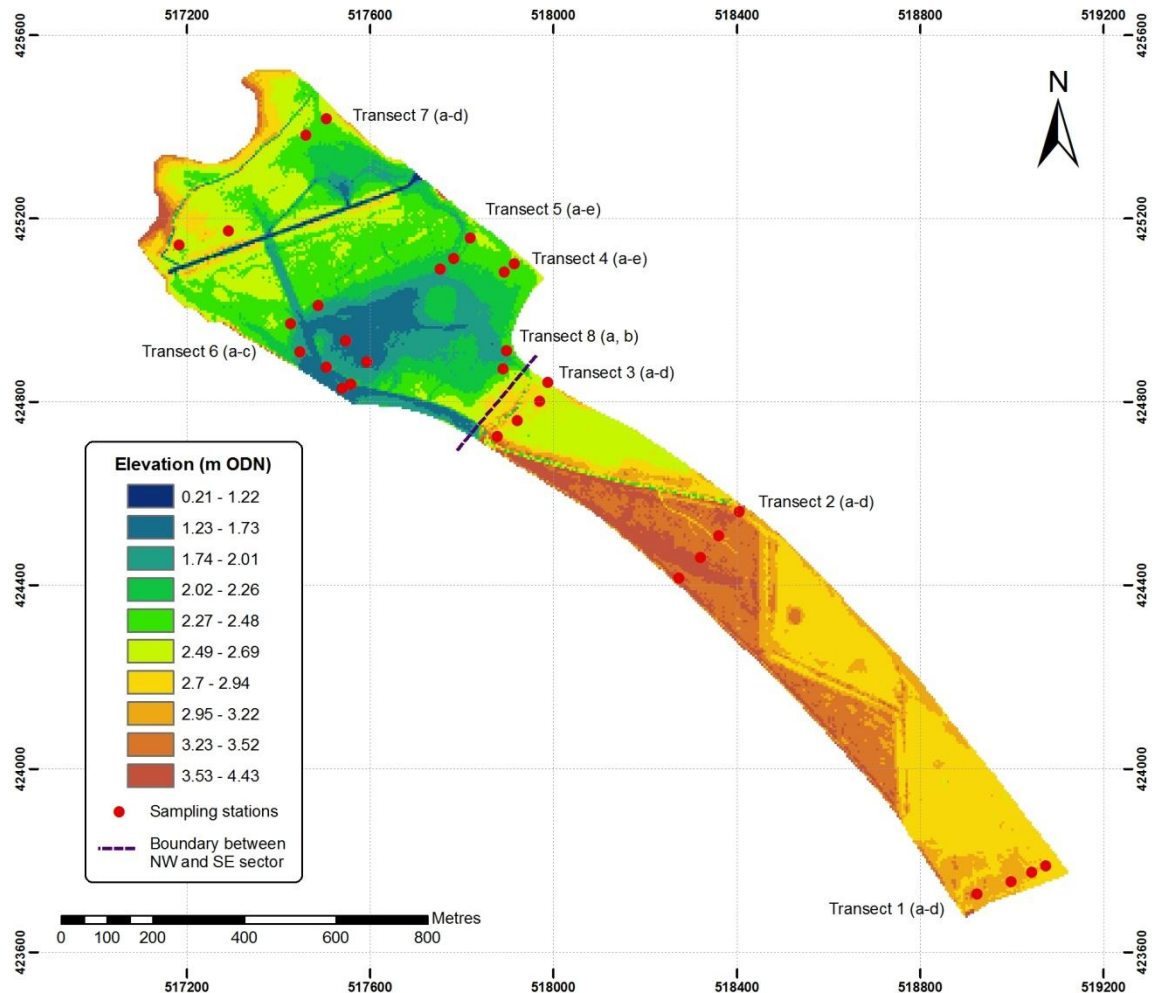
Figure 3.1: Location of accretion/erosion sampling stations across PHS.

Pairs of steel canes were placed across a wide area of PHS (see Figure 3.1 for locations). In the NW of the site, canes were placed around the breach in the first instance, as the EA observations do not cover this area; unfortunately canes could not be located further into the site behind the breach as this area was inaccessible. In the SE sector of the site canes were placed approximately every 100 m along three transects. Transects were used in this sector due to constraints of the site- drainage channels run along old field margins that make certain areas inaccessible as does ponding in some areas of this sector. The tall vegetation particularly along transect 2 meant canes were difficult to find during monitoring, if stakes had been placed randomly this would have made measurement taking difficult.

55

Figure 3.2: Site 1a showing set-up of metal canes.

At each location, five 1.5 m canes were placed one metre apart and hammered in until they were one metre above the sediment surface (see Figure 3.2). A spirit level was used to ensure the canes were at the same height. The accretion/erosion measurement was taken by placing the level on top of the two canes and then measuring down from the midpoint of the level to the sediment surface. Measurements were not taken near to the canes due to expected scour of this area that could provide misleading accretion/erosion measurements. An average from the four cane pairs was calculated at each sampling station. Care was taken not to disturb the area between the canes. The position of each cane was recorded using a differential global positioning system (DGPS, Leica GPS 1200) accurate to 10 mm (horizontal) and 20 mm (vertical) and the elevation of each site was calculated from this data using Leica Geo Office and ArcGIS software (see section 3.2.2.1). Photographs of all cane locations can be found in Appendix 2.

3.2.1.1 Confidence in results

Figure 3.3 below is an example of the mean monthly sediment accretion/erosion recorded at two sites on PHS for the full monitoring period. Site 3d on the SE sector had a slower rate of accretion, site 6b on the NW sector had a quicker rate of accretion. The standard deviations (representing the variation between the four measurements taken at each sampling station) for both sites are small throughout the majority of the monitoring period giving confidence in the pattern of accretion/erosion representing what was happening on the site and not due to measurement error. At some sites (to be discussed in Chapter 3) developing creeks and vandalised sampling sites have affected the

measurements. At all times this has been recorded whilst taking the measurement and highlighted when discussing the results.
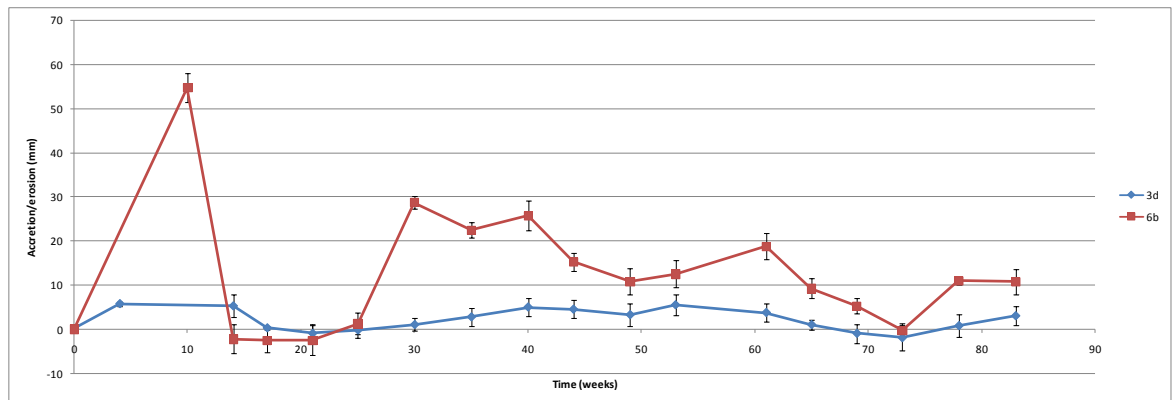
Figure 3.3: Example of monthly accretion/erosion measurements from the SE sector (site 3d) and the NW sector (site 6b). Standard deviations represent the variation between the four measurements taken at each sampling site.

3.2.2 Topography

The topography or relief of the site provides three dimensional data for the whole of PHS. A topographical map of the site was acquired using light detecting and ranging (LIDAR) data (Environment Agency, 2005). The LIDAR data were collected in 2005 and can be used to produce accurate topographical maps that provide the basis to map the inundation levels on the site and to track the formation of drainage channels and creeks. The topographic map produced using the LIDAR data is shown in Figure 3.4 below.
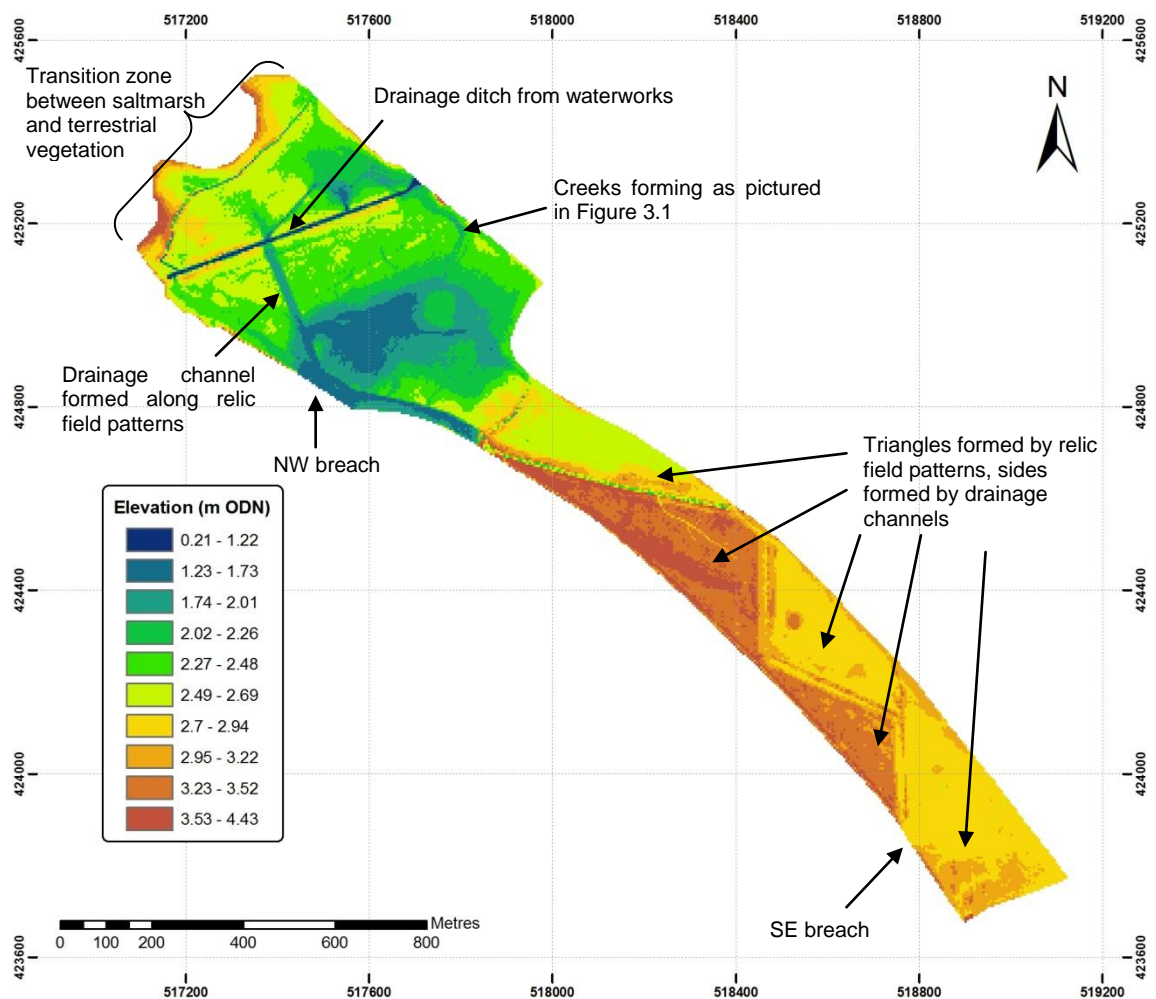
Figure 3.4: Topography of PHS produced using LIDAR data, locations referred to in later chapters are labelled.

Viewing of the LIDAR data was undertaken using the ArcGIS software package (© ESRI). The LIDAR data were provided as rasters that were clipped to the PHS boundary and displayed as five metre grids. The LIDAR data is accurate up to 100 mm (vertical and horizontal) (American Society for Photogrametry and Sensing, 2004).

3.2.2.1 Transforming DGPS data to GIS points

The Leica GPS 1200 system used for the data collection consists of a base station and rover (Leica Geosystems). The base station was set up at a high point on the flood embankment near to the sampling site locations (see Figure 3.5). The base station had to receive signals from a number of satellites for at least three hours to give a measurement precision of at least ±40 mm. The rover is a moveable antennae and data logger that was carried to the sampling locations to record a point.
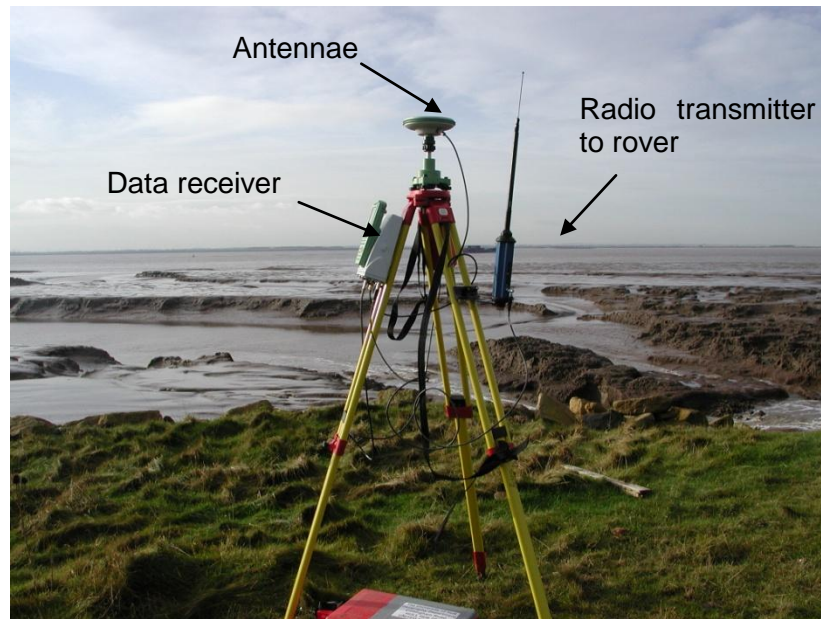
Figure 3.5: The DGPS base station on the old flood embankment next to the NW breach.

To process the DGPS data, firstly the position of the base station needed to be transformed using known DGPS Ordnance Survey points. The point used was for the nearest station of Easington (TA 39500 29600). These data were downloaded from the Ordnance Survey website to cover the same period of measurements as the base station was in place. The base station position was transformed using the more accurate OS point data from Easington using Leica Geo Office software to 'shift' the base station point providing a better accuracy of 10 mm (horizontal) and 20 mm (vertical). The recorded points from the rover of the stake locations and sampling stations were then plotted using the more accurate base station position.

3.2.3 Soil Samples

Soil samples were collected for various laboratory experiments (see section 3.3). The soil was initially collected from the 31 locations (see Figure 3.1) at the south-eastern end of each set of accretion stakes and analysed for moisture content, organic content and particle size.
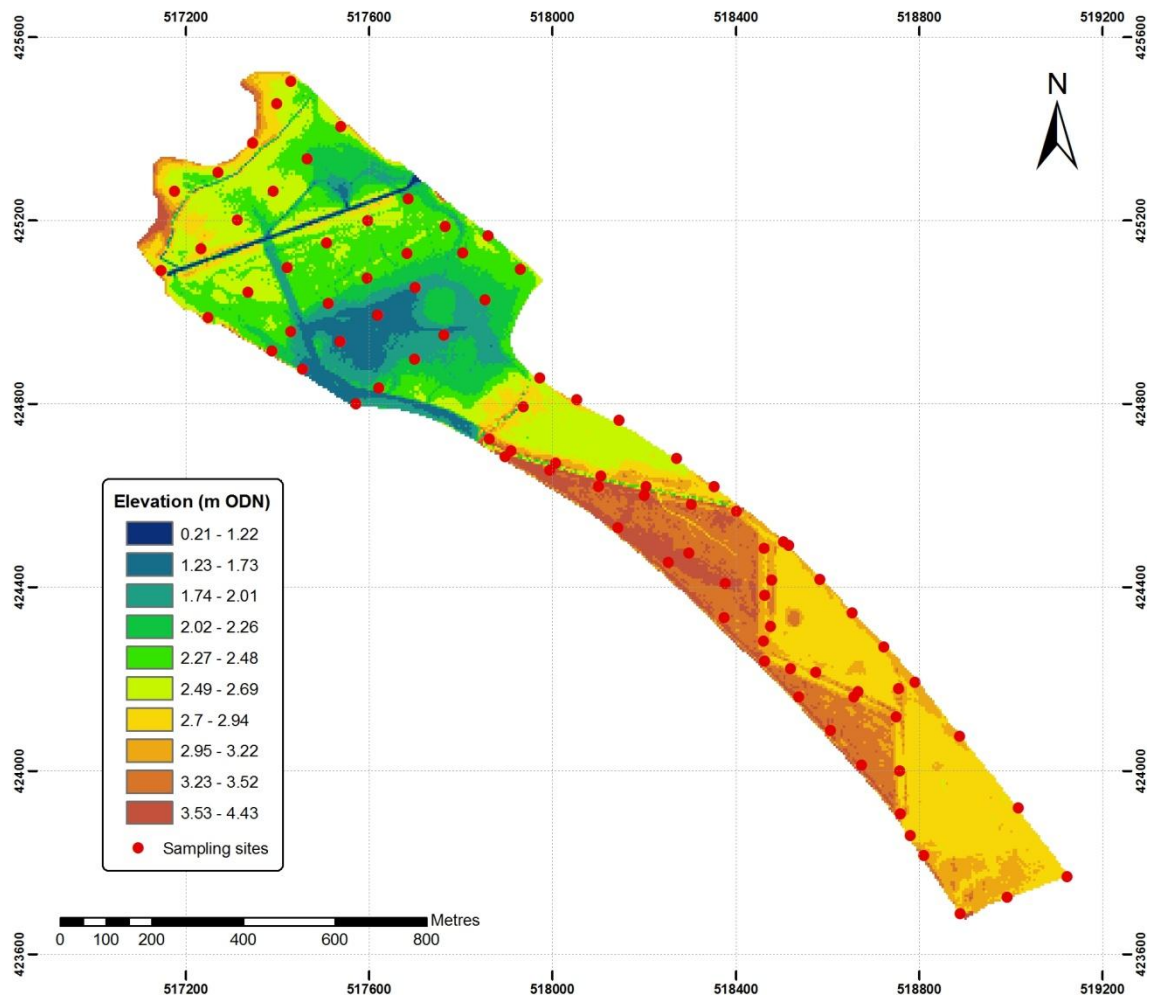
Figure 3.6: Bulk density sampling locations on PHS.

Further soil samples were collected during July 2006 and February 2007. Figure 3.6 shows the location of the sampling sites as recorded using a Leica DGPS. In the NW of the site 35 samples were collected along six transects approximately 100 m apart (avoiding the drainage ditch and gas pipeline). Along each transect a sample was taken every 100 m. Transects were used to give the greatest spatial coverage of the sector and so that the survey could be easily repeated using similar sampling positions. In the SE of the site, samples were taken following the path of the remnant drainage ditches that have resulted in this area being divided into a number of triangles (see Figure 3.3). The sediment in the central area of the three triangles closest to the new embankment was not sampled as it was too waterlogged to be accessible. Samples once again were collected at a spacing of 100 m, with 50 samples collected from this part of the site. Ten samples were collected on the mudflat outside of the NW breach at a spacing of 100 m. The samples were collected using a 610 x 610 x 520 mm piece of tubing that was pushed into the sediment surface, sealed and then stored in a cool box before

transporting back to a cold store. The samples were analysed for their wet bulk density properties within 24 hours of return to the laboratory to minimise sample degradation.

3.2.4 Equipment Set-up to measure hydrodynamics

The SonTek acoustic Doppler profiler (ADP, for operating principles see Section 3.2.6) used to measure flow velocity was mounted on a boat (see Figure 3.8) and then tethered to a scaffold pole located at a distance of approximately 20 m from the top of the eastern flood embankment at the NW breach (see Figure 3.7). The boat was tethered in place before the tide had reached the site and remained *in situ* throughout the tidal cycle.
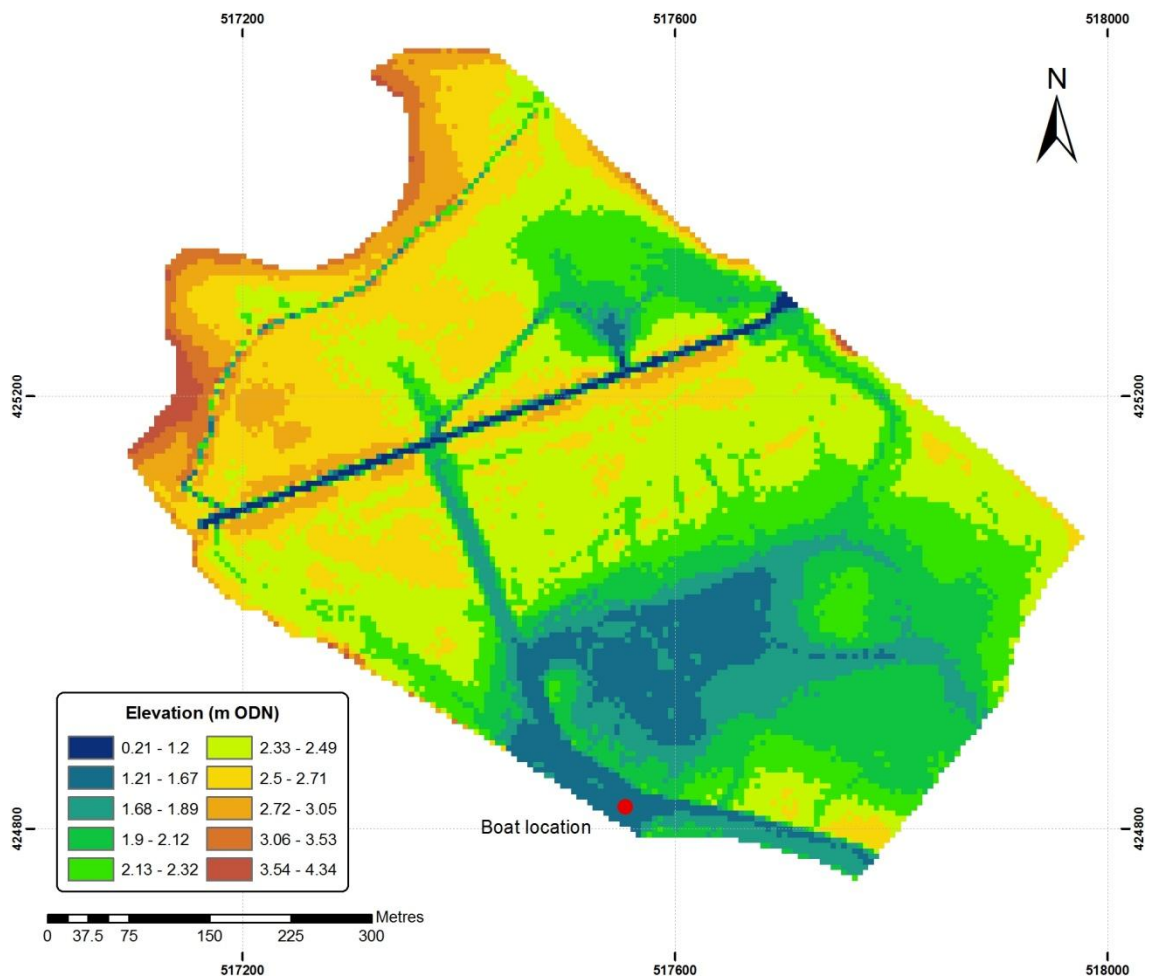
Figure 3.7: Location of boat during hydrodynamic modelling on PHS.

By using a second rope accessible from the flood embankment, the boat was moveable during deployment. The boat was designed to hold the ADP head and to minimise interference with the measurements. Some problems occurred during deployment of the equipment relating to the wind forcing the boat towards the embankment and waves moving the boat up and down. This can interfere with the readings from the equipment,

however the blanking distance (discussed fully in section 3.2.6.1) put in place removed the majority of the interference.

Figure 3.8: Boat on which the SonTek ADP was mounted.

3.2.5 Suspended Particulate Matter (SPM)

The different methods used to measure SPM are described and the advantages and disadvantages discussed in Table 3.2 below.

Table 3.2: Methods for measuring SPM, advantages and disadvantages given (adapted from Wren, *et al.*, 2000).

Method	Description of method	Advantages	Disadvantages
Gulp/ bottle samples	Water sample is taken by submerging bottle in water and then analysed for SPM and particle size later.	• Accepted, time-tested technique • Determines grain size and concentration • Inexpensive • Simple	• Poor temporal resolution • Intrusive • Requires lab analysis
Acoustic backscatter (ABS)	Sound pulses backscattered by sediment are measured to determine concentration and grain size.	• Good spatial and temporal resolution • Measures full vertical range • Non-intrusive	• Backscattered signal hard to translate/calibrate • Hard to calculate clay particles from data • Requires knowledge of technique • Expensive
Pump sampling	A water sample is pumped from the flow using a submerged line and taken to be analysed later.	• Accepted, time-tested technique • Determines grain size and concentration • Inexpensive • Simple	• Poor temporal resolution • Intrusive • Requires lab analysis • Does not sample isokinetically
Focused beam reflectance	A laser beam is focused on a small spot and rotated rapidly. The particles encountered by the beam reflect it and this can be used to calculate particle size.	• Not dependent on particle size • Wide range of size and concentration measured • Easily portable	• Point measurement only • Intrusive • Expensive
Laser diffraction	Particles in the laser beam scatter light at angles inversely proportional to their size. Concentration can be based on the measured particle sizes.	• Not dependent on particle size	• Point measurement only • Unreliable • Intrusive • Expensive • Limited particle size range
Nuclear backscatter	The backscatter of gamma or x-rays through a water sediment sample is measured. Three different types of gauge available.	• Low power consumption • Wide range of size and concentration measured	• Low sensitivity • Radioactive source decay • Regulations on use, licensing and training required

63

			• Intrusive • Point measurement only
Optical backscatter (OBS)	Similar to above, using infrared light.	• Simple • Good temporal resolution • Can be deployed remotely and logged • Relatively inexpensive compared to laser instruments	• Strongly particle size dependent • Intrusive • Point measurement only • Fouling of instrument
Remote spectral reflectance	The light reflected and scattered from a water body is measured remotely using a handheld, airborne or satellite based spectrometer.	• Can measure broad areas • Non-intrusive	• Poor resolution • Poor applicability in fluvial environment • Particle size dependent

Gulp sampling of the SPM at the NW breach was favoured over other methods as it is economic and quick to carry out and process the results. Several surveys measured both sediment flux and hydrodynamics at the NW breach, see Table 3.3 below.

Table 3.3: Hydrodynamic and SPM data recorded during high tide on different dates at PHS.

Date	Gulp Samples	ADP	Water Quality
08/12/2005	Yes	Yes	No
23/05/2006	Yes	No	Yes
19/07/2006	Yes	Yes	Yes
16/08/2006	Yes	Yes	Yes
11/09/2006	Yes	Yes	Yes
11/05/2007	Yes	No	No
14/09/2007	Yes	Yes	No
17/10/2007	No	Yes	No
31/10/2007	No	Yes	No

3.2.5.1 Gulp samples from NW breach

An initial survey to determine the optimum bottle volume was carried out in December 2005 using the large two litre bottles and ten smaller 500 ml bottles, results are shown in Table 3.2 below. Both methods yielded similar results, only the samples taken at 11:20 were more than 6% different and three out of the five samples were 5% different or less (see Table 3.4). The decision to use the larger bottles was based on the ease of transporting ten of this size instead of 100 of the smaller bottles.

Table 3.4: Results from comparison survey between 500 ml and 2 l bottles to be used for gulp sampling.

Time (GMT)	Mean SPM of 500 ml bottles (mgl^{-1})	Mean SPM of 2 l bottles (mgl^{-1})	Percentage difference
09:50	154.3	164.9	6
10:20	296.1	288.2	3
10:50	322.3	338.5	5
11:20	223.3	201.6	10
12:55	152.7	154.6	1

During a high tide at the NW breach a two litre bottle was filled once every half hour. The bottles were filled by immersing them below the water surface, as far into the water as possible. This equates to nine or ten water samples, as water was present at the breach for four or five hours of the tidal cycle depending on the depth of water (see Table 3.3 for collection dates). These were then filtered and weighed in the laboratory to calculate the SPM (see section 3.3.5 for full procedure).

3.2.6 Hydrodynamics

Hydrodynamic properties were measured at the NW breach to get a complete picture of the volume of sediment ingressing and egressing during various tides. This was used to provide a sediment budget for a year, and compared with the accretion data to ascertain if the net volume of sediment deposited on the site equates to the volume accreting. Different instruments that are used to measure flow velocity and the advantages and disadvantages of each method are discussed in Table 3.5 below.

Table 3.5: Methods to measure flow velocity.

Method	Description of method	Advantages	Disadvantages
ADP (includes pulse coherent and normal mode) (Betteridge, *et al.*, 2003)	Measures water velocity using the Doppler shift principle.	• Measures full velocity profile • Non-intrusive • Can measure sediment transport as well as velocity • Robust • Designed for estuarine and riverine deployment • High frequency results obtainable in pulse coherent mode	• Expensive • Cannot be deployed for small-scale flume measurements • Cannot measure near-bed velocities • Set-up requires in-depth understanding of instrument
Acoustic Doppler velocimeter (ADV) (MacVicar, *et al.*, 2007)	Measures water velocity using the Doppler shift principle.	• Non-intrusive • Useful for small-scale flume measurements • Measures near-bed velocities • Simple to use	• Only records point data • Relatively expensive compared to current meter
Current meter (impeller or electromagnetic) (MacVicar, *et al.*, 2007)	The impeller measures the speed of rotation of a helix in water. The electromagnetic current meter uses the Faraday principle (water moving in a magnetic field will produce a voltage proportional to the water velocity).	• Inexpensive • Useful for small-scale flume measurements • Measures near-bed velocities • Simple to use	• Only records point data • Can be unreliable

3.2.6.1 SonTek ADP

Current profiles were measured using a SonTek high resolution ADP. The ADP was chosen for this study as it provides a full velocity profile, and could be set-up to run *in situ* for the entire tidal cycle (see Table 3.5). The ADP is specifically designed to use in shallower water applications and measures water velocity using the Doppler shift principle. This principle dictates that if a source of sound is moving relative to the receiver, the frequency of the sound at the receiver is shifted from the transmit frequency. When applied to measuring sound in water the change in frequency is proportional to the velocity of the water. The change in frequency is calculated using the equation 3.1 below:

$$F_{doppler} = -2F_{source}\frac{V}{C}$$

Eq. 3.1

where $F_{doppler}$ = change in received frequency (Doppler shift), F_{source} = frequency of transmitted sound, V = relative velocity of particles and C = speed of sound. The velocity is a measure of the relative speed between the source and scatterers. If the motion is perpendicular to the two of them or stationary, there will be no Doppler shift (Betteridge, et al., 2003).

The ADP uses a monostatic Doppler current meter, with transducers that are transmitters and receivers. The ADP has three transducers each emitting a short sound pulse at a known frequency. The sound pulse is reflected as it travels through the water by micro bubbles and/or sediment and thus some will be received back into the transducer so that the frequency shift can be measured. The location of the particles reflecting the sound pulse is determined by the time elapsed from the pulse transmission. The velocity profile is built up by the ADP measuring the velocity from the returning signal at different times, thus equating to different distances from the transducer.
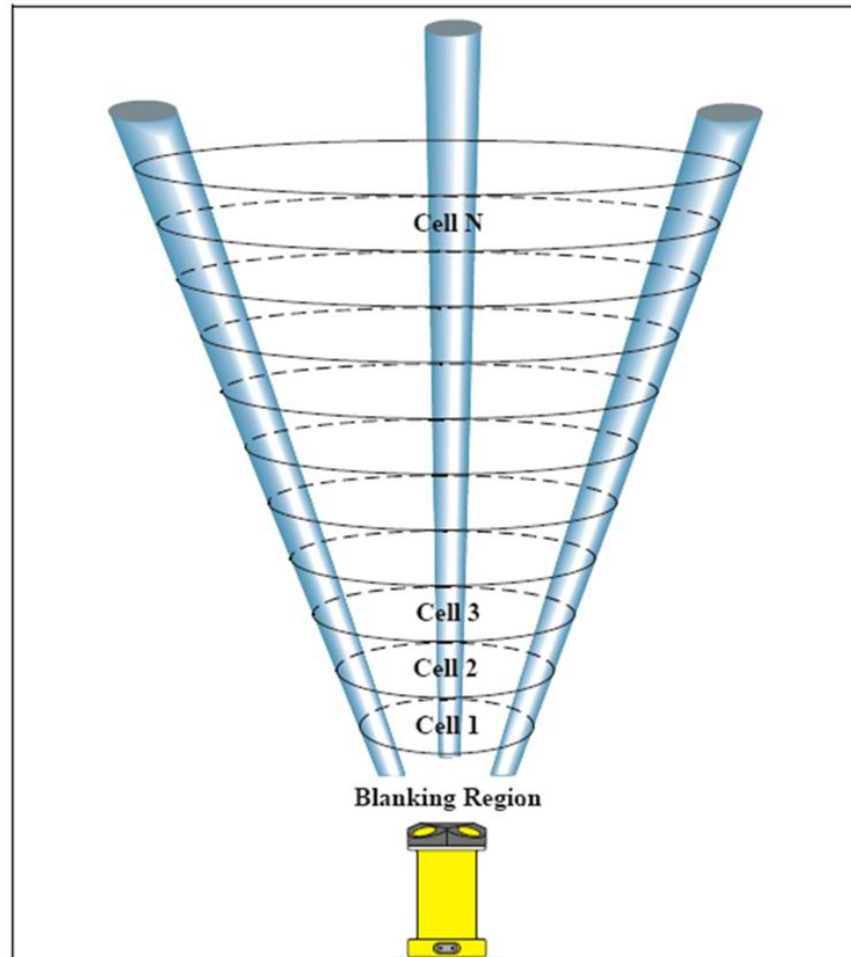
Figure 3.9: The beam geometry of the ADP and current profiling (SonTek, 2000).

The ADP has three transducer beams orientated at 15° off vertical to produce a 3D velocity profile, as can be seen in Figure 3.9. The three beam velocities are geometrically transformed in each range cell to calculate the 3D velocity for each depth layer. This means that the velocity is represented in a Cartesian coordinate system which can be transformed into the East-North-Up (ENU) coordinate system by calibrating the internal compass and tilt sensors.

As Figure 3.9 shows, in front of the measuring cells is a blanking region where measurements are not made. This is so that the transducers can recover electronically from the transmit pulse and get ready to receive the returning signal.

For the requirements of this study, the ADP was used in pulse coherent mode, the ADP is able to give greater precision recording velocity data in very high resolution cells, increasing the resolution from $\pm$ 0.5 cms^{-1} to $\pm$ 0.1 cms^{-1} (SonTek/YSI). The ADP transmits two pulses into the water and the change in phase between the pulse pair is measured by the ADP, not the change in the return signals. Each pulse pair produces a

single velocity value. The time between the two pulses being emitted does limit the maximum velocity that can be detected and also the range of the ADP, however it is this that results in the higher precision data (SonTek, 2000).

Parameters for ADP set-up in pulse coherent mode

Various parameters needed to be defined when using the ADP in pulse coherent mode so that the ADP operated to its best capabilities. Prior to the set-up an understanding of the study environment needed to be known- such as maximum velocity expected and maximum depth of water.

The first trade off is of velocity versus range. The greater the length of time between pulses of a pulse pair, the larger the velocity range the ADP can profile. Increasing the time lag will also increase the distance the particles move from the first pulse to the second. This time lag has to be set correctly to resolve the highest expected velocities. If this is not set correctly and the true velocities are actually greater than the maximum velocity resolvable by the ADP then the recorded velocity profiles will be ambiguous. For the purposes of this study the known velocities at PHS were up to 80cms^{-1} and so the ADP needed to be configured to record this. When defining the time lag both the profiling lag and the resolution profiling lag had to be considered (SonTek, 2004).

Profiling lag

The maximum unambiguous velocity in beam coordinates is:

$$U_a = \pm \frac{C^2 \cos\theta}{8 \, F_0 Z}$$

Eq. 3.2

and the maximum unambiguous velocity in the horizontal is:

$$U_h = \pm \frac{C^2 \cos\theta}{8 \, F_o Z \, \sin\theta}$$

Eq. 3.3

Where C is the speed of sound, θ is the slant angle of the ADP, F_o is the acoustic frequency (1.5 MHz) and Z is the profiling lag. The profiling lag is defined as half the distance the first pulse travels before the second pulse of the pair is transmitted (SonTek, 2004).

70

Ambiguity resolution cell

The profiling range may be increased by the use of the ambiguity resolution cell. This is a second set of pulse pairs that operate separately to the first set to build up a single cell. The lag for this cell is defined by the resolution profiling lag and needs to be less than the profiling lag so that the maximum resolvable velocity within the ambiguity cell will be greater than that within the regular velocity profile. Setting this ambiguity cell allows the software to resolve ambiguity errors. To set all the parameters for the ambiguity cell requires a resolution blanking distance and a resolution cell size (SonTek, 2004).

Rules for setting the ADP lags in pulse coherent mode

The profiling lag or the resolution profiling lag has to be small enough to resolve the maximum velocities and the profiling lag can be no greater than three times the resolution profiling lag. The ambiguity resolution cell needs to be in the region of true peak velocities, in reality this means the resolution blanking distance and cell size must be less than the resolution profiling lag. The velocity profile (blanking distance + (number of cells x cell size)) must be larger than the water depth so that the full velocity profile is resolved and has to be less than the profiling lag (SonTek, 2004).

Calibration of ADP

A Horiba water quality measuring system (W 22XD multiparameter monitoring, Horiba Ltd) was deployed during a high tide survey to measure salinity and temperature. These were measured every half hour synchronous with the gulp samples by placing the probe into the water flow and then logging each parameter on a data logger attached to the probe. These data were used in post-processing the SonTek ADP measurements and for setting up flume experiments (see section 3.4). For example, a temperature change of $5^{o}C$ results in a sound speed change of 1% as does a change in salinity of 12 ppt in the ADP results (SonTek, 2000).

3.2.8 Tidal heights for inundation mapping and tidal fluxes

Actual tide heights at PHS for a given elevation were needed to map inundation levels on PHS and produce estimates of tidal fluxes. To produce the on site tide heights required the DEM (from LIDAR data) and the tide heights provided by Admiralty TotalTide 2006 software (UK Hydrological Office, http://www.ukho.gov.uk/amd/productsServices.asp) for the nearest point of King George Dock, Hull (5 km upstream from PHS).

Tidal height data were collected on 30/03/2007 and 11/05/2007. Wooden stakes were hammered into the site at six different locations- four just behind the northern end of the NW breach and two at the deepest point of the NW breach at the southern end- and graduated ranging poles were attached to these stakes- the base level with the sediment (see Figure 3.10). During the high tide on the site, the water level was read off the poles every five minutes. The exact position of the poles was logged using DGPS.

Figure 3.10: Setup of ranging poles to measure tidal heights at PHS, looking inland from the estuary.

The two poles set up in the deepest part of the NW breach provided the most complete tide cycle and were used to transform the tidal data from King George Dock (KGD). The other four pole locations were used as 'test points' to compare the precision of the transformation.
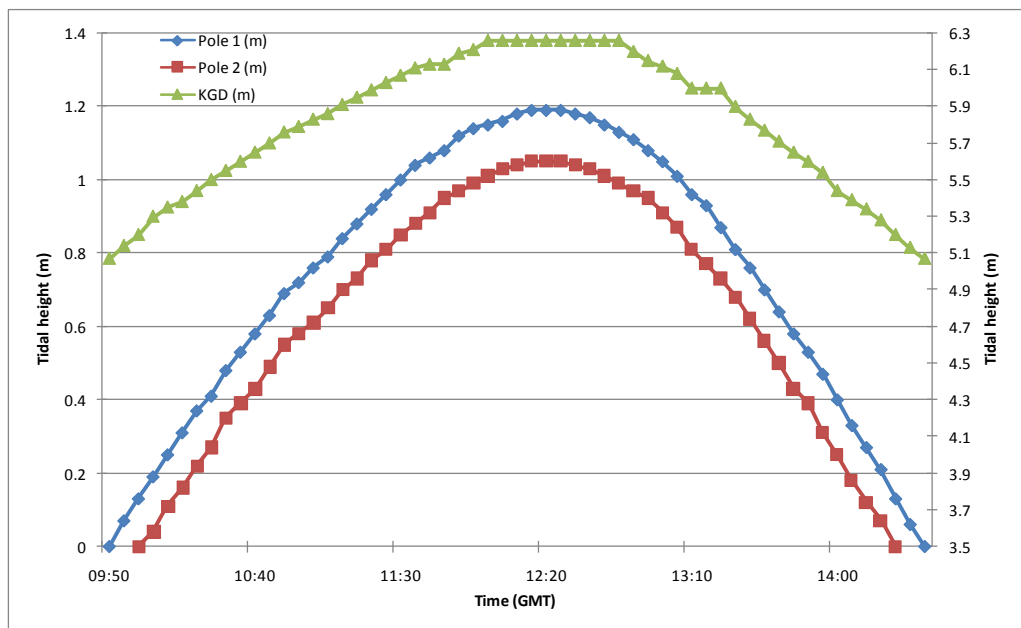
Figure 3.11: Tide heights for two locations at the NW breach compared to the tide height at King George Dock, Hull during the 11/05/2007.

The tide height data from KGD were transformed to account for the elevation on the site and the difference in coordinate systems- tide heights are predicted using chart datum not the Ordnance Datum Newlyn (ODN) used for mapping purposes (see Figure 3.11). There is also a difference of 10 minutes between high tide at the NW breach and high tide for King George Dock as the site is closer to the estuary mouth.

The difference between the two poles is 0.14 m (± 0.008), this value is the difference in elevation between the two locations of 0.15 m (pole 1 elevation: 1.07 m ODN, pole 2 elevation: 1.22 m ODN). The difference between the height at the poles and the tide height for King George Dock is 4.01 m (± 0.01) after subtracting the elevation. This constant can then be applied to a full year of tidal data to give the tide height at the breach. By using the range of elevations found across PHS, the inundation period for every location is known and can be mapped using the DEM of the site on ArcGIS.

Using the test point data from the 30/07/2007 (high tide at KGD 6.5 m), results are shown in Table 3.6 below of the high tide at these locations and the high tide predicted using the constant of 4.01.

Table 3.6: Comparison of test point data collected at PHS on the 30/03/2007 with predicted data using constant of 4.01.

Test point elevation (m)	Test point high tide (m)	Predicted high tide using constant (m)
1.61	0.86	0.88 (2.3% higher)
1.82	0.63	0.67 (6.3% higher)
2.07	0.4	0.44 (5.0% higher)
2.25	0.24	0.24 (0.0% higher)

Using the constant predicts the high tide correctly for one test point and is either 0.02 or 0.04 m higher for the remaining three test points. The highest percentage difference is a modest 6.3%, giving confidence in the use of the constant as a way of predicting the tide height for all elevations across PHS from the KGD tidal data.

3.2.9 Core collection for flume experiments

Cores were collected for the flume based erosion study (see section 3.4) from four sites around PHS (see Figure 3.12 below). The sites were chosen to reflect the different accretion rates recorded at PHS. The first site was in an area with very rapid rates of accretion near to the NW breach, the second and third sites had average rates of accretion (for PHS) but were in contrasting locations on the NW sector and the final site

was on the SE sector with slower rates of accretion. At each site, four 100 mm diameter cores were collected using plastic tubing to a depth of 750 mm. Each corer was pushed into the mudflat (taking care not to disturb the sediment surface), removed and then sealed. Taken alongside each core was a sample using the same tubing as that used for the bulk density samples (see section 3.2.3.2) so that testing for wet and dry bulk density, moisture content and organic content could be carried out on a mud sample similar to that being used in the flume. The cores and samples were transported back to the department and stored in a cold room until used in the flume. Cores were always used within 24 hours of collection.
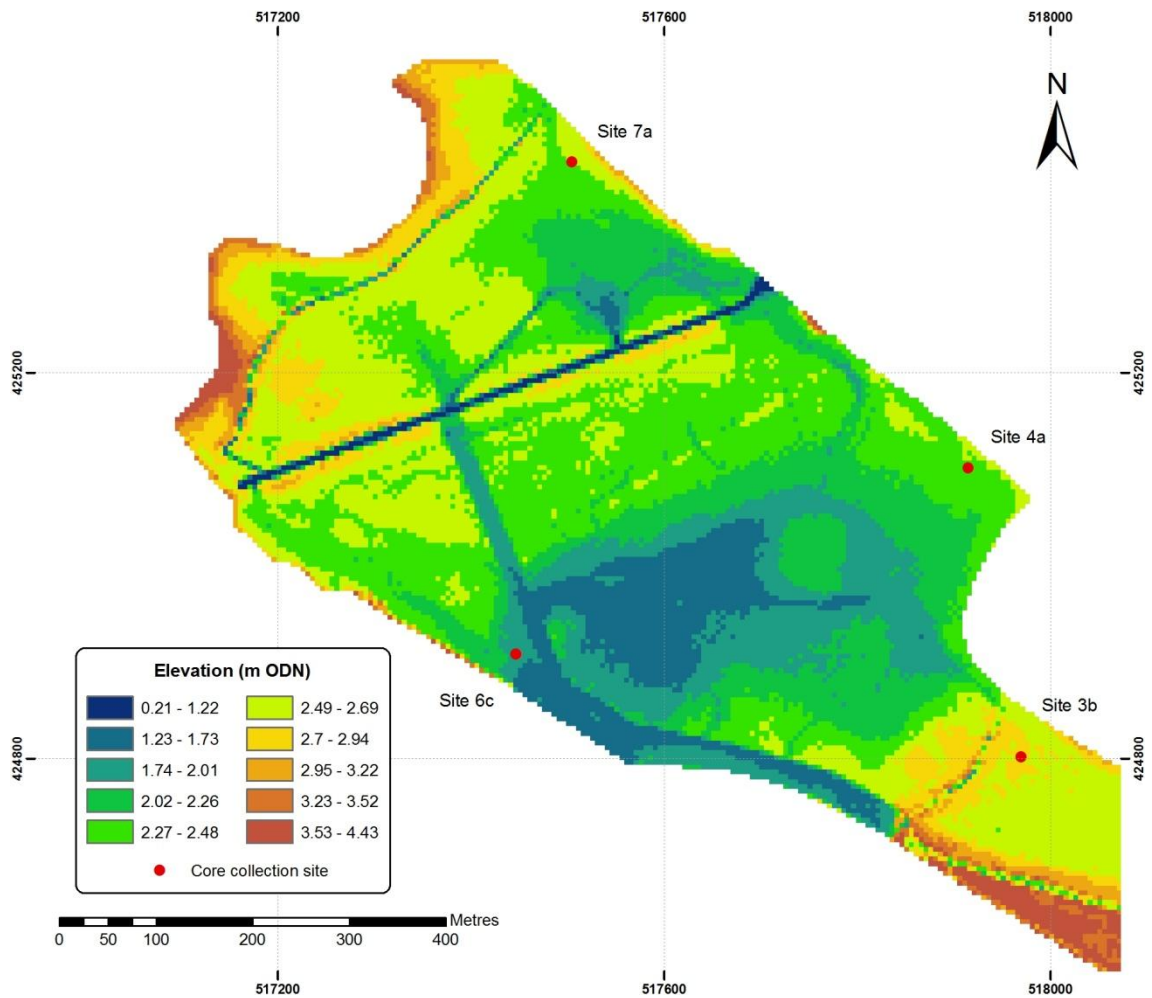
Figure 3.12: Location of core samples for erosion study on PHS.

3.3 Laboratory Methods

3.3.1 Particle Size Analysis

The sediment samples collected from PHS were analysed in the lab to determine particle size. Table 3.7 below gives details of all methods available for measuring particle size. Reasons for deciding on the methods used in this analysis are given in later sections. The analysis of the summer samples was undertaken using the sieving and sedimentation method and laser diffraction/imaging whereas the winter samples were only analysed using laser diffraction/imaging. The results from the sieving and sedimentation method during the summer were only used as a back-up; data presented in Chapter 5 are based on the laser diffraction/imaging results. Collecting from across the site and during different seasons should highlight both temporal and spatial differences in the sediment.

Table 3.7: Different methods of measuring grain size, from (Konert, *et al.*, 1997; Goossens, 2008)

Method	Principle of method	Advantages	Disadvantages
Sieving	Dry sediment is shaken through increasingly smaller meshed sieves.	• Simple • Inexpensive	• Number of grain classes limited by sieve mesh sizes • Unable to measure silt/clay particles so needs to be combined with another method if these particles are present
Laser diffraction	Particles in the laser beam scatter light at angles inversely proportional to their size. A number of companies produce laser diffraction machines including Malvern, Beckman Coulter, Fritsch and Horiba.	• High reproducibility under testing • Quick analysis time • Provides large range of information on particle size • Can measure full spectrum of particle sizes using different lenses	• Expensive • Can overestimate clay content depending on instrument used
Laser imaging	Particles in the laser beam scatter light at angles inversely proportional to their size. The particle image projected by the laser beam is collected by a high speed camera.	• High reproducibility under testing • Quick analysis time • Provides large range of information on particle size and particle shape • As an image gallery is produced, particles that are obviously organic can be removed	• Expensive • Unable to measure very small clay particles due to size of pixels
Sedimentation	Calculates the sediment size from the settling velocity of particles in a fluid. Range of equipment used: pipette, Atterberg cylinder, hydrometer, optical sensing and x-ray sensing.	• Can be inexpensive depending on equipment used (e.g. pipette method) • High reproducibility in some instruments (e.g. Atterberg, Sedigraph)	• Experimental protocol complex and introduces errors (Atterberg, pipette) • Long analysis time • Expensive depending on instrument used • Separate sieve analysis needed for coarser grains > 16 μm if using pipette method • Limited grain size classes analysed for some instruments

Electro-resistance particle counting (coulter counter instruments)	Particles are suspended in an electrolyte solution then sucked through a small aperture which has an electric current running across it. The pulse created by the particle moving through the current is directly comparable to its volume.	- Quick analysis time - Simple measuring protocol - Can analyse large spectrum of grain classes using different probe apertures	- Low reproducibility - Expensive
Time of transition	Particles are detected by a rotating laser beam. The interaction between the beam and the particle provides a direct measurement of its size.	Quick analysis time	- Low reproducibility - Expensive

From prior analysis of other sediment properties and knowledge of the accretion rates on PHS from the data collected on behalf of the EA (see Chapter 2, section 2.4.2), only those samples located on the NW sector (where the main, active breach is) and only those closest to the accretion stake locations were analysed using the laser diffraction and imaging machines (see Figure 3.13).
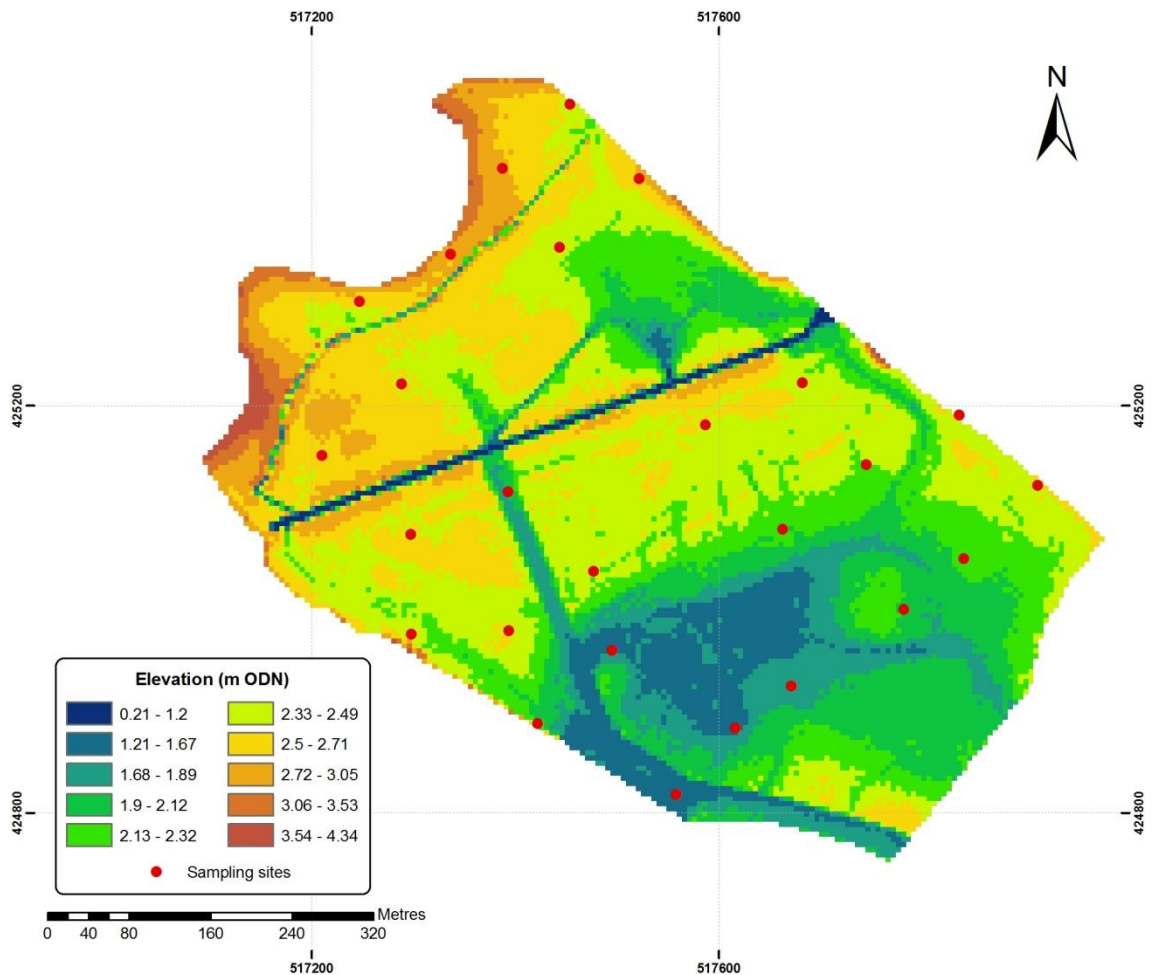
Figure 3.13: Chosen sampling stations for particle size analysis on the NW of PHS.

3.3.1.1 Measurements used to analyse grain size and shape

The two laser machines used to measure the grain size samples were the Sympatec QICPIC laser imaging machine to measure the sand fraction and the Sympatec HELOS machine to measure the silt and clay fraction. The various advantages and disadvantages of these techniques are discussed in Table 3.7 above. The laser diffraction and laser imaging instruments were chosen due to the speed and ease of measurement (important with a large number of samples), the availability of the instruments within the department and the high reproducibility of the results when compared with the sieving and pipette method. The operating principles are discussed in section 3.3.1.4. When investigating the grain size distribution of a sediment sample the concept of size and

what is actually being measured needs to be considered carefully. Sieving, for example, measures the smallest axis across a particle and thus defines the particle as the size of the square hole in the mesh through which it could pass (Konert & Vandenberghe, 1997). The grading of particles is also important to give size classes, for this the recognised scale is the Udden/Wentworth scale that classifies sediment into intervals that have rational definitions (Masselink, *et al.*, 2003; Eleftheriou, *et al.*, 2005; Soulsby, 1997).

Grain size measurements

At its most simple, a grain is defined by its long (L) intermediate (I) and short (S) axes. The I and S axes are measured at right angles to the L axis. The laser diffraction HELOS machine uses the high resolution laser diffraction (HRLD) iterative method for spherical particles, calculating the grain size in terms of an equivalent volume diameter, and can be compared with the EQPC (equivalent projected area of a circle) method that the QICPIC image analysis machine uses. This means that the particle is assumed spherical and gives the grain size as a function of the cross-sectional area of that particle (Eleftheriou, *et al.*, 2005; Goossens, 2008; Masselink, *et al.*, 2003).

A further grain size measurement used by the QICPIC machine is the Feret diameter. This measures the distance between parallel lines that are tangent to the profile of the particle- basically the particle size is the longest diameter of the particle. This diameter was useful in the removal of anomalous particles from the final grain size distribution; the QICPIC machine produces a gallery of every particle and from this a search for particularly large particles (over a certain Feret diameter) was made and these particles were then removed from the statistical analysis of the sample.

The sedimentation or pipette method has classically been used for the measurement of the clay and silt fraction of a sediment sample. This method defines the diameter of a particle as equivalent to that of a sphere settling in the same liquid with the same speed as the unknown particle as defined by Stokes law of settling. This assumes that the particles are spheres; however as clay particles are platy in structure they will settle differently (Konert, *et al.*, 1997).

Shape classification of grains

The shape of a grain affects how it will behave in the environment. Shape classification is only possible using the QICPIC image analysis machine. The shape variables that can be measured using this machine are sphericity, aspect ratio and convexity. Sphericity is

a measure of how closely the particle fits the dimensions of a true sphere and is measured on a scale of 0-1 with 1 being completely spherical. The aspect ratio (sometimes termed elongation) of a grain is the ratio of its longest dimension to that of its shortest dimension. Again measured on a scale of 0-1, this gives an idea of whether the sediment is tending towards spherical (1) or more ovate in shape (0). Convexity defines the surface roughness of a grain and is sensitive to the change in surface roughness of a particle but not of its overall form. It is calculated by dividing the convex hull perimeter by the actual particle perimeter and like sphericity is measured on a scale from 0-1 with 1 being smoothest and 0 being most 'spiky' (Blott, *et al.*, 2008).

3.3.1.2 Procedure to analyse grain size

Initial pre-treatment

The samples analysed were prepared in such a way as to optimise the results from the QICPIC and HELOS machines. All the particles need to fit the analytical range set-up within the machine and the volume of sediment needs to be just right to give the most accurate readings. As the samples were wet in their collection environment they were prepared to be used wet in the QICPIC and HELOS machines.

Approximately 30 g of sediment was measured into a pre-weighed large beaker, (an exact amount was not important as the sample was dried and then weighed). Organics had to be removed so as not to be included within the sediment analysis and skew the results. This was done by adding 100 ml of 6% hydrogen peroxide solution to the sediment and gently warming the beaker while the reaction takes place. The sample was stirred and extra 6% hydrogen peroxide solution added until no further reaction occurred. The sample was then dried out for at least 12 hours at 105°C to drive off the remaining 6% hydrogen peroxide.

The next step was to separate the sand fraction from the clay and silt fraction. This is so that the measuring range of the QICPIC machine will cover all the particles flowing through. To do this a dispersant, sodium hexametaphosphate solution, was added to the sample to separate the cohesive particles and then sonicated for 10 minutes. The sample was then wet sieved through a 63 μm mesh using distilled water. The separated samples were then dried for at least 12 hours at 105°C until a constant weight was achieved. The dry weight was noted at this point so that the data could be recombined after separate analysis.

This procedure was also followed during the sieving and sedimentation method with the difference that after the material was wet sieved the clays and silts were flushed into a 500 ml sedimentation tube.

Sieving and sedimentation method

The dried sand fraction was placed into a mortar to be lightly disaggregated with a pestle and then sieved into sand classes. The nest of sieves was shaken vigorously and the material remaining on each sieve weighed and recorded. The material left in the base pan was transferred into the corresponding sedimentation tube already holding the wet sieved clays and silts and filled to the 500 ml mark with distilled water.

The sedimentation tubes were left to stand for 12 hours in a water bath to obtain a constant temperature. The sedimentation tube was shaken vigorously for one minute then placed back into the stand taking note of the time. After four minutes a pipette was lowered into the tube to a depth of 10 cm and after 4 minutes and 48 seconds a sample was withdrawn from the tube. The contents of the pipette were then transferred into a 50 ml beaker. The sampling was repeated at one hour and eight hour time intervals. Once all the samples had been taken the beakers were dried for at least 12 hours at 105ºC until a constant weight was reached. This gives the percentage of material of the sample that is 20 µm, 6 µm and 2 µm using equation 3.4 below:

$$d = \left(\frac{W_d \mathrm{v}}{V} - W_{cal}\right)\left(\frac{100}{W_g}\right)$$

Eq. 3.4

where W_d = weight of material in pipette at time equivalent to diameter d, V = volume of sedimentation tube, v = volume of pipette, W_{cal} = weight of Calgon added to sedimentation tube, and W_g = total weight of gravel free soil.

Principles of operation of the QICPIC and HELOS machines

Two separate machines were combined for this analysis to give the best results for the range of grain sizes. The Sympatec HELOS machine is a standard laser diffraction machine and can analyse a range of particles from 0.1 µm to 10 mm, for this research the HELOS machine was used with the QUIXEL wet dispersing unit on the clay and silt fraction of the sediment samples. The Sympatec QICPIC machine produces image analysis of the particles to give highly accurate measurements and can measure a range of particles from 8 µm to above 10 mm. It is different from other laser diffraction

machines in that it provides an image of each sample while still processing at high speeds and can thus give shape data as well as size. QICPIC was used with the LIXELL liquid dispersing unit to measure the sand fraction of the sediment sample.
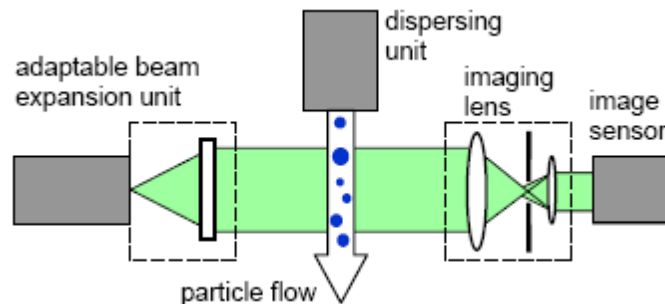
Figure 3.14: Optical set-up of the QICPIC image analysis sensor (Kohler, *et al.*).

The Sympatec QICPIC image analysis system uses a parallel beam of light which is directed to the measuring zone of the dispersing system. In principle, the illuminating light comes from a point light source and is then expanded to a parallel light beam in the expansion unit (see Figure 3.14). The light pulses are very short so that any motion blur effects are negated. The particles are then pumped through the narrow object plane and when here they interact with the light beam in the measuring zone of the LIXELL dispersing unit. The light beam then reaches the optical module in which the aperture stop blocks the stray light and the large angle diffracted light, caused by the particles. The imaging sensor (high speed camera) finally collects the information to be transferred to the computer for image evaluation.
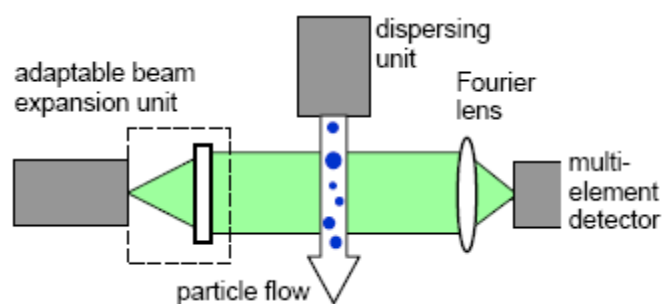
Figure 3.15: Optical set-up of the HELOS laser diffraction sensor (Kohler, *et al.*).

The HELOS laser diffraction machine also uses a parallel beam of light which is diffracted when the particle flow from the dispersing unit passes in front (see Figure 3.15). The Fourier lens transforms the diffracted light into a diffraction pattern which is in turn recorded by the multi element photo detector. The diffraction of the laser light is explained mathematically using the Fraunhofer theory (Sympatec GmbH, 2004).

Operation of QICPIC and HELOS machines

QICPIC machine to measure sand fraction

To measure the sand faction of each sediment sample QICPIC was set-up with the 2 mm flow cell and lens measuring range from 20 μm to 2 mm to cover all particles. The dry sample was rehydrated in 4000 ml of 1% sodium hexametaphosphate solution to give the optimum sediment dilution (Murray, 2002). A maximum of 5 g from each sand fraction was used- in most cases this accounted for the whole sand fraction of the sample. The beaker was stirred at 210 rpm and the LIXELL dispersant system pumped the sediment so that it constantly flowed through the machine. These conditions were used to give the optimum frame rate and were constant for all samples. Data were recorded during 30 second bursts with six replicates taken.

HELOS machine to measure fines fraction

To measure the clay and silt fraction of each sediment sample HELOS was set-up with the R2 lens which gives a measuring range of 0.2-80 μm. The QUIXEL dispersing system has a reservoir that is connected to the water supply and is emptied and refilled for each sample. The dry sample was rehydrated with 100 ml of sodium hexametaphosphate solution and 400 ml of distilled water and stirred constantly while sub-sampling took place. Care was taken while stirring so that the sample was uniformly suspended and thus no grading of material took place. From the wet solution, between 2 and 5 ml of sample was removed using a syringe and placed into the QUIXEL reservoir. From the software the dilution could be adjusted to be at or around 50%, the optimum for taking measurements. Three 30 second recordings were taken for each of three sub-samples creating a total of nine replicates.

Filtering of QICPIC data

Some of the data required post-processing to remove anomalies. These were the very large particles, either clays that had not dispersed or an organic particle not removed in the preparation stage and bubbles that were erroneously sampled. Filtering parameters were selected after examining the combined graphs of each sample which clearly shows those larger particles that were affecting the results. To remove these erroneous large particles a filter based on Feret diameter parameter or EQPC was applied and to remove bubbles a sphericity parameter was applied. Table 3.8 shows the stations that required filtering and the filter applied.

Table 3.8: Filter parameters used to post-process the sand faction for particle size analysis.

Sampling station	Filter parameter
2 winter	Diameter EQPC max ≤ 400 µm and sphericity ≤ 0.94
3 summer	Diameter Feret max ≤ 1400 µm
3 winter	Diameter Feret max ≤ 1000 µm
5 summer	Diameter Feret max ≤ 700 µm
5 winter	Diameter Feret max ≤ 1000 µm
7 summer	Diameter EQPC max ≤ 800 µm
9 winter	Diameter Feret max ≤ 1000 µm
10 summer	Diameter Feret max ≤ 1000 µm and sphericity ≤ 0.94
17 summer	Diameter Feret max ≤ 2000 µm
17 winter	Diameter EQPC max ≤ 1000 µm
21 winter	Diameter Feret max ≤ 1200 µm
23 summer	Diameter Feret max ≤ 100 µm
24 summer	Diameter Feret max ≤ 1800 µm
25 summer	Diameter Feret max ≤ 1800 µm, every 10th image
27 winter	Diameter Feret max ≤ 1500 µm
29 winter	Diameter EQPC max ≤ 300 µm and sphericity ≤ 0.94
30 summer	Diameter Feret max ≤ 1500 µm
30 winter	Diameter EQPC max ≤ 300 µm and sphericity ≤ 0.94
33 summer	Diameter Feret max ≤ 2900 µm
34 summer	Two replicates removed as too many bubbles
34 winter	Diameter Feret max ≤ 1300 µm
35 summer	Diameter Feret max ≤ 400 µm and sphericity ≤ 0.94
MF2 summer	Diameter Feret max ≤ 1500 µm
MF6 summer	Diameter Feret max ≤ 1500 µm
MF6 winter	Diameter Feret max ≤ 1000 µm
MF10 summer	Diameter Feret max ≤ 1000 µm

3.3.1.3 Confidence in results

The laser diffraction and imaging machines produced results with very low standard deviations (representing the variation in six to nine replicate measurements taken depending on machine used) giving high confidence in the results reflecting the true grain sizes of the samples measured (see Figure 3.16, below). Some of the lower percentages associated with the sand fraction have higher standard deviations than the

mean, for example at site 5. The volume of sand being sampled by the laser imaging machine to produce this result is extremely small and will lead to the higher standard deviations, however, the values would still be low even with the greatest standard deviation applied and do not impact on the overall profile of the sample.
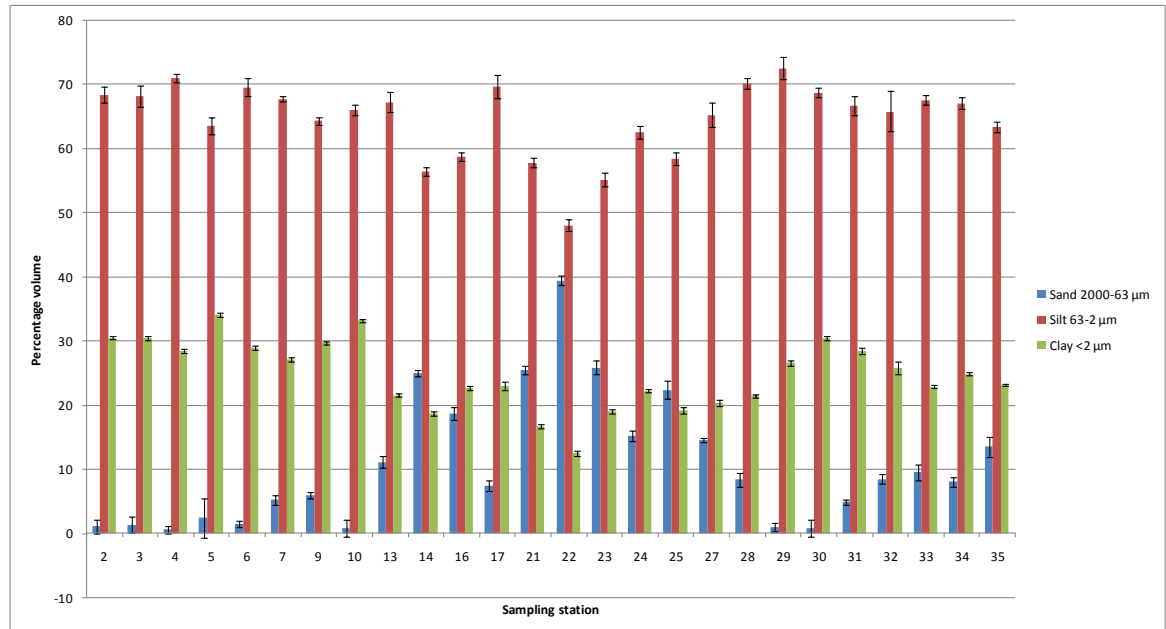
Figure 3.16: Example of particle size measurements from the NW sector of PHS, standard deviations represent the variation in six to nine replicate measurements taken depending on machine used.

Three sites have slightly larger standard deviations for the silt fraction. The largest is for site 32, however this still only equates to a difference of 5% from the mean value and so confidence in the value is still 95%.

3.3.1.4 Presentation of grain size distribution using ternary diagrams

Along with using histograms such as the one presented in Figure 3.16 above, the grain size distribution for the NW sector is also plotted using ternary diagrams. This allows the plotting of three variables (sand, silt and clay) on the same diagram and can indicate the type of sediment bed at that location or different groups of sediment across the sector. The type of bed is determined using the classification after Shepard (1954) presented on Figure 3.17 below (Eleftheriou, *et al.*, 2005).
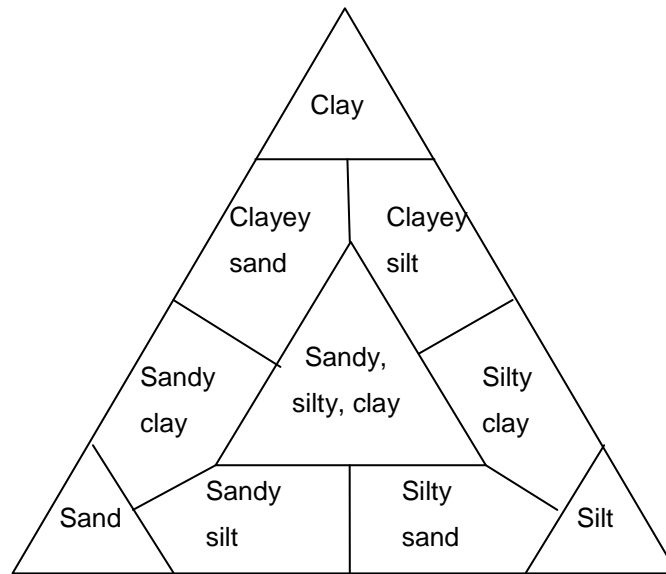
Figure 3.17: Classification of grain size distribution using a ternary diagram for sand, silt and clay after Shepard (Eleftheriou, *et al.*, 2005).

3.3.2 Calculating bulk density, absolute moisture content and organic matter content

The mass physical properties of sediment such as bulk density, moisture content and grain size are related to both mechanical strength and behaviour (Eleftheriou, *et al.*, 2005). This makes them important variables in the understanding of sedimentation on PHS.

Three samples were taken from each of the collected bulk density samples using a corer with a radius of 8.5 mm and length of 15 mm. The cores were transferred into pre-weighed labelled beakers and then weighed to calculate the wet bulk density, they were then dried for at least 12 hours at 105°C until they achieved a constant weight and weighed again to calculate the dry bulk density. The remaining sediment sample was placed into a separate pre-weighed beaker and used to measure particle size, organic content and moisture content. Equation 3.5 below was used to calculate the wet and dry bulk density (units: gcm^{-3}), where M is mass and V is volume (Flemming, *et al.*, 2000):

$$BD = \frac{M}{V}$$

Eq. 3.5

The absolute moisture content was calculated using equation 3.6 (M_w is mass of water, M_t is wet mass of sediment). The weighed sediment sample was dried in an oven for at least 12 hours at 105°C until a constant weight was achieved.

86

$$W_a = \left(\frac{M_w}{M_t}\right) \times 100\%$$

<div align="right">Eq. 3.6</div>

The absolute moisture content cannot exceed 100% (unlike relative water content used in some studies).

The organic matter content of all sediment samples collected was derived using the loss on ignition method (LOI). The pre-dried samples with no moisture were weighed and then each sample was placed into a furnace at 850°C for a time of 45 minutes to ensure that combustion of organic material had occurred. The samples were then re-weighed after cooling and the organic content was calculated using equation 3.7 below:

$$OC = \left[\frac{(M_s - M_{soc})}{M_s}\right] \times 100\%$$

<div align="right">Eq. 3.7</div>

Where M_s is mass after drying at 105°C and M_{soc} is mass after drying at 850°C.

3.3.3.1 Confidence in results

Confidence in bulk density measurements is shown by the example in Figure 3.18 below of the results obtained for samples from the mudflat in front of the NW breach. These results are typical of the full results to be presented for all sites in the NW sector in Chapter 5. The standard deviation (representing the variation between three replicate samples) never exceeds 5% of the wet bulk density mean, or 6% of the dry bulk density mean. This gives confidence that the method for measuring bulk density is reliable and any patterns seen in results are due to the sediment properties and not measurement error.
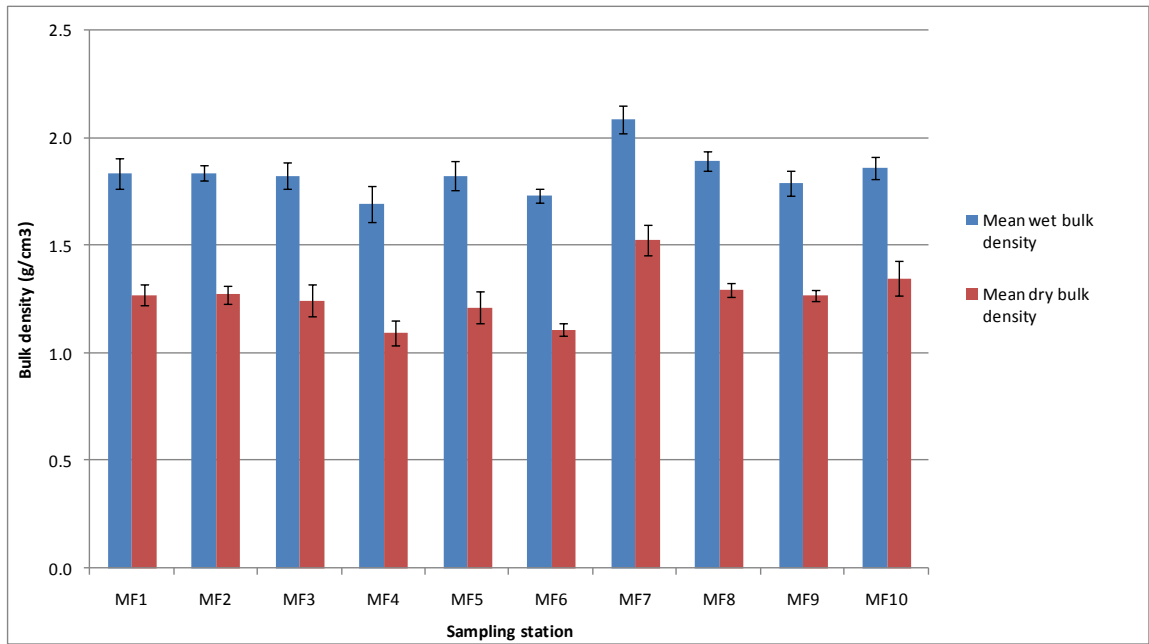
Figure 3.18: Example of bulk density measurements from the mudflat outside of the NW breach at PHS, standard deviations represent the variation between three replicate samples.

The mean absolute moisture content for the NW sector is shown in Figure 3.19 below. The majority of means have very small standard deviations, (representing the variation between three replicate samples) only four are more than 5% of the mean.
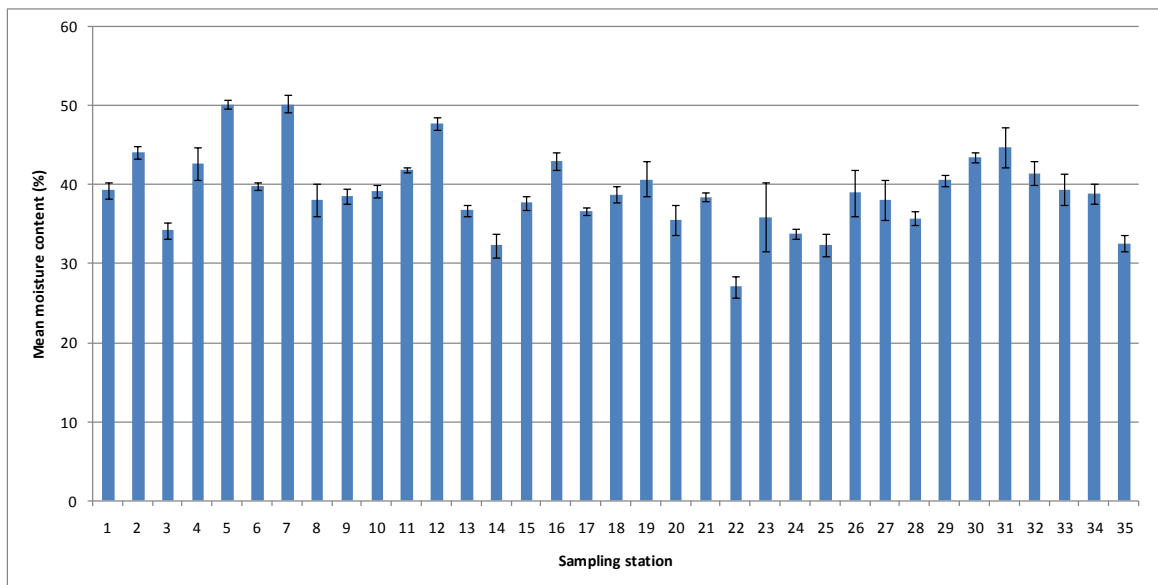
Figure 3.19: Example of absolute moisture content measurements using the mean for the NW sector of PHS, standard deviations represent the variation between three replicate samples.

As can be seen in Figure 3.20 below, the confidence in the organic content means is very high demonstrated by the small standard deviations (representing the variation between three replicate samples).
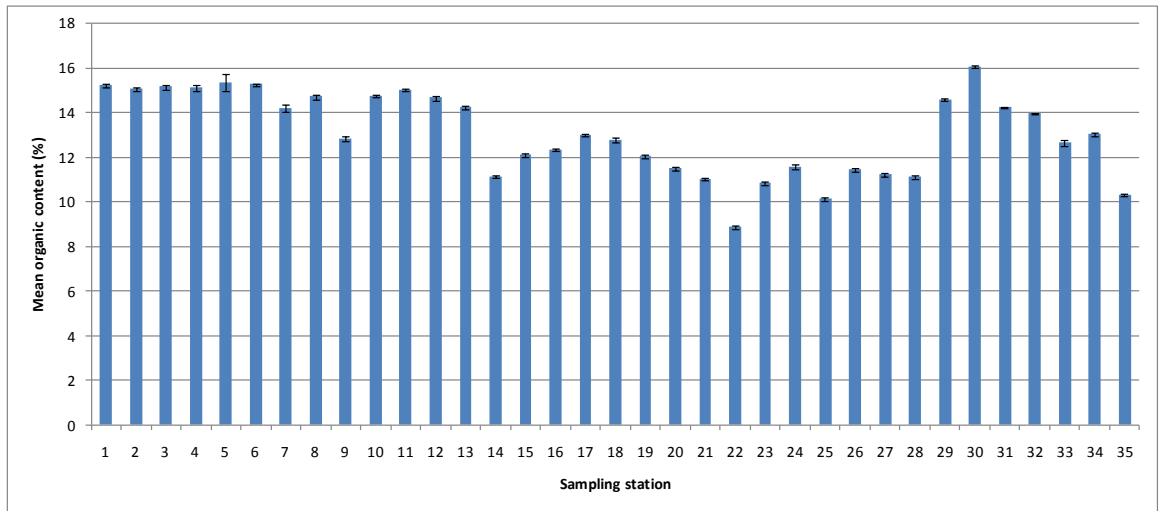
Figure 3.20: Example of organic content measurements using the mean for the NW sector of PHS, standard deviations represent the variation between three replicate samples.

3.3.3 Suspended Particulate Matter (SPM) - filtering of gulp samples and siphoned water from flume experiment

The gulp samples and siphoned water from the flume experiment described in section 3.4 was filtered to determine the concentration of SPM. Each water sample was sucked through a pre-weighed 2 μm filter paper into a flask. The filter paper was dried and weighed and the volume of the water in the flask calculated. The SPM (units: mgl^{-1}) was calculated using equation 3.8:

$$SPM = \frac{M_{sf} - M_f}{V}$$

Eq. 3.8

where M_{sf} is the dry mass of the sediment and filter paper, M_f is the dry mass of the filter paper and V is the volume of water.

The remaining filter paper was then back-washed into a beaker using distilled water and a dispersant (sodium heaxametaphosphate); a fine brush was used to make sure all the sediment was removed. This sample can be analysed for particle size to provide a comparison of the sediment size range coming through the breach at different times during the tide on PHS. The siphoned water from the flume experiments can also be compared with each other to examine the different size classes that are being eroded and how this compares with the sizes being carried by the tide at PHS.

3.4 Flume based erosion study

The flume at the Department of Geography, University of Hull (see Figure 3.21) has a working length of 7 m and a width of 0.3 m. The water was circulated using a pump with a maximum flow rate of around 70 cms^{-1}. The bottom of the flume for this study was lined with Styrofoam to a depth of 75 mm to accommodate the sediment cores. The foam at the centre of the channel was hollowed out so that the four cores fitted perfectly into the flume with a smooth surface up and downstream of the flow, a similar study by Pope, *et al*. (2006) used flume in the bottom of an annular fume so that the flow would be smooth and reproducible (Figure 3.21).
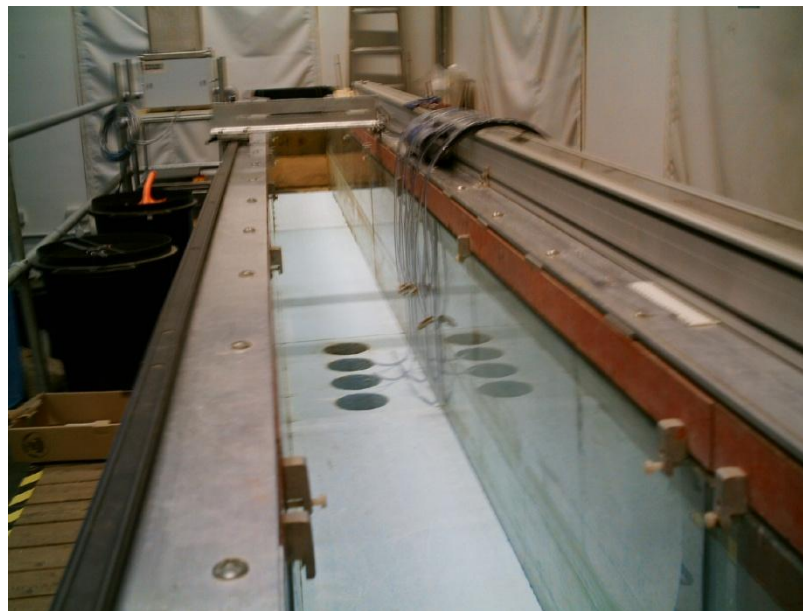
Figure 3.21: The flume used to perform erosion study showing blue Styrofoam with holes for sediment cores.

The four cores collected were placed into the foam and the flume was then filled with saline water (a salinity of 23ppt- the average from measurements at the site) to a depth of 10 cm above the sediment surface, giving a volume of approximately 600 litres. This depth was used for all four sets of cores so that any sidewall effects were reduced. The cores were left at least 12 hours to 'acclimatise' to the water conditions and for any loose sediment to settle out (Lau, *et al.*, 2000). A siphon was placed at the end of the run of cores to collect SPM during the experiment. An Acoustic Doppler Velocimeter (ADV, see section 3.4.1 below for operating principles) was mounted at a height of 4 cm above the front core to measure the velocity above the sediment, and to ensure that secondary turbulence did not interfere with the measurements (Schaaff, *et al.*, 2006). The ADV operated at a sampling frequency of 25 Hz and had a 50 mm gap to the sampling volume minimising any effect on the flow path.

Each experiment was run at a stepwise progression of increasing velocity. The initial velocity was 5 cms^{-1} and this was increased every 10 minutes by 5 cms^{-1} until a final speed of 50 cms^{-1} was reached. A temperature probe was placed downstream of the cores so that the ADV could be calibrated throughout the experiment. To measure the SPM, 100 ml of water from the flume was siphoned out after three minutes and then eight minutes during each velocity step to give the average SPM.

Once each experiment finished running the water was drained from the flume and cores were taken from the sediment to measure bulk density, moisture content, organic content and particle size. The holes in the sytrofoam to hold the cores were then cleaned out and the flume flushed for the next experiment.

3.4.1 Operating principles of the ADV

The ADV works using the same Doppler shift principle as the ADP. Details of this can be found in section 3.2.5.1. The ADV was chosen for the flume study as it is small and non-intrusive, simple to use and was available for the research (see Table 3.5 for comparisons of instruments to measure flow velocity). The system used was a Nortek, 3D, side-looking instrument. It has three acoustic transmitters that send out sound pulses, these are received by the acoustic receiver in the centre of the ADV sensor. The 3D profile measures an x-axis along the direction of the wave flume, a y-axis perpendicular to the flume and a z-axis vertically upwards. The correlation should always be between 70 and 100%, this was monitored throughout the experiment, drops occur if bubbles or debris interferes with the probe. Data can be filtered in post-processing if it falls below this threshold. The SNR (signal to noise ratio) is another important parameter that gives an indication of the quality of the data being collected. The strength of the echo being received back at the sensor head is quantified using the SNR, this is expressed in decibels (dB) and was viewed throughout the experiment. A reasonable level for the SNR is above 10dB, if the SNR drops below this level then cleaning the transducers may improve the signal.

3.4.2 Measuring bed shear stress

Bed shear stress was calculated using the Law of the Wall equation see Equation 3.9 (Masselink & Hughes, 2003).

$$u = \frac{u_*}{k} \ln\left(\frac{z}{z_o}\right)$$

<div align="right">Eq. 3.9</div>

where u_* is shear velocity, k is a constant of 0.4, z is the elevation above the bed and z_o is the bed roughness length. To calculate the bed shear stress from u_* Equation 3.10 below is used.

$$\tau_c = \rho\, u_*^2$$

<div align="right">Eq. 3.10</div>

where ρ is the water density calculated from the water temperature and salinity.

3.5 Statistics and Presentation of results

The Minitab statistics package was used for most statistical analysis along with SPSS. The actual statistics used will be discussed in the relevant results chapters. Most used was the correlation coefficient (Pearson's product moment correlation) to test for significance between variables. Other analysis done included the regression of factors to find which most predicted the change in accretion rates for each site.

Sediment properties and accretion needed to be analysed spatially so that the pattern of data across the site can be seen. This was done using ArcGIS Arc Map software. Using the point data already inputted from the recorded DGPS positions of accretion stakes and sediment sampling sites, data columns can be added to the point attributes and these can then be interpolated between points. The interpolation used was Inverse Distance Weighed (IDW), one of a range of different interpolation methods available on Arc Map that use point data to create a continuous surface. For each different interpolation method there is an associated model which makes assumptions of the data and produces a surface using different calculations. The interpolation method chosen (IDW), uses the basic principle that things closest together are likely to be more alike than those further apart. So, for a position on the surface with no point data, the model is influenced more strongly by the known points closest to this position. This explains the name: as the distance increases, the values will be inversely weighted. IDW is a deterministic technique creating a surface from measured points.

This chapter has set out the processes involved and the reasons these methods were used in collecting data at a managed realignment site to record accretion rate and sediment

properties, to produce a sediment budget and to study the erosion potential of sediment in a flume. The next chapters will present the results collected and will discuss the conclusions these results bring.

Chapter 4 : Accretion and erosion

Controls on the balance between sediment accretion and erosion since the site was first breached in 2003 are the key to the present research. Reasons for the extremely extensive accretion in some areas, compared with low rates of accretion and even erosion in other areas needs to be understood to manage the development of future realignment sites. The data from this study are designed to provide an important input into the modelling of managed realignment sites prior to breaching.

The controls on the balance between accretion and erosion on an intertidal mudflat are many and those assessed during this research are listed in Table 2.2 (Chapter 2). The results from investigation into these controls will be presented and discussed in subsequent chapters. The controls do not always work independently, each control may influence both accretion and erosion and may interact with other factors to some extent either lessening or exacerbating impacts.

The first section (4.1) presents the temporal changes in accretion/erosion including seasonal changes and monthly accretion rates; section 4.2 investigates the link between accretion/erosion and elevation and section 4.3 looks at the spatial patterns of accretion/erosion on the NW sector.

4.1 Temporal changes in accretion/erosion

Changes in mudflat levels since the start of the monitoring programme (February 2006) are presented in this section; this covers 19 months at most sites, however for some sites data collection had to be curtailed due to stakes being removed or bent. At these sites the new stakes were replaced as soon as possible and in most cases results could still be combined. At sites 2a and 3b, the stations were abandoned towards the end of the monitoring period due to repeated removal or bending of stakes. Two sites (4c and 8b) were inaccessible for the first few months of monitoring, however as the stakes were not disturbed readings could be taken when the stakes became accessible again.

The temporal changes indicate that the whole of PHS accreted sediment during the monitoring period (see Figure 4.2). This is in concordance with the EA monitoring results discussed in Chapter 2, section 2.3. The SE sector had much slower rates of accretion (range of -6.25 to 3.79 mm per month) and the NW sector had much faster rates of accretion in some areas (range of -1.82 to 17.34 mm per month). This general trend is shown clearly in Figure 4.2, below. The total height of sediment accreted or

eroded across the site for the full monitoring period and the monthly rate associated with each site is given in Table 4.1.

The site with the most sediment accreted throughout the 19 months was 6c- a total of 329.5 mm or approximately 17 mm per month. Sampling stations nearby also recorded very fast rates of accretion. Over 200 mm of sediment accreted at sites 6a, 6b, 5d and 4c during the monitoring period, over 10 mm per month. Four sites (2a, 2c, 3a, 5e) had eroded over the monitoring period. The most sediment eroded at site 2a, losing approximately 6 mm each month, the three other sites lost less than 2 mm each month.

Figure 4.1: Creeks forming close to sampling sites 5b and 5c affecting accretion readings, looking east from the new flood embankment.

The data recorded at sites 5b, 5c and 8b have large standard deviations from the mean (standard deviations representing the difference between four measurements at each sampling site, see Table 4.1 for values). All these sites were located in areas where creeks started to form towards the end of the monitoring period- in the case of site 8b directly between stakes. An example of the types of creeks near sites 5b and 5c is shown in Figure 4.1 above. Some of the recorded accretion rates at sites in the SE sector such as 1c and 2c, have large standard deviations compared to their means. However, these sites have only very slow rates of accretion (or slight erosion in the case of 2c) so even within the standard deviation the rates would still be slow and in keeping with the means of other sites in the SE sector.
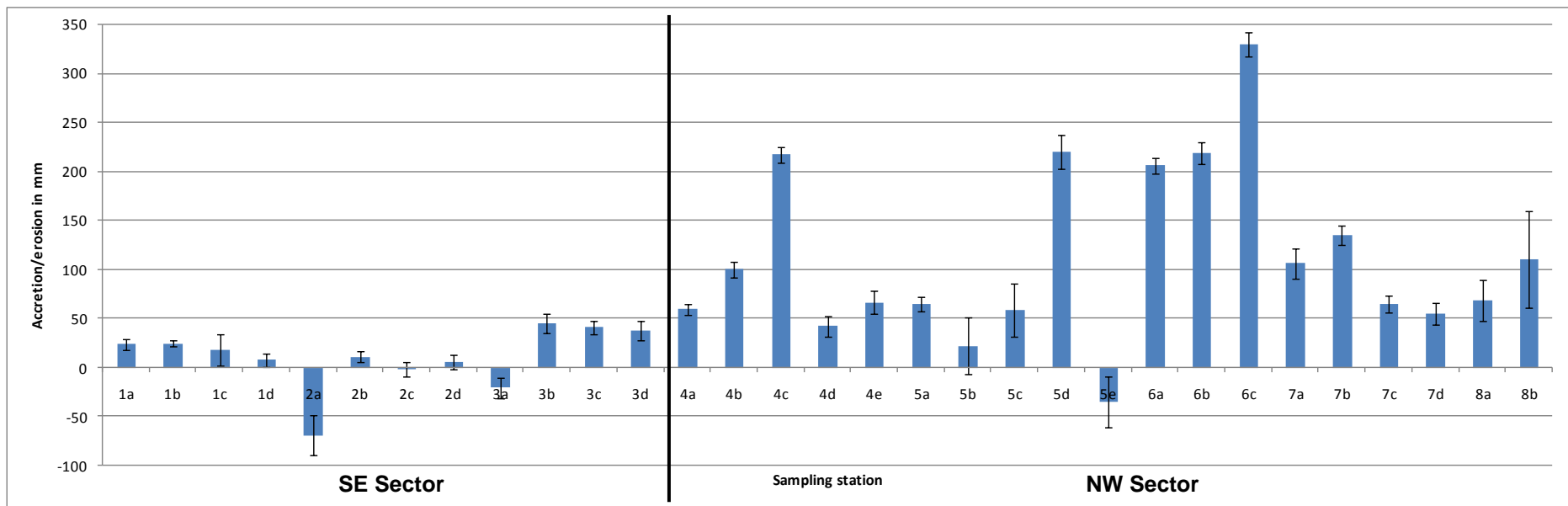
Figure 4.2: Cumulative mean accretion/erosion for the full monitoring period (February 2006 until September 2007) across all transects on PHS, standard deviations represent the variation between four measurements at each sampling station.

Table 4.1: Mean sediment level change across all sampling stations for the full monitoring period and the related monthly sediment level change across PHS, standard deviation represents the variation between four measurements at each sampling station. Full data are presented in Appendix 3.

Sampling Station	Mean accretion/erosion for full monitoring period (Feb 2006-Sep 2007) in mm	Monthly accretion/erosion in mm
1a	24 ± 5.7	1.26
1b	24.75 ± 2.9	1.3
1c	18.5 ± 16	0.97
1d	8 ± 6.8	0.42
2a	-68.75 ± 20.5	-6.25
2b	11.25 ± 5.3	0.59
2c	-1.5 ± 7.7	-0.08
2d	6 ± 7.8	0.32
3a	-20.5 ± 10.7	-1.14
3b	45.5 ± 9.7	3.79
3c	41 ± 6.8	2.41
3d	37.5 ± 9.6	1.97
4a	59.5 ± 5.3	3.31
4b	100 ± 8.5	5.56
4c	217.25 ± 8.2	12.07
4d	42.5 ± 10.4	2.24
4e	66.5 ± 11.4	6.5
5a	64.75 ± 7.1	3.6
5b	22 ± 29.1	1.22
5c	58.75 ± 27.3	3.26
5d	220 ± 17.8	12.22
5e	-34.5 ± 25.6	-1.82
6a	206.25 ± 7.9	10.86
6b	219 ± 11.4	11.53
6c	329.5 ± 12.1	17.34
7a	106 ± 15.3	5.89
7b	134.75 ± 9.9	7.49
7c	65.25 ± 8.4	3.43
7d	55 ± 10.8	2.89
8a	68.5 ± 21.3	5.71
8b	110.25 ± 48.8	6.13

4.1.1 Cumulative accretion/erosion on the SE sector

Table 4.2: Mean accretion/erosion and range in mm on the SE sector, standard deviation represents the variation between the sampling stations along each transect.

Transect	Mean accretion/erosion for full monitoring period (Feb 2006-Sep 2007) in mm	Range (mm)
1	18.8 ± 7.7	8-24.75
2	-13.3 ± 37.4	-68.75-11.25
3	25.9 ± 31.1	-20.5-45.5
Full sector	10.5 ± 31.3	-68.75-45.5

For the full monitoring period this sector shows a range of sediment level change from the sediment erosion along transect 2, to moderate rates of accretion along transect 3 (see Tables 4.1 and 4.2). Erosion was associated with the drainage channels; these can be seen on Figure 3.3 in Chapter 3. Transects 1 and 3 (when the erosion rate for site 3a is discounted) show constant slow rates of accretion. These two transects were located nearest to the water inputs: transect 1 at the smaller SE breach and transect 3 closest to the NW sector and the main breach.

4.1.2 Cumulative accretion/erosion on the NW sector

Table 4.3: Mean accretion/erosion and range in mm for the NW sector, standard deviation represents the variation between the sampling stations along each transect.

Transect	Mean accretion/erosion for full monitoring period (Feb 2006-Sep 2007) in mm	Range (mm)
4	97.2 ± 70.3	42.5-217.25
5	66.2 ± 94.6	-34.5-220
6	251.6 ± 67.8	206.25-329.5
7	90.3 ± 36.9	55-134.75
8	89.4 ± 29.5	68.5-110.25
Full sector	111.1 ± 89.0	-34.5-329.5

Erosion only occurred at site 5e on the NW sector for the full monitoring period (see Table 4.1). This site was the closest to the NW breach. Accretion rates have been fast at all other sites for the full monitoring period. The greatest amount of sediment accreted along transect 6 (see Table 4.3) to the north of the NW breach. Remaining transects exhibit a wide range of accretion rates, these differences will be discussed in further sections.

4.1.3 Comparison of accretion rates

To analyse the accretion rates in context, a comparison with the EA monitoring results, other managed realignment sites and natural saltmarshes is made on Table 4.4, below.

Table 4.4: Yearly accretion rates at PHS, other managed realignment sites and natural saltmarshes.

	Location		Accretion Rate (mma^{-1})
Managed realignment	PHS	Current research	NW sector: 15-208 (-22 at eroding site) SE sector: 4-45 (-75 at eroding site)
		EA data	NW sector: 10-159 SE sector: 2-39 (Brown, *et al.*, 2008)
	Blackwater Estuary, Essex, UK	Tollesbury	40 at low elevations 3-5 at high elevations (Cundy, *et al.*, 2002; French, 1999) 100-300 initially (Pontee, *et al.*, 2006)
		Abbot's Hall	0 for 1st 3 years Starting to accrete when vegetated (Pethick, 2002)
	Lantern Marsh, Orfordness, Suffolk, UK		40 (Pontee, *et al.*, 2006)
Historic breach failure	Pagham Harbour, UK		5 (from cores) (Cundy, *et al.*, 2002)
Natural saltmarsh	UK		2-20 (Pontee, 2003)
Mudflat	Spurn Bight, Humber Estuary, UK		Few mm during calm conditions (Christie *et al.* 1999)

There is some discrepancy between the accretion rates reported for the Tollesbury managed realignment site by different authors. This may arise from the faster accretion rates (100-300 mma^{-1}) occurring in the site during the first few years post-breach and the rates then reducing to 40 mm per year at higher elevations and 3-5 mm per year at lower elevations once the site has settled down. The initial accretion rates are similar in magnitude to those being experienced on PHS. Neither datasets (from the current research or EA monitoring) record accretion rates of 300 mm per year as reported for Tollesbury, however slower rates of 100-200 mm per year was recorded at a number of sites across the NW sector. All of these rates, even for the slower accreting SE sector were faster than those recorded at natural saltmarshes around the UK. This indicates that managed realignment sites create the conditions for fast accretion; either through the initial design of the site or the type of sediment present.

4.1.4 Monthly sediment level changes and seasonal differences

(a) Transect 1

(b) Transect 2

(c) Transect 3
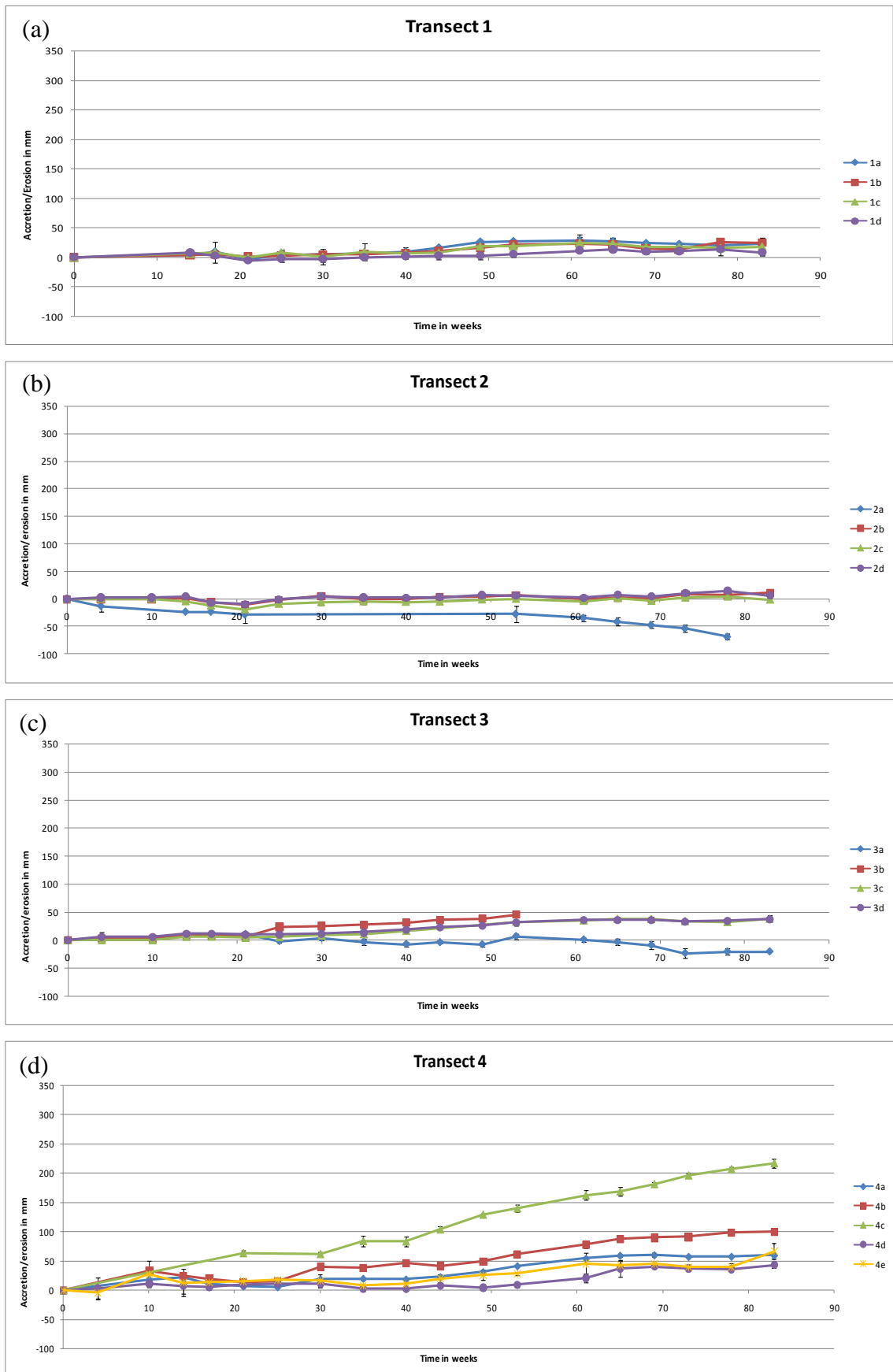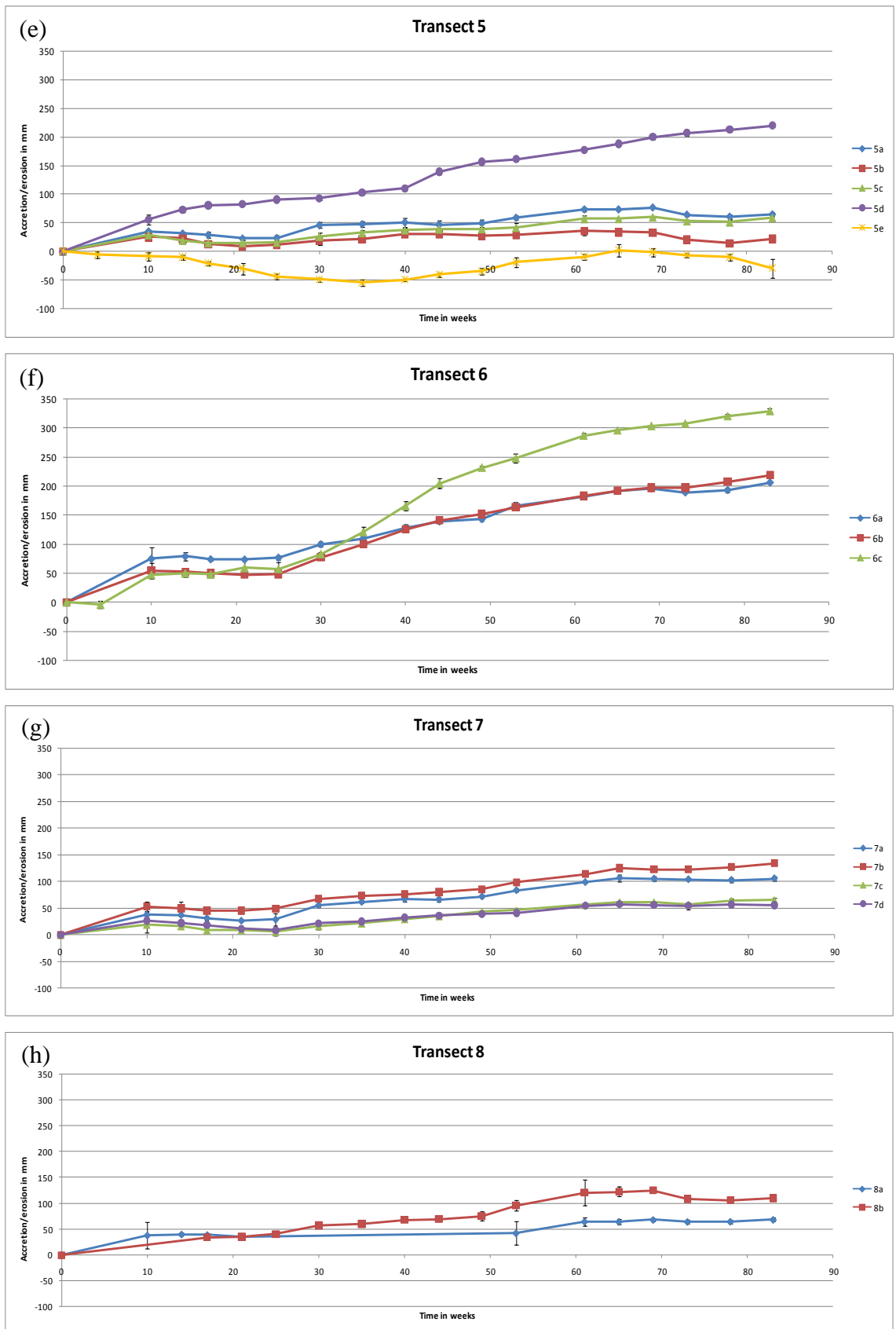
(d) Transect 4

Figure 4.3: Mean sediment level change for full monitoring period (February 2006- September 2007) across each transect on PHS, standard deviations represent variation between four measurements at each sampling station. (a) Transect 1, (b) Transect 2, (c) Transect 3, (d) Transect4, (e) Transect 5, (f) Transect 6, (g) Transect 7, and (h) Transect 8. For locations of transects see Figure 3.1, Chapter 3.

Figures 4.3 (a) to (h) show the changing levels of sediment at each sampling site. Along transect 1 (Figure 4.3 (a)) there was a slight increase in sediment height across all of the sampling stations, approximately 25 mm of sediment accreted- all stations show very similar patterns and all observations have small standard deviations. Sediment along transect 2 (Figure 4.3 (b)) has seen even slower rates of accretion during the 19 month monitoring period with one of the sites (2a) eroding fairly rapidly. The accretion of sediment was similar for the three remaining sites and slightly slower than for transect 1. Transect 3 (Figure 4.3 (c)) is the final transect on the SE sector. Again, sediment along this transect generally accreted slowly, however sediment at sites 3c and 3d has accumulated 50 mm in height. Site 3a has seen a fall in sediment height after 20 weeks of monitoring; the total eroded was less than the erosion at site 2a. Faster accretion rates occurred at site 3b than at sites 3c and 3d, however no data were recorded for the last seven months as the stakes were repeatedly vandalised and the site was abandoned.

Sediment along transect 4 (Figure 4.3 (d)) in the NW sector continuously accreted. Sediment at site 4c has the fastest accretion rate accumulating approximately 220 mm. The data recorded at other sites along this transect were similar; site 4b accumulated 100 mm of sediment and the remaining 3 sites more than 50 mm. The changes along transect 5 (Figure 4.3 (e)) were more diverse. Sediment at site 5d accreted by the greatest amount- approximately 220 mm; sites 5a and 5c accumulated over 50 mm, but site 5b only gained approximately 25 mm and site 5e eroded between weeks 15 and 40, started to accrete and then eroded again in the final weeks of monitoring. Sediment at sites 5a, 5b and 5c eroded slightly in the final 12 weeks of the monitoring period. Transect 6 (Figure 4.3 (f)) accreted the fastest. Sediment at site 6c accreted very rapidly especially after week 20 and finally accumulated 330 mm. Sites 6a and 6b were similar- both accumulating approximately 210 mm of sediment. All the sites on transect 6 had a slowing of accretion rate between weeks 10 and 25. Sediment at the sites along transect 7 (Figure 4.3 (g)) showed similar patterns of accretion over the 9 months of monitoring. The final accumulation of sediment was most similar between sites 7a and 7b, and 7c and 7d perhaps due to their proximity. The final transect on the NW sector only has two sampling sites (Figure 4.3 (h)). Sediment at both of these accreted; 8b accumulated just over 100 mm. No accretion occurred during the middle of the monitoring period at these two sites and the rates then fell at the end, similar to the pattern at sites along transect 5.
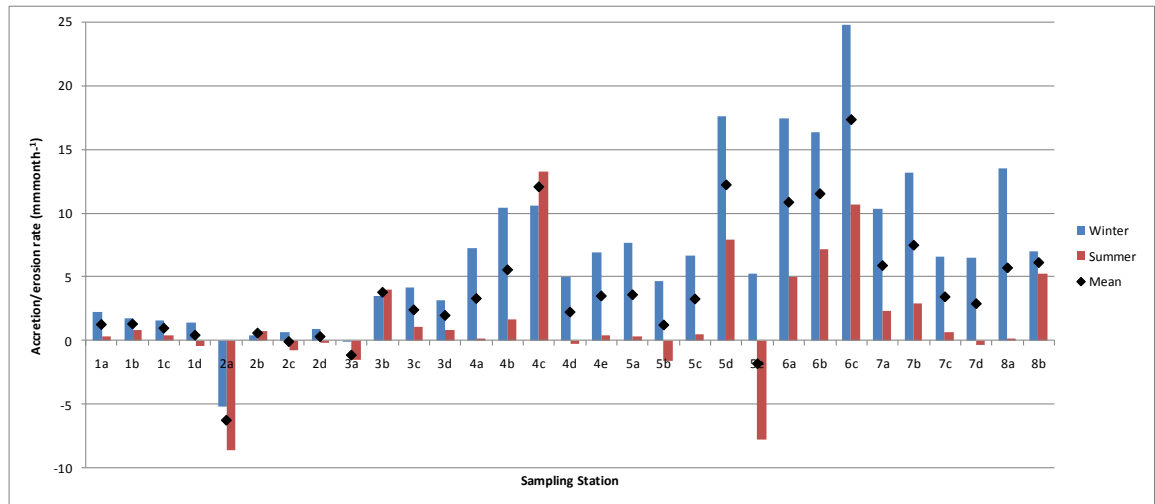
Figure 4.4: Cumulative sediment accretion/erosion across all sampling stations on PHS for the summer and winter periods of monitoring, mean indicated by black markers.

Figures 4.3 (d) to (h) of the NW sector show a seasonal trend with more sediment accreting during the winter months and slower accretion or erosion during the summer months. Figure 4.4 above shows this difference between the summer and winter months during the monitoring period; the number of summer and winter months were almost equal- nine winter and ten summer for those sites with full datasets. The amount of sediment accreted during the winter months was greater, apart from a few exceptions at sites 2b, 3b, and 4c. Using the Wilcoxon test for matched pairs, there was a significant difference between the median accretion rates for winter and summer (Z = -4.5, P < 0.000). At sites 1d, 2c, 2d, 4d, 5b, 5e and 7d there was erosion during the summer; sites 4a, 4e, 5a, 5c, 7c and 8a had very slow rates of accretion during the summer months compared to the winter.
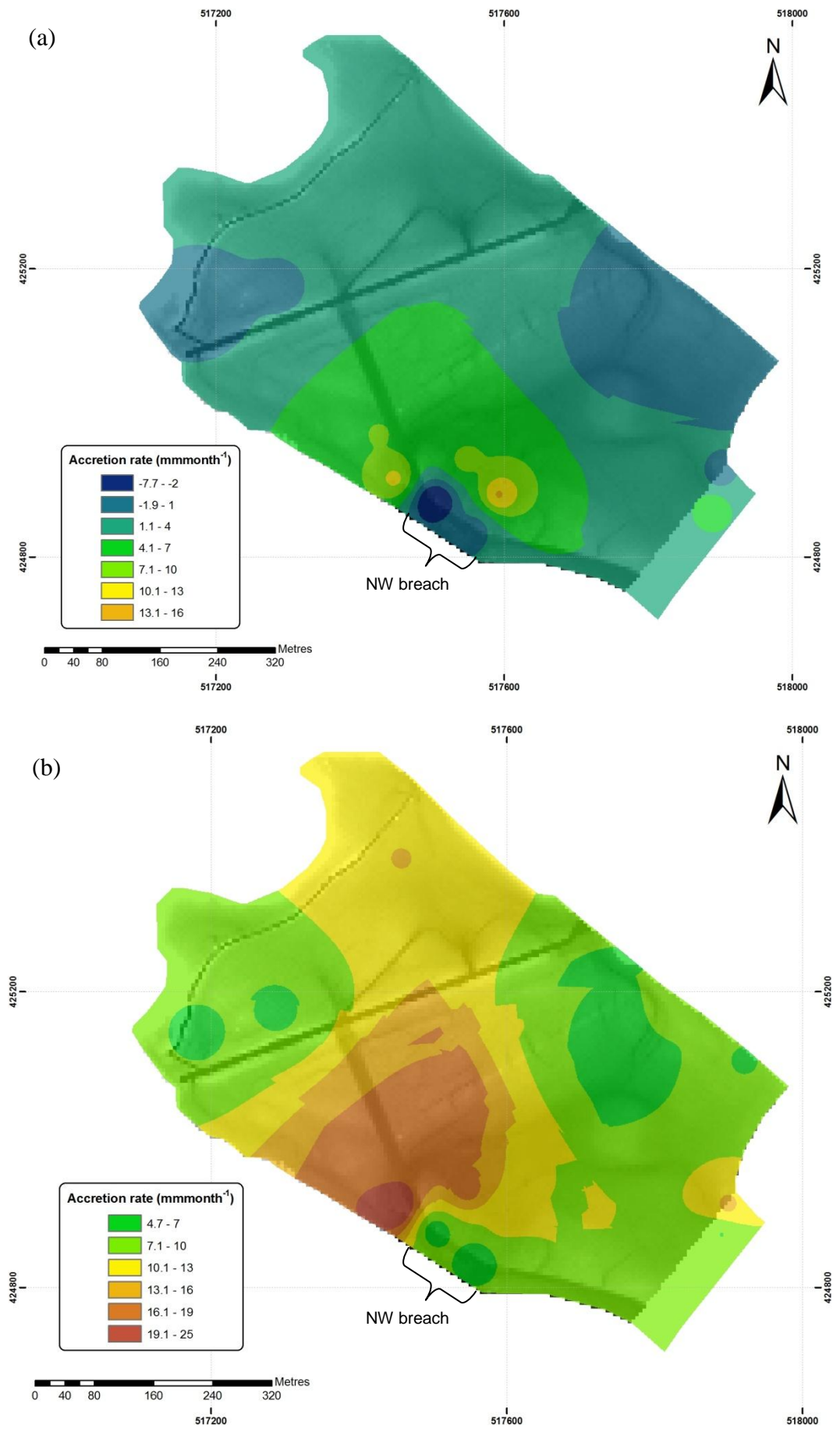
Figure 4.5: Interpolated map of monthly accretion rates in (a) summer and (b) winter.

Figures 4.5 (a) and (b) are of the seasonal differences between accretion rates on a spatial scale. The fastest accretion during the summer of 7 to 16 mm each month occurred at sites just to the north of and directly behind the NW breach. During the winter, the fastest accreting areas were again close to the NW breach, however they covered an area more towards the northern end of the site (indicated by the purple and dark brown areas). These areas were accreting at rates of 13 to 25 mm every month. The slower accreting areas during the winter and summer were in similar positions-immediately behind the NW breach and in the eastern and western corners.

4.1.5 Sediment level changes and elevation

The elevation of each sampling station determines both the amount of sediment accreted as well as colonisation by saltmarsh species. The colonisation by different species falls into different zones from the pioneer species right through to those more typical of terrestrial environments. Table 4.5 below shows the zones that have been identified in the EA monitoring programme and the saltmarsh vegetation that is found at each of these zones. The following Figures 4.6 (a-e) show the sampling stations at each of these zones, based on the site elevation recorded at the start of the monitoring period.

Table 4.5: Elevation zones on PHS and the associated saltmarsh vegetation zones.

Elevation (m ODN)	Saltmarsh vegetation zone
≤2.0	Mudflat
>2.0-2.3	Early pioneer
>2.3-2.6	Pioneer
>2.6-3.0	Lower-Mid marsh
>3.0-3.5	High marsh
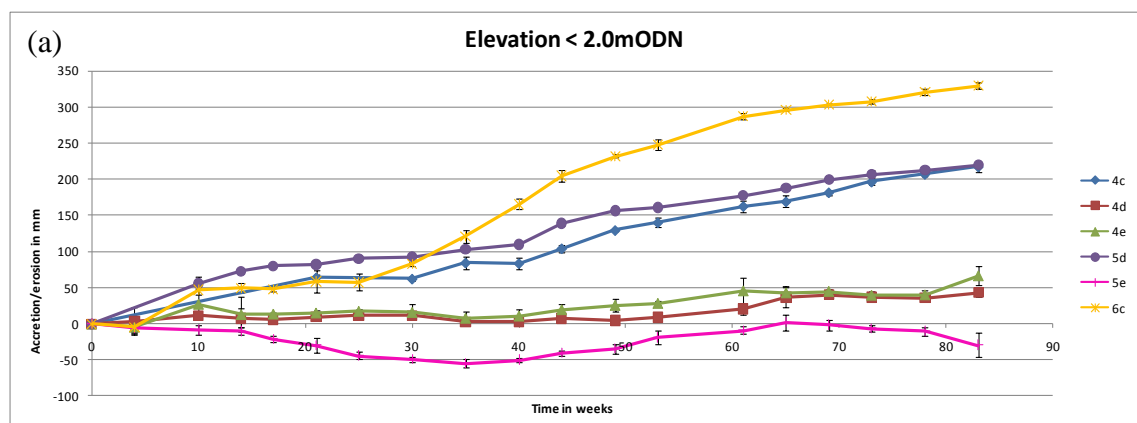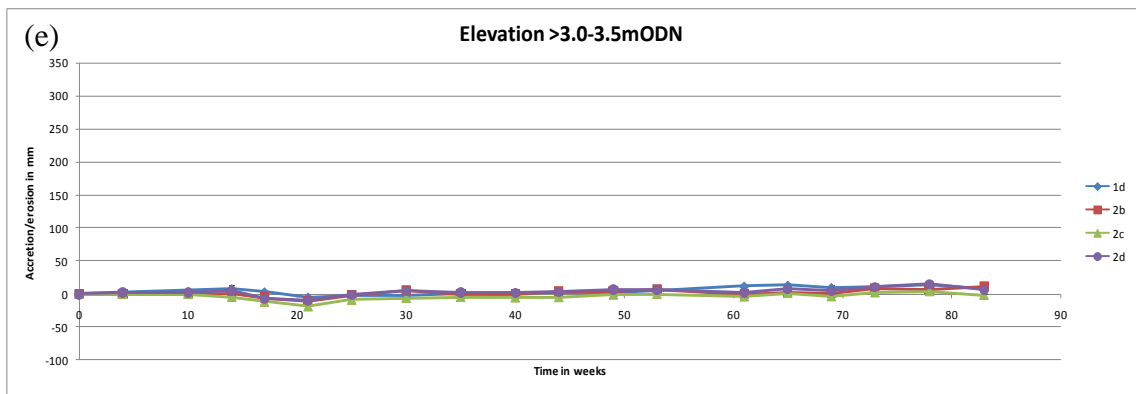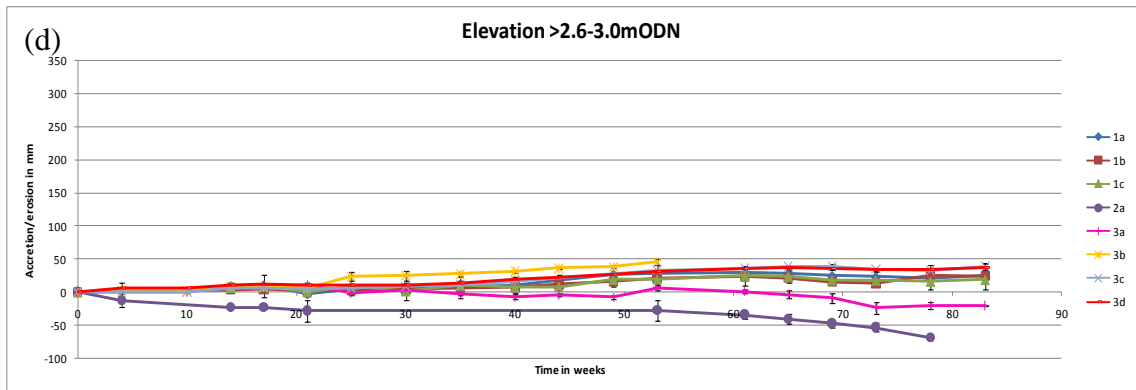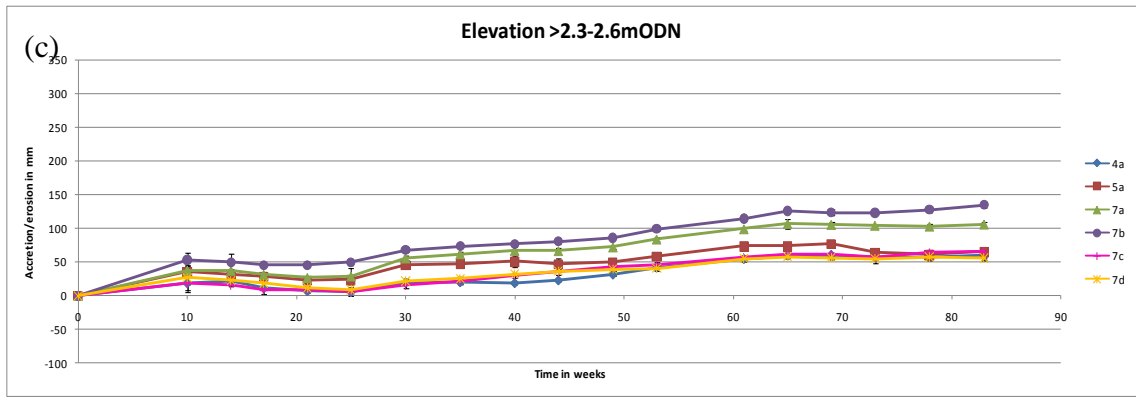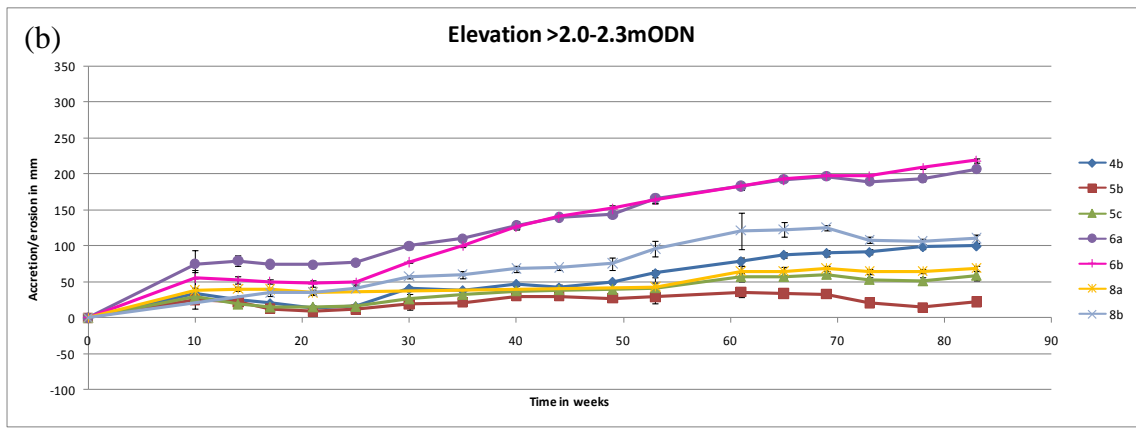
Figure 4.6: Sediment level changes across the full monitoring period (February 2006-September 2007) for sites at different elevations, standard deviations represent variation between four measurements at each sampling station, (a) elevations less than or equal to 2.0 m ODN, (b) elevations greater than 2.0 to 2.3 m ODN, (c) elevations greater than 2.3 to 2.6 m ODN, (d) elevations greater than 2.6 to 3.0 m ODN and (e) elevations greater than 3.0 to 3.5 m ODN. For locations of transects see Figure 3.1, Chapter 3.

Six sites were in the lowest elevation zone (less than or equal to 2.0 m ODN, Figure 4.6 (a)), and of these three were the sites with fastest sediment accretion (4c, 5d and 6c). All of the six sites are clustered around the NW breach and of the remaining three sites; two had moderate rates of accretion (4d and 4e) and sediment at the final site (5e) was eroding.

Seven sites were in the next elevation zone (greater than 2.0 to 2.3 m ODN, Figure 4.6 (b)). Two of these sites were very rapidly accreting sediment (6a and 6b) the remaining five sites were similar, only at one of the sites was the total sediment accreted less than 50 mm (5b) and this site was located in an area where creeks had formed thus reducing the effect of elevation.

Six sampling sites fall in the elevation zone: greater than 2.3 to 2.6 m ODN (Figure 4.6 (c)). This zone contains the remainder of the sites from the NW sector (4a, 5a, 7a, 7b, 7c and 7d). Two of the sites (7a and 7b) had recorded more rapid sediment accretion over the full monitoring period than the majority of the sites in the lower elevation zone. The remaining four sites had similar accretion rates to the majority of the sites in the lower elevation zone indicating that elevation was not the only control on the accretion rates recorded.

The highest two elevation zones contain all the sampling stations from the SE sector. Four sites (1d, 2b, 2c and 2d) fall into the highest zone (greater than 3.0 to 3.5 m ODN, Figure 4.6 (e)) all recorded very slow accretion over the monitoring period. The second highest elevation zone (greater than 2.6 to 3.0 m ODN, Figure 4.6 (d)) covers eight sites (1a, 1b, 1c, 2a, 3a, 3b, 3c and 3d). The two sites where sediment has eroded over the monitoring period are in this zone (2a and 3a). The rest of the sites have accreted similar amounts of sediment, all less than 50 mm over the monitoring period. The SE sector displays a much stronger relationship between elevation and accretion than the NW does.

Table 4.6: Mean accretion and range in mm for each elevation zone on PHS, standard deviation represents the variation between means of each sampling station in the elevation zone.

Elevation Zone (m ODN)	Sampling stations	Mean sediment accreted for full monitoring period (Feb 2006-Sep 2007) in mm	Range (mm)	EA Sampling stations	Mean sediment accreted for same period using EA data (mm)
≤2.0 (zone 1)	4c, 4d, 4e, 5d, 5e, 6c	140.2 ± 136.8	-34.5-329.5	4.2	185.9
>2.0-2.3 (zone 2)	4b, 5b, 5c, 6a, 6b, 8a, 8b	112.1 ± 74.5	22-219	2.1, 2.2, 2.3, 3.1, 3.3	125.5 ± 35.8
>2.3-2.6 (zone 3)	4a, 5a, 7a, 7b, 7c, 7d	80.9 ± 32.1	55-134.75	1.5, 2.4, 2.5, 3.2, 3.4, 4.1, 4.3, 4.4, 4.5, 4.6	94.6 ± 27.2
>2.6-3.0 (zone 4)	1a, 1b, 1c, 2a, 3a, 3b, 3c, 3d	12.8 ± 38.8	-68.75-41	1.1, 1.2, 5.1, 5.2, 5.3, 7.1, 7.2, 8.1, 8.2, 8.3, 8.4	43.4 ± 45.5
>3.0-3.5 (zone 5)	1d, 2b, 2c, 2d	5.9 ± 5.4	-1.5-11.25	1.4, 5.4, 6.1, 6.2, 6.3, 6.4, 7.3, 7.4	10.8 ± 4.4
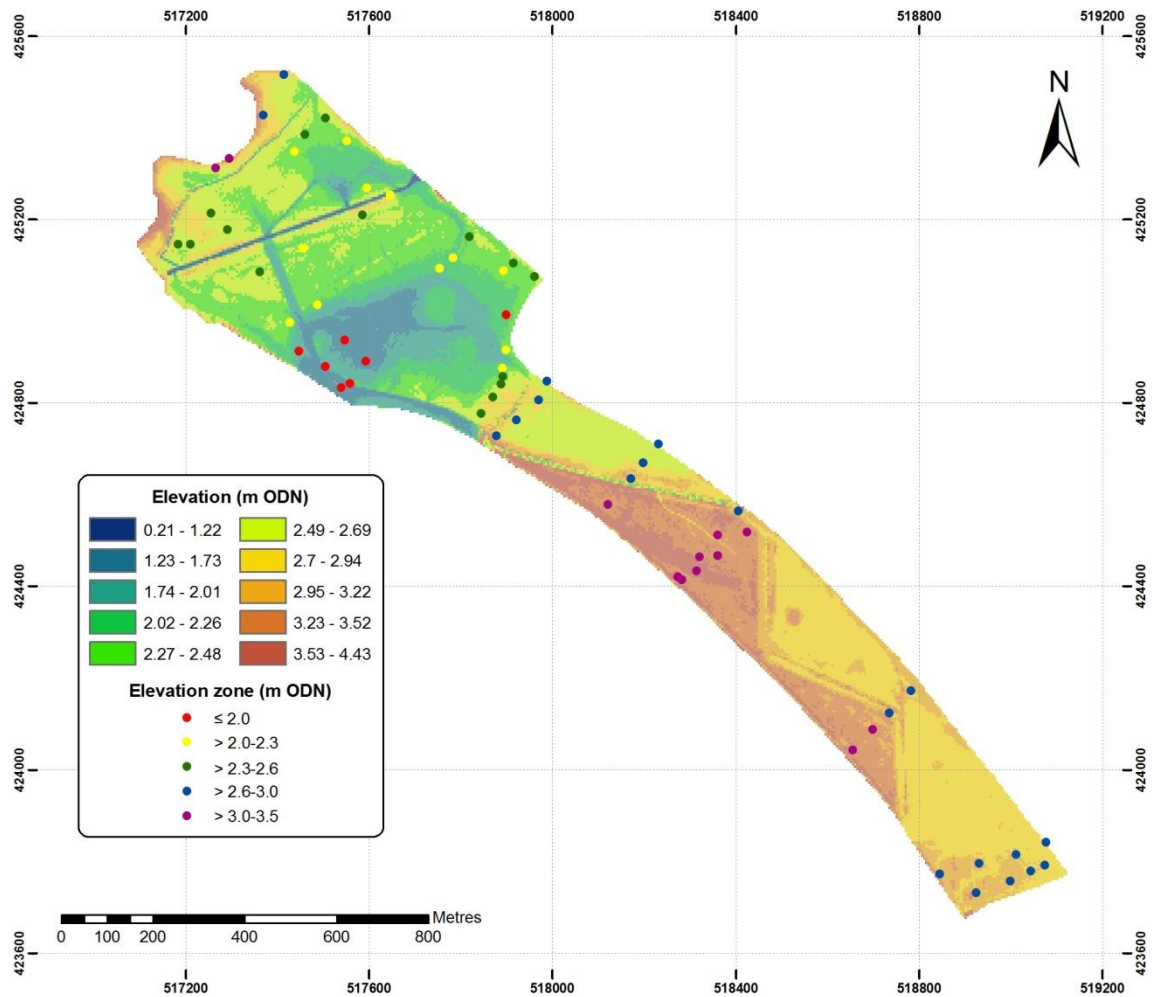
Figure 4.7: Locations of all sampling stations for each elevation zone on PHS.

From Table 4.6 and Figure 4.8 it is clear that the total mean sediment accreted falls with increased elevation. The fall in total mean sediment accreted for the monitoring period is greatest between the third and fourth elevation zones with a reduction of approximately 80%. The sites in the third zone are the highest elevated on the NW sector and in the fourth zone are the sites that are the lowest elevated on the SE sector (see Table 4.6 above). Even though the zones are grouping what is a continuous rise in elevation, this large difference in total sediment accreted still occurs, indicating a difference between the two sectors that influences the accretion rate.

In the highest two elevation zones (4 and 5) only three sites (all EA stake locations, see Figure 4.7) were in the NW of the site. These three sites were on the far north corner where the mudflat is in transition between very low inundation and continuous vegetation. The fall in total sediment accreted between the highest two zones covering the SE sector was about 50%. Figure 4.8 shows the range of total sediment accreted at each of the elevation zones. The lowest elevation zone is skewed by the one sampling

109

station (5e) that was eroding, however even with this station included in the mean the total sediment accreted was still greatest. Without the data from site 5e included in the calculations, the mean total sediment accreted rises to 175 ± 119 mm. There is still large variation about the mean but the mean moves closer to the EA monitoring site in this elevation zone.
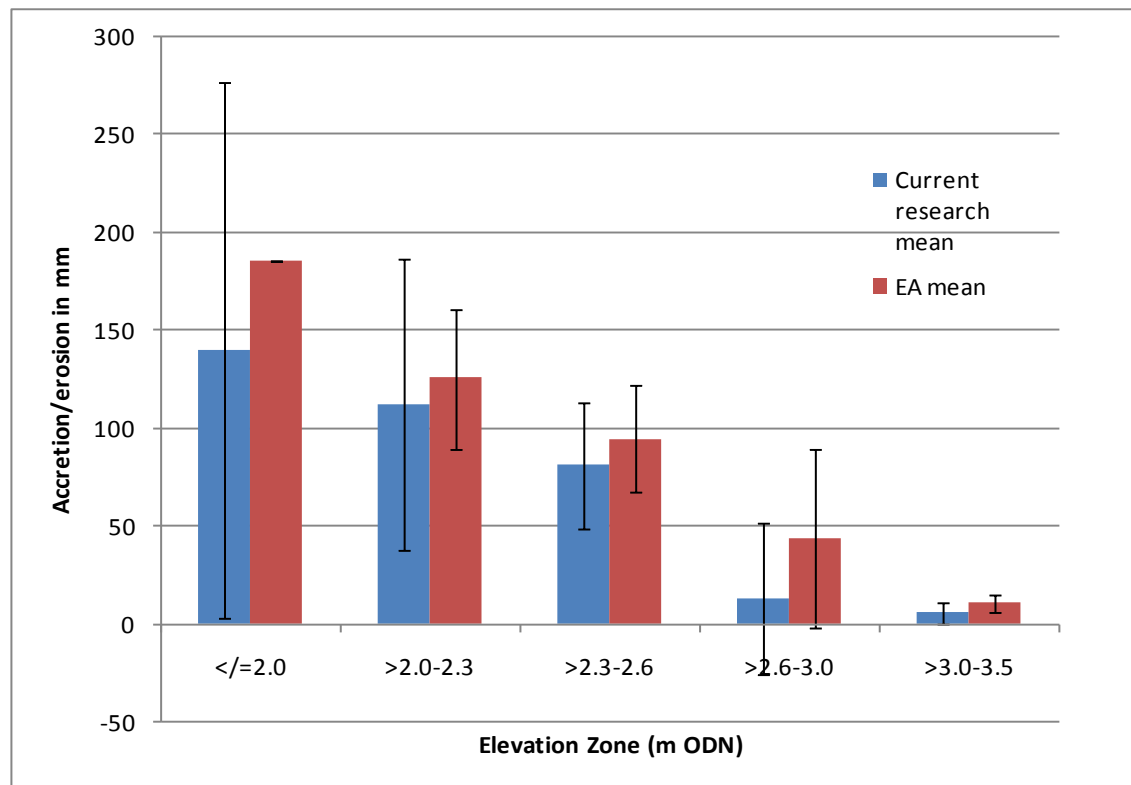
Figure 4.8: Mean accretion (both current research and EA monitoring) for the full monitoring period at different elevation zones across PHS managed realignment site, standard deviation represents the variation between means of each sampling station in the elevation zone.

When considering the mean total sediment accreted over the same time period at the EA monitoring sites (Table 4.6 and Figure 4.8) there was a similar reduction in total sediment accreted with rising elevation. The mean total sediment accreted for all the zones was greater at the EA sampling stations. For the lowest elevation zone this was because the EA measurement is based on just one site and will not be a representation of the elevation zone as a whole. In the other elevation zones the means were closer between the current research and the EA data. The result for zone 2 (greater than 2.0 to 2.3 metres) would have been affected by the low accretion at site 5b near to the NW breach. None of the EA sites were located near to the breach and so the higher mean accretion rates for the lower elevation zones would have been affected by this. The greatest difference between means is found at sites in zone 4 (greater than 2.6 to 3.0 metres). This zone also has large standard deviations indicating that the position of the

monitoring sites was influencing the accretion rates. The measurement of the EA stakes was biannually and will also affect the data collected perhaps contributing to the higher mean accretion.

4.2 The relationship between accretion rate and elevation

The fast rates of accretion across the NW sector are strongly linked to the elevation of the site (as discussed above), however other factors (as listed in Table 2.2, Chapter 2) will also be contributing to the patterns of sedimentation recorded on PHS. The results from the EA monitoring sites are shown in Figure 4.10. The EA data were not collected on as regular a basis and so the accretion/erosion rate was calculated from a smaller number of values.

The inverse relationship between accretion rate and elevation is identified in Figure 4.9 below. The slowest accretion occurred at the sites that had the highest elevation (data from February 2006 to September 2007) and the fastest accretion was recorded at the sites of lowest elevation. The Pearson's correlation coefficient is -0.583 with a significance of 0.001; indicating the strength of the relationship between these two factors. However, from looking at Figure 4.9 there are a number of points that do not conform to this relationship. The sites that were eroding have been mentioned in previous sections and reasons for this erosion proposed. There were, however, a number of sites that were at a low elevation but had a range of accretion rates associated with them. There was also a wide range of accretion rates amongst sites with an elevation of 2.0 to 2.3 m ODN (1.2 to 12.2 mm month^{-1}). These sites will be investigated more closely when other factors are discussed in the following chapters.
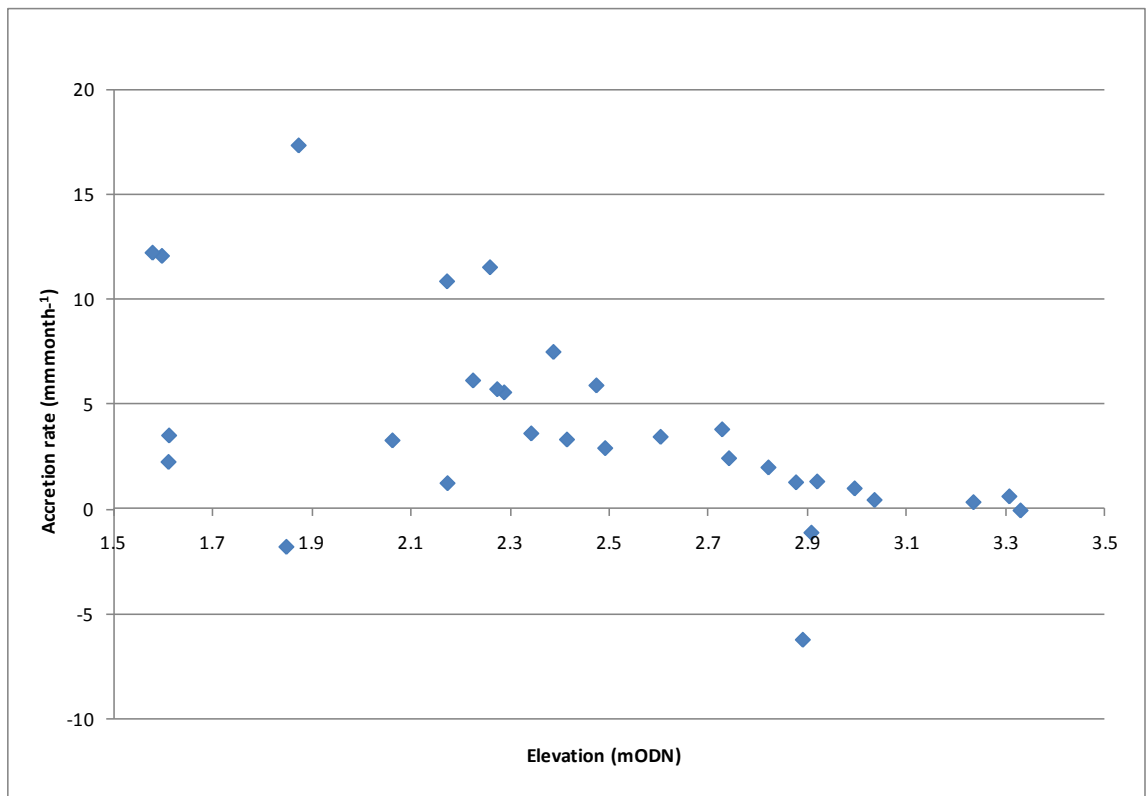
Figure 4.9: The accretion rate against elevation across PHS for the period Feb 2006- Sep 2007.
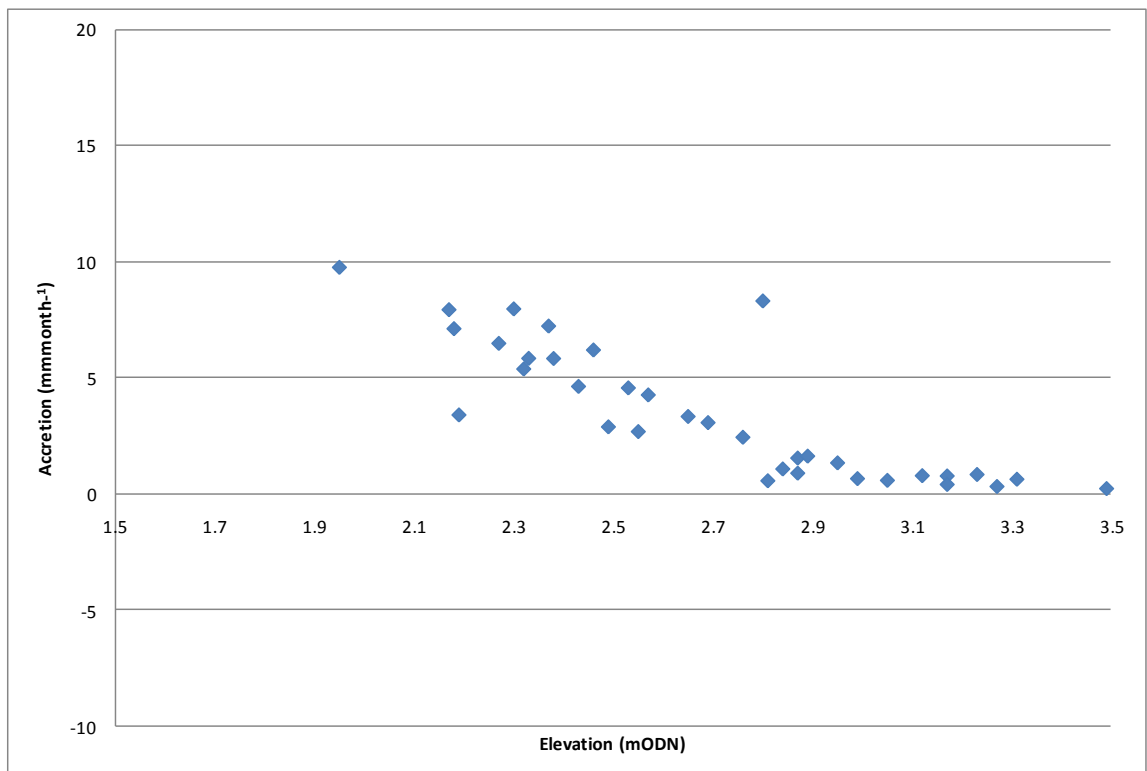
Figure 4.10: EA data for the period Feb 2006- Sep 2007. The accretion rate against elevation across PHS.

The relationship between accretion rate and elevation for the EA monitoring data also shows a clear trend with rapid accretion on sites at lower elevations (see Figure 4.10).

These data do not show as much variation at the lowest elevations as in the present research. However, none of the EA sites was lower than 1.9 m ODN which is where most data variation had been recorded in the present research (see Figure 4.9). The few outlying data points within the EA monitoring stations were at 2.2 m ODN and 2.8 m ODN.

The Pearson's correlation between accretion rate and elevation for just the SE sector (including the EA monitoring data) is -0.777, significant at P = 0.000. This is a more significant correlation than for the whole site indicating that the accretion rates recorded on the SE sector are most closely linked to the elevation of the site.

4.3 Spatial patterns of accretion

Sediment on the NW sector was accreting faster than on the SE sector, and sediment at sites closest to the NW breach appear to be either eroding or accreting rapidly depending on their location. The SE sector will not be considered in great detail as the accretion rates were relatively slow and very significantly linked to elevation alone. However, the accretion rates on the SE sector still require examination as the area was accreting faster than the mudflat sites monitored by the EA in front of the realignment site.

Figure 4.11 is an interpolation of the monthly accretion data incorporating EA data and results from this study. Details on the interpolation method and the GIS software used can be found in section 3.5. The interpolation map is superimposed over an elevation map of the NW sector. Further details on the areas referred to are found on Figure 3.3, Chapter 3.

Figure 4.11 shows the fastest accretion rate of 16-19 mm each month close to the NW side of the NW breach. Other areas of fast accretion were in the northern tip of the site and near to the bend in the embankment on the eastern side. These areas had rates of accretion around 7-10 mm each month. The areas that were eroding or accreting at very slow rates are directly behind the NW breach and halfway along the western edge of the site. Areas accreting fairly slowly for this sector at 1-4 mm per month were mainly in the eastern and western corners of the site. This rate of accretion was still fast for an area of mudflat and so classing it as 'slow accreting' is relative.
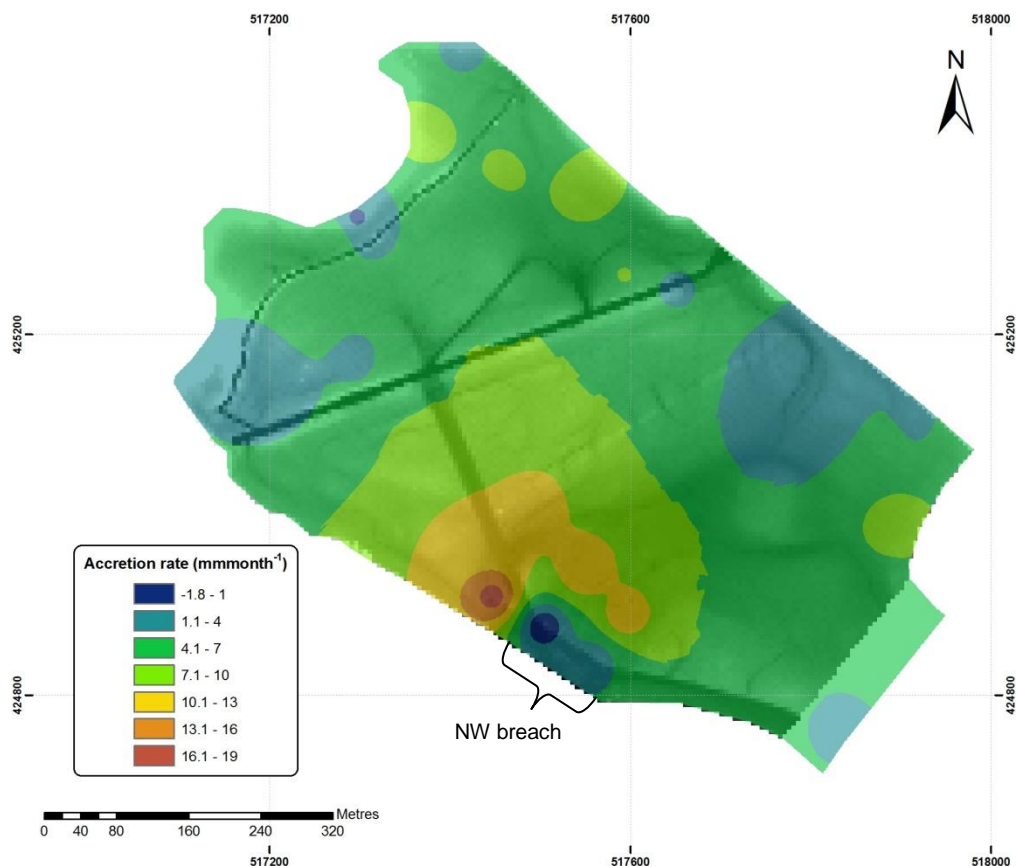
Figure 4.11: Interpolated map of the overall monthly accretion levels on the NW sector of PHS- both EA data and the present research.

4.4 Conclusions

From the results presented and discussed above it can be seen that PHS is still accreting at a fast rate when compared to other realignment sites opened in the UK. Some slowdown in this rate has been noted in the EA monitoring results however over the 19 month period of data collection, no such slowdown was in evidence, only a difference between seasons. The fastest accretion rates were present on the NW sector, particularly in the area to the NW of the breach. There was also fast accretion in the northern areas of the sector and the eastern area close to the new embankment. The SE sector was accreting at a slow but steady rate that is faster than the rate of accretion on the mudflat in front of the site. This accretion in the SE sector can almost solely be explained by the elevation of this sector. In the NW sector, elevation of the site does play an important part in the levels of sediment change seen, however it does not completely explain all of the fast accretion. For this to be explained properly more has to be understood about the other factors that control accretion and erosion as listed in Table 2.2, Chapter 2. Firstly, though an understanding of the source of the sediment accreting on the site is needed-this is provided in the next chapter.

Chapter 5 : Sediment net fluxes and inundation times

5.1 Introduction

This chapter discusses the sediment fluxes through the NW breach, the sediment load required for the accretion rates presented in Chapter 4, and the amount of tidal inundation across the site. Section 5.2 details the results from hydrodynamic surveys at the NW breach and the SPM concentration on six tides. Section 5.3 presents a sediment budget for a full year on PHS. Section 5.4 is a comparison of the sediment budget to the amount of sediment accreted on the NW sector for a year, calculated using accretion data. Section 5.5 presents the inundation patterns on the site.

The rapid accretion rates recorded, particularly across the NW sector, are sustained by a net flux of sediment onto these areas. This sediment could be derived from the erosion and reworking of sediment within the site feeding the depositional areas. This is unlikely due to the generally small and restricted pattern of erosion on the site. It is more likely that accretion is being driven by a net flux of sediment into PHS through the breaches, in particularly the larger NW breach that is closest to the fastest accreting areas (see Figure 3.4, Chapter 3). For a net flux into PHS to occur, there needs to be more sediment entering the site through this NW breach on the flood tide than is leaving on the ebb tide. Due to the effects of settling lag, this sediment entering the site is deposited when the tidal velocity drops inside the site and is not entrained on the ebb tide as the velocity rises again. Sediment flux is influenced by the volume of water entering and leaving the site, the amount and size distribution of the SPM, the velocity of the tide and the inundation time of the tide on the site (Balson, *et al.*, 2004; Black, 1998; Christie, *et al.*, 1999; Dyer, 1986; Masselink, *et al.*, 2003; Raudkivi, 1998).

The time and depth of inundation of PHS by the tide controls the type and amount of vegetation that can colonise the mudflat. For saltmarsh species to establish, the ground surface needs to be more exposed than it is flooded. A pioneer zone limit is at 40% inundation, anything below this limit will sustain a growing number of saltmarsh species up to 10% inundation sustaining middle and high marsh species (Boorman, 2003).

5.2 Net fluxes for tides through the NW breach

A spectrum of tidal and SPM data was collected during the monitoring period to observe different tide heights. For three tides, full data for velocity profiles and SPM

gulp samples were collected. These were for 0.48, 1.18 and 1.48 m high tides and these have been used to extrapolate net sediment flux data for the whole range of tides at the NW breach. The high tide depth refers to the mean depth across the full NW breach, calculated using the topographic map of the site and the KGD tide data (see section 2.2.8, Chapter 2). Further gulp samples to study the SPM were collected, comprising high tides of 1.28, 1.98 and 2.78 m.

5.2.1 Tidal velocity

The mean tidal velocities calculated from ADP data collected during surveys on the 16/08/2006 (1.48 m), 19/07/2006 (1.18 m) and 11/05/2007 (0.48 m) are shown in Figures 5.1 (a)-(c) below.
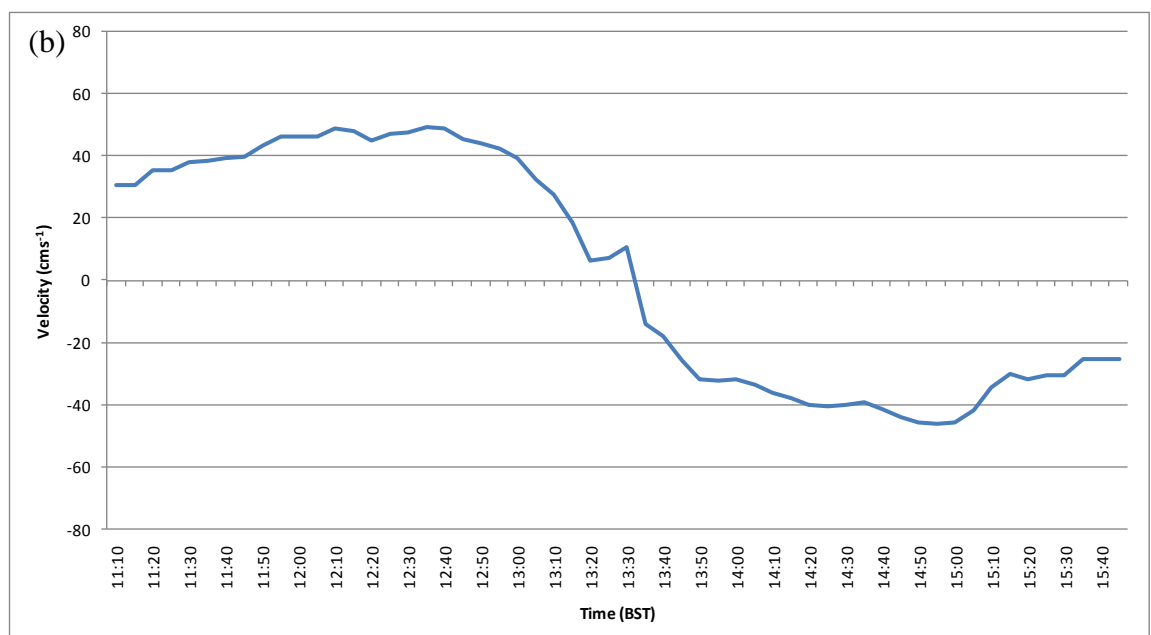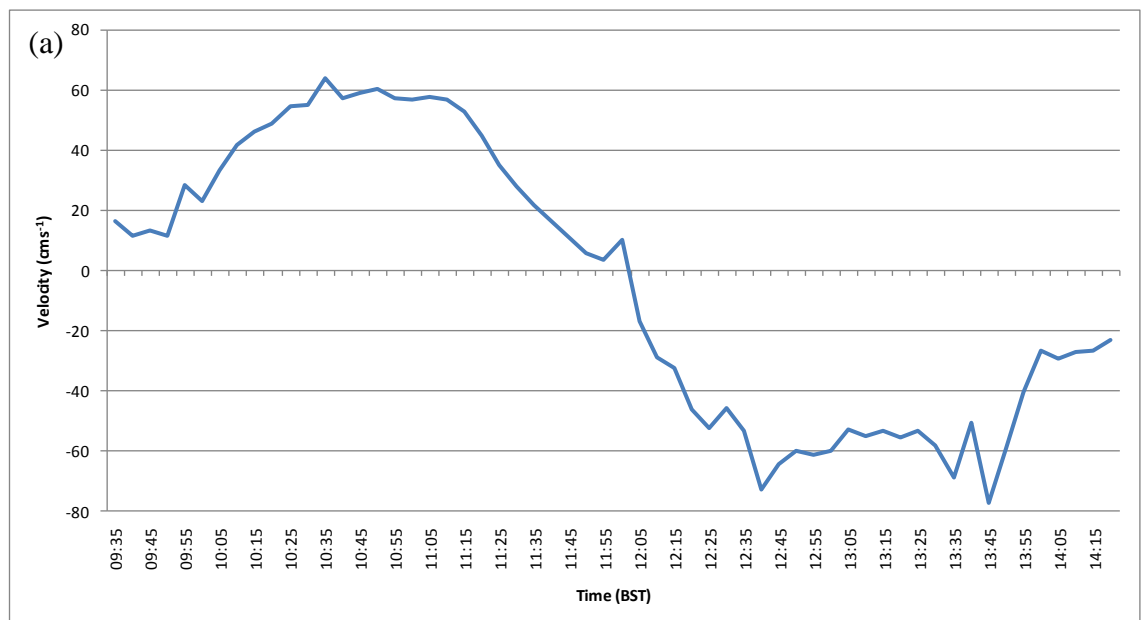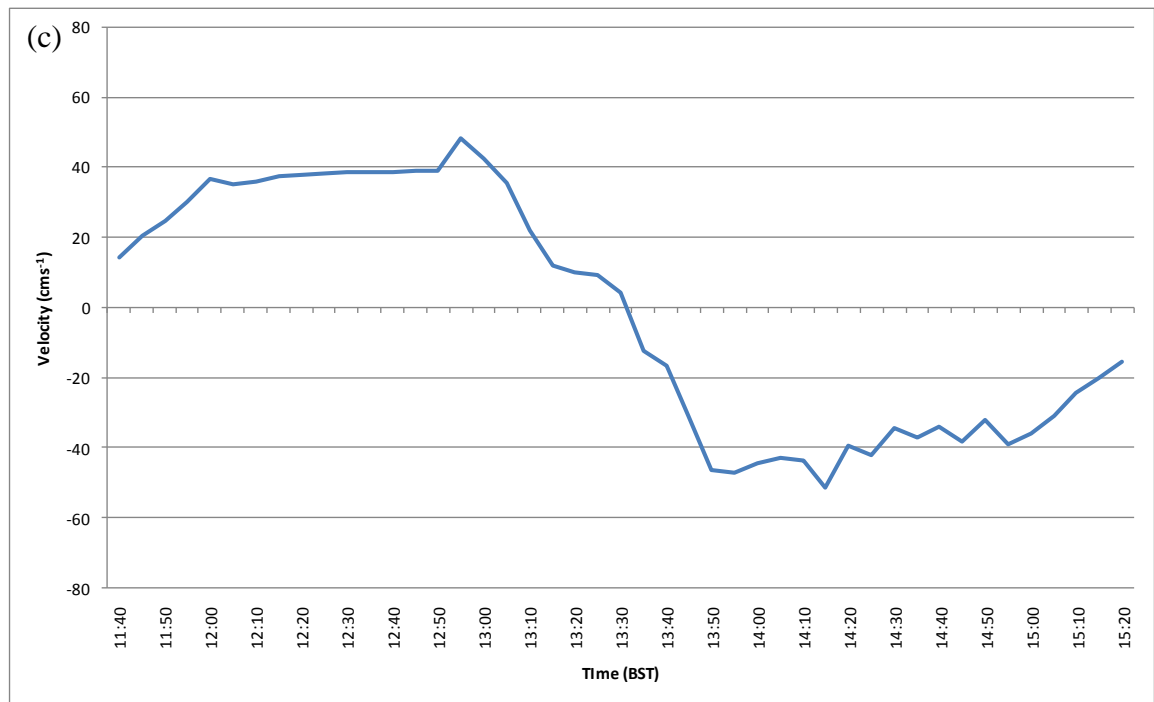
Figure 5.1: Mean tidal velocities during a tide at the NW breach on PHS, (a) during a 1.48m high tide on 16/08/2006, (b) during a 1.18m high tide on 19/07/2006, (c) during a 0.48m high tide on 11/05/2007.

Figures 5.1 (a)-(c) show the sinusoidal form associated with tidal velocity. The tidal flow was slow to start at the onset of flooding, rose to a peak about an hour after the water first entered the NW breach, then dropped to its slowest at slack water an hour later. The tide then changes direction as it ebbs, reaching peak velocity about an hour later and slowing towards the end of the tide. The tidal cycle on PHS lasts approximately four and a half hours.

A peak velocity of 80 cms^{-1} was reached on the largest tide (1.48 m, see Figure 5.1 (a)), both during flood and ebb. This large tide was on site at least 10 minutes longer than the smaller tides. The second largest tide achieved peak velocities of 50 cms^{-1} on flood and ebb whilst the smallest tide on site (0.48 m, Figure 5.1 (c)) achieved peak velocities of only 45 cms^{-1}.

5.2.2. SPM concentrations and water depth through the NW breach

The net SPM flux is dependent on the cross-sectional area of the breach and the sediment supply from the Humber estuary determining the transport capacity into and out of the NW breach. The cross-sectional area and flow velocity dictate the volume of water flowing into PHS and this is dependent on the water depth which is influenced by the stage in the tidal cycle and time of year. The sediment supply is also affected by the time of year and weather conditions in the Humber estuary (Balson, *et al.*, 2004;

Huntley, *et al.*, 2001; Pritchard, 2005; Wu, *et al.*, 1998). As was seen in the previous section, a larger cross-sectional area is associated with faster tidal velocities and thus larger sediment loads. The larger cross-sectional area means a greater volume of water entering the NW breach and if this is flowing faster, a greater volume of sediment may be entering the site during spring tides and vice versa during neap tides. Figures 5.2 (a)-(f) below indicate the actual water depth across the NW breach and SPM through the breach during six tidal cycles at PHS.
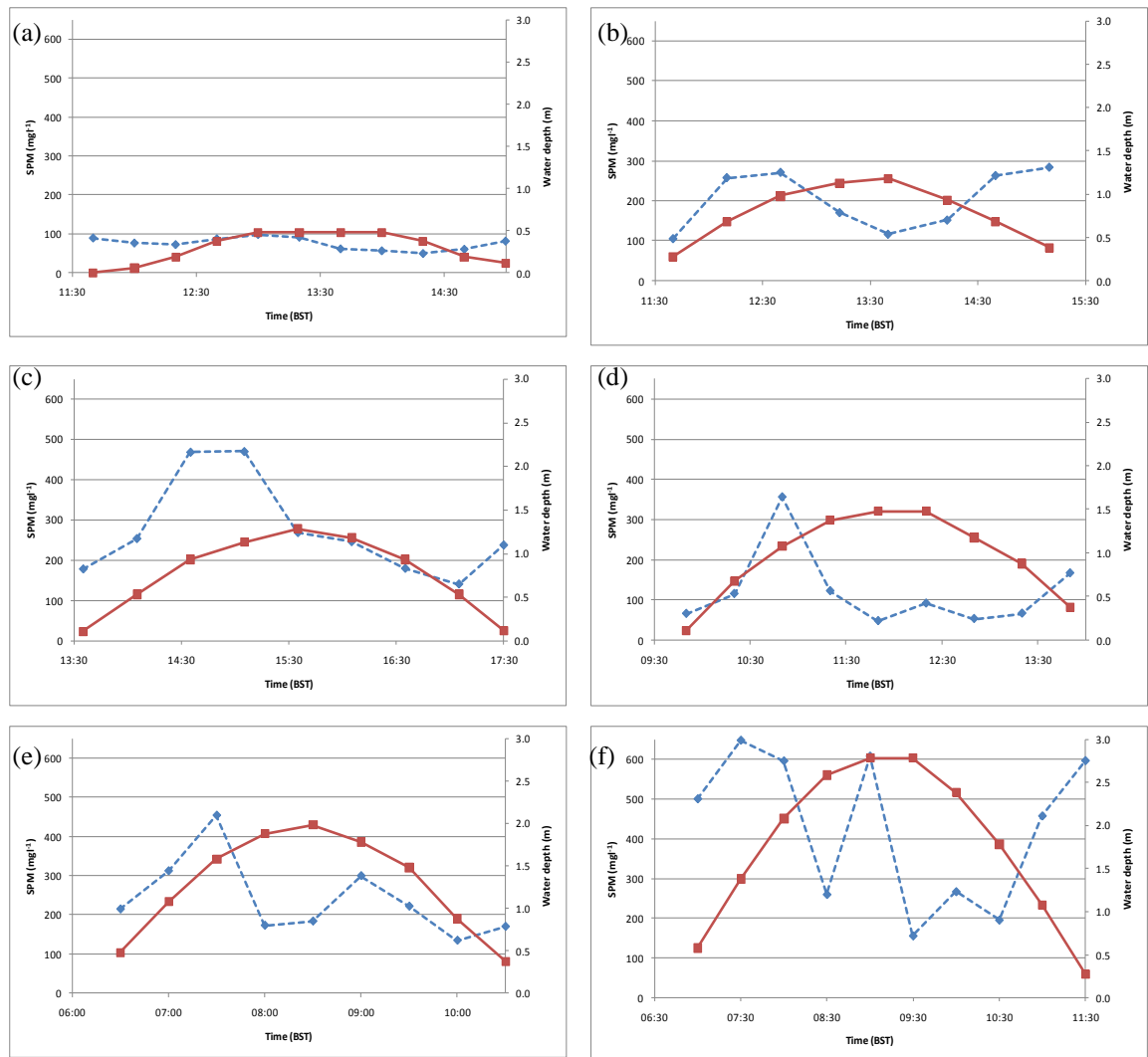
Figure 5.2: SPM (blue) and mean water depth (red) at the NW breach on PHS, (a) during a 0.48m tide on 11/05/2007, (b) during a 1.18m tide on 19/07/2006, (c) during 1.28m tide on 23/05/2006, (d) during a 1.48m tide on 16/08/2006, (e) during a 1.98m tide on 14/09/2007 and (f) during a 2.78m tide on 11/09/2006. Full data are presented in Appendix 4.

The basic pattern of SPM concentrations indicate that on all tides the SPM reaches a peak just prior to high water, dropping during the slack period as the tide turns, and then rising again on the ebb tide. This reflects the velocity data as faster velocities transport the larger SPM concentrations on the flood and ebb tides but slower velocities at slack

water led to settling of sediment and thus the SPM concentration drops, even though the water is at its deepest at this point. The largest quantity of SPM ($\sim$ 650 mgl^{-1}) was associated with the biggest tide (Figure 5.2 (f)), however the second largest SPM amount ($\sim$ 500 mgl^{-1}) was associated with the 1.28 m tide (Figure 5.2 (c)). The second greatest tide of 1.98 m had an associated peak in SPM concentration of approximately 450 mgl^{-1} (Figure 5.2 (e)). The sediment deposited on the 1.48 m tide (Figure 5.2 (d)) was fairly small ($\sim$ 350 mgl^{-1}), especially when considered in conjunction with the fast flow velocities through the breach during this tide (Figure 5.1 (a)). This could be due to a number of factors affecting the overall capacity of the tide on this day such as dredging in the estuary, prevailing weather conditions and season.

5.2.2.1 Differences in sediment load for similar tides

The peak SPM concentration on the 1.18 m tide is consistent with three other tides; however the 1.28 and 1.48 m tides are outliers from the relationship. Full SPM patterns for each tide are shown in Figure 5.3 below.
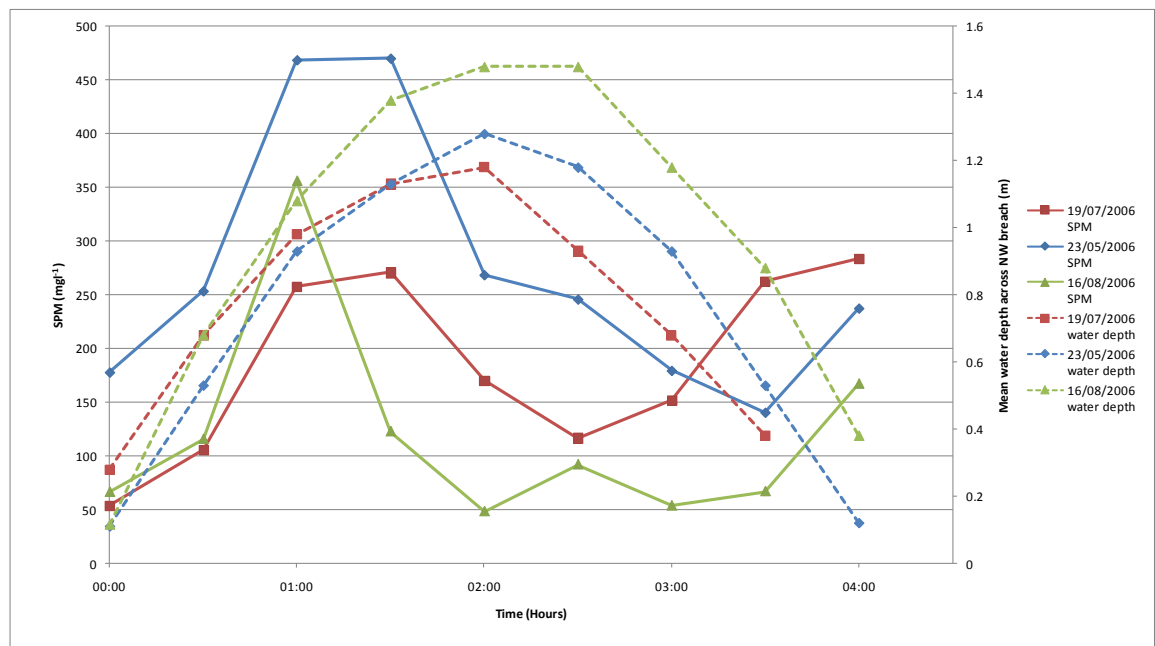
Figure 5.3: Comparison of SPM concentration recorded at the NW breach of PHS during three tides.

During the tidal cycle on the 23/05/2006, the peak SPM values of $\sim$470 mgl^{-1} occur prior to high tide and were very large compared to the other two tides which achieved peaks of $\sim$350 mgl^{-1} and $\sim$270 mgl^{-1}. The SPM concentration for the average tide of this height was closest to data from the 19/07/2006. The SPM concentrations during 16/08/2006 should be the largest out of the three shown on Figure 5.3 as this was the tide with greatest water depth and fastest velocity. This is not the case, apart from the

119

peak SPM concentration being slightly larger than the peak on the 19/07/2006, the rest of the SPM data points were small.
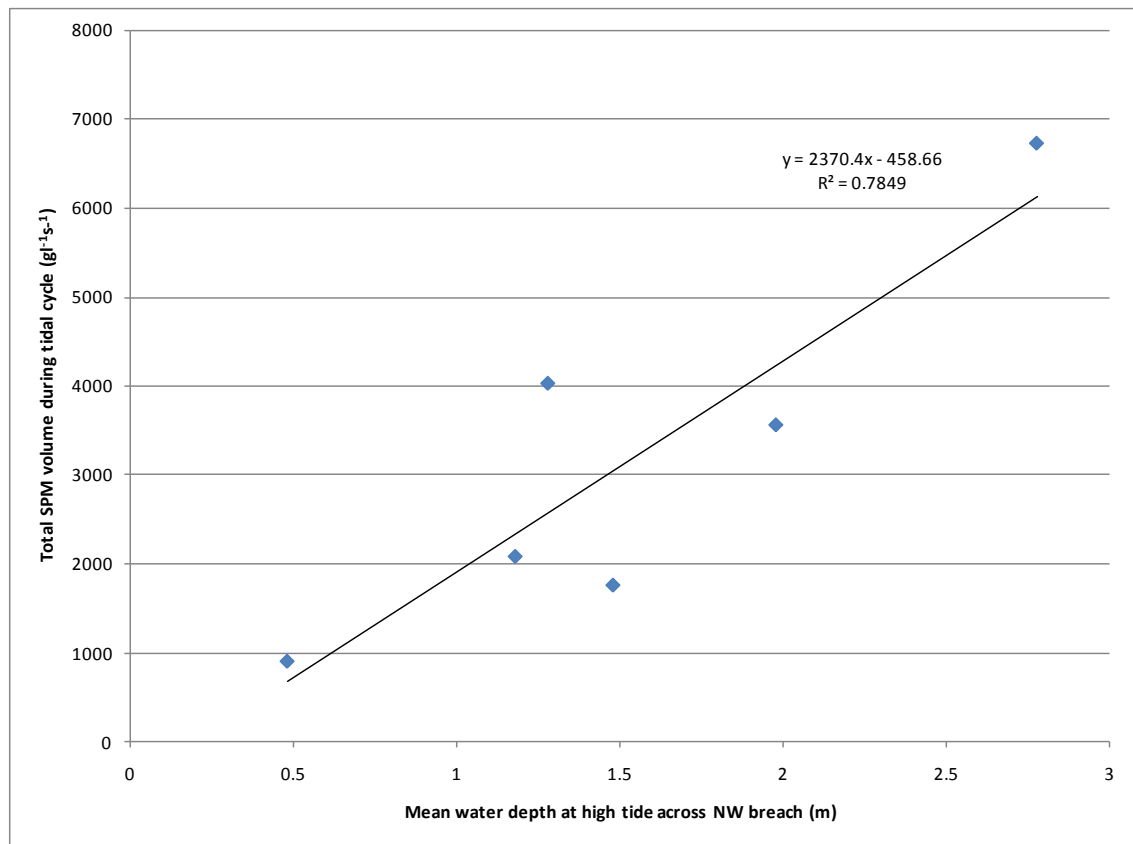
Figure 5.4: Relationship between SPM flux ($gl^{-1}s^{-1}$) and the mean water depth across six tides through the NW breach on PHS.

To give some indication of the volume of sediment measured during each tidal cycle and the relationship with mean tidal height across the NW breach, SPM concentration was integrated for the length of time the tide was on site. The results from integrating the SPM load during the six tidal cycles are shown in Figure 5.4, above. The SPM fluxes recorded for the same two tidal cycles on the 23/05/2006 and 16/08/2006 are again larger and smaller than predicted by the relationship between the remaining four SPM fluxes. When calculating the SPM flux for the two tides, the data for the 23/05/2006 are 64% larger than expected and the data for the 16/08/2006 are 57% smaller. Taking an average of both SPM fluxes over the full tidal cycle and of the mean tidal height produces an average point shown in red (Figure 5.5, below).
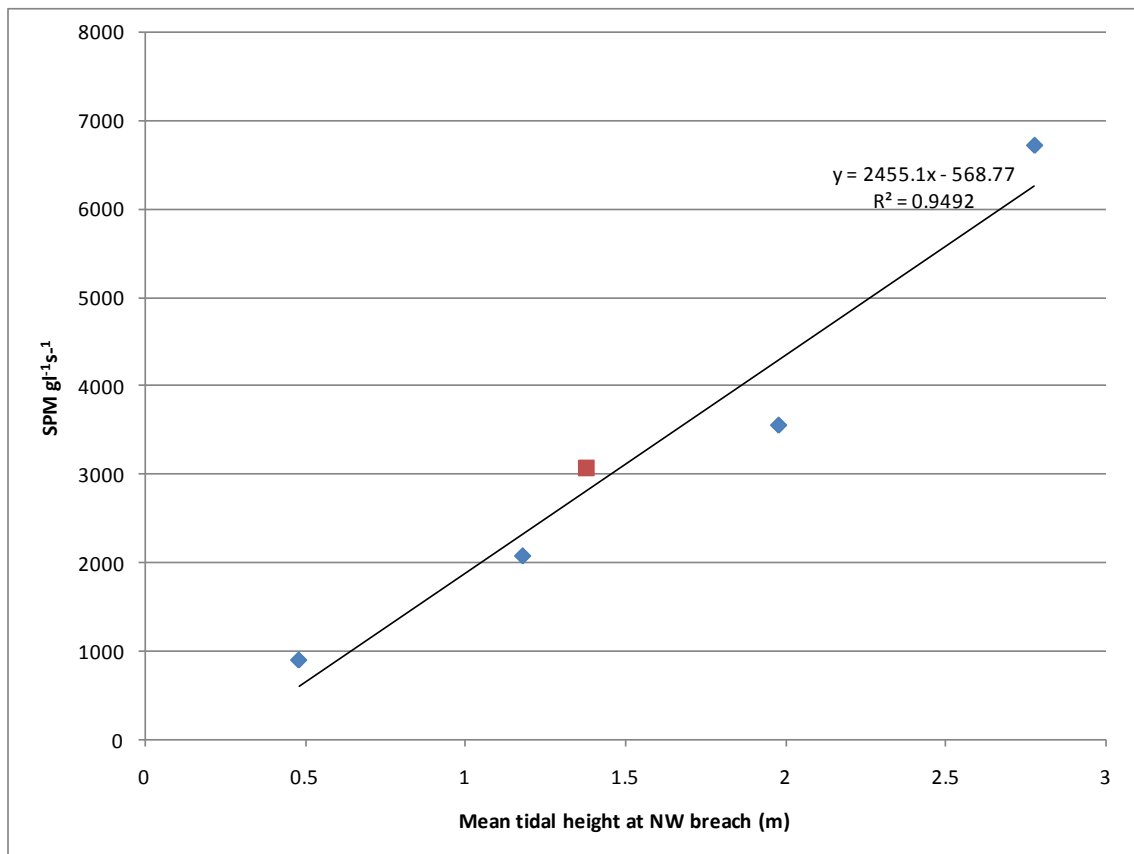
Figure 5.5: Relationship between SPM flux ($gl^{-1}s^{-1}$) and the mean water depth across six tides through the NW breach on PHS, mean value for 1.28 and 1.48 m high tides shown as red square.

Taking a mean of the SPM load and high tide depth moves the data set towards a very strong relationship with an R^2 value of 0.9492. This average was deemed necessary as the relationship created by using the average from the two datasets is stronger and will produce a more realistic sediment budget. As the other points clearly indicated a strong linear relationship, the data for the two tides that did not fit this relationship were averaged. Both datasets were for very similar tide heights and fell above and below the relationship by a similar percentage, as discussed above and so the averaging of these two values was deemed as adding to the validity of the relationship.

5.2.3 Net tidal flux for three tides

Using the velocity data combined with the SPM concentrations and known water depths across the full NW breach, a net tidal flux of water and sediment has been derived. This has been done for the tides of 11/05/2007 (0.48 m), 19/07/2006 (1.18 m) and the 16/08/2006 (1.48 m).

Full data to calculate all the tidal fluxes are presented in Appendix 5.

121

Table 5.1: Net tidal flux data for water and sediment at the NW breach of PHS during three tides.

	11/05/2007	19/07/2006	16/08/2006
Mean water depth at high tide across NW breach (m):	0.48	1.18	1.48
Water volume on flood tide (m^3s^{-1}):	253	869	1139
Water volume on ebb tide (m^3s^{-1}):	269	854	1222
SPM on flood tide (t):	22.5	200.7	338.3
SPM on ebb tide (t):	15.6	161.1	200.2
Tidal SPM (t):	6.9 ± 2.4 (34.3%)	39.7 ± 5.2 (13.1%)	138.1 ± 24.3 (17.6%)

Each tide carried more sediment into the NW of PHS than was removed on the ebb tide (see Table 5.1, above). Even for the smallest tide on the 11/05/2007 (0.48 m) 6.9 t of sediment was deposited on the site. During the largest tide on the 16/08/2006 (1.48 m) 138.1 t of sediment remained in the site and for the mid-range tide on the 19/07/2006 (1.18 m) 39.7 t were deposited on site. The errors given for the tidal SPM are calculated from the difference between the amount of water present during the flood and ebb tide as this should be completely equal. The biggest error is 34.3% for the smallest tide, the small amount of sediment deposited during this tide is accompanied by large errors, however even allowing for the maximum error of 2.4 t the tidal SPM is still positive. This does indicate that for smaller tides only a very small amount of sediment is retained on site, or on some tides, net sediment erosion from the site. The bigger tides of 1.18 m and 1.48 m have errors of 13.1% and 17.6% respectively. These errors are small compared to the values of SPM observed and the values give a measure of net SPM that have been used to calculate a yearly sediment budget for the NW sector.

5.3 Sediment budget for full year on PHS

5.3.1 Tidal data for full year

Tidal data for the nearest point of King George Dock (KGD), Hull was downloaded from the TotalTide Admiralty software package (UK Hydrological Office). This gives the details of the water heights every ten minutes for this location. The data covered a year from July 2006 until July 2007, incorporating most of the accretion monitoring and tidal surveying period. Using these data, the tidal heights across the NW breach were calculated using the conversion discussed in Chapter 3, section 3.2.8.

Table 5.2: Water depth statistics for a full year across the NW breach on PHS.

Statistic	Water depth (m) at high tide across NW breach
Mean	1.2
Median	1.18
Mode	1.38
Range	0 - 2.98

The mean water depth at high tide across the NW breach for a year (see Table 5.2, above), was 1.2 m, the median was slightly smaller at 1.18 m. The mode was larger at 1.38 m, and the range was 0 to 2.98 m. On some tides water does not reach the breach, this was the case for three tides between July 2006 to July 2007 (see Figure 5.6, below). During very small tides, for example 0.1 and 0.2 m mean water depth at high tide, there will only be a very small percentage of the site inundated and thus very small sediment fluxes. This has already been indicated by the small sediment flux recorded for the 0.48 m tide discussed in section 5.2.3.
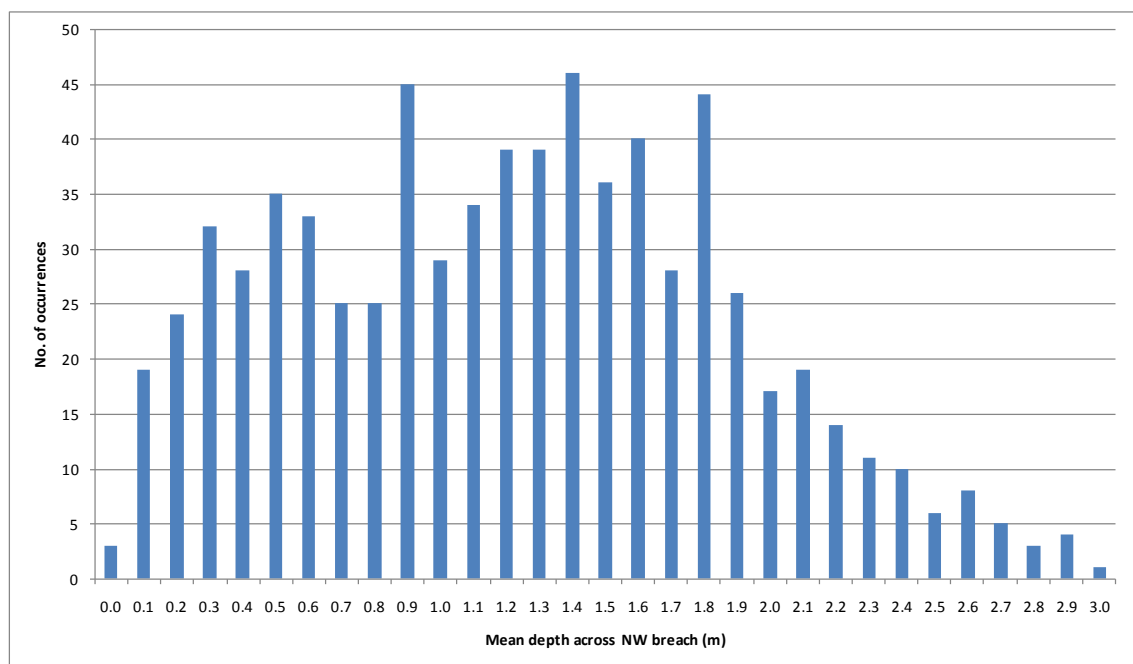
Figure 5.6: Frequency of each high tide during a year.
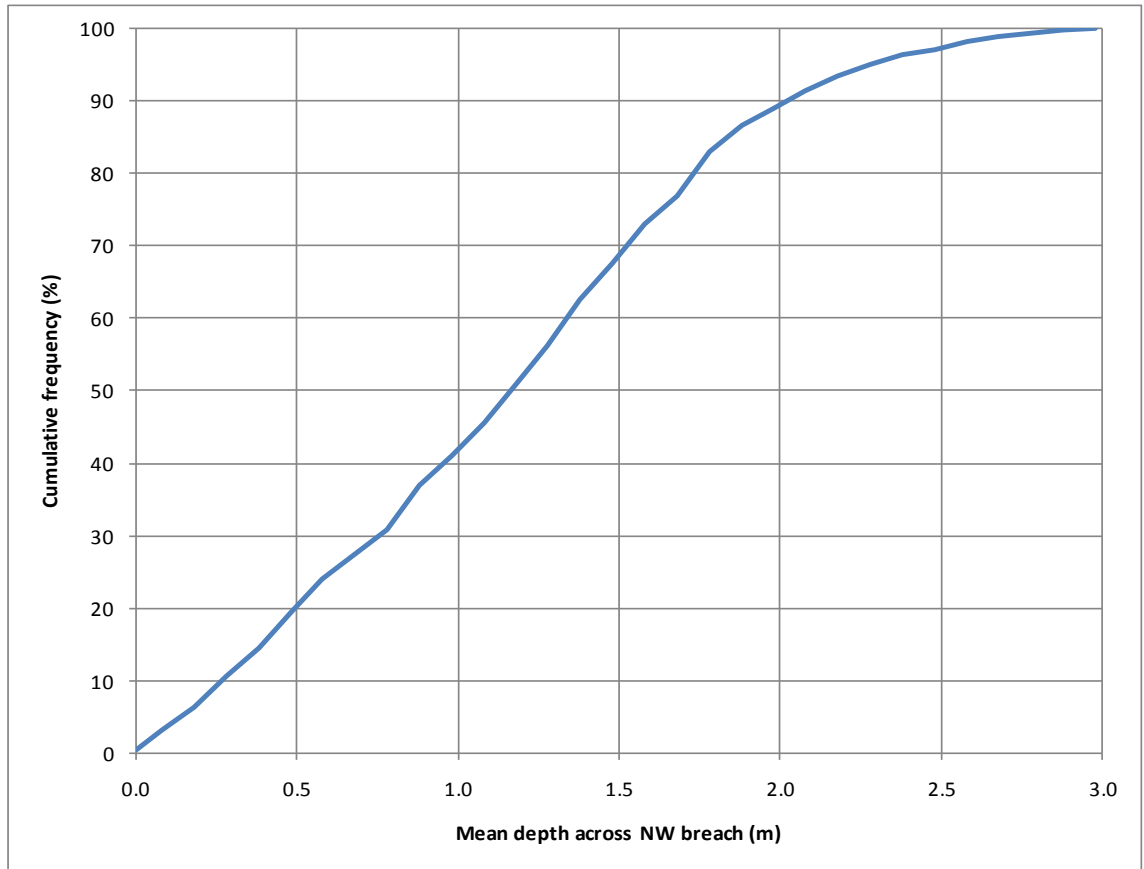
Figure 5.7: Cumulative frequency of high tides throughout a year.

Approximately 90% of the tides through the NW breach were less than 2 m in depth at high tide (see Figure 5.7, above). Even though the biggest tides were over 2.5 m deep at high tide throughout the year, these were infrequent and occurred only during spring tide cycles. Over 50% of the tides were between 1 and 1.5 m deep at high tide, which is reflected in the statistics in Table 5.2, above. The three most common water depths at high tide were 0.9, 1.4 and 1.9 m (Figure 5.6, above).

5.3.2 Estimated tidal fluxes for remaining recorded SPM values

The SPM data were used with the velocity data to estimate further net sediment fluxes for a wider range of tides. The mean data from the 1.28 and 1.48 m tide was used in conjunction with the velocity from the 1.18 m tide. The SPM data from both the 1.98 and 2.78 m tide was used with velocities from the 1.48 m tide.

Table 5.3: Net sediment flux data at the NW breach of PHS during three tides, using velocity data from the 19/07/2006 and the 16/08/2006.

	23/05/2006	14/09/2007	11/09/2006
Mean water depth at high tide (m):	1.28	1.98	2.78
SPM on flood tide (t):	263.4	626.4	1563
SPM on ebb tide (t):	138.7	447.8	918.3
Tidal SPM flux (t):	124.7 ± 28.7 (23.0%)	178.6 ± 32.2 (18.0%)	644.7 ± 77.0 (11.9%)

The bigger tides (see Table 5.3, above), although infrequent, provide the largest quantity of sediment to the site. The very deep spring tide of the 11/09/2006, close to the peak high tide recorded for the year, resulted in a positive net load of 644.7 (± 77) tonnes on each tide.

The errors (calculated from the errors in water volume flux as discussed in section 5.2.3) in these calculations are fairly small for the 1.98 m and 2.78 m tides, 18.0% and 11.9% respectively. The 1.28 m tide has a bigger error of 23.0%, which equates to the tidal SPM load of 124.7 potentially being different by 28.7 t either way.

The relationship between all six sediment loads through the NW breach and water depth at high tide has a linear trend and can be described by Equation 5.1 (see Figure 5.8, below).

$$y = 1.8512x + 1.67$$

Eq. 5.1
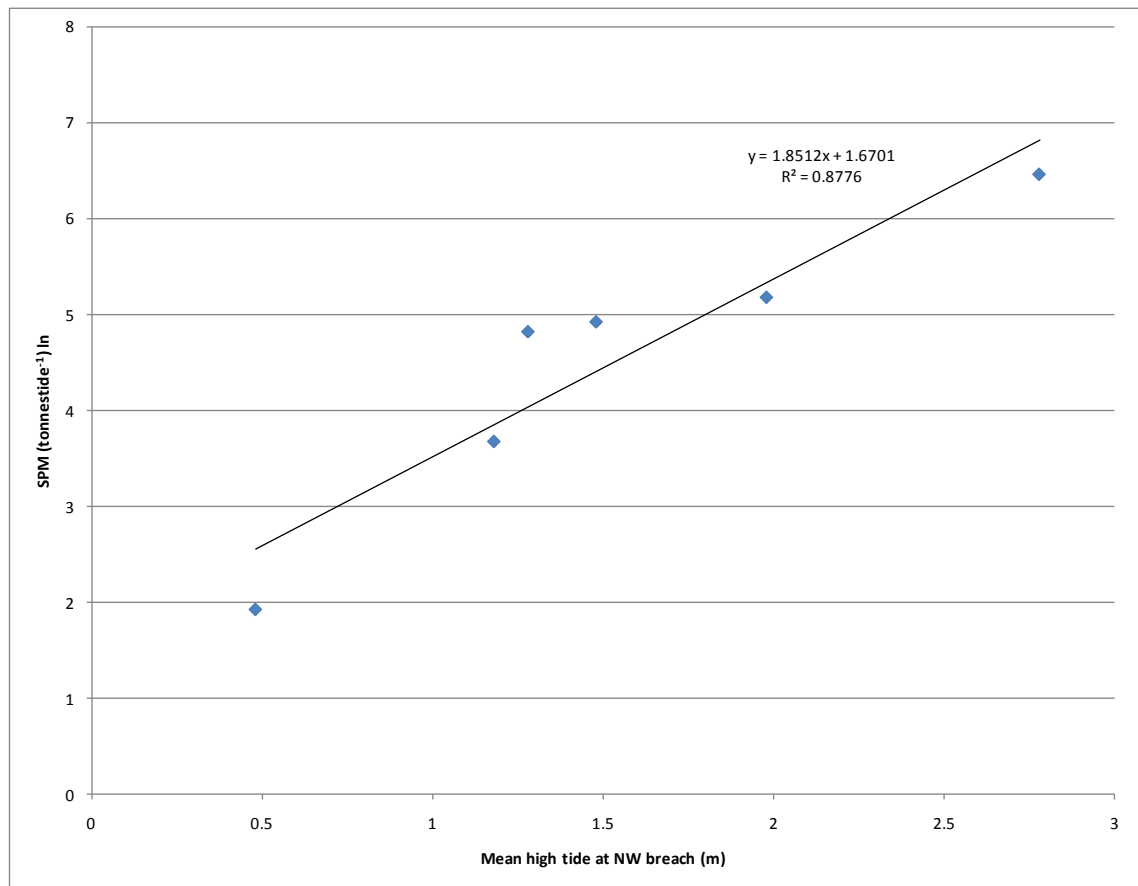
Figure 5.8: Relationship between all net sediment loads deposited and water depth at high tide at the NW breach on PHS.

Using equation 5.1 and the high tide data from section 5.3.1, a sediment budget for a full year has been produced.

5.3.3 A year's sediment budget

The sediment budget for the full year through the NW breach gives a positive result which was inevitable given the calculations of positive net sediment loads for the six SPM datasets in the previous sections (see Figure 5.9, below). The mean SPM deposited in the NW sector was 2113.6 t. The maximum amount deposited of 5373.3 t was during tides that had a maximum mean water depth at the NW breach of 1.78 m. This water depth occurred frequently throughout the year (see Figure 5.6, above), however was not the most frequent. The two tide heights with a greater occurrence were smaller (0.88 and 1.38 m) and so did not contribute as big a share to the overall sediment deposited. Approximately 50% of the sediment deposited on the NW sector was provided by tides that were 1.9 m deep or less at high tide (see Figure 5.10, below). Tides that were 1 m deep or smaller during high tide provided 10% or less of the sediment load. Tides

greater than 2.5 m deep at high tide (which occurred less than 5% of the time, see Figure 5.6) accounted for 20% of the total yearly sediment load.

The amount of sediment entering the site in a year calculated from sediment flux data was 63 400 tonnes (sum of SPM total from Figure 5.9, below). A comparison is now made between this sediment budget and the amount of sediment accreted on the site during the same time period.
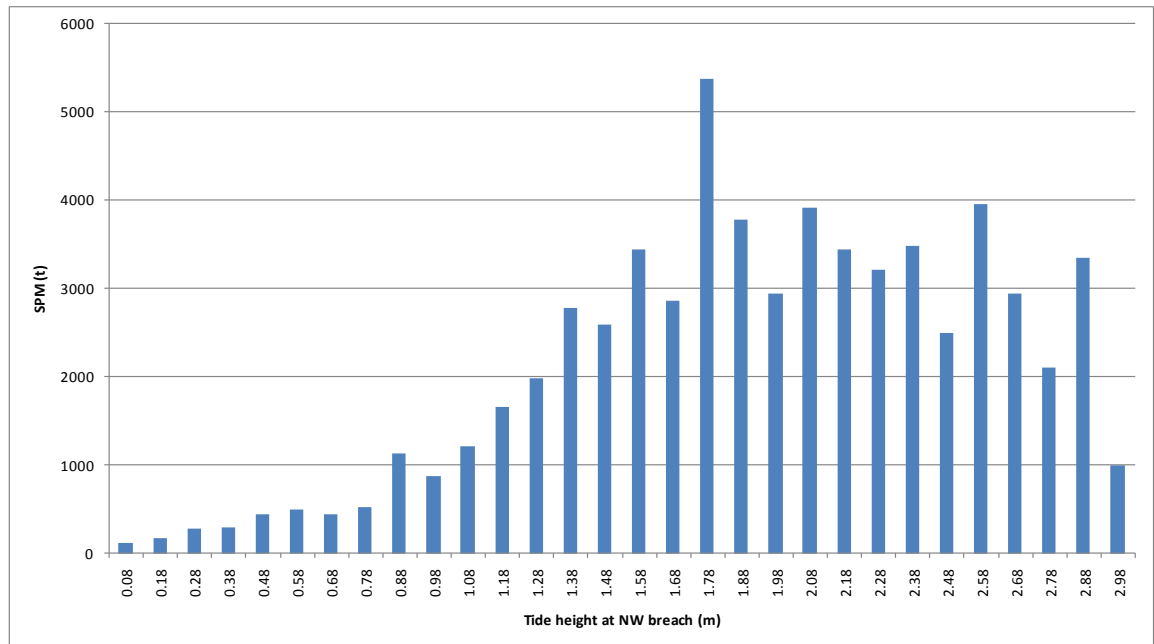
Figure 5.9: Amount of sediment deposited on the NW sector of PHS during every tide for a year.
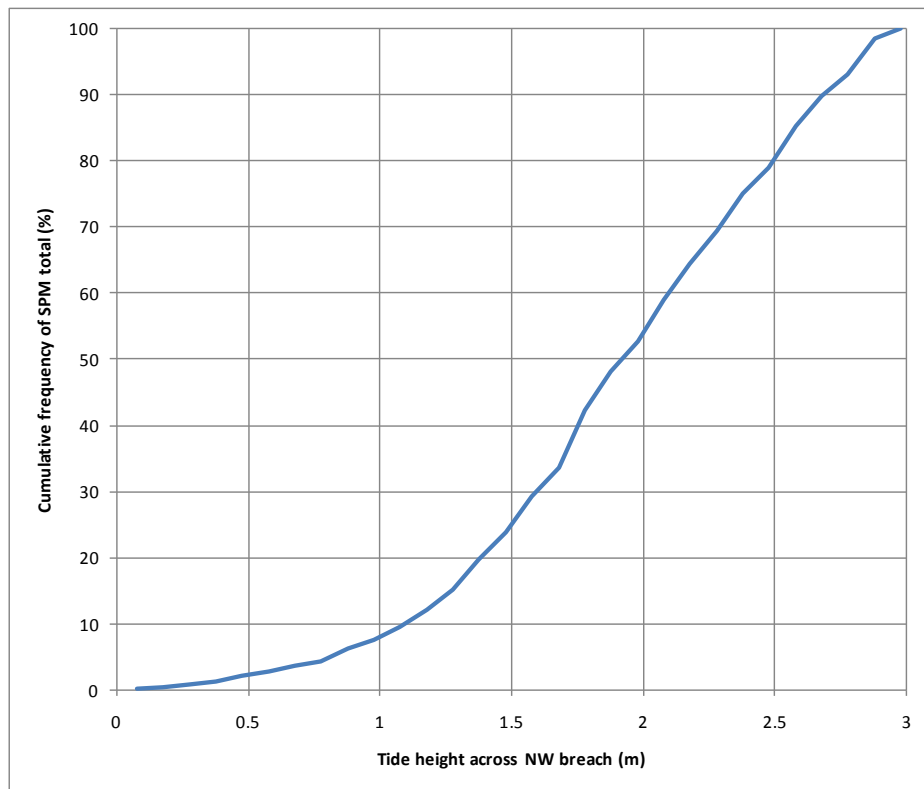
Figure 5.10: Cumulative frequency of SPM deposited over the NW sector throughout a year.

5.4 Comparing net sediment loads with accretion values across the NW sector

Using the mean accretion rate for each sampling site on the NW sector, an interpolation of the rates of accretion across the area was produced. Only this sector is being investigated as it was here where the most variation in accretion rates was found and also where the fastest accretion rates were recorded. The sediment budget presented above was for fluxes through the NW breach so it is expected that the sediment coming through this breach will be deposited in the NW sector. From the interpolation of accretion rates and utilising wet bulk density values (to be presented in chapter 5), an idea of the amount of sediment required to sustain such accretion rates is given. This can then be compared with the sediment budget presented in section 5.3.3.
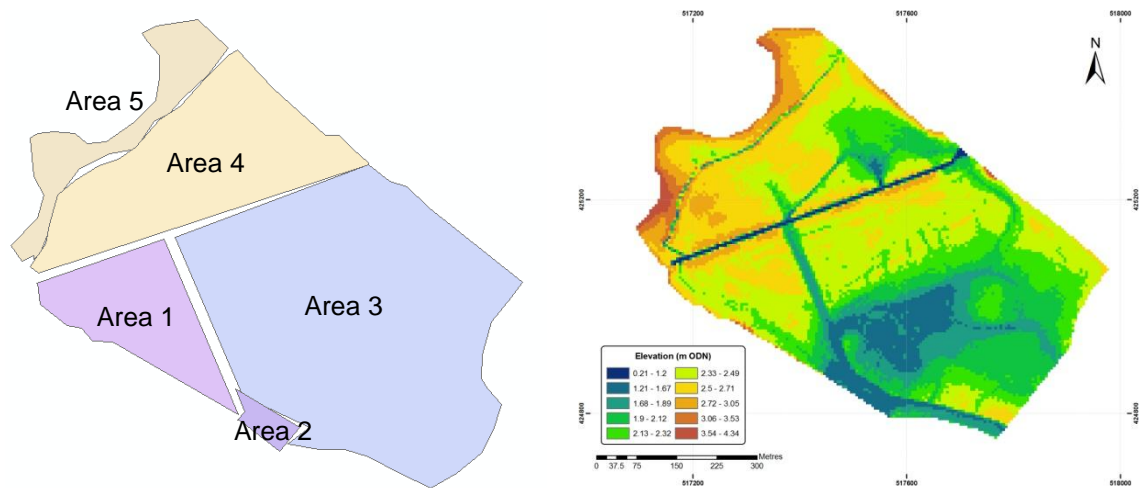
Figure 5.11: Areas of the NW sector of PHS used to interpolate bulk accretion; elevation map shown to highlight areas split along drainage channel boundaries. Blue areas on elevation map have lowest elevations.

The NW sector for the purpose of this calculation was divided into five areas (see Figure 5.11, above) so that a more accurate interpolation of the accretion rate across each area could be used. The areas were divided along channel boundaries as these influence the sedimentation patterns and most closely represent the sedimentation patterns. Area 2 contains the eroding sites so that values from faster accreting sites IN Areas 1 and 3 were not skewed.

Each area was interpolated using Arc GIS software and the IDW (inverse distance weighed) method of creating a surface (for more details see Chapter 3, section 3.5) to calculate a mean accretion rate.

Table 5.4: Calculating the bulk sediment present on the NW sector of PHS from interpolated accretion rates.

	Area 1	Area 2	Area 3	Area 4	Area 5
Area (m^2)	43032	4723	202862	89820	29583
Accretion rate (cma^{-1})	14.45	1.57	7.19	6.52	5.56
Wet bulk density (gcm^{-3})	1.74	1.81	1.69	1.72	1.68
Mass of sediment (t)	8823	183	26536	10684	2931
Daily sediment load (t)	24.2	0.5	72.7	29.3	8.0

The total daily sediment load required to sustain the recorded rates of accretion over the NW sector was 135 tonnes (see Table 5.4, total of daily sediment load, above). This equates to a yearly sediment load of 50 000 tonnes of sediment being deposited on the NW sector. This compares with the 63 400 tonnes of sediment estimated as deposited

on the site from previous sediment budget calculations. These two estimates of the amount of sediment being deposited on the NW breach either from hydrodynamic and SPM data or from accretion rates and bulk density values are closely comparable. To be able to predict the amount of sediment deposited on a managed realignment site using a small number of hydrodynamic and SPM surveys is extremely useful during the first years after breaching and offers an alternative to continuous monitoring of sediment level change as it occurs.

The sediment budget estimate is larger than the estimate of sediment load on the NW sector from accretion/erosion rates by 13 400 tonnes (26.8%). Some of this difference may be accounted for by sediment being deposited on the SE sector during very big tides. To improve the sediment budget prediction a wider range of hydrodynamic data is required, particularly for the bigger tides that carry the larger sediment loads into the site. The calculation of the net sediment flux for each tide had associated errors (see sections 5.2.3 and 5.3.2) that can be reduced with repeat data for a particular tide height to provide a mean tidal velocity and SPM load. However, the largest error of 34.3% was for the smallest tide (0.48 m) that only had a small SPM load and was infrequent. The only other error that was more than 20% was calculated for the next smallest tide of 1.18 m, again a small sediment load and low occurrence during the year. The bigger tides and loads all had errors less than 20%.

The error in this calculation actually equates to an increased height across the NW sector of approximately 2.1 cm. This has been calculated as follows:

$$increased\ height = \left(\frac{13\ 400\ x\ 100\ 000}{1.73}\right)\Big/ 3\ 700\ 200\ 000$$

Firstly the over estimate of 13 400 tonnes is converted to grams and then divided by the average wet bulk density across the full NW sector to find the volume in cm^3. This volume is then converted to a height by dividing by the area of the NW sector in m^2. Calculating the percentage error from the mean and standard deviation of the accretion rates measured across the NW sector (presented in Chapter 4) is potentially 25%. Both these measurements have errors associated that will influence the final amount of sediment measured across the NW sector, however the potential error associated with

the accretion rates is far greater than the majority of the errors associated with the tidal flux data which are between 11.8% and 34.4% (see Tables 5.1 and 5.3, above).

To collect further data for a wider range of tides and repeat data for the same tide heights increases the work needed for the prediction of a sediment budget. Considering the relatively low number of hydrodynamic surveys that were required to produce a sediment budget that can be confidently compared with sediment load from accretion rate measurements, only a small number of extra surveys may be required for prediction of a more comparable budget. To decide which method is more useful to other studies of accretion rates on a managed realignment site, looking at the associated errors calculated above would indicate that the estimation of sediment budget using hydrodynamic surveys results in lower errors and therefore would make this method more robust. Time spent on the hydrodynamic surveys is shorter and equipment such as a tidal gauge could be used to receive more precise tide heights. However, this equipment is expensive and may not be available to everyone. For a study such as this one with a breach that is easily accessible and conditions at the breach easily recorded compared to some of the areas in the mudflat being inaccessible for the placement and measurement of sediment level change, hydrodynamic surveys appear the better method for assessing sediment load. Coupled with a good topographic map of the site, areas of fastest and slowest accretion can be calculated and total sediment load easily seen.

5.5 Inundation and flow patterns

The supply of sediment to the areas of rapid accretion on the NW sector is driven by the inundation time of the tides and the flow of water across the site. The lower elevated areas on PHS are likely to be inundated for longer than the higher elevations. From experience on the site, some areas on PHS were constantly inundated during wetter, colder months and periods of high tides when the site was unable to fully drain before the tide turns.

5.5.1 Patterns of inundation

The inundation map was created using the topographic map of the site from LIDAR data collected in 2005 (see Chapter 2, section 2.2.2) and the transformed King George Dock data (details to be found in Chapter 2, section 2.2.8). Using this, a percentage time that an area was covered by the tide was calculated for PHS (see Figure 5.12, below).
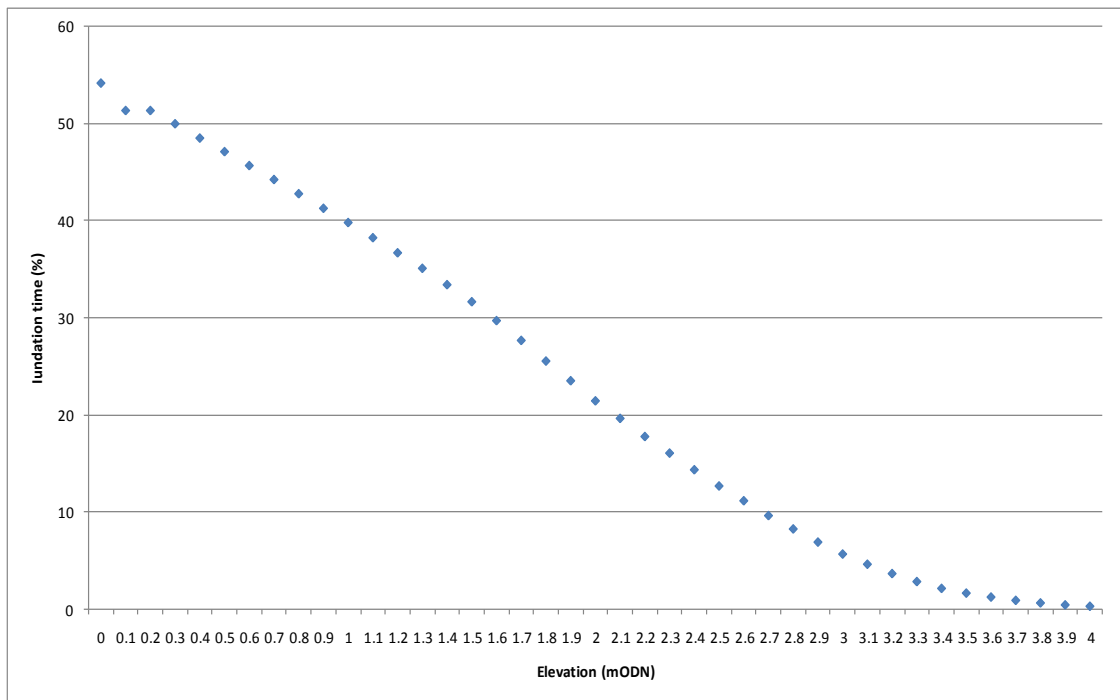
Figure 5.12: Percentage of time inundated plotted against topographic height.

Only the very lowest points are inundated for more than 50% of the time (see Figure 5.12, above). The height at which sites are not inundated at all is 4 m ODN.
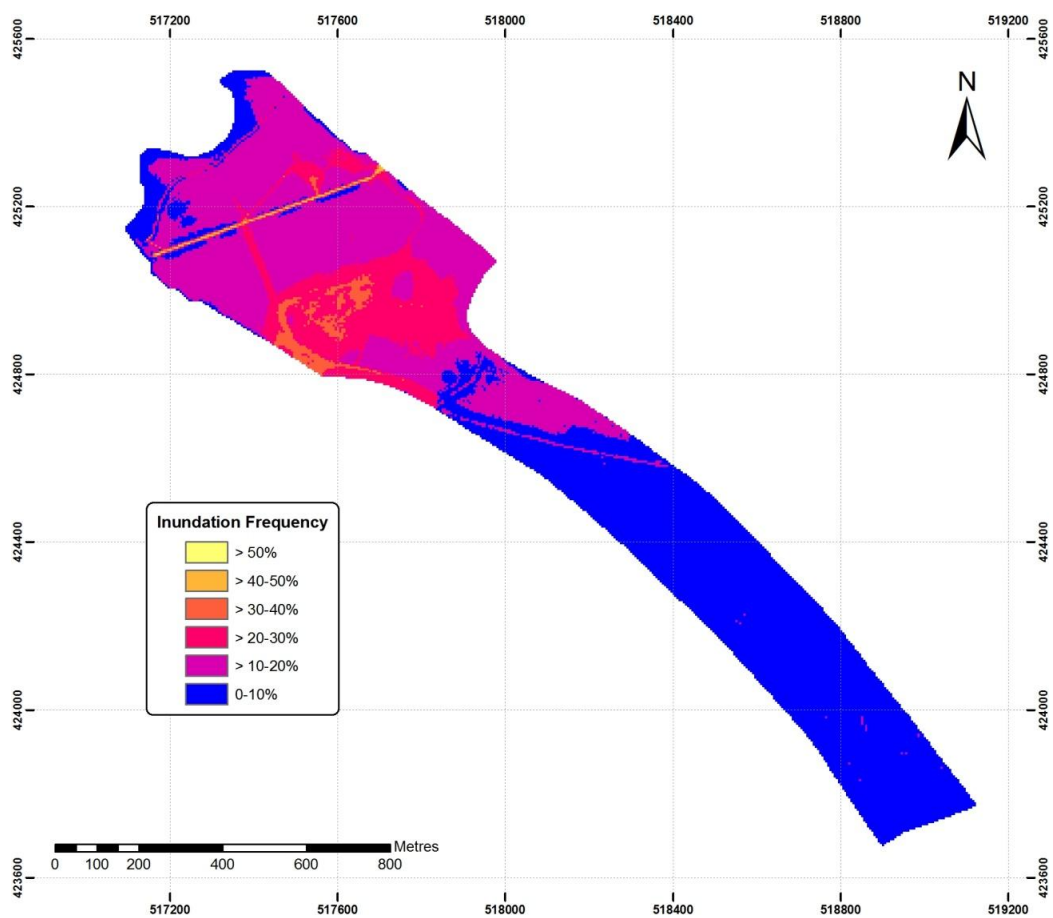
Figure 5.13: Percentage of time land is inundated on PHS.

The area that is inundated for longest (disregarding the drainage ditch running across the northern part of the site) is closest to the NW breach and is inundated between 30 and 40% of the tide (see Figure 5.13, above). A large area behind the NW breach is inundated for 20 – 30% of the tide, as are small areas in the northern corner of the site and along a channel created by the former field patterns on the site.

5.5.2 Introducing a time factor for inundation

The time taken for the tide to inundate the NW sector of PHS has been modelled within the Geography department, University of Hull. Using these data improves the precision of the tidal inundation information shown in Figure 5.13, below. The modelled data are for four different tides on the site: 0.98, 1.48, 1.98, and 2.48 m (water depth across NW breach at high tide), starting with a completely dry site.
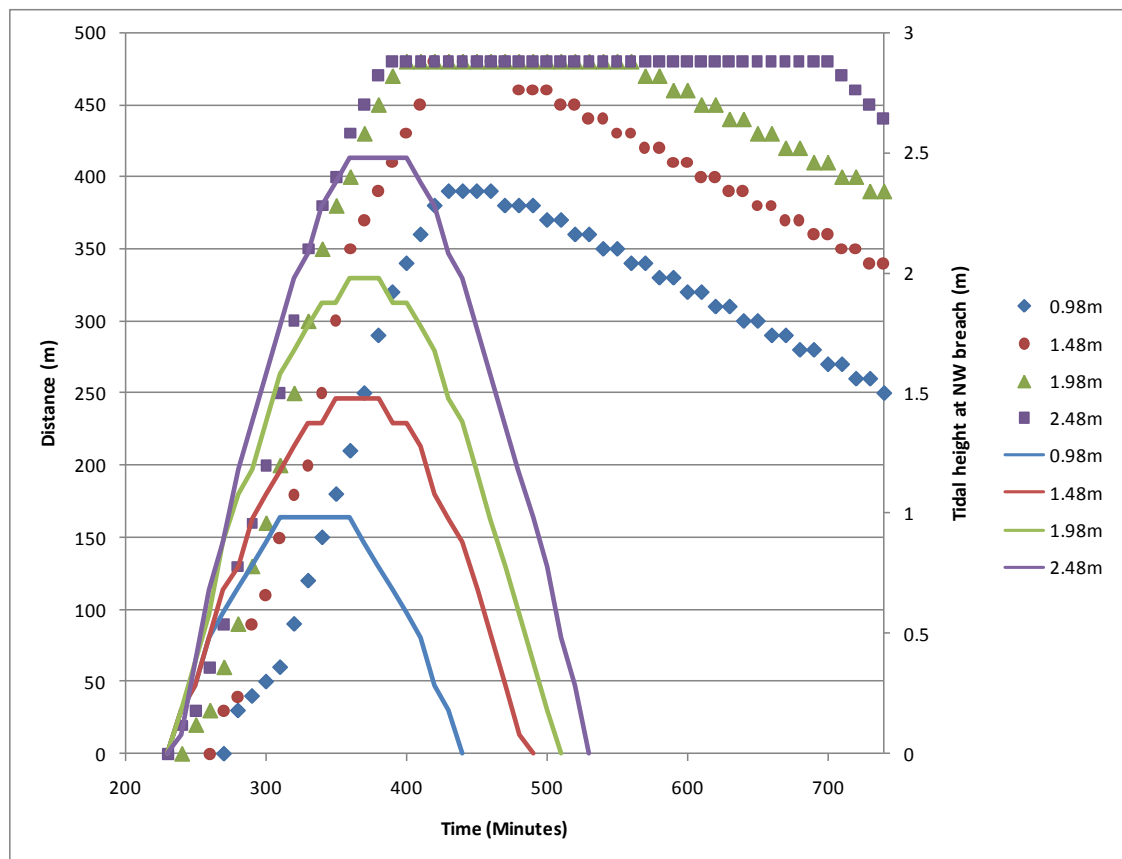
Figure 5.14: Relationship between time and distance from NW breach during four different high tides on PHS, based on model output. Mean tide height across the NW breach shown on right axis.

The tide flows very quickly over the NW sector even during the relatively small 0.98 m tide, reaching high tide about 2.5 hours after entry. This smallest tide was the only one not to reach the new embankment 480 m NE of the breach. Figure 5.14, above, gives

the appearance that much of the tidal water stays on site even after the tide has dropped. Knowledge of the site does indicate that some areas still have water covering the sediment once the tide has ebbed, however this is only a very thin layer in lower parts of the site. On the largest tides especially, the water does not flow out of the site through the small channel in the NW breach as quickly as the actual water depth is dropping, leaving some areas slow to clear of water. The actual depth of the water on the site cannot be calculated from the modelling data provided.

Table 5.5: Stages in tidal inundation for four tides through the NW breach on PHS, locations in bold type are identified on Figure 5.16.

	Mean high tide across NW breach (m)			
	0.98	**1.48**	**1.98**	**2.48**
Tide in **channel** reaches **drainage ditch** (minutes since start of tidal cycle)	410	380	360	350
Tide reaches far **embankment** (minutes since start of tidal cycle)		420	410	390
Tide overtops into Area 4 (see Figure 4.14) (minutes since start of tidal cycle)		430	410	380
Tide reaches peak (minutes since start of tidal cycle)		450	460	490
Tide floods into Area 4 at top of **drainage ditch** (minutes since start of tidal cycle)		480	450	420
Tide reaches **drainage ditch** (minutes since start of tidal cycle)			460	440
Tide still covering Area 4 (minutes since start of tidal cycle)		740	740	740
Tide out of **drainage ditch** (minutes since start of tidal cycle)	550			

As the water depth at high tide increases, the key locations listed in Table 5.5 are inundated more quickly by the tide (see Figure 5.15 below for the locations on PHS). For example, the tide reaches the far embankment 420 minutes after the start of the tidal cycle during a 1.48 m tide, after 410 minutes during a 1.98 m tide and after 390 minutes during a 2.48 m tide. During the smallest 0.98 m tide, the far embankment is never reached; this tide is the only one that appears to fully drain from the NW sector before the tide turns again. All other tides overtop into area 4 (northern part of sector, see Figure 5.11, above) and stay in this location until the end of the tidal cycle. Even with the additional data about the pattern of flooding and the route of water across the NW sector during four different tides, quantifying the inundation remains difficult. However, the pattern of tidal inundation may help to explain the error in the sediment budget calculation.
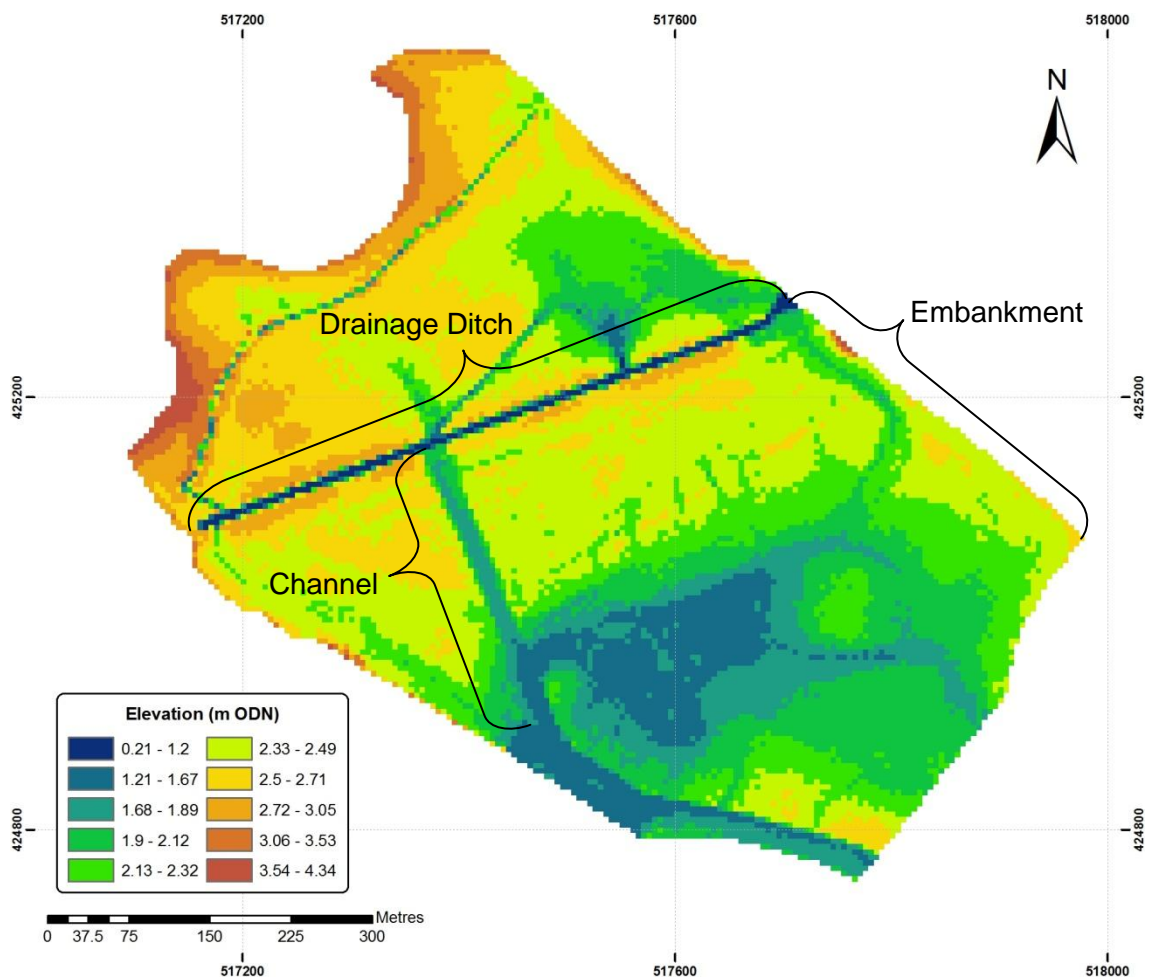
Figure 5.15: Key locations on the NW sector of PHS when discussing inundation patterns.

5.6 Conclusions

The sediment budget calculated using the hydrodynamic and SPM flux data estimated a total net flux into PHS through the NW breach of 63 400 tonnes. On all six separate tidal cycles for which SPM was measured, there was a net flux of sediment into the site; these included tides at very low heights and spring tides during the autumn. The varying SPM fluxes were not directly linked by the tide height and thus the tidal volume into the site for two tides of height 1.28 and 1.48 m (these heights represents the mean high tide across the NW breach) were averaged to provide the strongest relationship between tide height and SPM volume. Various factors will affect the amount of sediment held in suspension within the Humber estuary, which include the weather conditions, such as wind direction forcing more water onshore or offshore, wave height (related to wind and pressure), dredging in the estuary and time of year (again related to the weather conditions and temperature) (Christie, *et al.*, 1999; Robinson, *et al.*, 1998; Townend, *et al.*, 2003). When collecting the measurements the weather conditions were generally

135

good with little rain and lower winds as high wind conditions made measurements of hydrodynamics extremely difficult.

The LOIS study found that the amount of sediment held in suspension in the estuary could vary on a day to day basis (Cave, *et al.*, 2003) and that the suspended sediment loads are high with a turbidity maximum that moves between Hull and Selby (Townend, *et al.*, 2003), generally closer to Hull (and PHS) during the winter. The paper by Townend *et al.*, (2003), outlining a sediment budget for the Humber estuary, proposed that on average there is 1.2×10^6 tonnes of dry sediment resident in the estuary at any one time. A study by Christie, *et al.* (1999) found that the residual flux onto the mudflat at Skeffling in the Humber estuary (for exact location see Figure 2.9, Chapter 2) was significantly correlated with the following 'forcings': water temperature at high water, maximum current speed, maximum and minimum SSC, river flow, mean wind speed and wave height.

Despite the calculation errors discussed in sections 5.2.3 and 5.3.2, the sediment budget calculated from the tidal and SPM data closely matched the amount of sediment that had been deposited on the NW sector during a year using mean accretion rates and wet bulk density values. This gave a prediction of 50 000 tonnes of sediment needed to sustain the accretion of the site at the rates recorded during the monitoring period. This link between the two calculations of sediment deposition on the NW sector provides the basis of a way of calculating the amount of sediment to be deposited on a managed realignment site using sediment flux data through a breach.

The overall inundation of the site is based on the elevation. To include a time factor using flow rate information would improve the estimation of inundation periods, but this has not been possible. Analysis of the time taken for water to enter and drain from parts of the site has provided an insight into the route the tidal flow takes across the NW sector, highlighting the old field margin channel as a means for the tide to quickly reach the drainage ditch from the water treatment works and then flow into the northern tip of the sector. There is also some indication that the water remains in this area of the sector longer while the site drains. The variations in inundation period may explain some of the differences between SPM estimates of accretion rates and the direct measurements of accretion.

So far, the accretion rates, sediment fluxes and inundation of the site have been presented. The next chapter will present the properties of the sediment and discuss comparisons between these properties and the accretion rates.

Chapter 6 : Sediment properties

The properties of the sediment across PHS, especially in the fast accreting NW sector, are important to investigate for a number of reasons. The previous two chapters have highlighted the different areas of the site and their associated accretion rates, and the amount of sediment entering through the NW breach equating with the amount accreting on the NW sector. The link between the accretion rate and sediment elevation has also been noted, for the SE sector the link was stronger. In the NW sector, there were other factors influencing the rapid accretion rates that could not be explained through site elevation alone. Coupled with this and the information on inundation patterns, an investigation of the sediment properties should add further evidence and help explain more fully what is influencing sedimentation patterns on the site. The properties investigated for the NW sector were: bulk density, moisture content, grain size and organic content. These properties are important in terms of sediment stability and indicate areas suitable for colonisation by vegetation. They are also easily measured over a spatial and temporal scale and comparable with similar studies done on mudflat environments (see Table 2.2, Chapter 2, for a comprehensive assessment of sediment properties controlling accretion and erosion).

The wet bulk density of the sediment on an intertidal area has been found to correlate positively with erosion potential (Andersen, *et al.*, 2005; Bale, *et al.*, 2006; Mitchener, *et al.*, 1996; Quaresma, *et al.*, 2004). This implies that a higher wet bulk density for a site is indicative of a less erosive environment. A low bulk density could also indicate areas of fast accreting sediment- areas that are accreting quickly are likely to be less consolidated and would have a lower bulk density; it could also indicate areas where water pools. The inundation map of the NW sector presented in the previous chapter highlights areas that are inundated most frequently and are therefore more likely to be unconsolidated. Saltmarsh development on a new intertidal area is generally accompanied by consolidation of the sediment, and therefore by areas of higher bulk density. Moisture content is a product of the difference between wet and dry bulk density and will be presented as an indicator of waterlogging- a factor in the failure of vegetation colonisation on the Tollesbury managed realignment site (Garbutt, *et al.*, 2006). The ratio between the wet and dry bulk density is also informative. A small ratio (and large moisture content) would indicate an unconsolidated sediment regardless of the wet bulk density being higher.

Grain size can also be used to identify fast accreting areas. This is because the larger and heavier particles are expected to fall out of suspension first as the water decelerates on the site, thus creating areas of relatively fast accretion. In a study on the Tollesbury managed realignment site, coarser material was recorded in the central area of the site and attributed to a high energy environment where the small particles were unable to settle (Chang, *et al.*, 2001).

The ratio of mud (grain size less than 63 μm) to sand in a sediment bed is also indicative of erosion potential (Mitchener, *et al.*, 1996). Different studies have found that by increasing the mud content of a bed increases erosion resistance (van Ledden, *et al.*, 2004) but conversely adding small amounts of sand to a cohesive bed also increases erosion resistance. The study by Mitchener *et al.* (1996) found that a sediment bed will be more resistant to erosion up to an optimum between 50 and 70% sand; more sand than this will decrease the resistance. These ratios on the NW sector were used to provide evidence of areas of different susceptibility to erosion. A higher cohesive content may also indicate the presence of flocs in suspension (Raudkivi, 1998).

The organic content of the sediment bed on the NW sector should indicate areas of vegetation cover and thus more stable sediment. On an intertidal site the presence of vegetation is likely to be positively correlated with the height of the bed and negatively correlated with the inundation time (itself a factor of bed height), as areas covered for shorter periods by water will be better able to support vegetation. Vegetation also has a buffering effect on water velocity, reducing flow and waves thus providing conditions for increased sediment settling (Boorman, 2003). Increasing organic content has been found to correlate with increased erosion resistance of sediment (Mitchener, *et al.*, 1996).

The flocculation of sediment particles in suspension is beyond the scope of the present research, however it is expected that this process would affect the properties of the sediment at PHS. Flocculation removes the fine grains from suspension and thus would influence the distribution of these fine grains upon the site. Bulk density would also be affected by the flocculation process- the strings of flocs created are less dense than their constituent particles and would lead to a less compacted surface and thus a lower bulk density. Temperature also affects the formation of flocs- when water temperature is high less and smaller flocs form so a seasonal difference of the impact of flocculation may be expected (Dyer, 1989; Dyer *et al*., 1999).

6.1 Wet and dry bulk density

The wet and dry bulk density of the sediment was fairly constant across all sites on the NW sector (see Figure 6.1 below).

Full data for wet and dry bulk density are presented in Appendix 7.
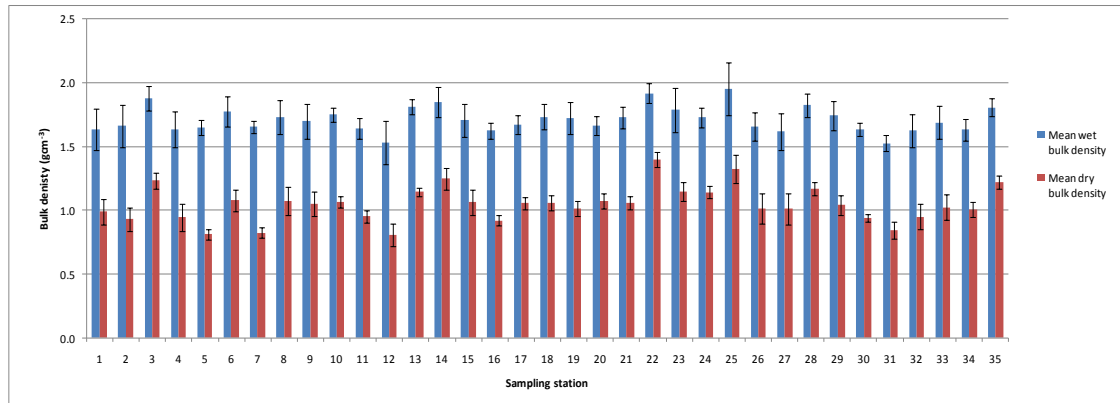
Figure 6.1: Mean wet and dry bulk density on the NW sector of PHS, standard deviation represents the variation between three repeat samples at each station.

The mean wet bulk density for the NW sector was 1.71 gcm^{-3} and for dry bulk density the mean value was 1.05 gcm^{-3} (see Table 6.1). The ranges of the two sets of values do not intersect, the lowest wet bulk density was 1.53 gcm^{-3} (site 32) and the highest was 1.95 gcm^{-3} (site 25), the lowest dry bulk density was 0.81 gcm^{-3} (site 5) and the highest was 1.4 gcm^{-3} (site 22).

Table 6.1: Mean and range bulk densities for the NW sector of PHS.

	Mean wet bulk density (gcm^{-3})	Mean dry bulk density (gcm^{-3})
Mean	1.71 ± 0.1	1.05 ± 0.14
Range	1.53-1.95	0.81-1.4

6.1.1 Dry: wet bulk density ratio
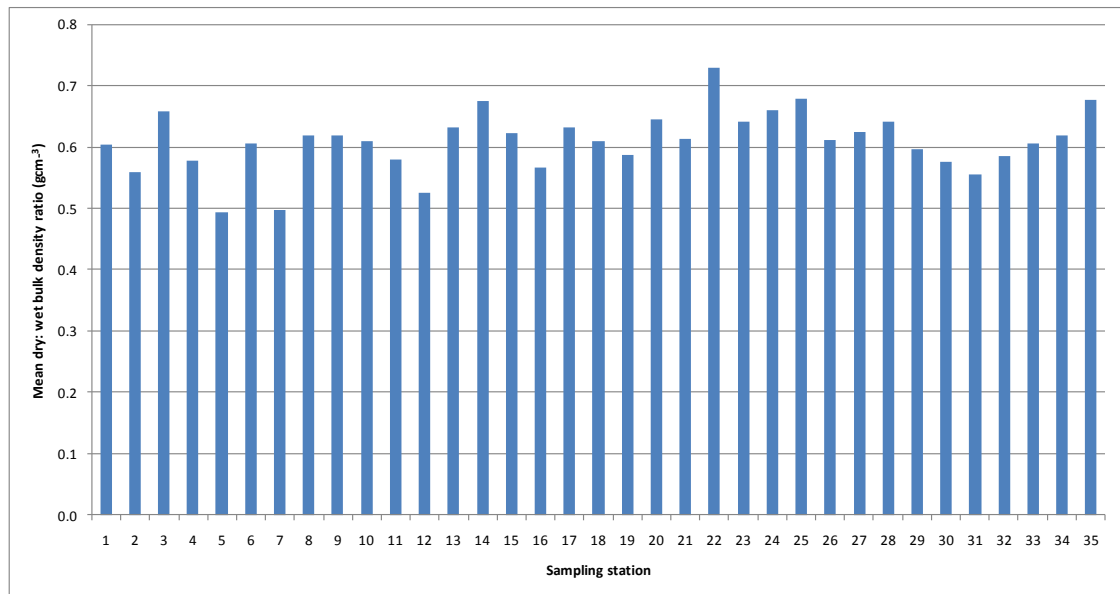
Figure 6.2: Mean dry: wet bulk density ratio for the NW sector of PHS.

The dry to wet bulk density ratio (see Figure 6.2, above) is an indicator of consolidated sediment. For the mean dry and wet bulk densities the ratio varies from just below 0.5 to just above 0.7. The three sites with the lowest ratios (5, 8, and 12) recorded wet bulk density values that were nearly double the dry bulk density value for the sediment. The three sites with the highest ratios (14, 22 and 35) were ones where the wet bulk density was 25 to 30% greater than the dry bulk density value.

6.1.2 Spatial differences in mean bulk density
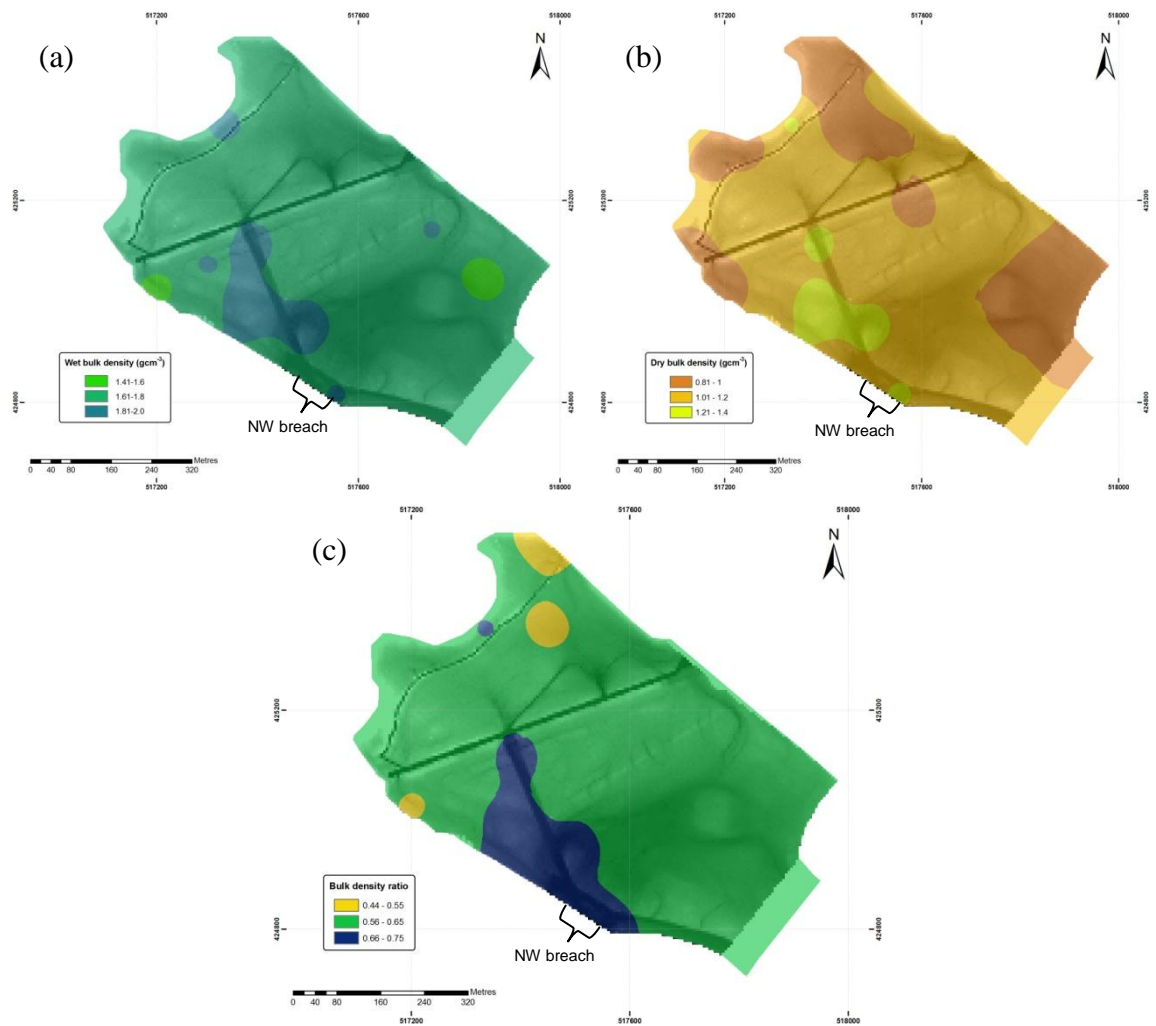
Figure 6.3: Mean bulk density on the NW sector of PHS, (a) wet, (b) dry and (c) the dry: wet bulk density ratio.

The wet and dry bulk density varied only slightly across the NW sector. The largest wet bulk densities on Figure 6.3 (a) were concentrated around the SW of the sector. This area recorded the faster accretion rates, and includes the old field margin channel. The lower dry bulk densities were also recorded in this area (see Figure 6.3 (b)), implying less consolidated sediment with higher moisture content. The higher dry bulk densities were situated in the north, east and west corners of the sector, closest to the new embankments. These are transitional areas between intertidal and soil sediment. The areas on the NW sector that had a ratio closest to unity (i.e. with least difference between wet and dry bulk density) were located along the old field margin channel and behind the breach (see Figure 6.3 (c)). The smaller ratios (i.e. those where the wet and dry bulk density were most different) were recorded in a small area to the northern corner of the sector.

6.1.3 Seasonal differences in bulk density

From Figure 6.4 there is little systematic difference between the summer and winter bulk density values. The mean wet bulk density during summer was 1.67 gcm^{-3} and the mean dry bulk density was 1.13 gcm^{-3}; during winter the respective means were 1.76 gcm^{-3} and 0.97 gcm^{-3} (see Table 6.2 below). The dry bulk density is lower in the winter in all but 5 of the sites, this difference is significant (matched pairs t-test, P = 0.002). The trend for wet bulk density was for higher values in winter: the difference between the summer and winter values are significant (matched pairs t-test, P = 0.02), however considerably smaller than for the dry bulk densities. This may indicate that during the winter months the sediment was less compacted.

Table 6.2: Mean and range bulk densities during summer and winter for the NW sector of PHS.

		Mean wet bulk density (gcm^{-3})	Mean dry bulk density (gcm^{-3})
Summer	**Mean**	1.67 ± 0.13	1.13 ± 0.16
	Range	1.40 – 2.08	0.78 – 1.53
Winter	**Mean**	1.76 ± 0.17	0.97 ± 0.22
	Range	1.46 – 2.27	0.66 – 1.65
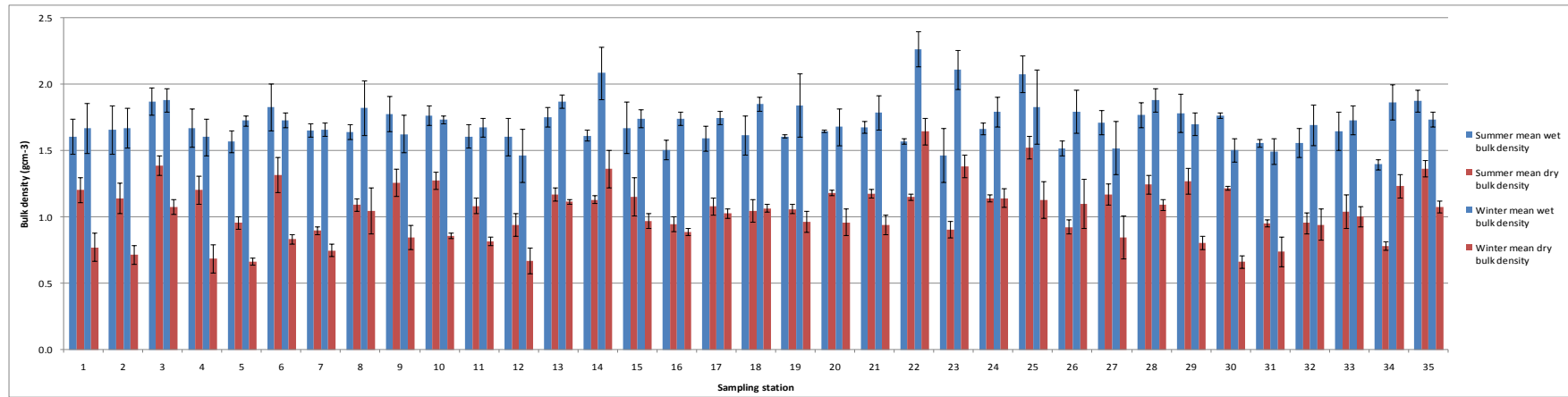
Figure 6.4: Mean wet and dry bulk density on the NW sector of PHS during summer and winter, standard deviation represents the variation between three repeat samples at each station.
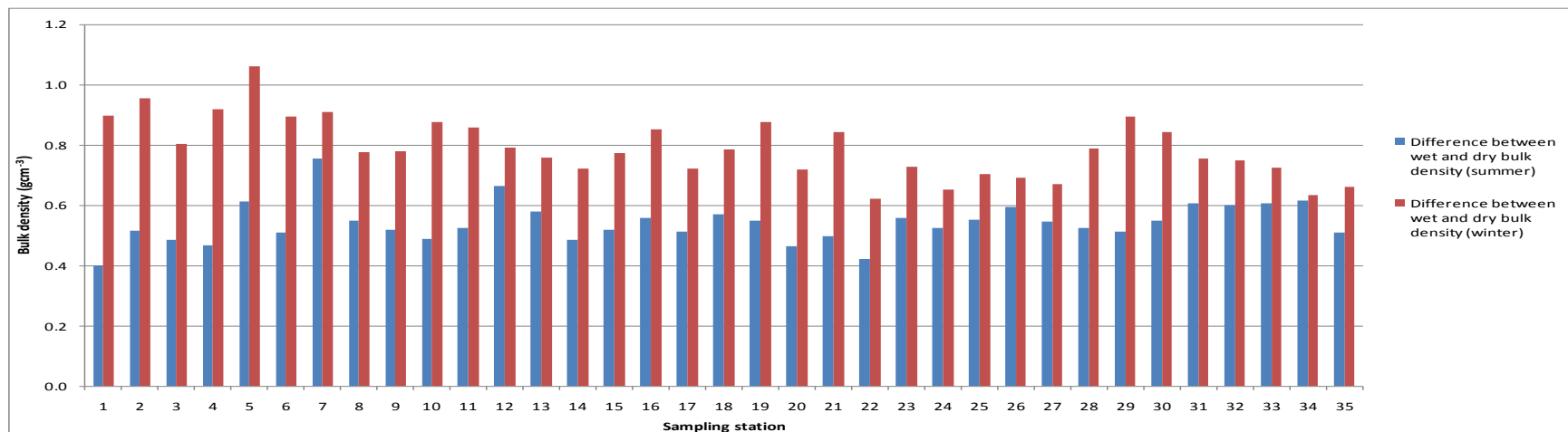
Figure 6.5: Differences between wet and dry bulk density during the summer and winter across the NW sector of PHS, standard deviation represents the variation between three repeat samples at each station.

144

6.1.3.1 Dry: wet bulk density ratio
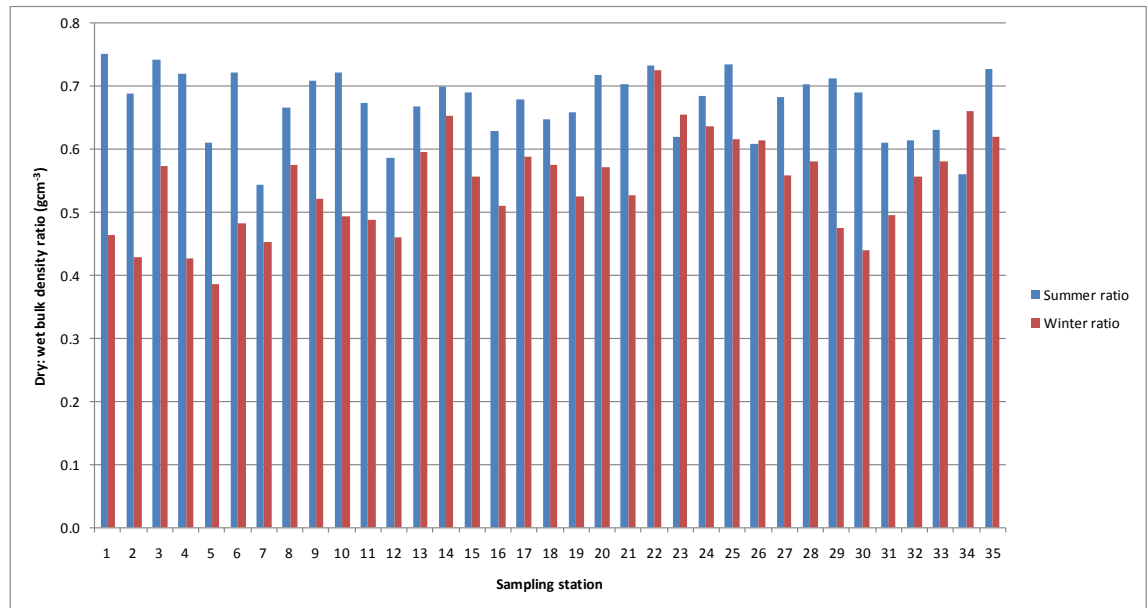
Figure 6.6: The dry: wet bulk density ratio over the NW sector of PHS for summer and winter.

The dry: wet bulk density ratios for both winter and summer are shown in Figure 6.6 above. The summer ratios are always bigger than the winter ones (apart from at site 34) and are significantly different (matched pairs t-test, P = 0.000). This indicates that during the summer the difference between wet and dry bulk density values was smaller than during the winter. During the winter, one third of the sites recorded wet bulk densities more than double the associated dry bulk densities. All of the sites had dry bulk densities less than double the wet equivalents during winter.

6.1.3.2 Spatial differences
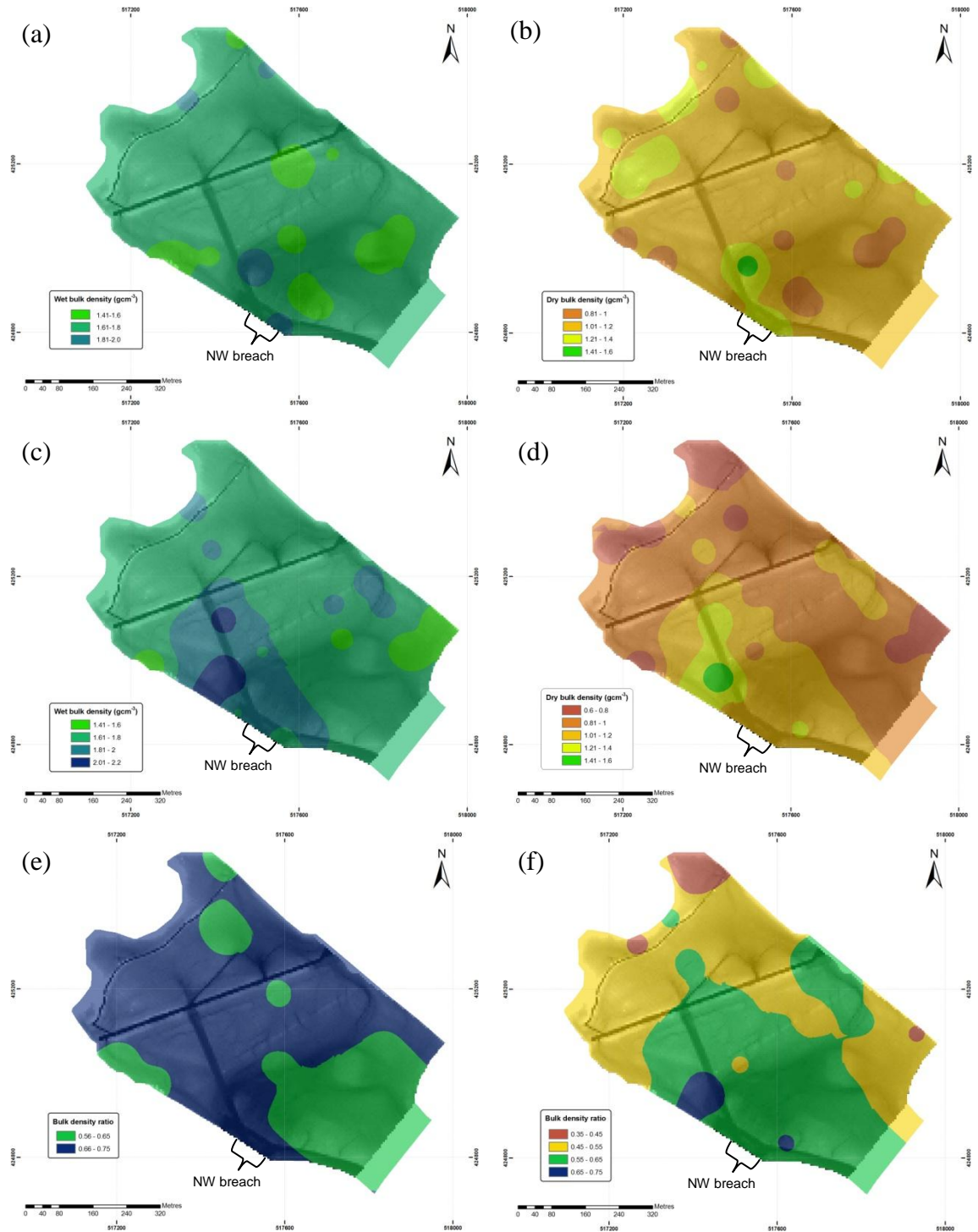
Figure 6.7: Bulk density on the NW sector of PHS, (a) summer wet, (b) summer dry, (c) winter wet, (d) winter dry, (e) the summer dry: wet ratio, (f) the winter dry: wet ratio.

The summer values of dry and wet bulk density (Figures 6.7 (a) and (b)) do not appear to exhibit any spatial patterns although there may be a slight concentration of higher dry bulk density in the area just behind the NW breach. The pattern was clearer during winter (Figures 6.7 (c) and 6.7 (d)), with the spatial variability similar to the mean bulk density shown in Figures 6.3 (a) and (b). The lower dry bulk densities and higher wet

146

bulk densities around the SW of the sector indicate higher moisture content and less consolidated sediment in this area. During the summer, the higher dry: wet bulk density ratios were mainly concentrated to the south of the NW sector with only isolated pockets to the north. During the winter, the pattern of the dry: wet bulk density ratio changed with the lower ratios concentrated around the NW breach and in the south of the sector. The higher ratios were in the northern most corner.

6.2 Moisture content

The mean moisture content varied up to 20% over the NW sector (see Figure 6.8). The smallest moisture content of 27.1% indicates that the driest sediment was at station 22 and the highest moisture content of 50.2% was at stations 5 and 7. The remaining values were mainly in the high 30s (mean moisture content 39.1%).

Full data for moisture content are presented in Appendix 7.
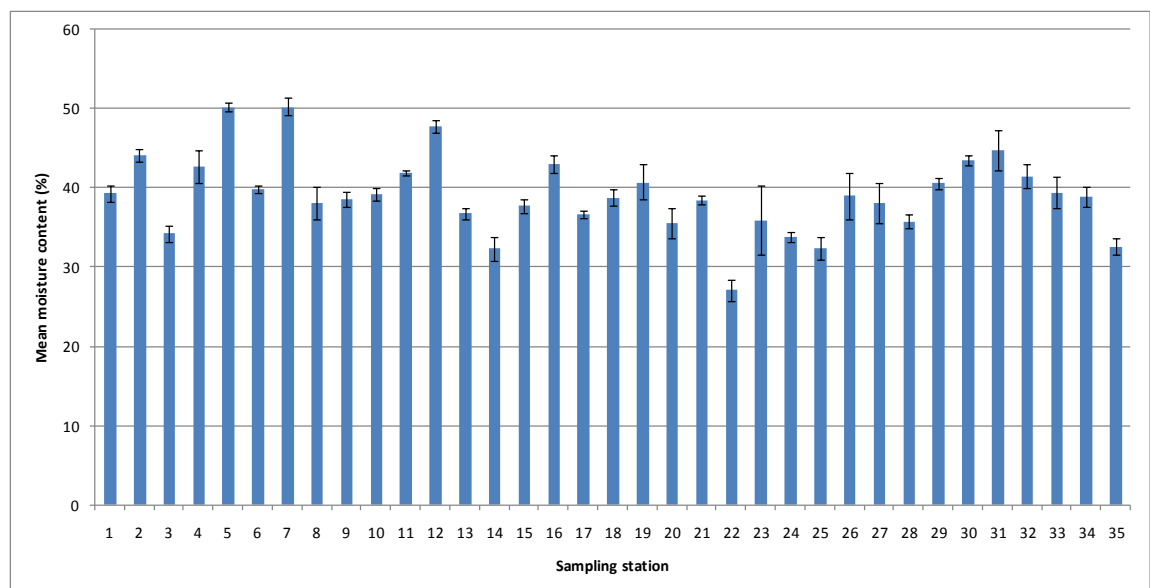
Figure 6.8: Mean moisture content on the NW sector of PHS, standard deviation represents the variation between three repeat samples at each station.

6.2.1 Spatial distribution

The sediment holding the least amount of moisture in the NW sector was located directly behind the NW breach, along the old field margin channel running towards the drainage ditch (see Figure 6.9, below). This area recorded the fastest accretion rates. Other areas of moist sediment occurred towards the north, east and west corners of the sector, notably in the northern corner in front of the new embankment. This area usually filled during inundation of the site and continued to have surface water even when the

tide was ebbing, as discussed in the previous chapter. This indicates an area where water pools and this leads to the higher moisture content recorded at these sampling stations.
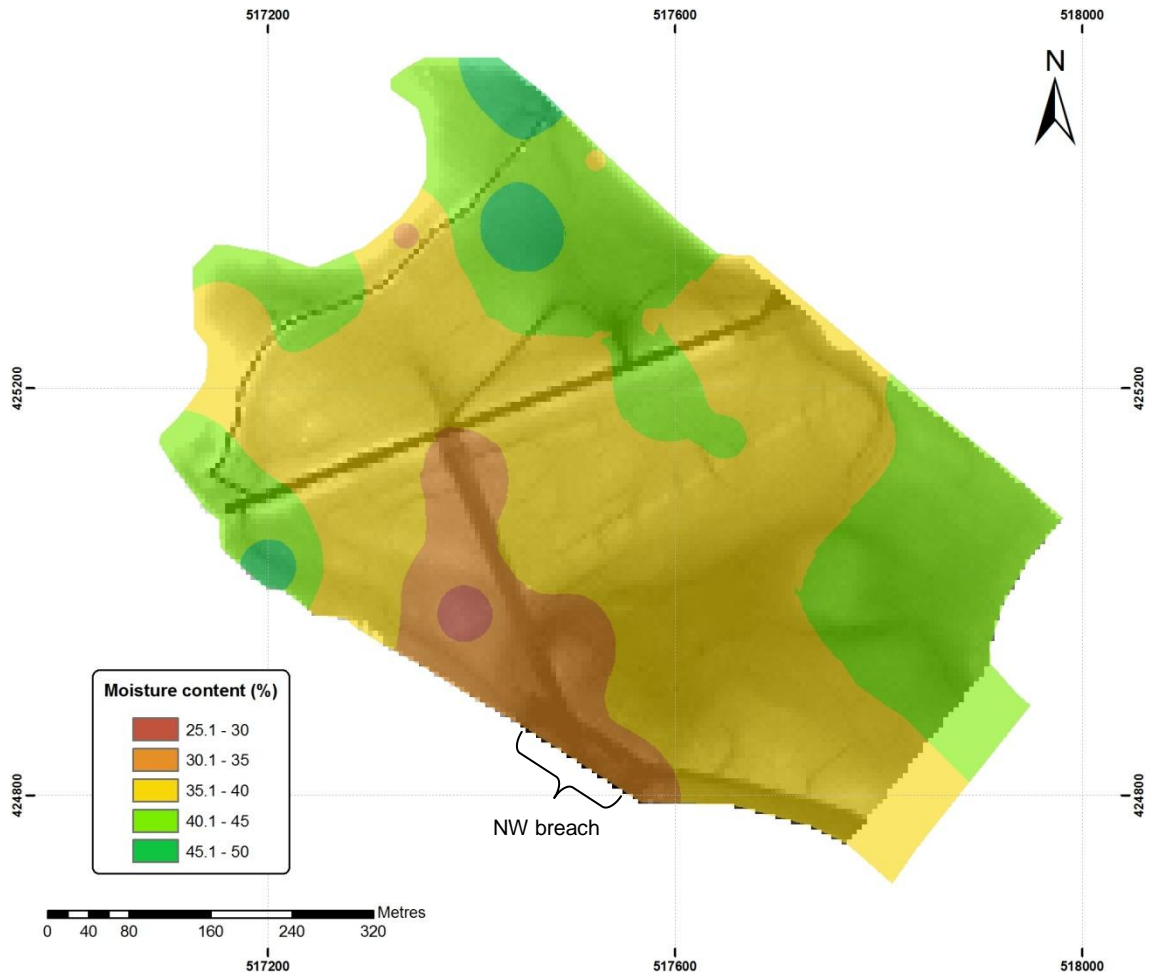
Figure 6.9: Mean moisture content on the NW sector of PHS.

6.2.2 Seasonal differences

Moisture content across the NW sector was generally highest during the winter (see Figure 6.10, below); only three sites recorded higher moisture content in the summer: 23, 26, and 34. At site 23 the standard deviation of the summer samples was very large indicating that the sediment sample may have been unrepresentative. The standard deviation of the winter sample at site 26 was also large and again may indicate an unrepresentative sample. The high standard deviations also demonstrate the variability over very small areas of mudflat. The moisture contents recorded showed seasonal differences (matched pairs t-test, P=0.000) indicating that the site was wetter during the winter. This result is expected as the colder and wetter conditions in the winter will lead to the sediment retaining more moisture.

148
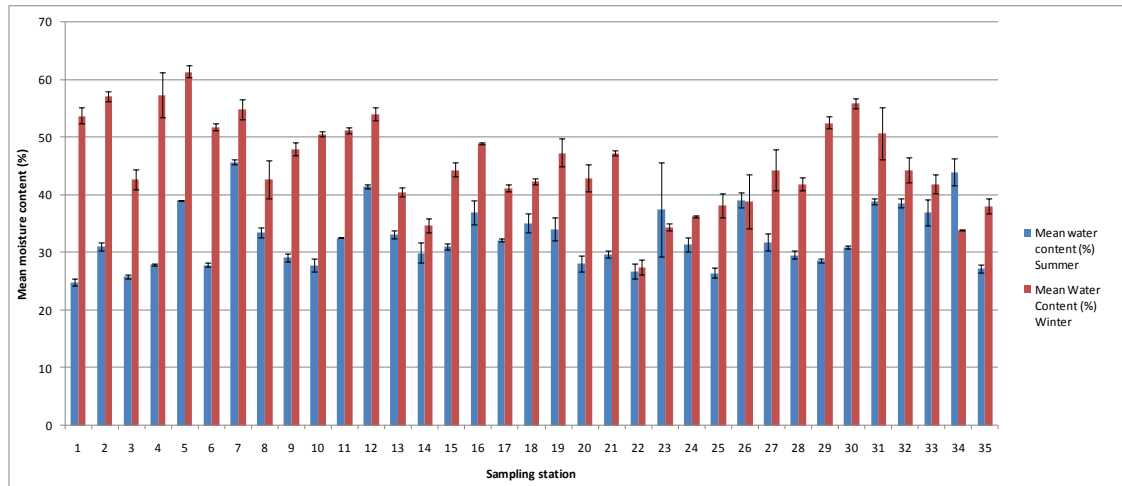
Figure 6.10: Mean moisture content during winter and summer on the NW sector of PHS, standard deviation represents the variation between three repeat samples at each station.

The mean moisture content during the winter was 45.5% (see Table 6.3), over 10% higher than the summer mean. The lowest moisture content for both seasons was similar, (24.8% in summer and 27.4% in winter), however the highest moisture content during the winter was almost a third greater than the highest summer moisture content. This indicates that the dryer sites were dry during both seasons but the wettest sites were wetter during the winter.

Table 6.3: Moisture content statistics on the NW sector of PHS, standard deviation represents the variation between sampling stations.

Moisture content	Mean (%)	Summer (%)	Winter (%)
Mean	39.1 ± 4.9	32.7 ± 5.3	45.5 ± 7.9
Range	27.1 – 50.2	24.8 – 45.7	27.4 – 61.4

6.2.2.1 Spatial distribution

The summer moisture content does not exhibit any spatial patterns (Figure 6.11 (a) below). The sediment with lowest moisture content appears to have been in the area just to the north of the NW breach and in the western corner of the sector. The areas of sediment with highest moisture content were spread around the sector, one to the east behind the NW breach, a further area in the northern tip and the final area near to the west end of the drainage ditch. The winter sediment moisture content showed a clearer pattern (see Figure 6.11 (b), below). The lowest moisture content was in sediment behind the NW breach and to the west along the old field margin channel. The sediment with most moisture content was found to the north, west and east corners of the sector in front of the new flood embankments.
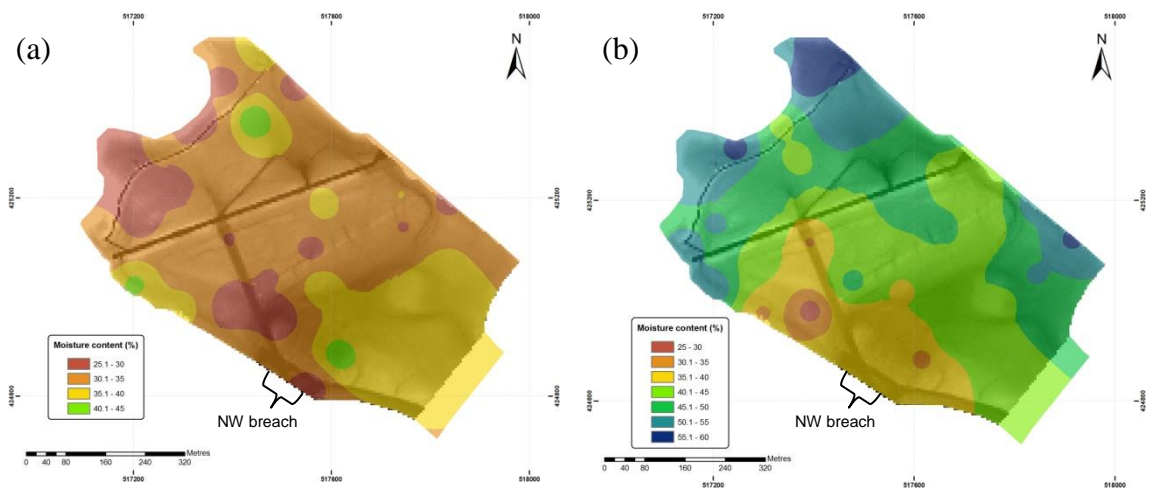
Figure 6.11: Mean moisture content on the NW sector of PHS, (a) during summer, (b) during winter.

6.3 Grain size

Across the NW sector, mean grain size ranges between sand (up to 2 mm diameter) and clay (less than 2 μm). The biggest proportion of sediment at every sampling station was silt, usually followed by clay and then sand (see Figure 6.12, below). At the following stations, (14, 21, 22, 23, and 25) the sand fraction exceeded clay.

Full grain size data is presented in Appendix 8.
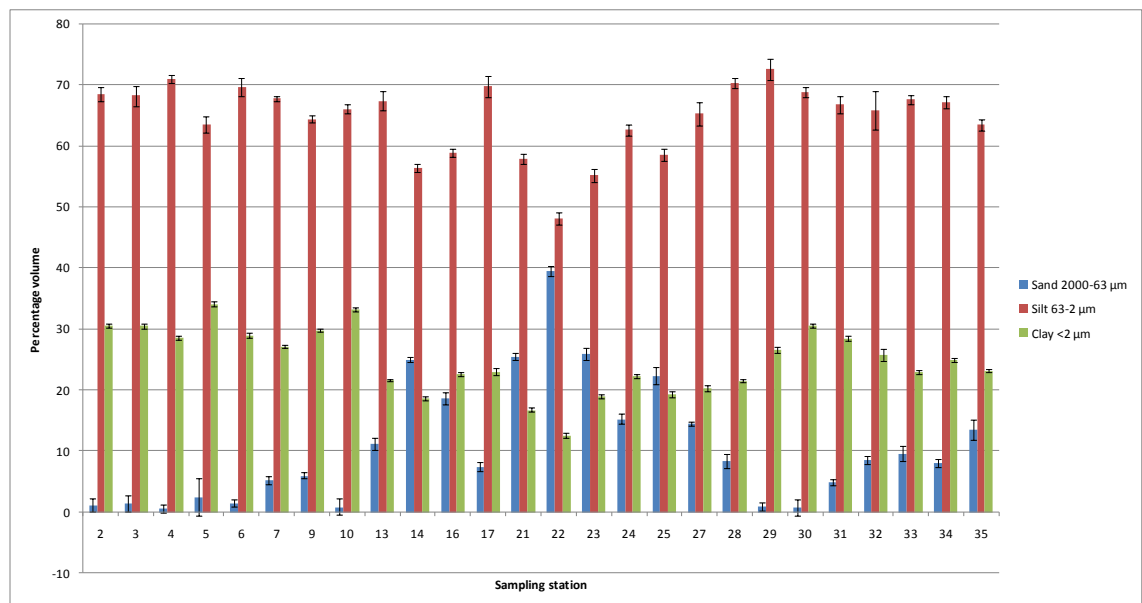
Figure 6.12: Mean sand, silt and clay fraction across selected sites on the NW sector of PHS, standard deviation represents the variation between three repeat samples at each station.
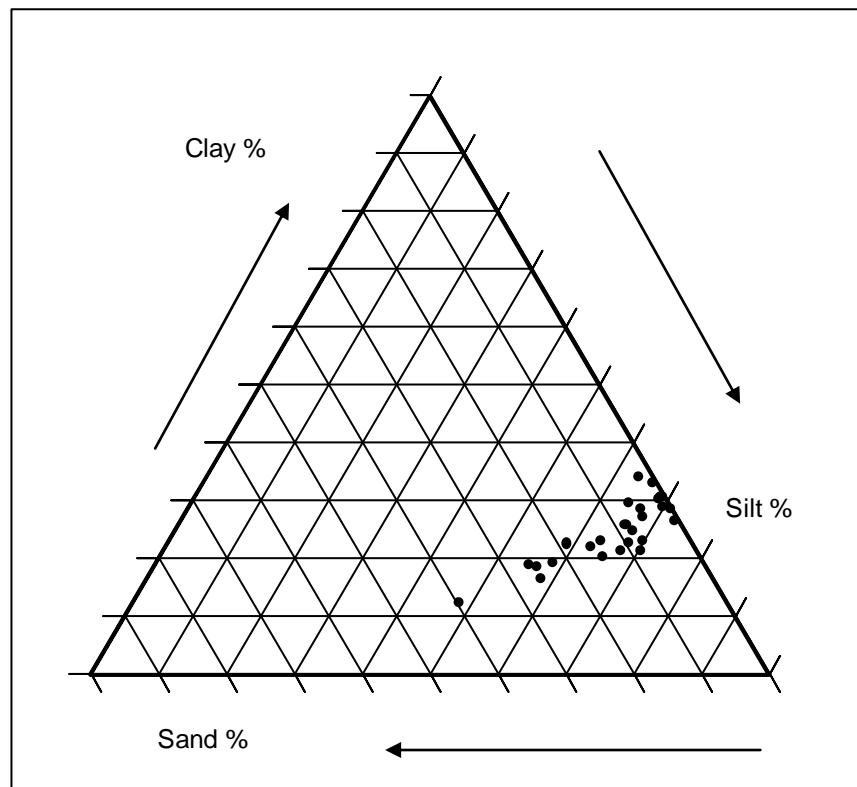
Figure 6.13: Mean grain size across selected sites on the NW sector of PHS.

The grain size was grouped fairly closely together at all of the sites (see Figure 6.13, above). The most variation was within the sand fraction, both the clay and silt fraction of the grain size distribution were within about 20% ranges. This classifies the mean sediment over the NW sector as silty clay and a few sampling stations as sandy, silty, clay according to the classification presented in Chapter 3, section 3.3.1.3.

The sand fraction ranged from 0.6% (station 4) to 39.5% (station 22). The sand fraction was the most variable across all sites as the large standard deviation: mean ratio demonstrates (values in Table 6.4, below). The silt and clay fractions had smaller ranges and standard deviations. The silt fraction at every station was always above 45% and never more than 75%, the clay fraction was always less than the silt, between 10 and 35%.

Table 6.4: Mean and range for sand, silt and clay percentage volume at selected sites on the NW sector of PHS, standard deviation represents the variation between sampling stations.

	Mean (%)	**Range (%)**
Sand (2000-63 μm)	10.7 ± 10.1	$0.6 - 39.5$
Silt (63-2 μm)	64.6 ± 5.8	$48.1 - 72.6$
Clay (< 2 μm)	24.7 ± 5.4	$12.5 - 34.1$

In comparison, at three plots on Tollesbury managed realignment site, the sand fraction was similarly low (6-7%), however the amount of clay was higher (52%) and silt was lower (52%) (Watts, *et al.*, 2003), these measurements were taken six years post breach, two years more established than PHS.

The grain size distribution of sediment at Skeffling mudflat on the Humber estuary is presented in Table 6.5 below (Christie, *et al.*, 1999). Site A at 3km from the mean low water spring (MLWS) was just below the upper limits of the MHWS. The amount of sand steadily increases from 4% at site A to 54% at site D, 0.75 km from MLWS. Conversely, the amount of silt and clay both dropped from 63 and 33% respectively at site A to 27 and 19% at site D. The mean values of sand, silt and clay on the NW sector of PHS most closely resemble the values recorded at sites A and B on the Skeffling mudflat.

Table 6.5: Grain size distribution along transect on Skeffling mudflat, Humber estuary (modified from Christie, *et al.*, 2000).

Distance from low water	Sand %	Silt %	Clay %
A 3 km	4	63	33
B 2.5 km	13	60	27
C 1.25 km	28	41	31
D 0.75 km	54	27	19

6.3.1 Spatial distribution of mean grain size

The sediment with the largest fractions of sand (30 to 40 %) were located to the west of the NW breach (see Figure 6.14 (a), below), the sediment in this area also had the lowest silt (45 to 55 %, see Figure 6.14 (b), below) and clay fractions (10 to 20 %, see Figure 6.14 (c), below). This area was where the fastest accretion rates were recorded. The smallest fractions of sand (0 to 5 %) were found in sediment near to the old embankments furthest from the breach. These coincide with the largest fractions of silt (65 to 75 %) and clay (24 to 35 %).
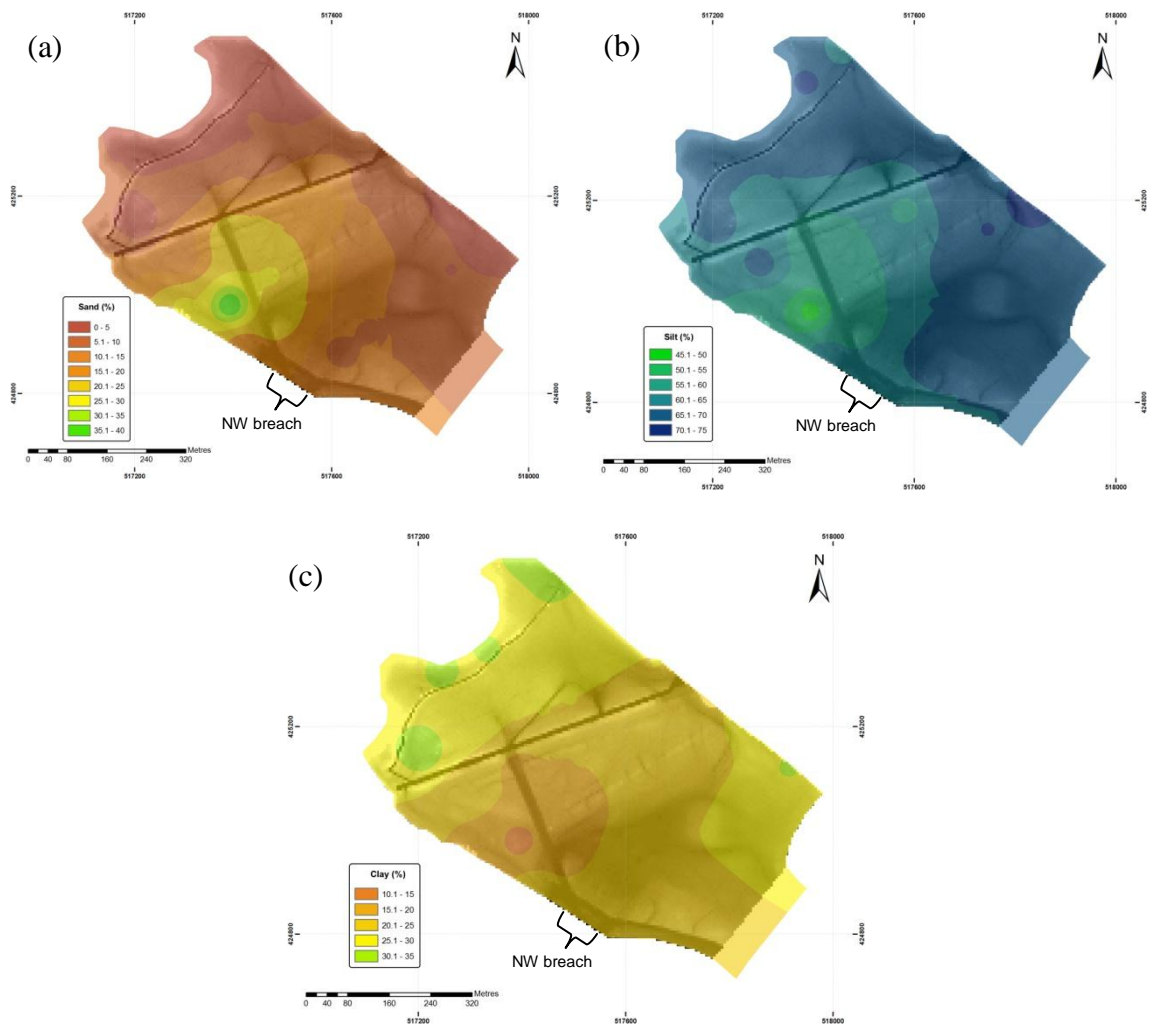
Figure 6.14: Mean grain fractions across the NW sector of PHS, (a) sand, (b) silt, and (c) clay.

6.3.2 Seasonal differences

The grain size fractions for each sampling station on the NW sector showed a summer to winter contrast, as can be seen in Figures 6.15 (a) and (b), below. During summer, the silt fraction remained fairly constant with only three sites dipping below 60% silt (5, 14 and 25). The clay fraction was also fairly constant across all the stations, the largest fraction was at site 5- (40%), and the rest of the values remained between 20 and 35%. The sand fraction was a lot more variable- at most sites values were below 5% but at 20% of the sites the values were between 10 and 20% (14, 16, 21, 22, 25).
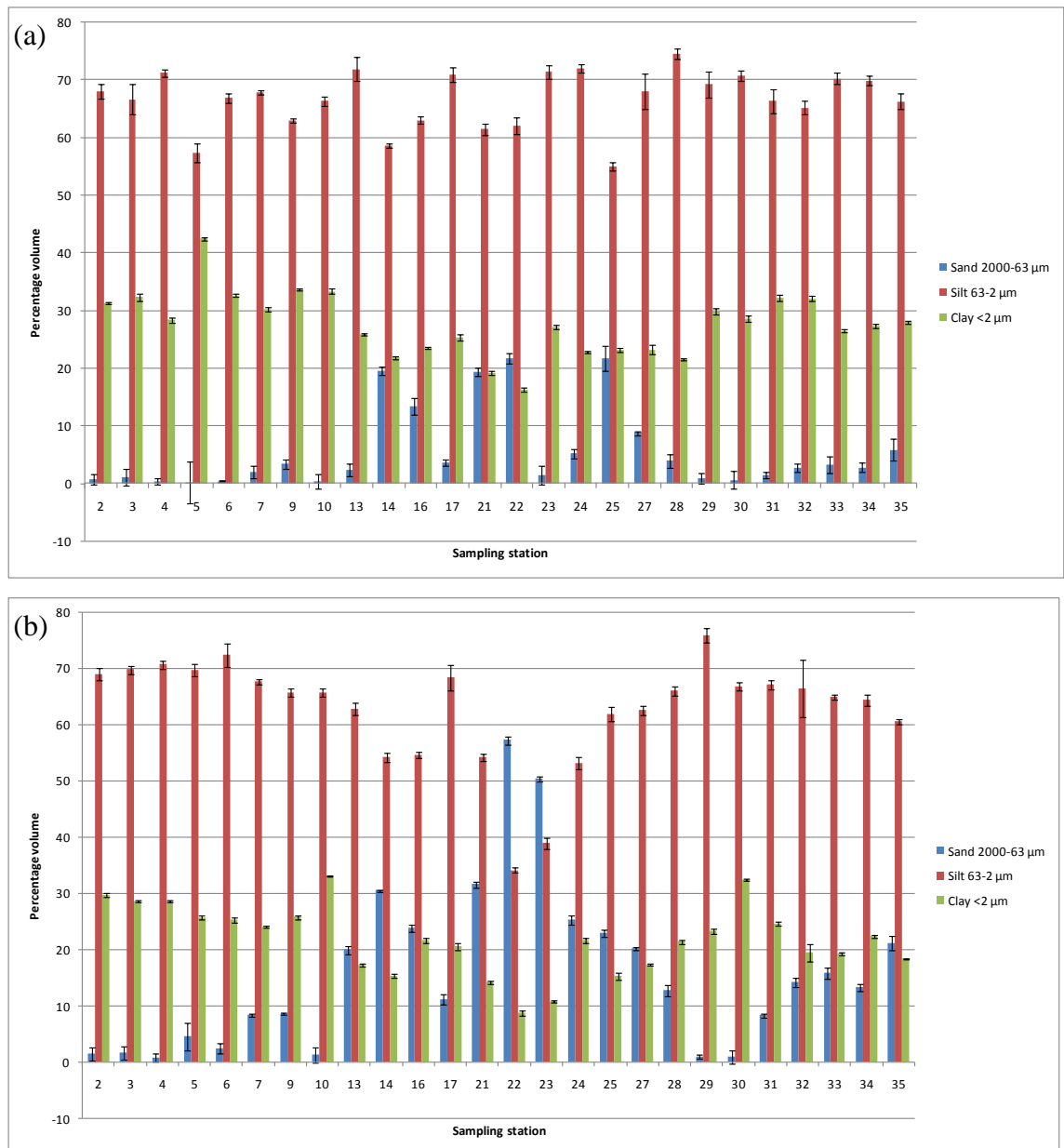
Figure 6.15: Mean sand, silt and clay fraction across selected sites on the NW sector of PHS, (a) during summer, (b) during winter, standard deviation represents the variation between repeat samples at each station.

The grain size fractions between stations were more variable during the winter. On a fifth of the sites the silt fraction of the sediment falls below 60% (14, 16, 21, 22, 23, 24) and at two of these sites the silt fraction was lower than 40% and also less than the sand fraction (22, 23). At the remaining sites, the amount of silt was similar to summer values (between 60 and 70%). At just over half of the sites the clay fraction of the sediment was between 20 and 30%. At two sites the clay fraction was higher than this (10, 30), one site had less than 10% clay (22) and the remaining sites were between 10 and 20% clay. The sand fraction was again very variable. At two sites (22, 23) the sand fraction was above 50% and two sites were above 30% (14, 21). Just fewer than half the

sites have sediment with a sand fraction lower than 10% and the remaining sites were between 10 and 25% sand.
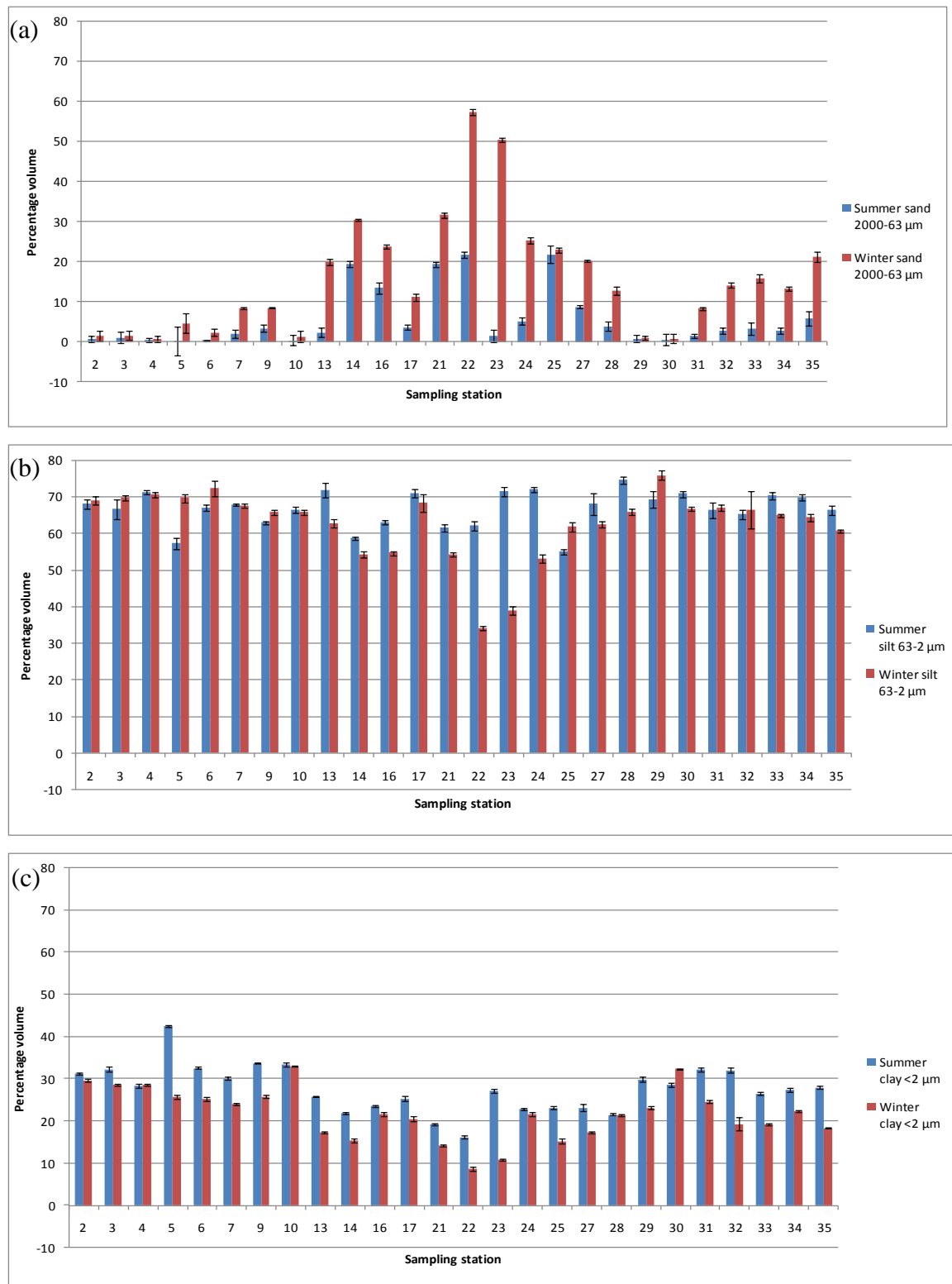
Figure 6.16: Mean grain fraction for summer and winter across selected sites on the NW sector of PHS, (a) is sand, (b) is silt, and (c) is clay, standard deviation represents the variation between repeat samples at each station.

Figures 6.16 (a)-(c), above, show the grain size fractions for each season. They were statistically significantly different for each fraction (using the t-test for matched pairs): both sand and clay have a P value of 0.000; silt has a P value of 0.045. The large amounts of variability in the sand fraction can be seen very clearly in Figure 6.16 (a).
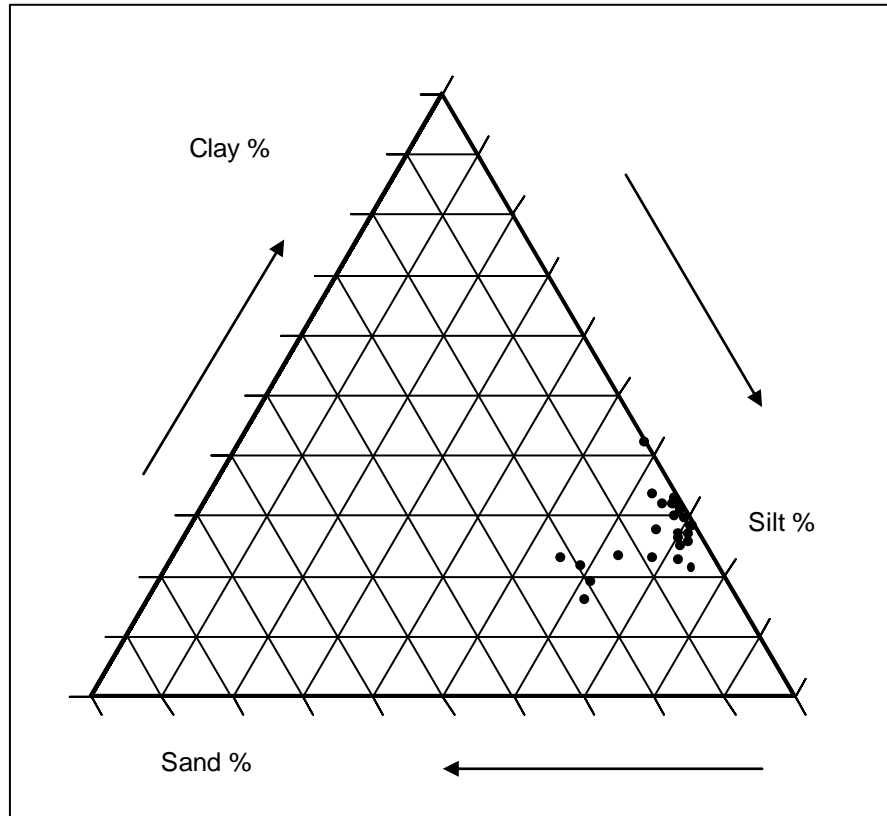
Figure 6.17: Summer grain size across selected sites on the NW sector of PHS.

The overall pattern of grain size distribution during the summer, as shown on the ternary diagram of Figure 6.17 above, was fairly constant for all sampling stations. There is some indication that the sites fall into a larger group of low sand (less than 10%), high silt and clay (silty clay using the classification after Shepard, Chapter 3, section 3.3.1.3) and a small group of 4 or 5 sites that fall into a sandy, silty, clay grouping.
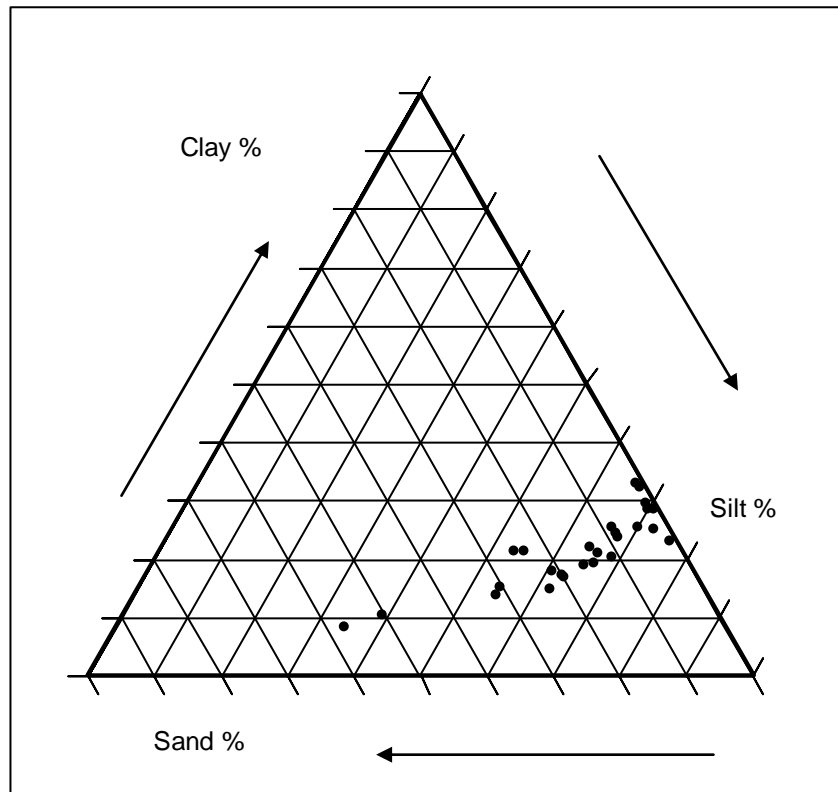
Figure 6.18: Winter grain size across selected sites on the NW sector of PHS.

Grain sizes were more varied during the winter (see Figure 6.18, above). Both the silt and sand fractions vary considerably between the sampling sites, with two sites in particular separated from the main grouping. These two sites fall into the sandy silt area of the diagram (classification after Shepard, see Chapter 3, section 3.3.1.3). The remainder of the sites were in the silty clay and sandy, silty, clay groupings with no clear division between them.

The statistics associated with the grain size fraction for summer and winter are summarised in Table 6.6, below.

Table 6.6: Grain size statistics for the summer and winter on the NW sector of PHS, standard deviation represents the variation between sampling stations.

	Summer		Winter	
	Mean (%)	**Range (%)**	**Mean (%)**	**Range (%)**
Sand fraction	5.6 ± 7.1	$0.2 - 21.7$	15.7 ± 14.8	$0.7 - 57.2$
Silt fraction	66.7 ± 4.9	$55.1 - 74.6$	62.6 ± 9.6	$34.1 - 75.9$
Clay fraction	27.6 ± 5.5	$16.3 - 42.5$	21.7 ± 6.2	$8.7 - 33.1$

The mean winter sand fraction was 15.7%, three times larger than that during the summer (5.6%), however the standard deviation was almost as large as the mean. The silt fraction was smallest during winter (mean of 62.6% compared to 66.7%) and the clay fraction was also smallest during winter (21.7% mean to 27.6%).

6.3.2.1 Spatial distribution

The spatial distributions for each season depict similar spatial patterns to the mean (Figures 6.19 (a)-(f), below). The seasonal differences in the sand fractions are clear in Figures 6.20 (a) and (b). The area of sediment with a larger sand fraction during the winter was closer to the new embankment than during the summer; however it still encompassed the old field margin that forms a channel towards the drainage ditch. The spatial distribution of the silt and clay fractions altered similarly between the seasons, with lower values closer to the new flood embankment during the winter than in summer.
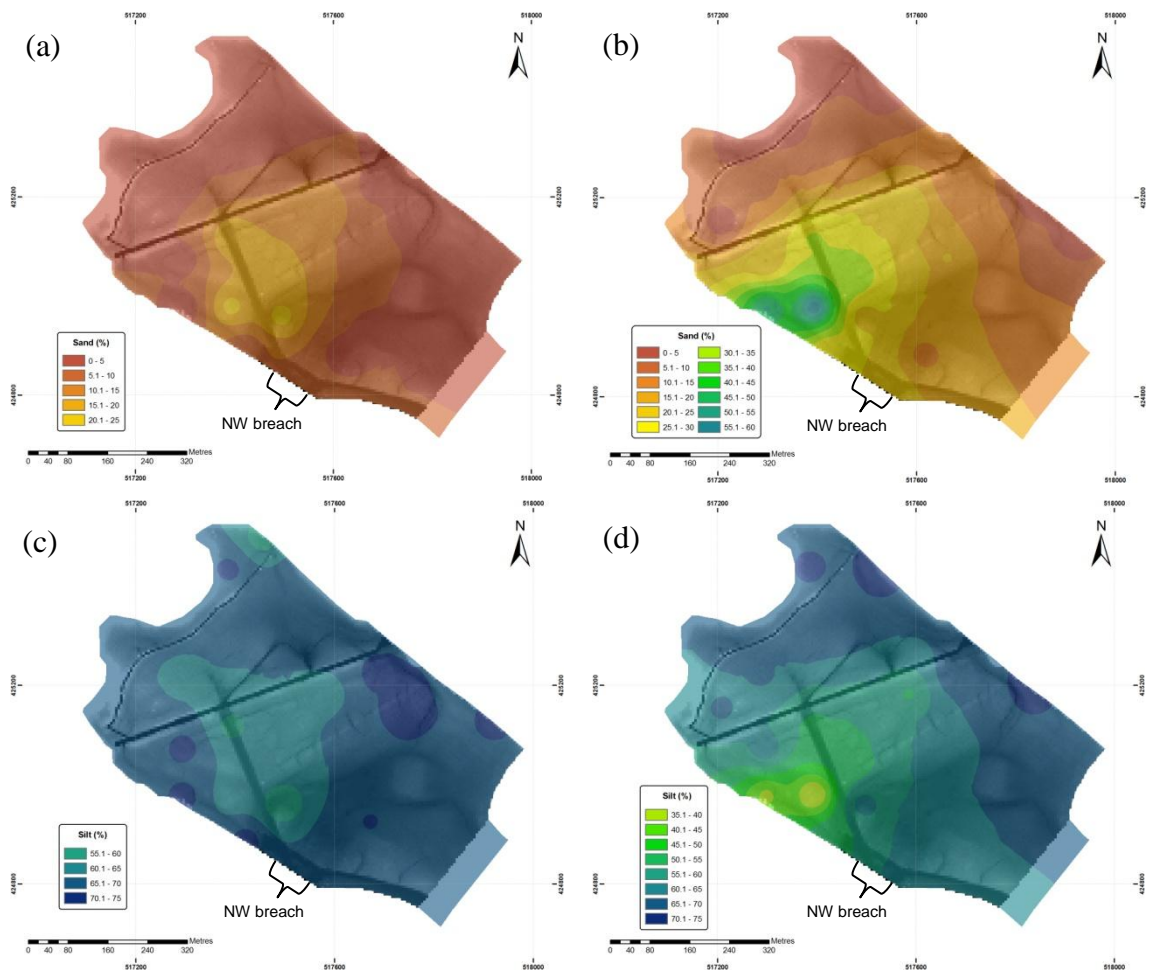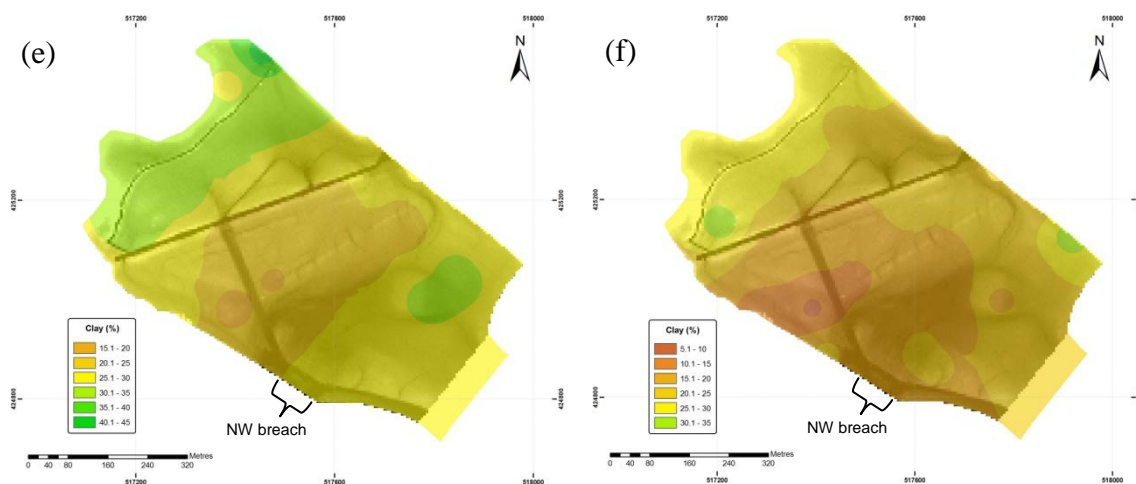
Figure 6.19: Mean grain fractions on the NW sector of PHS, (a) sand during summer, (b) sand during winter, (c) silt during summer, (d) silt during winter, (e) clay during summer, and (f) clay during winter.

6.3.3 Grain size statistics

For the full monitoring period, the mean grain size was 16 µm and median grain size was 10 µm (see Table 6.7, below). This is in the fine silt fraction. The summer median and mean grain size were smaller than over the full monitoring period at 8 and 11.85 µm respectively and the winter median and mean grain size were larger at 15 and 21.4 µm. All values are still within the silt fraction of the grain size distribution. The grain size is most dispersed during the winter (18.6 µm) and least in summer (10.2 µm). The skewness of the grain size distribution was positive reflecting the dominance of fine sediments. For the full monitoring period and during the winter the skewness was higher (6 and 6.4 respectively) than during the summer alone (3.85). Kurtosis is almost identical for the full monitoring period and each season.

Table 6.7: Grain size statistics for full data on NW sector.

	Full monitoring period	**Summer**	**Winter**
Median (µm)	10	8	15
Mean (µm)	16	11.85	21.4
Dispersion/ Sorting	14.0	10.2	18.6
Skewness	6	3.85	6.4
Kurtosis	0.22	0.21	0.2

6.4 Organic content

The mean organic content of the sediment across the NW sector ranged from 8 to 16% (see Figure 6.20, below). The lowest value was around 10% on three sites (22, 25, and 35), and nearly half the sites had organic contents above 14%.

Full organic content data are presented in Appendix 9.
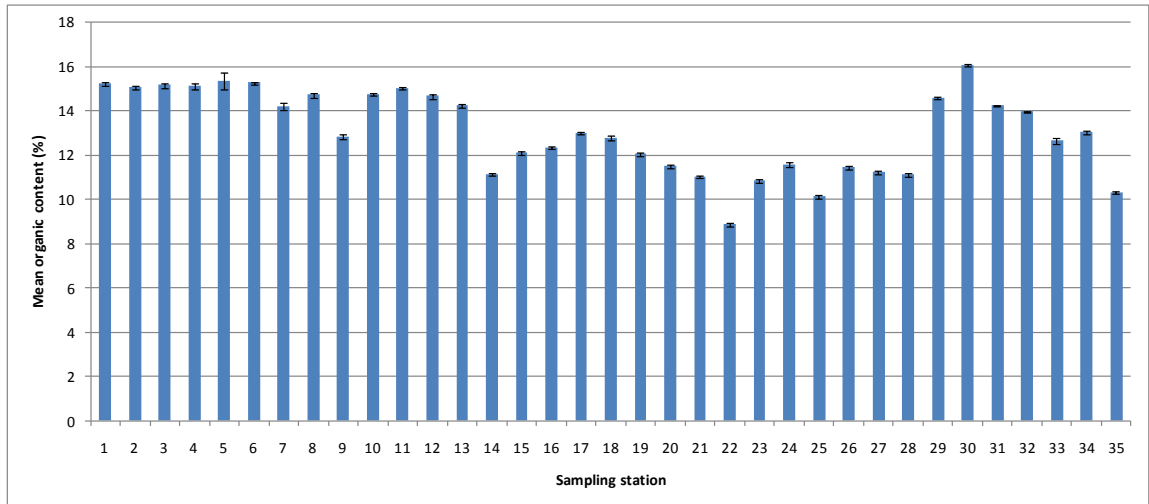
Figure 6.20: Mean organic content on the NW sector of PHS, standard deviation represents the variation between three repeat samples at each station.

6.4.1 Spatial distribution

The organic content of the sediment was lowest in the area behind the NW breach and to the west behind the old flood embankment (see Figure 6.21, below). The higher organic contents were found in sediment in the north western area, which was near the transition zone where the mudflat grades into terrestrial soil. A final area of sediment that had higher organic content was in the eastern corner.
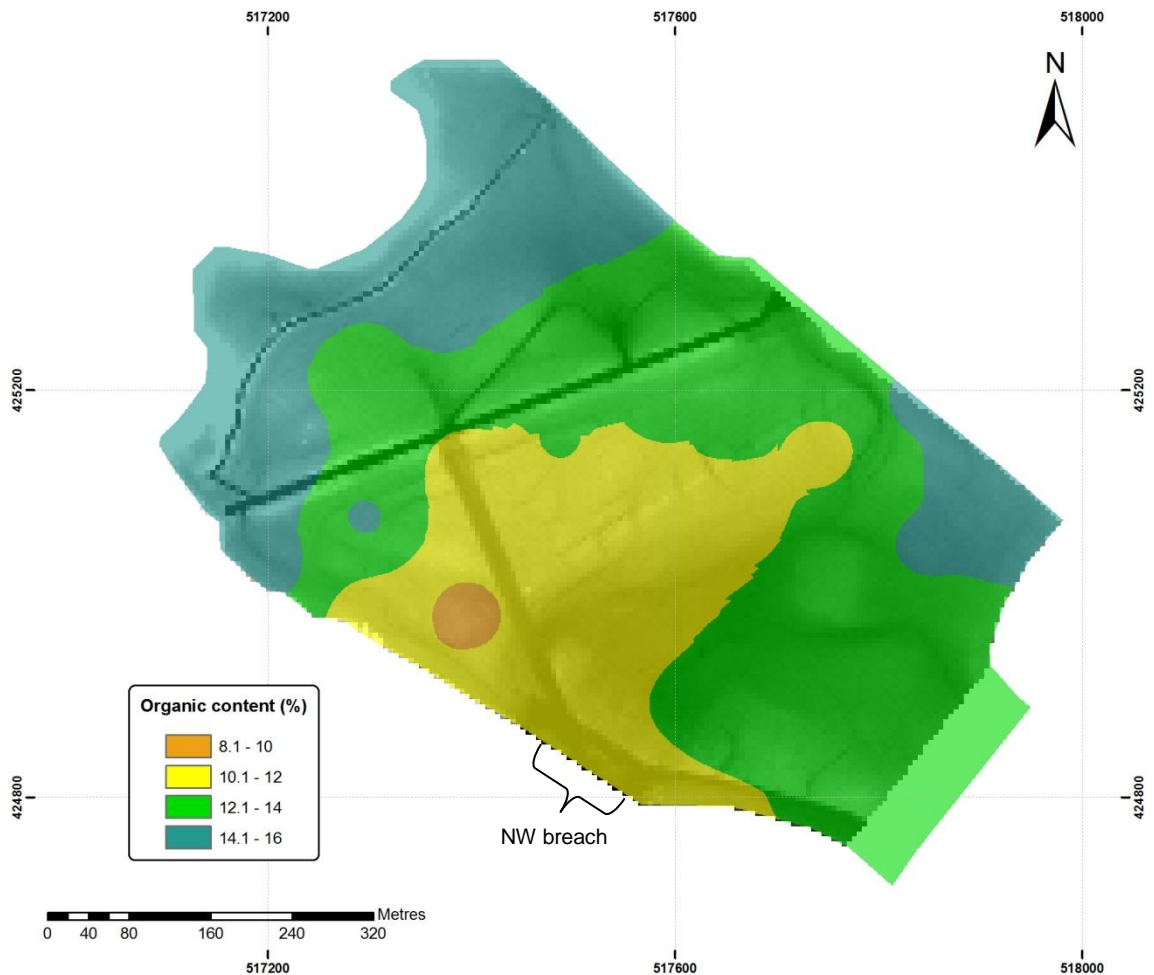
Figure 6.21: Mean organic content on the NW sector of PHS.

6.4.2 Seasonal differences

As expected at almost all sites, the organic content was higher in summer than in winter (see Figure 6.22, below). The variation within the summer and winter organic content values was similar to that of the mean organic content already discussed in previous sections. The summer mean organic content was higher than winter (14.48% compared to 11.64%, see Table 6.8, below) and the lowest recorded organic content for winter was over 3% lower than the comparable summer one. The highest percentage in the winter was 2% lower than that of summer.

Table 6.8: Organic content statistics on the NW sector of PHS, standard deviation represents the variation between sampling stations.

	Mean (%)	Summer (%)	Winter (%)
Mean organic content	13.06 ± 1.87	14.48 ± 1. 96	11.64 ± 2.10
Range	8.86 – 16.05	10.06 – 18.02	6.77 – 16.13

161
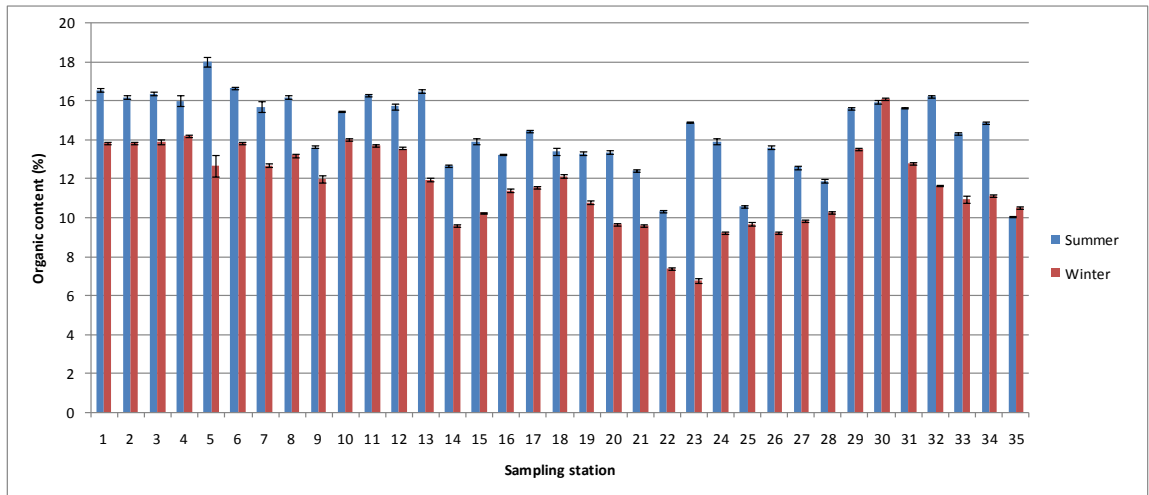
Figure 6.22: Organic content during summer and winter on the NW sector of PHS, standard deviation represents the variation between three repeat samples at each station.
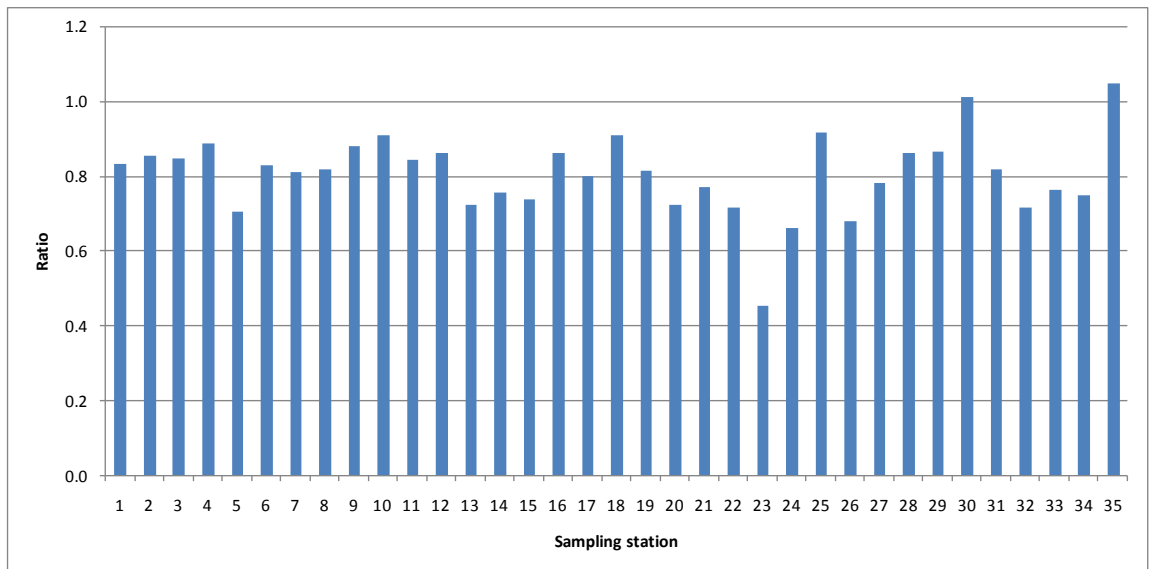
Figure 6.23: Winter: summer organic content on the NW sector of PHS.

The ratio between winter and summer organic content clearly shows the sites where the winter: summer contrast was greatest (see Figure 6.23, above). The biggest difference was at site 23 where the winter organic content of the sediment was only half that of summer. This suggests a situation where vegetation was able to develop during summer but was removed in the winter due to strong tidal flows. At over half the sites, winter organic content was at least 80% of the summer value. Three sites had almost no contrast (25, 30, and 35) and at the remaining sites the ratio was between 0.8 and 0.6.

6.4.2.1 Spatial distribution

The distribution of organic content across the NW sector was similar for both winter and summer (see Figures 6.24 (a) and (b), below). The areas of mudflat with lowest

organic content were concentrated in the area behind the NW breach and to the NW of this behind the old embankment. The areas of sediment with higher organic content were to the NW and the east.
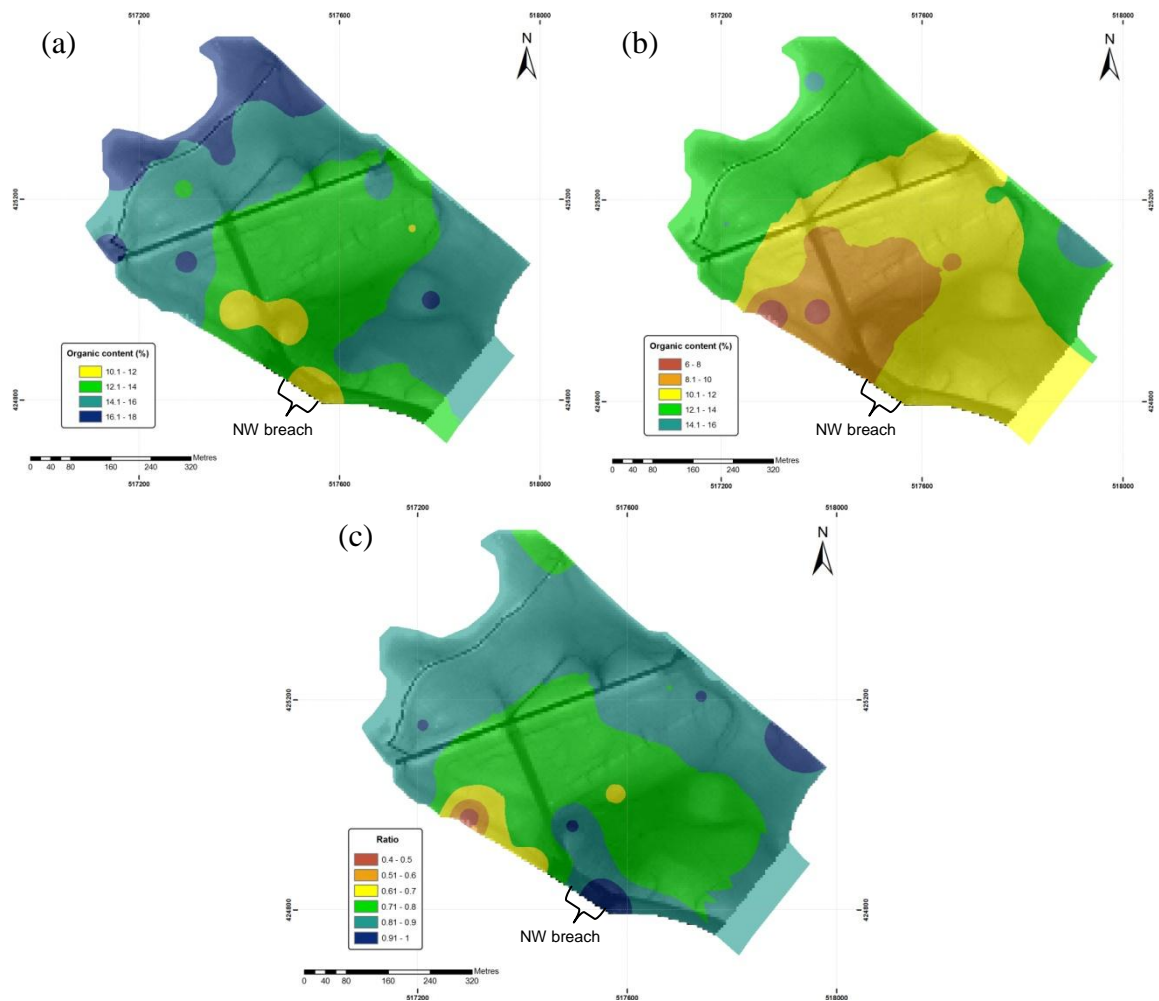
Figure 6.24: Organic content on the NW sector of PHS, (a) is during summer, (b) is during winter, and (c) is the winter: summer ratio.

The biggest contrast between winter and summer values was at a location midway along the old flood embankment (see Figure 6.24 (c)). The smaller ratios were mainly concentrated in the area behind the NW breach and near to the old field margin channel.

6.5 Summary of sediment properties

The sediment properties on the NW sector all show spatial and temporal patterns that may help explain the variation in the accretion data, in particular the fastest accretion rates at the lowest elevations where most variation between the elevation and accretion rate relationship was seen (see section 4.2, Chapter 4). The mean values for each of the four sediment properties investigated are shown in Table 6.9 below. This suggests that the sediment is cohesive in nature, contains some organics, holds a lot of moisture but is still fairly well consolidated.

163

Table 6.9: Mean sediment properties for NW sector of PHS, standard deviation represents the variation across sampling stations.

Sediment property	Mean
Wet bulk density (gcm^{-3})	1.71 ± 0.1
Dry bulk density (gcm^{-3})	1.05 ± 0.14
Sand (%)	10.7 ± 10.1
Silt (%)	64.6 ± 5.8
Clay (%)	24.7 ± 5.4
Moisture content (%)	39.1 ± 4.9
Organic content (%)	13.1 ± 1.87

During the summer wet bulk density, sand percentage, and moisture content are all lower, dry bulk density, organic content, silt and clay percentage are higher- these differences are all statistically significant. The summer sediment is drier and more compacted, contains less sand (or less sand was deposited during the summer) and is richer in organic matter. These statistics are in stark contrast to those for winter.
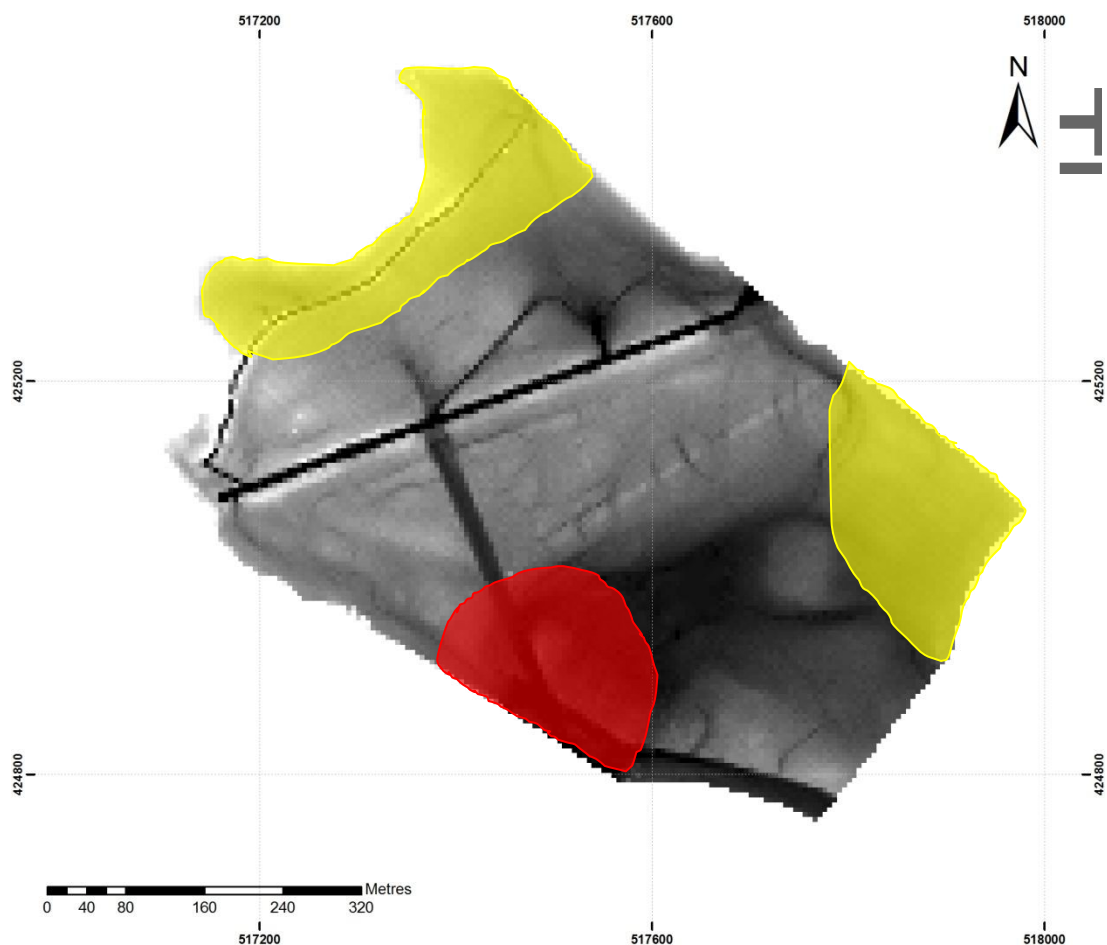
Figure 6.25: Location of two main classifications of sediment characteristics over NW sector of PHS. First area is in red, two remaining areas are in yellow.

The spatial pattern of the mean sediment properties across the NW sector suggests two key locations. The first is the area behind and to the north of the NW breach and the second is in the northern edge and corner of the site and the eastern corner (see Figure 6.25 above).

Table 6.10: Sediment properties in the red and yellow areas of the NW sector of PHS.

Sediment property	Red area	Yellow area
Wet bulk density	Higher	Lower
Dry bulk density	Higher	No pattern
Sand content	Higher	Lower
Silt content	Lower	Higher
Clay content	Lower	Higher
Moisture content	Lower	Higher
Organic content	Lower	Higher

Table 6.10 above shows a summary of the sediment properties in the two contrasting areas of the NW sector. The sediment in the red area around the NW breach is more likely to have higher wet and dry bulk density, and lower moisture content indicating more consolidated sediment. The higher sand and lower organic content in this area could be indicative of faster flows. In the yellow areas the sediment has lower wet bulk density, and higher moisture content possibly indicating that these are areas where water pools (see discussion on inundation of the NW sector, section 5.5, Chapter 5). The organic content is higher and sand content lower. These areas are more elevated and can sustain saltmarsh vegetation. It is therefore not surprising they have higher organic matter contents and less sand since flows over the surface are always both slow and attenuated by the vegetation.

Without knowing the relationships between the different sediment properties on the NW sector and the comparisons with accretion rate and elevation, the full picture of sedimentation cannot be discussed completely. The following sections consider the links among sediment properties in more detail and also evaluate links between sediment properties, accretion rates and elevation.

6.6 Comparisons between factors

Sections 6.1 to 6.5 presented the bulk density, particle size and organic content of the sediment for the NW sector of the site, looking at temporal and spatial patterns. This section will continue to investigate the relationships between properties on the NW sector, making reference to the relationships between each of these properties and

accretion rate and site elevation finally comparing all independent variables with accretion rate to determine those that were most influential in determining the accretion rate.

Relationships among sediment properties and elevation are important because elevation is a key determinant of accretion rate but there may be additional factors causing the scatter in the lower elevated areas of the site.

6.6.1 Comparisons with bulk density

6.6.1.1 Dry bulk density and mud content

The mud content of the sediment is related to cohesion, a high content means that the bed is more cohesive than a deposit with a lower content.

There is a significant negative correlation between mud content and dry bulk density for winter values (Pearson's correlation = -0.776, P = 0.000), see Table 6.11, below. In summer, the relationship, although still negative is not significant (Pearson's correlation = -0.186, P = 0.325).

Table 6.11: Pearson's correlation of mud content and dry bulk density parameters.

Factors for comparison	Pearson's Correlation	P value
Mean mud content, mean dry bulk density	**-0.559**	**0.001**
Summer mud content, summer dry bulk density	-0.186	0.325
Winter mud content, winter dry bulk density	**-0.776**	**0.000**

6.6.1.2 Dry bulk density and organic content

The mean and winter dry bulk density of the sediment, (but not summer), was significantly correlated with organic content with Pearson's correlations of -0.635 (P = 0.000) and -0.765 (P = 0.000), respectively (see Table 6.12, below). The correlation was negative for all sets of parameters, regardless of significance. This indicates that areas with lower bulk densities, organic content is greater, particularly during the winter. This is particularly evident close to the NW breach.

Table 6.12: Pearson's correlation of organic content and dry bulk density parameters.

Factors for comparison	Pearson's correlation	P value
Mean organic content, mean dry bulk density	**-0.635**	**0.000**
Summer organic content, summer dry bulk density	-0.288	0.093
Winter organic content, winter dry bulk density	**-0.765**	**0.000**

6.6.1.3 Dry bulk density and elevation

Mean and winter dry bulk density are negatively correlated with site elevation on the NW sector (Pearson's correlations of -0.442, P = 0.005 and -0.472, P = 0.003, respectively, see Table 6.13, below). In higher areas, mainly towards the new embankments on the NW sector the dry bulk density is less indicative of unconsolidated sediment.

Table 6.13: Pearson's correlation of elevation and dry bulk density parameters.

Factor compared with elevation	Pearson's correlation	P value
Mean dry bulk density	**-0.442**	**0.005**
Summer dry bulk density	-0.095	0.570
Winter dry bulk density	**-0.472**	**0.003**

6.6.1.4 Dry: wet bulk density ratio and organic content

The dry: wet bulk density ratio of the sediment on the NW sector was significantly correlated with organic content for the overall mean and during the winter with Pearson's correlations of -0.675 (P = 0.000) and -0.780 (P = 0.000) respectively (see Table 6.14, below). The correlation during the summer was not significant, however it was still a negative correlation in line with the significantly correlated factors. This indicates that in areas where the sediment had less organic material, the difference between dry and wet bulk density was also low.

Table 6.14: Pearson's correlation of dry: wet bulk density ratio and organic content.

Factors for comparison	Pearson's correlation	P value
Mean dry: wet bulk density ratio and organic content	**-0.675**	**0.000**
Summer dry: wet bulk density ratio and organic content	-0.285	0.098
Winter dry: wet bulk density ratio and organic content	**-0.780**	**0.000**

6.6.1.4 Dry: wet bulk density ratio and sand content

Similar to the correlation with organic content, dry: wet bulk density ratio and sand content was significantly correlated for the overall mean and during the winter with Pearson's correlations of 0.619 (P = 0.001) and 0.756 (P = 0.000) respectively, but not during the summer (see Table 6.15, below). The correlation was positive for all factors regardless of significance and the correlation was strong for both the mean and winter values. Sandier sediments were less moist and more compacted when wet.

Table 6.15: Pearson's correlation between dry: wet bulk density ratio and sand content.

Factors for comparison	Pearson's correlation	P value
Mean dry: wet bulk density ratio and sand content	**0.619**	**0.001**
Summer dry: wet bulk density ratio and sand content	0.282	0.164
Winter dry: wet bulk density ratio and sand content	**0.756**	**0.000**

6.6.1.5 Dry: wet bulk density ratio and elevation

The mean and winter dry: wet bulk density ratio is significantly negatively correlated with elevation (see Table 6.16, below). This suggests that for sediment at higher elevations on the NW sector, the dry: wet bulk density was low.

Table 6.16: Pearson's correlation of elevation and dry: wet bulk density ratio.

Factors compared with elevation	Pearson's correlation	P value
Mean dry: wet bulk density ratio	**-0.485**	**0.002**
Summer dry: wet bulk density ratio	0.011	0.949
Winter dry: wet bulk density ratio	**-0.593**	**0.000**

6.6.2 Comparisons with sand content

Sand content of the sediment is not significantly correlated with the distance from the NW breach (see Table 6.17, below). This suggests that it is not proximity to the breach that determines the amount of sand in the deposited sediment, even though flow velocity declines away from the breach.

Table 6.17: Pearson's correlation of sand content and distance from NW breach parameters.

Factors for comparison	Pearson's correlation	P value
Distance from NW breach, mean sand content	0.061	0.714
Distance from NW breach, summer sand content	-0.006	0.973
Distance from NW breach, winter sand content	0.112	0.504

All parameters of mean, summer and winter sand content were correlated negatively with elevation (see Table 6.18, below). This suggests that as elevation increases the sand content of the sediment was decreasing.

Table 6.18: Pearson's correlation of elevation and sand content parameters.

Factor compared with elevation	Pearson's correlation	P value
Mean sand content	**-0.425**	**0.008**
Summer sand content	**-0.327**	**0.045**
Winter sand content	**-0.429**	**0.007**

6.6.3 Comparisons with organic content

There was a significant correlation between mean and winter moisture and organic contents (Pearson's correlations of 0.686, P = 0.000 and 0.780, P = 0.000, respectively), but not for summer (see Table 6.19, below). For the mean values and during the winter, higher moisture content in sediment is related to higher organic content. The wetter areas during the winter were in the northern, eastern and western corners of the sector, areas that are the most vegetated.

Table 6.19: Pearson's correlation of moisture content and organic content parameters.

Factors for comparison	Pearson's correlation	P value
Mean moisture content, mean organic content	**0.686**	**0.000**
Summer moisture content, summer organic content	0.285	0.097
Winter moisture content, winter organic content	**0.780**	**0.000**

All organic content values are significantly correlated with elevation (see Table 6.10, above). The positive correlation indicates that as site elevation rises, the organic content of the sediment was also higher. The areas that are higher elevated can support vegetation because of the lower inundation leading to better sediment conditions for vegetation colonisation and growth.

Table 6.20: Pearson's correlation of elevation and organic content parameters.

Factor compared with elevation	Pearson's correlation	P value
Mean organic content	**0.569**	**0.000**
Summer organic content	**0.553**	**0.000**
Winter organic content	**0.479**	**0.002**

6.6.4 Comparisons of sediment properties with accretion rate

6.6.4.1 Dry bulk density and accretion rate

Dry bulk density and the dry: wet bulk density ratio were compared with the accretion rate. Four parameters were selected for this comparison: mean dry bulk density, summer dry bulk density, winter dry bulk density and the summer to winter dry bulk density ratio (see Table 6.21, below). The two parameters that significantly correlate with accretion rate are summer dry bulk density and the dry bulk density winter: summer ratio. Both of these correlations are negative (-0.348 and -0.354, respectively). This indicates that during the summer in areas where the accretion rate was slow, dry bulk density was higher. This could indicate that more consolidated areas were less frequently inundated and so would experience slower accretion rates, however, looking at Figure 5.5 (b) the spatial pattern of summer dry bulk density does not reflect this, with highest values mainly around the breach. This suggests that more than one factor is important in determining bulk density.

The ratio between summer and winter dry bulk densities decreases as accretion rate increases. More rapid accretion is observed in areas where the summer dry bulk density is lower than the winter value. This ratio gives an idea of the sites where changes in sediment between seasons were greatest.

Table 6.21: Pearson's correlation of accretion rate with dry bulk density parameters.

Comparing to accretion rate	Pearson's Correlation	P value
Mean dry bulk density	0.155	0.353
Summer dry bulk density	**-0.348**	**0.032**
Winter dry bulk density	0.307	0.061
Summer: winter dry bulk density	**-0.354**	**0.029**
Mean dry: wet bulk density ratio	0.103	0.583
Summer dry: wet bulk density ratio	-0.280	0.089
Winter dry: wet bulk density ratio	0.223	0.178

6.6.4.2 Grain size and accretion rate

The three parameters that correlate significantly with accretion rate were the mean and winter sand content and the sand: clay ratio also for winter (see Table 6.22, below). In all cases the relationship was positive. This suggests that areas with faster accretion had more sand present. Looking back at Figure 5.8 (a), the sediment with highest sand content occurred near to the NW breach, particularly during the winter (Figure 5.11 (b)). The deposition of sand may indicate an area of high deposition hence the faster accretion rates.

The ratio of sand to clay content was positively correlated with accretion rate during the winter, however this relationship was influenced strongly by two outlying data points. These data suggest that sand is associated preferentially with faster accretion rates.

Table 6.22: Pearson's correlation of accretion rate with sand content parameters.

Comparing to accretion rate	Pearson's correlation	P value
Mean sand content	**0.475**	**0.003**
Summer sand content	0.302	0.069
Winter sand content	**0.502**	**0.002**
Summer sand: clay %	0.298	0.073
Winter sand: clay %	**0.543**	**0.001**

6.6.4.3 Organic content and accretion rate

The mean and winter organic content were negatively correlated with accretion rates, higher organic contents relating to lower accretion rates (see Table 6.23, below). The winter: summer ratio is also negatively correlated with accretion rate. This suggests that when the organic content of the sediment during winter was less than the summer, the accretion rate in that area was faster. As the ratio tends towards unity (i.e. organic content in the sediment for both seasons were equal) the accretion rate was generally slower. In areas with more established vegetation (indicated by the similar organic content of the sediment for both seasons), accretion rate was also slower. Areas where organic content falls during the winter may be those where vegetation is less well established.

Previous studies have shown that saltmarsh vegetation is positively linked to accretion rates (e.g. Boorman, 2003; Reed, *et al.*, 1999). This is because incoming sediment is trapped by the developing vegetation, re-suspension is reduced and further material is

added to the surface through organic matter deposits. This link is not evident on the NW sector as vegetation is still sparse and the areas that were accreting rapidly were too low in the tidal frame for the colonisation of pioneer species. However, when saltmarsh species do colonise this sector more fully, a positive correlation with accretion rate could develop.

Table 6.23: Pearson's correlation of accretion rate with organic content parameters.

Comparing to accretion rate	Pearson's Correlation	P value
Mean organic content	**-0.348**	**0.032**
Summer organic content	-0.037	0.827
Winter organic content	**-0.348**	**0.032**
Winter: summer organic content	**-0.383**	**0.018**

6.6.5 Multivariate analysis of factors

To understand the interactions amongst the sediment properties, accretion rates and site elevation a number of multivariate techniques have been used to identify the most important factors influencing sedimentation patterns in the NW sector. An initial stepwise regression has been carried out to identify any components not related to accretion rate, then a multiple regression analysis of the remaining components was carried out to identify the contribution made by each factor to the accretion rate.

6.6.5.1 Mean values

Stepwise regression carried out on the independent values of accretion rate, elevation, organic content, sand content and dry bulk density indicates that sand content, organic content and elevation are the main predictors of the mean accretion rate for the NW sector (see Table 6.24, below).

Table 6.24: Results from stepwise regression to determine factors influencing mean accretion rate on the NW sector PHS.

Step	1st	2nd	3rd
Sand content (coeff)	0.190	0.392	0.422
P value	0.003	0.001	0.000
Organic content (coeff)		1.13	1.68
P value		0.031	0.003
Elevation (coeff)			-4.3
P value			0.023
S	3.30	3.13	2.94
R^2	19.49	31.55	41.34

The results of the stepwise regression indicate that both mean sand and organic content correlates positively and that elevation correlates negatively with accretion rate. The R^2 value for the 3rd step is 41%- this means that these three factors predict 41% of the variation in the accretion rate. A regression analysis was then carried out with these three factors to see which best predicted the accretion rate (see Equation 6.1).

$$Accretion = -10.4 - 4.3 \; Elevation + 1.68 \; Organic \; content$$
$$+ 0.422 \; Sand \; content$$

Eq. 6.1

6.6.5.2 Winter values

Comparing just the values recorded for accretion rate, elevation, sand content, organic content and dry bulk density during the winter using a stepwise regression gives the results presented in Table 6.25, below.

Table 6.25: Results from stepwise regression to determine factors influencing winter accretion rate on the NW sector PHS.

Step	1st	2nd	3rd
Sand content (coeff)	0.174	0.308	0.301
P value	0.002	0.004	0.004
Dry bulk density (coeff)		-9.3	-11.3
P value		0.122	0.065
Elevation (coeff)			-3.4
P value			0.143
S	4.11	4.03	3.96
R^2	24.07	29.16	33.55

The third step of the regression model included sand content, dry bulk density and elevation, however sand content was the only parameter with a significant P value. This indicates that it is sand content which most closely predicts accretion rates over the NW sector during winter. The R^2 value for the final step was quite low at 34% indicating that only a third of the variance in the accretion rate was explained by these three factors.

6.6.5.3 Summer values

A stepwise regression for summer values of accretion rate, elevation, sand content, organic content and dry bulk density using a stepwise regression gives the results presented in Table 6.26, below.

Table 6.26: Results from stepwise regression to determine factors influencing summer accretion rate on the NW sector PHS.

Step	1st	2nd
Dry bulk density (coeff)	-8.6	-10.5
P value	0.032	0.007
Sand content		0.25
P value		0.018
S	3.94	3.68
R^2	12.09	25.29

During the summer it appears that only two parameters explain the variance in the accretion rate- firstly dry bulk density and secondly sand content. The results for both parameters were significant with P values less than 0.05. The R^2 value, however, was only 25% so these two factors only explain a quarter of the variance seen in the accretion rate.

$$Accretion = 14.1 + 0.249\ Sand\ content - 10.5\ Dry\ bulk\ density$$

Eq. 6.2

6.7 Conclusions

This chapter has presented the results from studying the sediment properties across the NW sector to see if they are significantly correlated with the sedimentation patterns on this sector presented in Chapter 4. In general, there are areas on the NW sector that have similar sediment properties and these were discussed in section 6.5. The relationships presented in section 6.6 are inconclusive as to whether any of the sediment properties studied were significantly correlated with the accretion rate. The strong relationship between elevation and many of these properties appears to indicate that it is elevation that is primarily responsible for the sedimentation patterns on the NW sector and the other factors may explain some of the variation within this relationship. Depending on the season, either bulk density, sand content or organic content had some relationship with the accretion rate. It is very likely from the different relationships presented throughout this chapter that it is an interaction among these factors that cause the wide range of accretion rates on the NW sector. In winter months, the site was accreting fastest and relationships are clearest. During the summer, relationships between sediment properties and the accretion rates are less evident. All of these properties were studied as they have been cited in the literature as having either a positive or negative correlation with sediment stability and accretion (see introduction at the start of this

chapter), however, it appears that for a fast accreting managed realignment site, these sediment properties are not correlated with the accretion rate.

The next chapter presents the results of a flume based experiment that compares areas of the site that have differing sediment properties and accretion rates to see the effects of these on erosion potential under increasing flow velocities. This will show whether sediment properties on a smaller scale have an effect on sediment stability.

Chapter 7 : Erosion study

The erosion potential of sediment is influenced by a number of factors listed in Table 2.2, Chapter 2. Many of these factors have been presented in the previous chapters on sediment characteristics and sediment fluxes for the NW sector. The critical erosion shear stress of the sediment at locations across PHS has not so far been identified. To measure the shear stress of sediment and its relation to sediment properties and accretion, a flume-based study was undertaken.

The erosion study focuses on the volume of SPM measured in the flume as the bed shear stress is increased (section 7.3) over the surface of the sediment cores (section 7.4) from different locations across the site. The difference in SPM concentrations as velocity increases can be used as an indication of the threshold of erosion for a given sediment surface and how much sediment is eroded at different shear stresses. The erosion of the bed material on the site will be triggered at a certain shear stress related to the current velocity and depth of the tide and influenced by the sediment properties at that location.

The sediment properties of the cores used in this study are presented in sections 7.1 and 7.2. The critical shear stress in cohesive sediment has been found to decrease as moisture content increases, this is proposed to be linked with the strength of the bonds between clay particles weakening as they become less compacted (Raudkivi, 1998). A number of studies have also found a positive correlation between the critical shear stress of sediment and the bulk density (Amos, *et al.*, 2004; Bale, *et al.*, 2006; Quaresma, *et al.*, 2004; Riethmuller, *et al.*, 2000; Tolhurst, *et al.*, 2000). However, not all studies report a link between sediment properties and erosion highlighting that different results are expected when studying different sites, and the difficulty in studying cohesive sediments (Paterson, *et al.*, 2000). The bulk density is also negatively correlated with mud content (Delefontaine *et al.* 1996), linking the critical shear stress of sediment to the particle size. For the NW sector, mud content and dry bulk density were significantly negatively correlated for the mean values and during the winter (see Chapter 6, section 6.6.1.1). A study by Bale, *et al.* (2006) investigated the *in situ* links between CET and sediment properties. The CET was found to be most strongly linked with the bulk density (positive correlation), then moisture content and silt content (negative correlations). These correlations were also found to significantly link with the critical erosion shear stress in a study by Friend, *et al.* (2003).

Details of sediment core location, collection and running of the study are found in Chapter 3, section 3.2.9.

7.1 Sediment conditions at erosion study sites

The accretion rate at the four selected sampling sites is shown in Figure 7.1 below. The fastest accretion rate (and fastest on the whole of PHS) was at site 6c. The accretion rate at site 7a of 5.89 mm month^{-1} was the closest to the mean accretion rate over the whole NW sector (5.85 mm month^{-1}). Both sites 4a and 3b had similar accretion rates, however their locations were inundated 0 to 10% of the time (site 3b) compared to 10 to 20% of the time (site 4a). This difference in inundation is reflected in the lower moisture content for site 3b of 41% compared to 57% at site 4a (see Chapter 5, section). Site 3b was at the highest location (2.73 m ODN), sites 4a and 7a were similarly elevated (2.41 and 2.47 m ODN, respectively) although had different accretion rates. Site 6c was the lowest at 1.87 m ODN and closest to the NW breach.
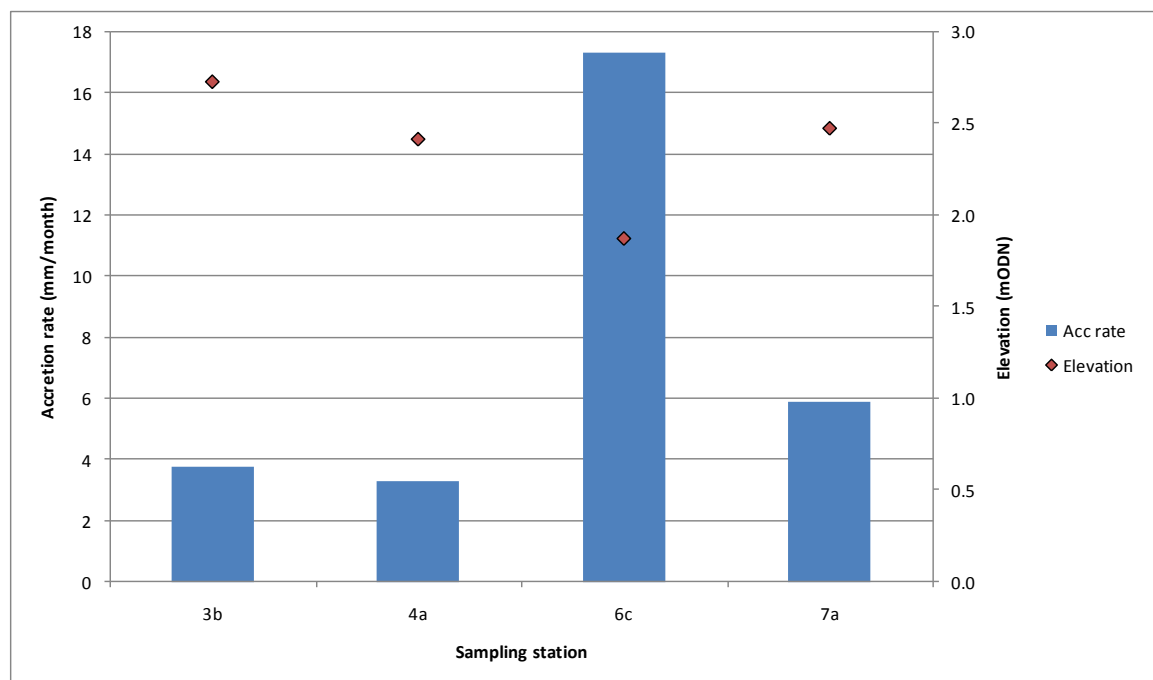
Figure 7.1: Monthly accretion rate at sites sampled for erosion study.

When comparing the grain size for each sampling station, it is the fastest accreting site 6c that has the greatest sand fraction of 25% (15% more than the average for the NW sector) and consequently the lowest silt and clay fractions (see Figure 7.2, below). Sites 4a and 7a are very similar in their grain size fractions, both with very small amounts of sand, and nearly 70% silt and 30% clay (both about 5% less than the mean for the NW sector). Site 3b on the SE sector has a greater silt fraction than the other three sites

(closer to 80%) and consequently a lesser clay fraction of 15%. The sand fraction is greater than both sites 4a and 7a at 3.5% but still not as great as site 6c.

The smallest organic content is found at site 6c (see Figure 7.3, below), however site 3a is similar; both around 14%, close to the mean organic content for the NW sector of 14.5%. The other two sites have a greater organic content; site 7a is the slightly higher of the two, both around 17%.
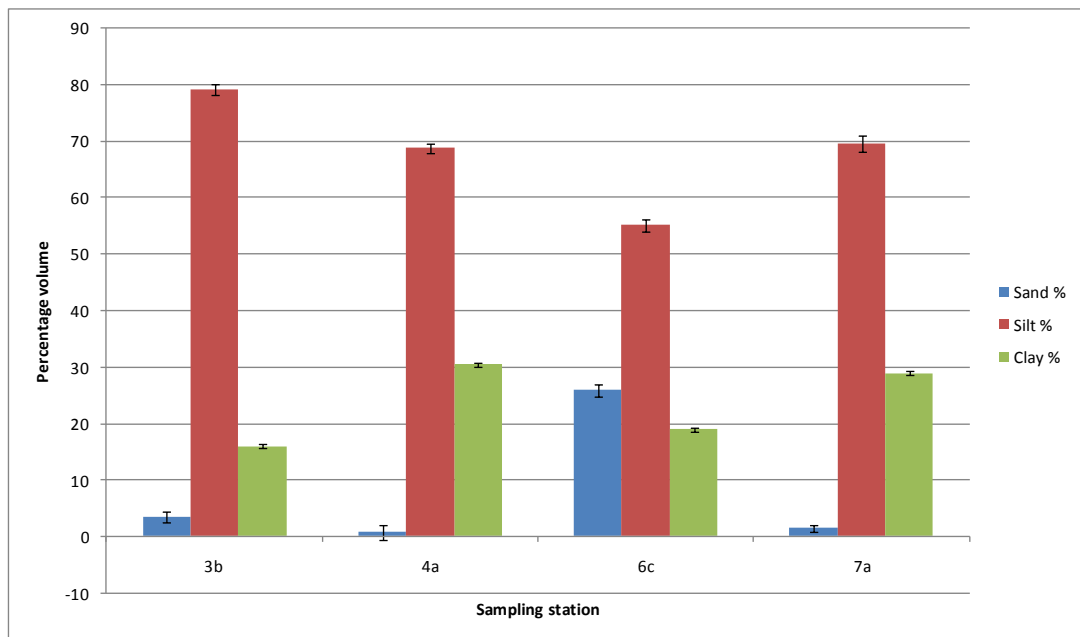
Figure 7.2: Grain size at the sites used for erosion study, standard deviation represents the variation between three repeat samples at each site.
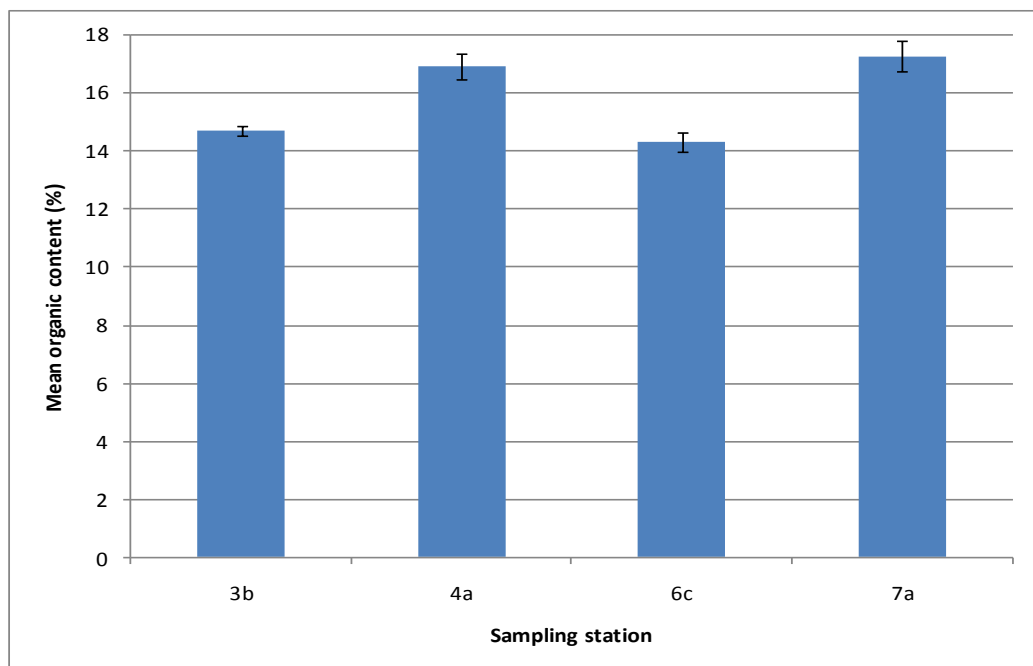
Figure 7.3: Organic content at the sites used for erosion study, standard deviation represents the variation between three repeat samples at each site.

7.2 Changing sediment conditions

The bulk density and moisture content of the sediment used in the erosion study was analysed before and after the study to see the effects of exposing the sediment from different areas across the site to a range of flow conditions. The conditions of the sediment cores from site 6c were different to those from the remaining three sites as mean wet and dry bulk density and moisture all either increased or were similar before and after the study. The mean dry bulk density was around 1.7 gcm^{-3} and the dry bulk density around 1.0 gcm^{-3} (see Figures 7.4 (a) and (b)). The mean moisture content was around 38% (see Figure 7.4 (c)). The large standard deviation indicates spatial variability of the sediment after the study.

The sediment conditions of the cores from the remaining three sites all decreased after the cores were exposed to the different flow conditions during the erosion study. The wet and dry bulk density was greatest at site 3b (see Figures 7.4 (a) and (b)). The wet bulk density of the sediment before the study was 2.16 gcm^{-3} and the dry bulk density was 1.58 gcm^{-3}, both greater than the average wet and dry bulk density for the summer (when cores were collected) on the SE sector (1.76 and 1.31 gcm^{-3} respectively). The mean wet bulk density before the study of the sediment cores from sites 4a and 7a was close to 1.7 gcm^{-3}, which is slightly higher than the mean of 1.67 gcm^{-3} on the NW sector during summer. The mean dry bulk density before the erosion study was just below 1.0 gcm^{-3} again this is close to the mean dry bulk density for the NW sector of 1.13 gcm^{-3}. After the study, the mean wet and dry bulk density decreased between 1.5 and 2 gcm^{-3}.

The moisture content was least in the sediment from site 3b, the site with smallest bulk density, just over 25% before and around 33% after the erosion study (see Figure 7.4 (c)). The mean moisture content in the SE sector was 25.3%, very close to the 'before' value. Sediment cores from sites 4a and 7a had moisture contents of around 47% after the study; before the study site 4a had a moisture content of just over 45% and site 7a had a moisture content of around 42%. The mean moisture content on the NW sector during summer was lower than these values at 32.7%.
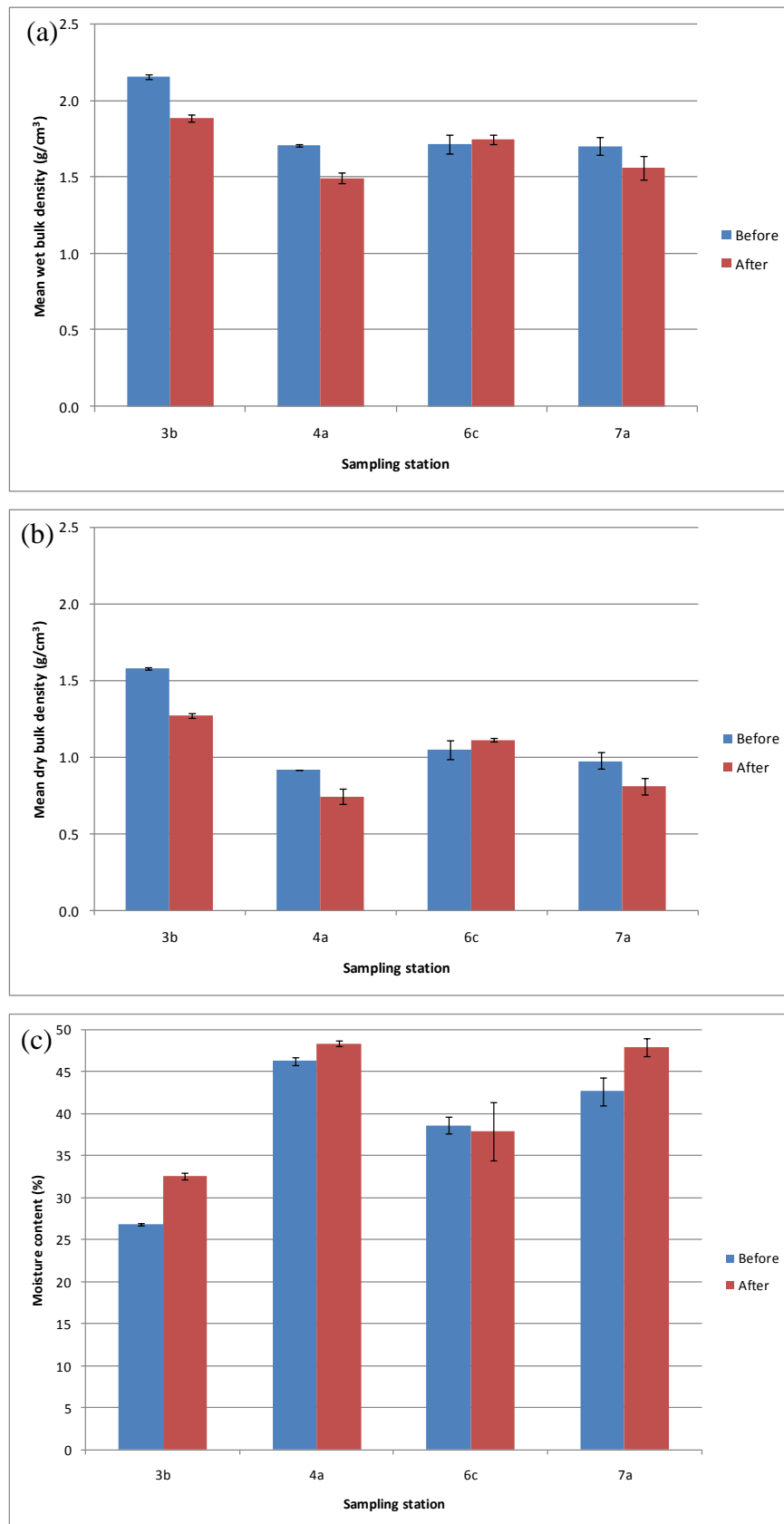
Figure 7.4: Sediment properties before and after the erosion study, (a) mean wet bulk density, (b) mean dry bulk density, (c) mean moisture content, standard deviation represents the variation between three repeat samples at each site.

When including results from site 6c, the mean wet and dry bulk density before and after the erosion study were not significantly different (paired t-tests, P = 0.11 and P = 0.16, respectively) however with the results from this site removed the bulk densities were significantly different (paired t-test, P = 0.03 and P = 0.04, respectively). The difference between the moisture content before and after the erosion study was not significant (paired t-test, P = 0.14), however with the data from site 6c removed the difference was significant (paired t-test, P = 0.03).

7.3 SPM during the study
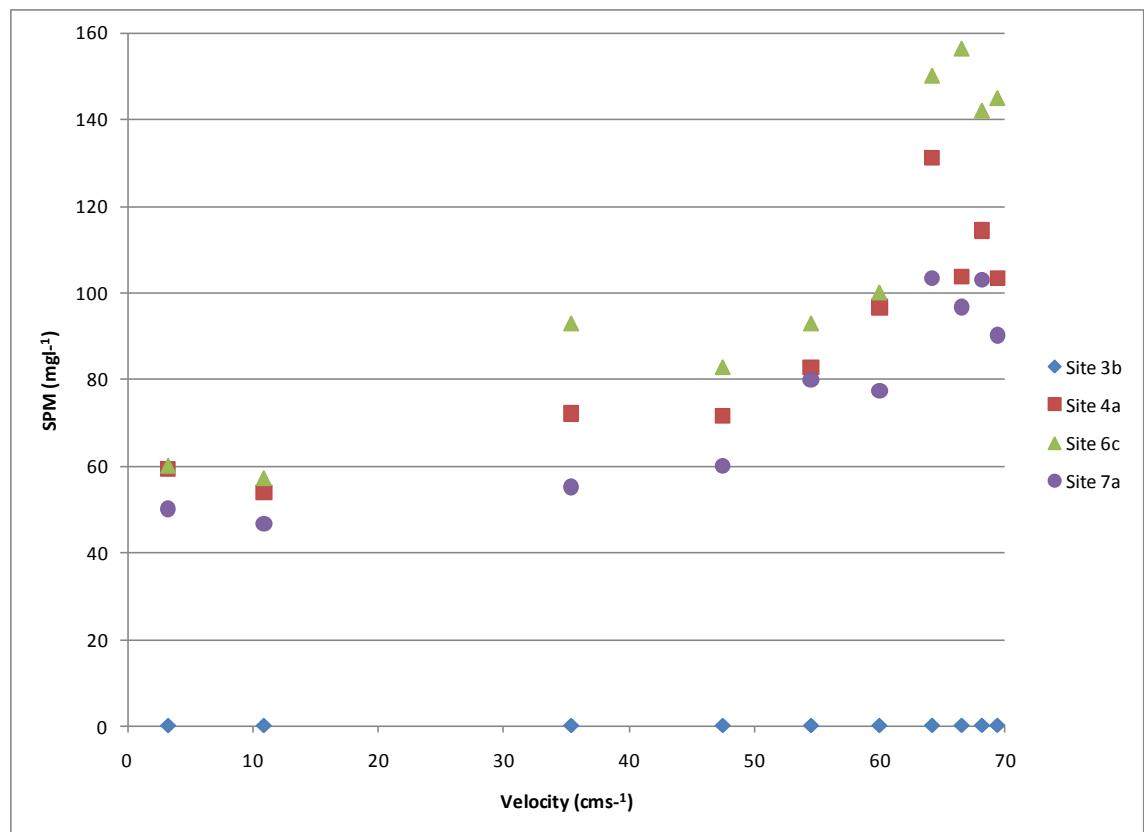
Figure 7.5: SPM concentration over the sediment cores for sites 3b, 4a, 6c and 7a as near-bed velocity increases.

Figure 7.5 above is a comparison of the near-bed velocity recorded 4 cm above the sediment cores by an ADV and the SPM concentration, indicating associated periods of erosion. Sediment from site 3b did not erode as the velocity in the flume increased. The concentration ranged from 0.03 mgl^{-1} when near-bed velocity was around 5 cms^{-1} to 0.07 mgl^{-1} after 60 cms^{-1} was recorded.

The sediment cores from the remaining three sites eroded as shown by the higher SPM concentrations as near-bed velocity in the flume increased. These three sites showed an initial fluff layer (similar to the study by Schaaff, *et al.* (2006)) when the velocity was

around 5 cms^{-1} as loose sediment not part of the bed was suspended. SPM concentration then decreased to below 55 mgl^{-1} when the near-bed velocity increased to 10 cms^{-1}.

The next stepwise increase of flow velocity in the flume was 15cms^{-1}, however the near-bed velocity increased to 30 cms^{-1}. This increase was met with an increase in SPM concentration in the flume from all three sites, the highest increase recorded over sediment from site 6c. As velocity increased to 60 cms^{-1}, SPM concentration over cores from sites 6c and 4a rose to 100 mgl^{-1}, and over cores from site 7a to 80 mgl^{-1}. Between 60 and 70 cms^{-1}, erosion of the cores from site 6c sustained SPM between 140 and 160 mgl^{-1}. Sediment erosion dropped on cores from the remaining two sites from a high of 130 mgl^{-1} at site 4a and a high of 100 mgl^{-1} at site 7a to lows of 100 mgl^{-1} (site 4a) and 90 mgl^{-1} (site 7a).

The results of the erosion study indicate that at the site with fastest accretion and sand content, the sediment was eroded the fastest as the near-bed velocity increased. The sediment did not erode earlier than at the other sites in the NW sector, however the amount of sediment eroded from the cores was greater and faster when near-bed velocity reached 30 cms^{-1}.

The cores from site 3b that did not erode during the study were visually different from the other cores. The lower moisture content, higher bulk density and greater amount of cohesive sediment point towards sediment that is more resistant to erosion, the cores were more compacted than those from the other sites. Less tidal inundation at this site may also lead to compaction of the sediment.

7.4 Bed shear stresses

From the previous section, the sediment was not eroding at site 3b but was at the other three locations when the velocity across the cores increased. At these three sites the threshold for erosion occurred between 10 and 30 cms^{-1}. The bed shear stress on these cores calculated using the Law of the Wall equation (Equation 3.9 and 3.10 in Chapter 3, section 3.4) is shown in Table 7.1 below.

As a comparison, values of critical shear stress for estuarine tidal mudflats, as reported in Black, *et al.*, (2002) range between 0.02 and 2.0 N m^{-2}. Measurements of natural shear stresses in the Humber estuary at the Skeffling mudflats during a relatively calm period were in the range of 0-1.0 Nm^{-2} (Tolhurst, *et al.*, 1999).
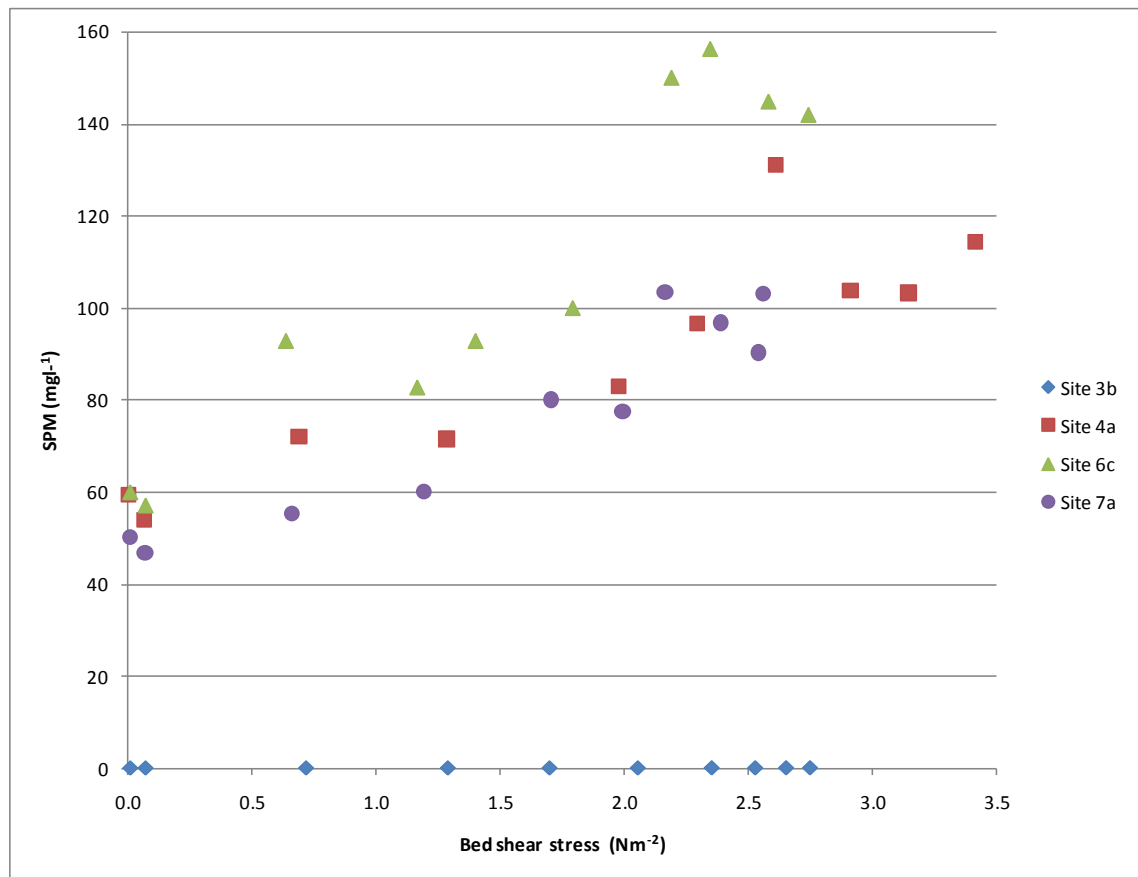
Figure 7.6: Changing bed shear stress and SPM concentration across sediment cores for sites 3b, 4a, 6c and 7c.

Table 7.1: Bed shear stress measured in a flume for sediment cores from four sites on PHS at increasing near-bed velocities.

Mean near-bed velocity (cms⁻¹)	Bed shear stress τ_{cr} (Nm⁻²)			
	Site 3b	Site 4a	Site 6c	Site 7a
3.1	0.006	0.003	0.005	0.007
10.8	0.068	0.068	0.067	0.065
34.4	0.715	0.691	0.634	0.658
46.5	1.287	1.286	1.165	1.193
54.4	1.698	1.980	1.400	1.703
59.7	2.054	2.296	1.793	1.992
63.9	2.352	2.615	2.192	2.164
66.8	2.528	2.914	2.348	2.388
69.5	2.749	3.150	2.584	2.541
70.5	2.652	3.417	2.745	2.558

The values of critical bed shear stress are similar for sediment from all sites tested in the flume (see Table 7.1, above). When mean velocity over the sediment cores had reached 10 cms^{-1}, critical shear stress was between 0.065-0.068 Nm^{-2}. This coincides with a slight decrease in the amount of SPM in the flume (see Figure 7.6, above). By the time mean velocity in the flume has reached 35 cms^{-1}, critical shear stress is much greater (between 0.634 and 0.715 Nm^{-2}). This coincides with a period when SPM in the flume over all sediment cores was increasing, indicating that erosion was taking place. As the critical shear stress was similar for all sediment cores collected from the four sites, the differences in erosion seen by the differing SPM amounts are related to sediment properties of the cores.

A similar study to this one by Schaaff, *et al.* (2006) reported critical shear stress values of 0.02 Nm^{-2} when the initial fluff layer eroded, increasing to 0.05 Nm^{-2} in the second phase of erosion, which was for mud cores collected from the Gulf of Fos in France. Both these values are different to those recorded over the cores from the current research site; the initial critical erosion shear stress is higher than for the current study and the final value is lower than for the current study.

Watts, *et al.* (2003) investigated the shear stress of sediment at the Tollesbury managed realignment site using a cohesive strength meter (CSM). They found that after six years of tidal inundation, for the sediment above mean high water neap (MHWN) the critical erosion shear stress was 2.45 Nm^{-2}, and below MHWN (where accretion rates were fastest) the critical erosion shear stress was lower at 1.5 Nm^{-2}.

7.5 Conclusions

The sediment cores that exhibited least erosion under flume conditions were from site 3b, just into the SE sector. Table 7.2, below, lists the sediment properties of all the cores that were reported in previous studies to be significantly correlated with erosion of sediment (see section 7.1). For both bulk density and moisture content, the suggestion is that this site should be the most resistant to erosion, however, a high silt content has been found to correlate with low critical erosion threshold. This may not have affected the sediment cores as much as at a site that was frequently inundated and where the sediment was less compacted than at site 3b.

Table 7.2: Comparison of sediment properties of sediment cores used in flume study that correlate with erosion of sediment according to published literature.

Site	Silt content	Bulk density	Moisture content
3b	Highest (80%)	Highest, before and after study	Lowest, before and after study (25-35%)
4a	70%		45-50%
6c	Lowest (55%)	Slightly lower out of NW sector sites, before and after study	Lowest of NW sector sites, before and after study (35-40%)
7a	70%		40-50%

Of the three sites from the NW sector, it is site 6c that most exhibits sediment properties best suited to resist erosion. The silt content was the lowest of all four sites, the bulk density was slightly lower of the three NW sector sites and the moisture content was again the lowest of the NW sector sites. All these factors have been reported to be significantly correlated with a high critical erosion shear stress and critical erosion threshold. During this study, however, the three NW sector sites all eroded with similar SPM values and increases and also had similar critical erosion shear stresses associated with that erosion. Out of these three sites it was probably site 6c that eroded the most over the whole study. This could be linked to the higher sand content of sediment from the site and thus a lower cohesion between sediment particles, increasing the erosion potential. Overall, this points towards the conclusion also made from the results presented in Chapter 6, that the accretion of sediment on the NW sector is primarily dictated by factors other than the sediment properties, namely elevation and in turn the tidal inundation.

A laboratory based study of the erosion of cohesive sediment such as this one needs to ensure that the condition of the sediment cores remains as close as possible to the conditions of the sediment at the site. Studies by Pope *et al.* (2006) and Schaaf *et al.* (2006) both compare data from flume experiments to those recorded *in situ*. Both found that comparable results were obtained using these two methods and the study by Schaaf *et al.* (2006) used a similar experimental set-up as the one in the current study. However, there are always going to be constraints when removing sediment from a site to a flume that will inhibit the results from such a study. Some deterioration of the cores is inevitable, however carefully the cores are collected, this has been seen in the current study as an initial erosion of a fluff layer occurred removing loose sediment that had

accumulated on the core surface. A further constraint to examining erosion of a cohesive sediment is the ability to determine when erosion is starting. In the current study this was done by examining the relationship between the amount of SPM in the flume and time, to try to pin-point when the threshold for erosion had been attained. This method is still subjective. This flume study has highlighted the difficulties that researchers have in studying cohesive sediments and the erosion of such sediments.

This chapter completes the presentation of results, a brief summary of all the results chapters follows and the final chapters will then discuss these findings and present conclusions.

Summary of Results

The rapid accretion rates recorded on the NW sector during the monitoring period were reported in Chapter 4, section 4.3, to be significantly linked with elevation across the site. Fastest accretion was found in the area landwards of the NW breach and behind the old flood embankment to the north. A seasonal difference exists with faster accretion rates during the winter months.

Chapter 5 outlined a sediment budget for a year through the NW breach on PHS. The amount of sediment entering the NW sector during a year of approximately 63 400 tonnes was found to be comparable to the sediment load of approximately 50 000 tonnes required to sustain the recorded accretion rates. The inundation patterns and time lag as sediment is carried across the site were proposed as a reason for the difference between the two methods of calculation.

In Chapter 6 the properties of the sediment on the NW sector were presented to examine patterns. Three distinct areas were identified where sediment properties were similar (see section 6.5). These sediment properties were then compared with each other and with accretion and elevation, identifying a seasonal trend in significant correlations, showing that the winter values were more likely to correlate than the summer values recorded. However, after investigating all of these sediment properties, only elevation was found to be strongly correlated with accretion rate; all other properties were proposed as increasing the 'noise' in this relationship at lower elevations, especially sand content and in some cases bulk density.

The flume study presented in Chapter 7 indicated that despite flume cores being collected from different areas of the NW sector, they all eroded continually as water velocity increased. The site that did not erode was on the SE sector- at a higher elevation, characterised by slower accretion, less inundation and thus a more compacted bed, resistant to erosion.

Chapter 8 : Discussion

Measurements of accretion rates taken on PHS post-breach were found to be an order of magnitude faster than those predicted by modelling produced when designing the site. These faster rates of accretion will affect the floodwater storage potential of the site and the rates of ecological change, thus altering the capacity of the site to meet the main aims of creating PHS that are flood alleviation and habitat creation. The purposes of this study were to examine the cause of accelerated rates of accretion, investigate the sediment properties and plant colonisation of a newly created intertidal habitat, to understand the relationship between patterns of sedimentation and the sediment budget, and to develop a conceptual model that could be used to design other sites. To answer these aims, a full monitoring programme was undertaken at PHS, a sediment budget was produced and the erosion potential of key areas studied. The previous chapters have presented the results of this study; this chapter will integrate these results and propose a conceptual model of PHS which is applicable to other similar fast accreting managed realignment sites, discussing how a site such as this one passes through a series of stages towards becoming a more stable intertidal area. Reasons will be discussed for the difference between this site and other managed realignment sites and recommendations will be made for flood managers in the design and monitoring of future sites so they can successfully create intertidal land and negate the effects of global warming induced sea level rise.

8.1 A conceptual model for fast-accreting managed realignment sites

The NW sector has been found to accumulate sediment at a very fast rate as soon as the site was breached and continued to accrete at similar rates to the end of the monitoring period, five years after breaching. In comparison, the managed realignment sites in the Blackwater estuary, Essex (discussed in section 2.1.4, Chapter 2) have reported different rates of sediment accretion. Three of the sites did not accrete until vegetation cover was established. The site at Orplands accreted nearly 50 mm in two years and Tollesbury accreted between 40 mm and 300 mm per year, depending on the time elapsed since breaching (Cundy, *et al.*, 2002; French, 2006; Pethick, 2002; Pontee, *et al.*, 2006).

On fast-accreting managed realignment sites, the following conceptual model of the site's propagation and the expected changes to sediment properties, elevation, inundation, accretion rate and vegetation colonisation is proposed. Compaction of the

sediment has not been taken into account as values for this were not part of the present research. The data to produce this model are provided by the results from the present research that have been summarised previous to this chapter. Figures 8.1 and 8.2 (a) propose the different zones to explain the sedimentation patterns across the NW sector at the end of the period of monitoring. The model simulates the area perpendicular to the NW breach between this and the new embankment on the NE of the site. This is a coherent section of the site where rapid accretion is occurring and where the control variables are similar, and has been chosen for this reason. The underlying field was graded to slope down towards the NW breach previous to breaching. By the end of the monitoring period (five years after breaching) only three of the five elevation zones identified on PHS are represented on the NW sector. Elevations are approximate based on the LIDAR elevation map from 2005 that has been used in previous chapters, e.g. Figure 3.4, Chapter 3, and accretion rates measured during the monitoring period. The zones referred to are those that have been identified during the EA monitoring programme as changing vegetation zones for saltmarsh species on PHS (see Table 4.5, Chapter 4). Associated with these zones are mean accretion rates that have been calculated in Chapter 4 (see Table 4.6 and Figure 4.8). These accretion rates slow as the elevation of the site rises, a correlation between elevation and accretion rate was found to be significant and presented in Chapter 4 (see section 4.2).
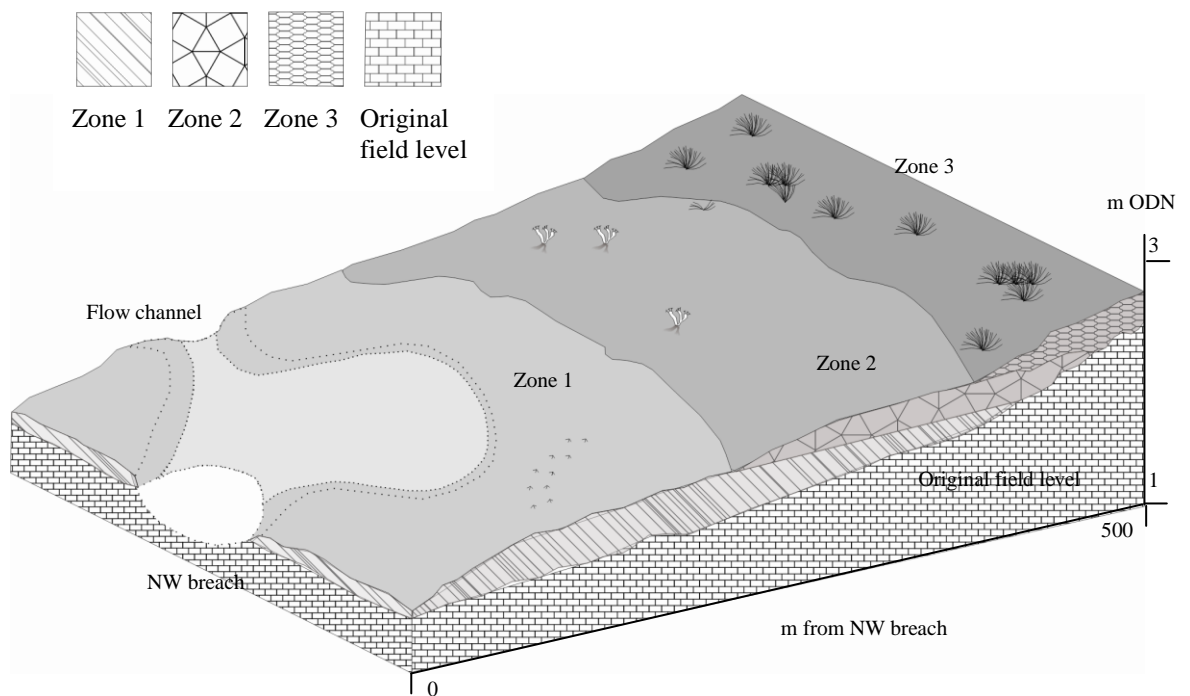
Figure 8.1: Conceptual model of a managed realignment site five years after old sea defences have been breached at a single point.

189

The model in Figure 8.1 is driven by the changes in elevation over the NW sector which in turn drives the tidal inundation time and residence time of sediment on the site. This is the most important factor in the accretion of sediment over the NW sector and thus the accretion rates dictate how the zones propagate in the future modelling of the site, shown in further plan models (see Figure 8.2 (b) and (c)).

The lowest zone 1 (less than or equal to 2 m ODN, in the case of PHS) is present as a base layer above the old field soil and the extent of coverage will be controlled by the initial grading. In the case of the NW sector, this covers much of the site. The sediment in this layer has been characterised as fast accreting (a mean of approximately 90 mma^{-1}), has the highest sand content (still less than 50% of the total grain fraction), and the lowest organic content and dry bulk density. Such properties are to be anticipated in an area that is regularly accreting large quantities of sediment. This sediment is also easily eroded, demonstrated by the channels forming behind the breach that are exposed to the fastest flows and by the recorded erosion at station 5e just behind the breach. Periods of tidal inundation are longest in this zone (between 30-40% of the time) and the area is classified as mudflat; no vegetation species have been recorded on PHS in this zone.

In zone 1 on the NW sector, there is a flow channel (shown on Figure 8.1) that routes the tidal flow across this zone and towards the drainage ditch from the water treatment plant (for a map showing these features see Figure 5.15, Chapter 5). This drainage channel is at a lower elevation than the surrounding sediment and is not accreting sediment as quickly due to the fast flows through it. Also on zone 1, when considering the NW sector, there is an area where water ponds during high spring tides. This area is at a slightly lower elevation, however the accretion rates are still as fast, for example at site 4c at the edge of the ponded area, accretion rates averaged 66 mma^{-1}.

Zone 2 (greater than 2 to 2.3 m ODN, in the case of PHS) begins about 250 metres landward of the NW breach. This zone is at an elevation where mean accretion rates have slowed to 70 mma^{-1} and tidal inundation occurs between 20-30% of the time. The zone can support early pioneer species such as *Spartina anglica* and *Salicornia europaea* but vegetation cover is still very limited and averaged less than 5% over the monitoring period. The sediment is slightly more compacted with higher dry bulk densities, less sand and more silt and clay and slightly higher organic content.

400 metres landwards of the NW breach is zone 3 (greater than 2.3 to 2.6 m ODN, in the case of PHS), where accretion is even slower than in other zones averaging rates of

50 mma^{-1}, and tidal inundation is between 10-20% of the time. This is the pioneer zone, supporting up to 10% vegetation coverage including species such as *Spartina anglica*, *Aster tripolium*, *Puccinellia spp.*, and *Suaeda maritima*, all typical pioneer saltmarsh species for saltmarshes in this area of England (Boorman, 2003).

The following plan models of the NW sector of PHS show the site as it is expected to develop if current rates of accretion are sustained for each elevation zone (Figures 8.2 (b) and (c)) and the plan model of the site five years post-breach as a comparison (Figure 8.2 (a)). As a rough estimate using current mean accretion levels calculated for PHS: for every five years zone 1 will accrete by 450 mm, zone 2 will accrete by 350 mm, zone 3- 250 mm, zone 4- 50 mm and zone 5- 20 mm. As the height difference between zones is 300 to 500 mm, the zones will quickly propagate across the NW sector.

Ten years after breaching (see Figure 8.2 (b)) zone 1 will only extend for the first 100 metres landwards of the breach. Zone 2 will have propagated towards the breach so that the area between 100 and about 200 metres landwards of the breach will have been transformed into the early pioneer zone. From 200 to 400 metres landwards of the breach, the NW sector will be zone 3 (pioneer zone) and a new zone will develop 400 metres seaward of the breach- zone 4 (greater than 2.6 to 3 m ODN, in the case of PHS). This zone will become the equivalent of a lower mid-marsh community with up to 50% vegetation cover, mean accretion rates of 10 mma^{-1}, and tidal inundation only up to 10% of the time.
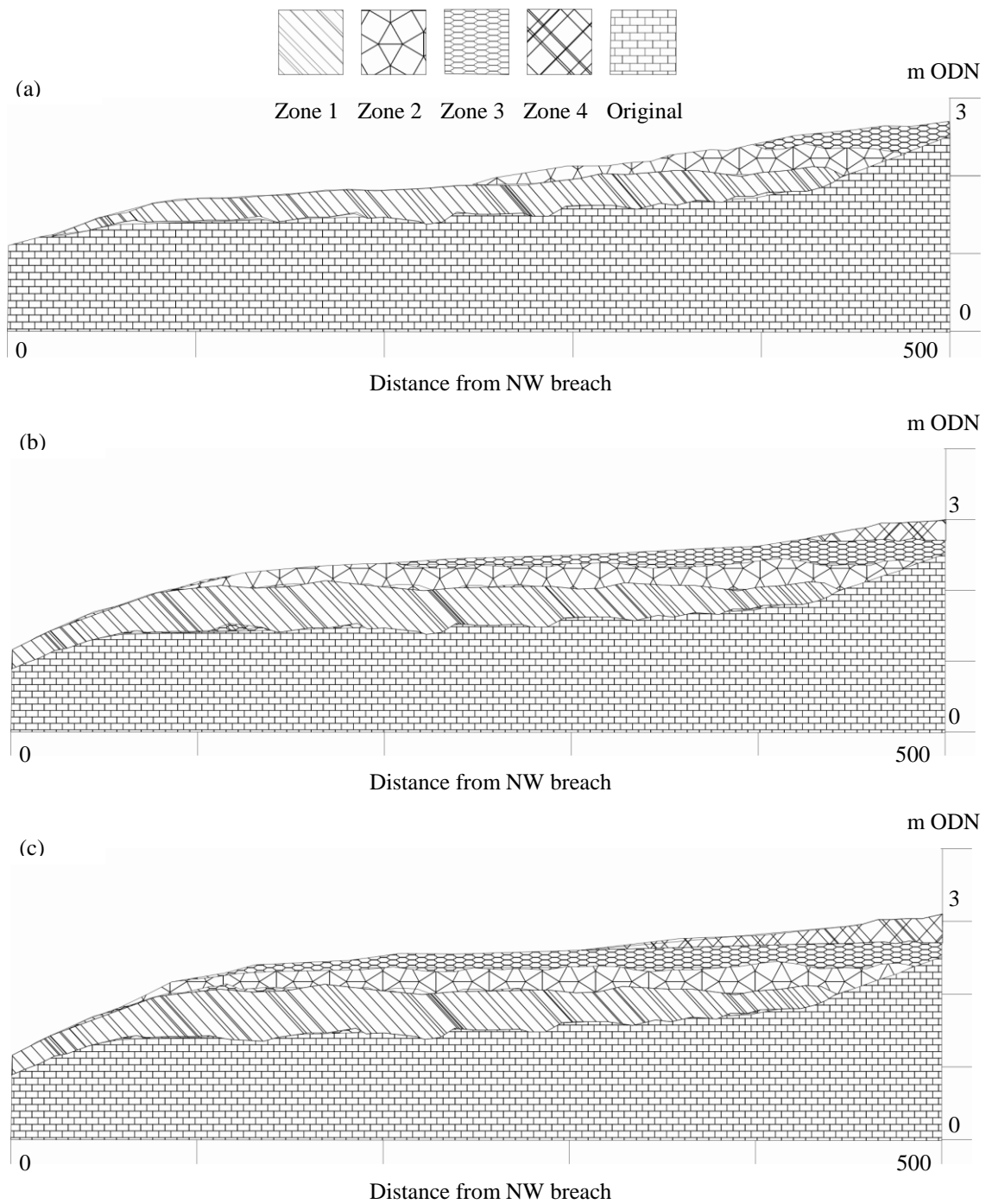
Figure 8.2: Cross-section views through conceptual model of managed realignment site showing temporal development. (a) is 5 years after breaching (also presented in Figure 8.1), (b) is 10 years after breaching and (c) is 15 years after breaching.

Fifteen years after breaching (see Figure 8.2 (c)), the site will have developed even further. Vegetation will then be established across large areas of the NW sector, mirroring the saltmarsh already present on the SE sector. Only at the area closest to the NW breach will there still be evidence of zone 1 conditions, which is currently where the fastest tidal flows are recorded and, as mentioned before, easily eroded areas persist preventing the site at this location from evolving beyond zone 1. Zone 2 will stretch to 130 metres landwards of the breach, zone 3 type conditions will be present for a further 150 metres and the remainder of the site will have developed zone 4 type features. As the accretion rate on zone 4 is slow (10 mma^{-1}) it could take more than 40 years for zone 4 to develop zone 5 characteristics (greater than 3 to 3.5 m ODN, in the case of PHS). Zone 5 features are currently evident on the SE sector and the area is characterised by a high marsh community of plants with up to 70% vegetation cover and very slow accretion rates of 4 mma^{-1}, similar to those recorded for natural saltmarshes in England (see Figure 4.4, Chapter 4). Tidal inundation is very short (less than 5% of the time) and as a result of this and slow accumulation, the sediments are more compacted with the highest bulk densities, lowest sand contents and highest organic contents. Zones 4 and 5 will have more stable sediment and plant communities due to the shorter time spent inundated and the slower accretion rates. It is on these more stable communities that the impact of sediment properties and biotic parameters over a small spatial scale may become pronounced. For example, a study of the sediment stability on the Skeffling mudflat in the Humber estuary (see Figure 2.9, Chapter 2 for a location map) by Paterson *et al.* (2000) found that the diatom biomass was the most significant factor controlling sediment stability.

This conceptual model of managed realignment is essential for the management of such sites and the prediction of intertidal habitats that they will support. The original aims of creating the managed realignment site at PHS were to provide intertidal habitat to compensate for losses in other schemes in the estuary that could support various invertebrate assemblages similar to other locations in the Humber estuary and at least 30 species of feeding, wintering birds. The original expectation was that the site would create 45 ha of mudflat and 35 ha of saltmarsh (Environment Agency, 2005). This conceptual model, created from the results collected during the monitoring period shows that these aims will not be achieved. The area of mudflat will gradually diminish over 10 years, presently the majority of the SE sector is already saltmarsh and the majority of the NW sector will be colonised by pioneer and mid-marsh communities

during the next ten years if accretion rates continue at the present rates for each elevation zone. This will in turn affect the invertebrate and bird communities that the site is able to support. A study of the macrofaunal communities on PHS by Mazik, *et al.* (2007) found that they were still representative of an early successional community with low species diversity, high abundance and small body size. The reduction in mudflat will mean invertebrates that live in this substrate are less prevalent, and in turn the bird communities that feed off these invertebrates will not be supported. Saltmarsh will obviously support its own assemblages of species including birds, however the original aim of the site did not include such a large coverage of this type of habitat.

The NW sector of PHS has yielded data that have allowed the development of a model for managed realignment sites that are accreting quickly. From the literature, Tollesbury managed realignment site in Essex had initial accretion rates that matched PHS. Tollesbury managed realignment site also showed significant links between elevation similar to PHS; at lower elevations accretion rate was faster than at higher elevations, supporting the sedimentation patterns depicted in the conceptual model (Watts, *et al.*, 2003). A review of the literature on managed realignment produced by French (2006) also discussed the important link between elevation and the rates of sedimentation reported for managed realignment sites both in the UK and the US, as did a study by Wolters *et al.* (2005) which compared over 70 European managed realignment sites, further supporting the design of this conceptual model. At managed realignment sites with fast accretion rates and ones planned to require fast accretion, it might be expected that the sedimentation patterns cause the site to develop in a similar manner to those modelled above, with strong links between elevation, tidal inundation and accretion rates.

8.2 Discussion of proposed conceptual model

The proposed conceptual model described in section 8.1 is driven by the results obtained from the current research that show fast rates of accretion on a breached managed realignment site. The reasons for these fast accretion rates are discussed further in this section.

The fast accretion on the NW sector is primarily driven by the underlying site elevation. The most significant correlation found when synthesising the results for all sediment properties known to influence sediment stability was with elevation. It is proposed that for this site, it is the height of the intertidal land post-breach that determines the amount

of sediment that will accrete. Other authors have shown a number of sediment properties and biological factors that are also driving accretion and erosion rates (e.g. Andersen, 2001; Bale, *et al.*, 2006; Riethmuller, *et al.*, 2000). During this study, close examination of the relationship between accretion and all of these factors failed to reveal any significant impact on deposition and erosion. None of these factors were found to have a systematic affect on accretion; the monitoring of these properties on a large scale as at PHS neither adds to the knowledge of accretion rates nor helps to explain them. Even on a very small scale, such as in the flume experiments, differences in sediment properties between the samples taken from sites on the NW sector did not translate into differences in their behaviour under flowing water. The big difference in results of the flume study was related to differences in tidal inundation time between the NW and SE sector.

Sediment properties such as grain size did exhibit small but significant correlations with accretion rate and these explain some of the apparently random fluctuations in the relationship between accretion and elevation. In the lowest elevation zone where a greater range of accretion rates were recorded, it was concluded that the variation was due to the locations of the sampling stations. The sites that were accreting slowly and the single site that exhibited net erosion were directly behind the NW breach and experiencing the greatest flow velocities as the tide flooded into and ebbed from the site. The more sheltered sampling sites along transect 6 that recorded the fastest accretion rates were also in this low elevation zone, but due to their position landward of the old flood embankment, the sites were not exposed to the faster flows and thus fast accretion occurred.

A number of studies have recorded inverse correlations between bulk density and erosion potential, a higher wet bulk density indicating areas resistant to erosion (Amos, *et al.*, 2004; Andersen, *et al.*, 2005; Bale, *et al.*, 2006; Mitchener, *et al.*, 1996; Quaresma, *et al.*, 2004; Riethmuller, *et al.*, 2000). For example, the study by Bale *et al.* (2006) explored the erosion of sediment *in situ* using a CSM and examined the relation to both bulk properties and biological factors at a number of locations around the Tamar Estuary in Devon. The main conclusion of the study was that the best predictor of sediment erodibility was the wet bulk density of the sediment. Research by Bale *et al.* (2006) dealt with different sediments in contrasting locations across the full estuary, so covered a larger spatial scale than the current research. Even so the research still showed a correlation with bulk density. The contrast between the results of the previous

study and from the present research is probably due to the fact that the intertidal area being studied is not a naturally developing site. In a managed realignment site the entry and egress of sediment is controlled and accretion is encouraged. Thus the sediment is all newly accreted and will not behave the same as established mudflat. Even though estuaries are rapidly changing environments, the newness of the sediment surface on managed realignment sites is likely to mean the results from a study of sites such as this do differ from established patterns of cohesive estuary sediments. The fast accretion rates measured on PHS are not evident in other areas of the estuary (see Table 4.4, Chapter 4) and so no comparison can be made between data from these sites and those for other estuarine sediments.

The flume experiment reported in Chapter 7 concluded that for the sediment cores taken from the site none of the measured sediment properties (bulk density, moisture content and organic content) showed any significant correlation with the rates and patterns of entrainment recorded across the cores, again suggesting no links between these factors and erosion potential for a site such as this one. The cores from the NW sector all began eroding as flow was established over them and erosion increased as velocity increased. No critical erosion threshold was identifiable for the NW sector cores, so no variation in this property could be linked with differing sediment properties. The SE sector sediment cores were the only samples that resisted erosion and for these sites long residence time facilitated by consolidation was the cause. The studies that found links with bulk sediment properties are a mix of both *in situ* and laboratory based experiments, so the fact that the current research studied erosion in a flume is not a reason for the lack of correlation between sediment entrainment and sediment properties. For example, the study by Quaresma *et al.* (2004) was carried out under laboratory conditions using a settled cohesive bed (sediment taken from Southampton Water) and found an inverse correlation between wet bulk density and entrainment.

There was not a strong significant correlation between accretion rate and either wet or dry bulk density (reported in Chapter 6) adding further evidence to the assertion that the relationships detected in other studies are not applicable to a fast accreting managed realignment site. The sediment samples were collected from the site and measured as soon as possible after return to the laboratory. The method of measurement is a standard one and minimises effects of transportation of the sample. As all samples are treated similarly, it should be expected that any deterioration of the sample would affect all

samples equally and so the results are internally consistent- so this is not the cause of the lack of a relationship.

Grain size and the ratio of mud to sand have been extensively studied and related to potential for erosion and sediment stability. Erosion of sandy sediments is more widely understood than erosion of cohesive silts and muds (e.g. Aberle, *et al.*, 2004; van Ledden, *et al.*, 2004), which are influenced by a large range of properties such as chlorophyll *a* and carbohydrate content, climatic changes, and bed properties; each one to a greater or lesser extent explaining the erosional behaviour of the sediment (Friend, *et al.*, 2003; Mitchener, *et al.*, 1996). Perhaps this is a reason for the lack of correlation between sediment parameters and accretion within PHS. The number of factors that have been independently shown in different studies to be either directly or inversely correlated with the erosion of cohesive sediment can be difficult to measure on a large temporal and spatial scale. Added to these problems are the issues associated with the constantly changing environment created by the fast accretion rates producing a site that changes on each tide, with vertical changes of up to one centimetre a month at some sites during the high spring tides. This ever changing environment is challenging to study and makes coming to a clear conclusion about the influence of numerous factors that may each be influencing the accretion rate very difficult. Some of the significant correlations amongst sediment properties, namely sand content, dry bulk density, and organic content, were discussed in Chapter 6. They may be influencing the accretion rate to some extent, however because they are overwhelmed by the strong significant effect of elevation, their effects are negligible.

An often cited link is between the degree and type of vegetation cover and accretion, namely that faster accretion is occurring at sites that are more vegetated (Armstrong, 1988; Boorman, *et al.*, 2001; Boorman, 2003; French, 2006). Again, this relationship is not evident at PHS; in fact just the opposite is occurring. Barren mudflats are accreting fastest and the highly vegetated areas on the SE sector are accreting slowest. This contradictory result can also be attributed to the nature of the site. A study by Boorman, *et al.* (2001) found that when planting two species of saltmarsh plant that exist naturally in pioneer zones, both responded well to the rapid accretion of sediment so it is not that the plants cannot survive in an intertidal environment with fast accretion levels. It is the persistence of tidal inundation, waterlogging and high salinities that will inhibit the growth of these species. Thus, on PHS the fast accretion is occurring in the areas of most persistent inundation where waterlogging occurs, making the conditions unsuitable

for colonisation by saltmarsh species. The correlation between accretion and vegetation cover is reported for well-established saltmarsh where the plants are themselves contributing to the increased sediment height through both baffling incoming tidal flows causing sediment deposition and the breakdown of organic matter. A study at the eastern end of the Humber estuary by Brown *et al.* (1998) found that long-term vertical marsh accretion was influenced by a number of factors including compaction, marsh age and the accumulation of organic matter and surface litter. When PHS becomes more established as saltmarsh in the next 20 years it can be expected that the mid to high marsh areas might begin accreting more than the lower zones, moving towards the models established for unmanaged marshes.

The influencing factors on sediment stability discussed above have all been investigated when looking at intertidal areas and were studied during this research because of the body of evidence that supported the correlations that they had with sediment stability. The observations presented here have important implications for site monitoring strategies. For a site such as PHS, there is no benefit from monitoring sediment properties and vegetation while the site is still accumulating sediment at a fast rate. Instead, the measurement of elevation prior to breaching coupled with calculations of inundation frequency around the site will give the site manager enough information to predict the rates and patterns of sedimentation. Once the site is more developed and changes are occurring more slowly, more detail of sediment properties may help predict accretion rate and erosion potential.

Elevation of the site, whilst explaining the majority of the sedimentation patterns found on the NW sector, cannot explain fully the volume of sediment that has settled onto the site. This is due to the important impact of variations in sediment supply into the site from the Humber estuary. If the volume of sediment coming into the site through the NW breach is smaller, then it follows that the accretion rate has to be slower. The concentration of sediment entering through the NW breach is driven by the high concentration of suspended sediment within the Humber estuary. On most days the estuary waters are dark brown in colour reflecting the amount of sediment held in suspension. The sediment load is swelled by the addition of the products of erosion within the NW breach and the creeks incised into the mudflat seawards of the breach. Whether this was modelled prior to breaching is not known, however in the newer managed realignment site on the Humber estuary at Alkborough (breached 2006), a flow channel in between the breach was engineered perhaps in response to the

unexpected deep channel that has formed at PHS. The sediment from the channel at the NW breach may be amplifying the sediment load measured passing through the breach. The channel has become noticeably wider and deeper throughout the monitoring period, as has the channel through the mudflats, (see Figure 8.3 for an idea of the depth and width of the channel over the mudflat).

Figure 8.3: Tidal channel flowing towards the Humber estuary from the NW breach.

Another factor in the fast accretion of the NW sector is the design of the site. This is very important to the final functioning of the managed realignment site and several of the important aspects of design (French, 2006; Pontee, *et al.*, 2006; Leggett, *et al.*, 2004; Pontee, 2007; Townend, 2008a) were outlined in Chapter 2, section 2.2.2. Most important among these in accelerating the accretion rates are the shape and breach design. The shape of the NW sector and the design of the breach at this end of the site have facilitated the fast accretion rates. This is because the breach funnels flows through a narrow deep channel as the tide starts flooding the site. This causes erosion and the breach has continued to grow as the site develops. The fastest accreting sites are sheltered behind the old embankment. The sheltering of much of the site by the remaining banks and the existence of only a narrow tidal entry point instead of to completely remove the old embankment together provides conditions that enhance the deposition of sediment.

The assumption was made at the commencement of this research that the physical and biological factors that affect the sediment stability and thus erosion and accretion of sediment on intertidal areas could be applied to a managed realignment site. The results from this study have proved otherwise and indicate that only elevation of the site needs to be considered when predicting accretion rates on a breached managed realignment site such as this. As these accretion rates slow, the expectation should be that the factors such as wet bulk density and grain size will become more significant controls on the sediment stability of the site.

8.3 Management and monitoring

The findings from this research provide a range of important implications for the management and monitoring of a managed realignment site, some of which have already been touched upon in this chapter. As the only significant factor controlling the accretion rates on this site was elevation, it is evident there needs to be careful consideration given to site design in order to optimise the required outcomes of the site. A knowledge of elevations in the estuary where the proposed site is located and the frequency of tidal inundation that these elevations equate to will determine the expected accretion rates. Coupled with this is knowledge of the amount of potential sediment load within the estuary at that particular location to drive these accretion rates. With these data, the decision can be made as to the rate of accretion required at the site. For a site where low accretion rates are desired the elevation should be one which restricts inundation, for a site where faster accretion rates are planned then a lower elevation and more frequent inundation is needed. The design of the site is also very important in determining the initial accretion rates, especially the breach design and use of creeks to channel tidal flows. For a more sheltered site creating saltmarsh such as the one created at PHS then breaching the old flood embankment is advisable and possibly the use of a channel so that less erosion of mudflat in front of the site occurs. For a site where the purpose is to create mudflats, it is more advisable to remove the full embankment in front of the site. In this case, as long as elevation is similar to the surrounding mudflat, erosion and deposition of sediment should balance and the increased exposure to tidal forcing will limit the accretion rate of sediment so reducing the probability of the site becoming saltmarsh.

These management proposals are simple, however in reality there are many more limits to the designing of the optimum managed realignment site. Flood managers should not

lose sight of the fact that in designing a managed realignment site compromises will be needed that affect the final functioning of the intertidal area and to mitigate these affects detailed modelling of the site prior to breaching and intensive monitoring of the site after breaching is essential to bring about a successful outcome. This study shows that when monitoring a fast accreting managed realignment site with breaches, it is best to use a small number of hydrodynamic surveys that measure velocity profile, SPM and tide height through the breach (see section 5.4, Chapter 5). When accretion rates have slowed, then investigation of other factors such as bulk properties and biological factors will be useful in determining whether they are now controls on the sediment stability, as indicated by studies mentioned throughout this chapter. A further recommendation for the monitoring of a managed realignment site which has been created to provide intertidal habitat, is to measure vegetation cover in relation to elevation on the site. This only needs to be done on a yearly basis as demonstrated by the measurements collected by the CEH reported in section 2.4.2.2, Chapter 2 which are comprehensive and indicate the changes occurring on the site.

Chapter 9 : Conclusions and Future Work

This study of Paull Holme Strays has yielded very significant results which bring with them implications for other managed realignment sites across the UK and internationally. If the objective of countering the decline in saltmarsh habitat is anticipated as accompanying climate change induced sea-level rise, then such sites must be planned and managed to retain appropriate habitats.

The conclusions presented in section 9.1 will encompass those that are relevant to the NW sector, to the whole of PHS, and to managed realignment sites in general. This study has revealed contrasts within the site, and has produced results which contradict those for 'unmanaged' saltmarsh and mudflat sites in this and other estuaries. The conclusions that can be drawn from these differences are presented in section 9.2.

9.1 Conclusions

The fast accretion rates recorded on PHS are primarily driven by the position of the site relative to the tidal frame. This is reflected in tidal inundation time, water depth and therefore the time available for settling by the sediment.

The shape and breach design of the site also determines the accretion rates over the site. The sheltering given to areas of the site by the use of limited breaches instead of removing the old embankment produces conditions entirely favourable to fast accretion. The deeper NW breach channelled the tide into the NW sector and the growth of the channel cut through the mudflat in front of the site must also have acted as a source of sediment to feed the accretion rates.

The large suspended sediment load in the Humber estuary is the final important factor in supplying the fast accretion rates recorded on the NW sector as it controls sediment availability. It is these factors which have created the fast accreting site evident during the monitoring period.

The conceptual model of site progression proposed in Chapter 8 indicates that this site will quickly progress to becoming mainly saltmarsh within ten years and to the beginnings of a high marsh community on the NW sector within 40 years. This conceptual model can be used to determine the progression of other fast accreting managed realignment sites as long as some details about the annual accretion rates and site elevation are known.

The design of a management realignment site needs to be carefully considered and modelled prior to breaching, paying particular attention to the important control of elevation, and the sediment load available in the estuary. Knowledge of other intertidal areas within the estuary are essential in providing this information, however the resulting site evolution will not be controlled by sediment properties or biological factors during the fast accreting phase of development. The current research stemmed from prior modelling predicting slower accretion rates and highlights the problems that can occur when the models' initial conditions and assumptions are not sufficiently accurate.

A particular problem with the modelling of PHS was the lack of a previous comparable managed realignment site with sufficient available data. Without knowing measured outcomes from similar sites, the modelling of PHS was inevitably more difficult.

More extensive research is needed on managed realignment sites as their importance in flood management and intertidal habitat creation grows. In the Humber estuary, for example, a further five managed realignment sites are planned for completion between 2010 and 2050 ((Environment Agency, 2008).

9.2 Future work and recommendations

Looking to the future, the management of the Humber estuary faces many challenges, in particular the issues of intertidal habitat loss due to expected climate-change induced sea level rise and increased storminess. The creation of managed realignment sites is central to the Humber Flood Risk Management Strategy (Environment Agency, 2008), and so any study highlighting the influences and monitoring the changes on such a site is important.

There needs to be a greater emphasis on modelling prior to site design that actually uses all data available for the estuary and from previous studies on managed realignment sites. In similar estuary settings, this will benefit the modelling of the proposed site's development once breaching occurs. This includes focusing on sediment cycling through the estuary and the erodibility of mudflats seawards of the breached embankment. Secondly, modelling should use accurate topographic data to model flows into and around the site. The topography of PHS was crucial in routing the flow through the NW sector thus influencing accretion rates and sedimentation patterns. The local topography and shape were also important in this site, almost splitting it into two separate sites that behaved very differently.

Continued accretion monitoring on PHS would give a large dataset on accretion rates during the first 5 to 10 years after breaching of a managed realignment site which could prove vital to the management of other sites. It would also prove or disprove whether the site develops as proposed in the conceptual model presented in Chapter 8. More information on the rates and whether any slowdown in accretion is recorded as the fast accreting sites become higher in elevation would be important to ascertain habitat development on this site and similar sites in the longer term.

A second set of LIDAR or DGPS topographic data to compare with the data collected during 2005 would help identify the changes taking place on the site and more clearly demonstrate the sedimentation patterns as well as help quantify the sediment deposited, allowing comparison with the sediment budget calculated for the NW sector.

A more detailed study of how the creeks form on the site, both at the NW breach and towards the new embankment, is of considerable interest to flood managers and to those involved in navigation within the estuary. It is reported that some of the eroded material has formed subaqueous 'banks' seawards of the mudflats which have had to be excavated by ABP (personal communication) More information such as this would increase the ability of modellers to predict accurately the effects of both natural creek formation and the impact of new creeks on the proposed site.

Further hydrodynamic data are necessary to produce a more accurate sediment budget for the site, which includes the SE sector to see whether net sediment flux through the SE breach is also linked to the accretion rates for this sector,. Although the SPM data collected during this study were sufficient to allow the development of a sediment budget for the NW sector, extra tidal data for tides during different seasons would increase the accuracy of the budget and lower the associated errors.

These further studies would add to the conclusions from this study on the formation of a new intertidal habitat and be of importance to flood managers both in the Humber estuary and within the UK and Europe, where similar schemes are gaining in popularity. Within the Humber estuary, the challenge for the future is to provide continuing protection to homes, industry and farmland, whilst adapting to and coping with the predicted sea-level rise and increased storminess which is set to result from the changing climate.

References

Aberle, J., Nikora, V., & Walters, R. (2004). Effects of bed material properties on cohesive sediment erosion. *Marine Geology , 207*, pp. 83-93.

ABP mer. (2004a). *Geomorphological Modelling of Setback Sites in the Humber Estuary: report for Environment Agency R.1055.* Southampton: ABP Marine Environmental Research Ltd.

ABP mer. (2004b). *Humber Holocene Chronology, Humber Estuary Geomorphology Study- Stage 2.* ABP mer.

ABP mer. (2004c). *Hydrodynamic Modelling of Setback Sites in the Humber Estuary: report for Environment Agency R.1057.* Southampton: ABP Marine Environmental Research Ltd.

Alvisi, F., Albertazzi, S., Frignani, M., Marozzi, G., & Ravaioli, M. (2001). Sampling and dating strategies in studying environments with high spatial and temporal variability. *Archives of Oceanography and Limnology , 22*, pp. 207-216.

American Society for Photogrammetry and Remote Sensing. (2004). ASPRS Guidelines Vertical Accuracy Reporting for Lidar Data. *ASPRS.* [Online] May 2004. http://www.asprs.org/society/committees/Downloads/Vertical_Accuracy_Reporting_for_Lidar_Data.pdf

Amos, C. L., Bergamasco, A., Umgiesser, G., Cappucci, S., Cloutier, D., DeNat, L., et al. (2004). The stability of tidal flats in Venice Lagoon- the results of in-situ measurements using two benthic, annular flumes. *Journal of Marine Systems , 51*, pp. 211-241.

Andersen, T. J. (2001). Seasonal Variation in Erodibility of Two Temperate, Microtidal Mudflats. *Estuarine, Coastal and Shelf Science , 53*, pp. 1-12.

Andersen, T. J., Lund-Hansen, L. C., Pejrup, M., Jensen, K. T., & Mouritsen, K. N. (2005). Biologically induced differences in erodibility and aggregation of subtidal and intertidal sediments: a possible cause for seasonal changes in sediment deposition. *Journal of Marine Sediments , 55*, pp. 123-138.

Andrews, J. E., Burgess, D., Cave, R. R., Coombes, E. G., Jickells, T. D., Parkes, D. J., et al. (2006). Biogeochemical value of managed realignment, Humber estuary, UK. *Science of the Total Environment , 371*, pp. 19-30.

Anisfeld, S. C., Tobin, M. J., & Benoit, G. (1999). Sedimentation Rates in Flow-Restricted and Restored Salt Marshes in Long Island Sound. *Estuaries , 22* (2A), pp. 231-244.

Armstrong, W. (1988). Life in the Humber (A) Salt-marshes. In J. N. V (Ed.), *A Dynamic Estuary Man, Nature and The Humber* (pp. 46-57). Hull: Hull University Press.

Atkinson, P. W., Crooks, S., Drewitt, A., Grant, A., Rehfisch, M. M., Sharpe, J., et al. (2004). Managed realignment in the UK- the first 5 years of colonsation by birds. *Ibis , 146* (1), pp. 101-110.

Bale, A. J., Widdows, J., Harris, C. B., & Stephens, J. A. (2006). Measurements of the critical erosion threshold of surface sediments along the Tamar Estuary using a mini-annular flume. *Continental Shelf Research , 26*, pp. 1206-1216.

Balson, P. S., & Philpott, S. L. (2004). *Sediment sources, sinks and pathways at the mouth of the Humber Estuary.* British Geological Society.

Begon, M., Harper, J. L., & Townsend, C. R. (1996). *Ecology.* Oxford: Blackwell Science.

Bernstein, L., Bosch, P., Canziani, O., & Chen, Z. (2007). *Climate Change 2007: Synthesis Report. An Assessment of the Intergovernmental Panel on Climate Change.* Cambridge: Cambridge University Press.

Betteridge, K. F., Williams, J. J., Thorne, P. D., & Bell, P. S. (2003). Acoustic instrumentation for measuring near-bed sediment processes and hydrodynamics. *Journal of Experimental Marine Biology and Ecology , 285-286*, pp. 105-115.

Black, K. S. (1998). Suspended Sediment Dynamics and Bed Erosion in the High Shore Mudflat Region of the Humber Estuary, UK. *Marine Pollution Bulletin , 37* (3-7), pp. 122-133.

Black, K. S., Tolhurst, T. J., Paterson, D. M., & Hagerthey, S. E. (2002). FORUM: Working with Natural Cohesive Sediments. *Journal of Hydraulic Engineering* , pp. 2-7.

Blott, S. J., & Pye, K. (2004). Application of LIDAR digital terrain modelling to predict intertidal habitat development at a managed retreat site: Abbotts Hall, Essex, UK. *Earth Surface Processes and Landforms , 29*, pp. 893-905.

Blott, S. J., & Pye, K. (2008). Particle shape: a review and new methods of characterisation and classification. *Sedimentology , 55*, pp. 31-63.

Boorman, L. A. (2003). *Saltmarsh Review. An overview of coastal saltmarshes, their dynamic and sensitivity characteristics for conservation and management.* JNCC Report, No. 334.

Boorman, L. A., Hazelden, J., & Boorman, M. (2001). The effect of rates of sedimentation and tidal submersion regimes on the growth of salt marsh plants. *Continental Shelf Research , 21*, pp. 2155-2165.

Boumans, R., & Day Jr, J. W. (1993). High precision measurements of sediment elevation in shallow coastal areas using a sedimentation-erosion table. *Estuaries , 16*, pp. 375-380.

Boyes, S., & Mazik, K. (2004). *Paull Holme Strays- Accretion/Erosion Monitoring.* Hull: Institute of Estuarine and Coastal Studies, University of Hull.

Brown, S. L., & Brown, S. (2008). *Paull Holme Strays Intertidal Vegetation, Accretion and Erosion Monitoring 2007.* Wallingford: Centre for Ecology and Hydrology.

Brown, S. L., & Garbutt, A. (2004). *Paull Holme Strays Monitoring Intertidal Vegetation, Accretion and Erosion Monitoring.* Wallingford: Centre for Ecology and Hydrology.

Brown, S. L., & S, B. (2006). *Paull Holme Strays Intertidal Vegetation, Accretion and Erosion Monitoring 2006.* Wallingford: Centre for Ecology and Hydrology.

Brown, S. L., Garbutt, A., & Brown, S. (2005). *Paull Holme Strays Intertidal Vegetation, Accretion and Erosion Monitoring 2005.* Wallingford: Centre for Ecology and Hydrology.

Brown, S. L., Warman, E. A., McGrorty, S., Yates, M., Pakeman, R. J., Boorman, L. A., et al. (1998). Sediment fluxes in intertidal biotopes: BIOTA II. *Marine Pollution Bulletin , 37* (3-7), pp. 173-181.

Cahoon, D. R., & Lynch, J. C. (1989). Accretion and canal impacts in a rapidly subsiding wetland: II. Feldspar marker horizon technique. *Estuaries , 12*, pp. 260-268.

Cave, R. R., Andrews, J. E., Jickells, T., & Coombes, E. G. (2005). A review of sediment contamination by trace metals in the Humber catchment and estuary, and the implications for future estuary water quality. *Estuarine, Coastal and Shelf Science , 62*, pp. 547-557.

Cave, R. R., Ledoux, L., Turner, K., Jickells, T., Andrews, J. E., & Davies, H. (2003). The Humber catchment and its coastal area: from Uk to European perspectives. *The Science of the Total Environment , 314-316*, pp. 31-52.

Chang, Y.-H., Scrimshaw, M. D., Macleod, C. L., & Lester, J. N. (2001). Flood Defence in the Blackwater Estuary, Essex, UK: The Impact of Sedimentological and Geochemical Changes on Salt Marsh Development in the Tollesbury Managed Realignment Site. *Marine Pollution Bulletin , 42* (6), pp. 470-481.

Christie, M. C., Dyer, K. R., & Turner, P. (1999). Sediment Flux and Bed Level Measurements from a Macro Tidal Mudflat. *Estuarine, Coastal and Shelf Science , 49*, pp. 667-688.

Christie, M. C., Dyer, K. R., Blanchard, G., Cramp, A., Mitchener, H. J., & Paterson, D. M. (2000). Temporal and spatial distributions of moisture and organic contents across a macro-tidal mudflat. *Continental Shelf Research , 20*, pp. 1219-1241.

Cloutier, D., LeCouterier, M. N., Amos, C. L., & Hill, P. R. (2006). The effects of suspended sediment concentration on turbulence in an annular flume. *Aquatic Ecology , 40*, pp. 555-565.

Communities and Local Government. (2006). *Planning Policy Statement 25: Development and Flood Risk.* London: The Stationery Office.

Crooks, S., Schutten, J., Sheern, G. D., & Pye, K. D. (2002). Drainage and Elevation as Factors in the Restoration of Salt Marsh in Britain. *Restoration Ecology , 10* (3), pp. 591-602.

Cundy, A. B., Long, A. J., Hill, C. T., Spencer, C., & Croudace, I. W. (2002). Sedimentary response of Pagham Harbour, southern England to barrier breching in AD 1910. *Geomorphology , 46*, pp. 163-176.

de Brouwer, J. F., Bjelic, S., de Deckere, E. M., & Stal, L. J. (2000). Interplay between biology and sedimentology in a mudflat (Biezelingse Ham, Westerschelde, The Netherlands). *Continental Shelf Research , 20*, pp. 1159-1177.

de Deckere, E. M., Tolhurst, T. J., & de Brouwer, J. F. (2001). Destabilization of Cohesive Intertidal Sediments by Infauna. *Estuarine, Coastal and Shelf Science , 53*, pp. 665-669.

Defew, E. C., Tolhurst, T. J., & Paterson, D. M. (2002). Site-specific features influence sediment stability of intertidal flats. *Hydrology and Earth System Sciences , 6* (6), pp. 971-982.

Dyer, K. R. (1986). *Coastal and Estuarine Sediment Dynamics.* John Wiley and Sons.

Dyer, K. R., & Manning, A. J. (1999). Observation of the size, settling velocity and effective density of flocs, and their fractal dimensions. *Journal of Sea Research , 41*, pp. 87-95.

Edwards, A. M., & Winn, P. S. (2006). The Humber Estuary, Eastern England: Strategic planning of flood defences and habitats. *Marine Pollution Bulletin , 53*, pp. 165-174.

Eleftheriou, A., & McIntyre, A. (2005). In *Methods for the Study of Marine Benthos* (3rd ed.). Blackwell.

Environment Agency. (2005). *HUMBER ESTUARY FLOOD DEFENCE STRATEGY PAULL HOLME STRAYS ENVIRONMENTAL MONITORING REPORT 2005.* Leeds: Halcrow Group Ltd.

Environment Agency. (2007). *Paull Holme Strays Environmental Monitoring Report.* Leeds: Environment Agency.

Environment Agency. (2008). *Planning for the Rising Tides: The Humber Flood Risk Management Strategy.* Leeds: Environment Agency.

Environmental Systems Research Institute (ESRI). (2008, February 29). *About TIN surfaces*. Retrieved January 27, 2009, from ArcGIS 9.2 Desktop Help: http://webhelp.esri.com/arcgisdesktop/9.2/index.cfm?TopicName=About_TIN_surfaces

Erlingsson, U. (1991). A sensor for measuring erosion and deposition. *Journal of Sedimentary Petrology , 61*, pp. 620-622.

Flemming, B. W., & Delafontaine, M. T. (2000). Mass physical properties of muddy intertidal sediments: some applications, misapplications and non-applications. *Continental Shelf Research , 20*, pp. 1179-1197.

French, P. W. (2006). Managed realignment- The developing story of a comparitively new approach to soft engineering. *Estuarine, Coastal and Shelf Science , 67*, pp. 4069-423.

French, P. W. (1999). Managed retreat: a natural analogue from the Medway estuary, UK. *Ocean & Coastal Management , 42*, pp. 49-62.

Friend, P. L., Ciavola, P., Cappucci, S., & Santos, R. (2003). Bio-dependent bed parameters as a proxy tool for sediment stability in mixed habitat intertidal areas. *Continental Shelf Research , 23*, pp. 1899-1917.

Friend, P. L., Lucas, C. H., & Rossington, S. K. (2005). Day-night variation of cohesive sediment stability. *Estuarine, Coastal and Shelf Science , 64*, pp. 407-418.

Garbutt, R. A., Reading, C. J., Wolters, M., Gray, A. J., & Rothery, P. (2006). Monitoring the development of intertidal habitats on former agricultural land after the managed realignment of coastal defences at Tollesbury, Essex, UK. *Marine Pollution Bulletin , 53*, pp. 155-164.

Goossens, D. (2008). Techniques to measure grain-size distributions of loamy sediments: a comparative study of ten instruments for wet analysis. *Sedimentology , 55*, pp. 65-96.

Hazelden, J., & Boorman, L. A. (2001). Soils and 'managed retreat' in South East England. *Soil Use and Management , 17*, pp. 150-154.

Huntley, D. A., Leeks, G. J., & Walling, D. E. (Eds.). (2001). *Land-Ocean Interaction Measuring and modelling fluxes from river basins to coastal seas.* London: IWA Publishing.

Jarvie, H. P., Neal, C., & Robson, A. J. (1997). The Geography of the Humber catchment. *The Science of the Total Environment , 194/195*, pp. 87-99.

Kohler, U., List, J., & Witt, W. *COMPARISON OF LASER DIFFRACTION AND IMAGE ANALYSIS UNDER IDENTICAL DISPERSING CONDITIONS.* PARTEC Sympatec System Partikel Technik.

Konert, M., & Vandenberghe, J. (1997). Comparison of laser grain size analysis with pipette and sieve analysis: a solution for the underestimation of the clay fraction. *Sedimentology , 44*, pp. 523-535.

Lau, Y. L., & Droppo, G. (2000). RESEARCH NOTE: INFLUENCE OF ANTECEDENT CONDITIONS ON CRITICAL SHEAR STRESS OF BED SEDIMENTS. *Water Resources , 34* (2), pp. 663-667.

Law, M., Wass, P., & Grimshaw, D. (1997). The hydrology of the Humber catchment. *The Science of the Total Environment , 194/195*, pp. 119-128.

Leggett, D. J., Cooper, N., & Harvey, R. (2004). *Coastal and estuarine managed realignment- design issues.* London: CIRIA.

Leica Geosystems. (n.d.). *Leica GPS1200+*. Retrieved January 27, 2009, from http://www.leica-geosystems.com/corporate/en/ndef/lgs_4521.htm

MacVicar, B. J., Beaulieu, E., Champagne, V., & Roy, A. G. (2007). Measuring water velocity in highly turbulent flows: field tests of an electromagnetic curretn meter (ECM) and an acoustic Doppler velocimeter (ADV). *Earth Surface Processes and Landforms , 32*, pp. 1412-1432.

Manning, A. J., & Dyer, K. R. (1999). A laboratory examination of floc characteristics with regard to turbulent shearing. *Marine Geology , 160*, pp. 147-170.

Manning, A. J., & Dyer, K. R. (2002). The use of optics for the in situ determination of flocculated mud characteristics. *Journal of Optics A: Pure and Applied Optics , 4*, pp. S71-S81.

Manning, A. J., Friend, P. L., Prowse, N., & Amos, C. L. (2007). Estuarine mud flocculation properties determined using an annular mini-flume and the LabSFLOC system. *Continental Shelf Research , 27*, pp. 1080-1095.

Manning, C. J. (2006). *Humber Management Scheme.* Humber INCA.

Masselink, G., & Hughes, M. G. (2003). In *Introduction to Coastal Processes and Geomorphology.* Hodder Arnold.

Mazik, K., Smith, J. E., Leighton, A., & Elliott, M. (2007). Physical and biological development of a newly breached managed realignment site, Humber estuary, UK. *Marine Pollution Bulletin , 55*, pp. 564-578.

Mitchell, S. B., Couperthwaite, J. S., West, J. R., & Lawler, D. M. (2003). Measuring sediment exchange rates on an intertidal bank at Blacktoft, Humber Estuary, UK. *The Science of the Total Environment , 314-316*, pp. 535-549.

Mitchener, H., & Torfs, H. (1996). Erosion of mud/sand mixtures. *Coastal Engineering , 29*, pp. 1-25.

Morgan, P. A., & Short, F. T. (2002). Using Functional Trajectories to Track Constructed Salt Marsh Development in the Great Bay Estuary, Maine/New Hampshire, U.S.A. *Restoration Ecology , 10* (3), pp. 461-473.

Murray, M. (2002). Is laser particle size determination possible for carbonate-rich lake sediments? *Journal of Paleolimnology , 27*, pp. 173-183.

Neumeier, U., Lucas, C. H., & Collins, M. (2006). Erodibility and erosion patterns of mudflat sediments investigated using an annular flume. *Aquatic Ecology , 40*, pp. 543-554.

O'Riordan, T., Andrews, J. E., Samways, G., & Clayton, K. (2000). Coastal Processes and Management. In T. O'Riordan (Ed.), *Environmental Science for Environmental Management* (2nd ed., pp. 243-266). Harlow: Prentice Hall.

Pasternack, G. B., & Brush, G. S. (1998). Sedimentation cycles in a river-mouth tidal freshwater marsh. *Estuaries , 21* (3), pp. 407-415.

Paterson, D. M., Tolhurst, T. J., Kelly, J. A., Hoenywill, C., de Deckere, E. M., Huet, V., et al. (2000). Variations in sediment properties, Skeffling mudflat, Humber Estuary, UK. *Continental Shelf Research , 20*, pp. 1373-1396.

Pethick, J. (2001). Coastal management and sea-level rise. *Catena , 42*, pp. 307-322.

Pethick, J. (2002). Estuarine and Tidal Wetland Restoration in the United Kingdom: Policy Versus Practice. *Restoration Ecology , 10* (3), pp. 431-437.

Pethick, J. (2002). *Humber regime modelling: sea level rise and managed realignment Report to HESMP Consortium.* HESMP Consortium.

Pethick, J. S. (1988). The physical characteristics of the Humber. In N. V. Jones (Ed.), *A Dynamic Estuary Man, Nature and The Humber* (pp. 31-45). Hull: Hull University Press.

Pilcher, R., Burston, P., & R, D. (2002). *Seas of Change.* Royal Society for the Protection of Birds.

Pontee, N. (2003). Designing sustainable estuarine intertidal habitats. *Proceedings of the Institution of Civil Engineers: Engineering Sustainability* (ES3), pp. 157-167.

Pontee, N. I., Whitehead, P. A., & Hayes, C. M. (2004). The effect of freshwater flow on siltation in the Humber Estuary, north east UK. *Estuarine, Coastal and Shelf Science , 60*, pp. 241-249.

Pontee, N. (2007). Realignment in low-lying coastal areas: UK experiences. *Proceedings of the Institution of Civil Engineering: Maritime Engineering* (MA4), pp. 155-166.

Pontee, N., Harvey, R., Tovey, E., Brown, T., Osment, J., Bowell, H., et al. (2007). Large, innovative and realigned: Hesketh Out Marsh West. *42nd DEFRA Conference of River and Coastal Engineers*, (pp. 1.1.1-1.1.10). York.

Pontee, N., Hull, S., & Moore, J. (2006). Banked realignment: a case study from the Humber Estuary, UK. *Proceedings of the Institution of Civil Engineers: Engineering Sustainability* (ES3), pp. 99-108.

Pope, N. D., Widdows, J., & Brinsley, M. (2006). Estimation of bed shear stress using the turbulent kinetic energy approach- A comparison of annular flume and field data. *Continental Shelf Research , 26*, pp. 959-970.

Pritchard, D. (2005). Suspended sediment transport along an idealised tidal embayment: settling lag, residual transport and the interpretation of tidal signals. *Ocean Dynamics , 55*, pp. 124-136.

Pritchard, D., & Hogg, A. J. (2003). Models of settling lag in coastal and estuarine settings.

Quaresma, V. d., Amos, C. L., & Flindt, M. (2004). The influences of biological activity and consolidation time on laboratory cohesive beds. *Journal of Sedimentary Research , 74* (2), pp. 184-190.

Raudkivi, A. J. (1998). Cohesive Sediments. In *Loose Boundary Hydraulics.* Rotterdam: A A Balkema.

Reed, D. J. (1989). Patterns of sediment deposition in subsiding coastal salt marshes, Terrebonne Bay, Louisiana: the role of winter storms. *Estuaries , 12* (4), pp. 222-227.

Reed, D. J., Spencer, T., Murray, A. L., French, J. R., & Leonard, L. (1999). Marsh surface sediment deposition and the role of tidal creeks: Implications for created and managed coastal marshes. *Journal of Coastal Conservation , 5*, pp. 81-90.

Riethmuller, R., Heineke, M., Kuhl, H., & Keuker-Rudiger, R. (2000). Chlorophyll a concentration as an inder of sediment surface stabilisation by microphytobenthos? *Continental Shelf Research , 20*, pp. 1351-1372.

Robinson, M.-C., Morris, K. P., & Dyer, K. R. (1998). Deriving Fluxes of Suspended Particulate Matter in the Humber Estuary, UK, Using Airborne Remote Sensing. *Marine Pollution Bulletin , 37* (3-7), pp. 155-163.

Rupp, S., & Nicholls, R. J. (2002). Managed Realignment of Coastal Flood Defences: A Comparison between England and Germany. *Proceedings of "Dealing with Flood Risk" An interdisciplinary seminar of the regional implications of modern flood management.*

Schaaff, E., Grenz, C., Pinazo, C., & Lansard, B. (2006). Field and laboratory measurements of sediment erodibility: A comparison. *Journal of Sea Research , 55*, pp. 30-42.

Shepherd, D., Burgess, D., Jickells, T. A., Cave, R., Turner, R. K., Parker, E. R., et al. (2007). Modelling the effects and economics of managed realignment on the cycling and storage of nutrients, carbon and sediments in the Blackwater estuary UK. *Estuarine, Coastal and Shelf Science* , pp. 355-367.

SonTek. (2000). *Acoustic Doppler Profiler Principles of Operation.* SonTek.

SonTek. (2004). *PC-ADP- Read ME First!* SonTek.

SonTek/YSI. (n.d.). *PC-ADP- Pulse-Coherent Acoustic Doppler Profiler*. Retrieved February 2009, from SonTek: http://www.sontek.com/pc-adp.html

Soulsby, R. (1997). In *Dynamics of Marine Sands: a manual for practical applications*. London: Telford.

Shennan, I., & Horton, B. (2002). Holocene land- and sea-level changes in Great Britain. *Journal of Quaternary Science, 17 (5-6)*, pp. 511-526.

Symonds, A. M., & Collins, M. B. (2007). The establishment and degeneration of a temporary creek system in response to managed coastal realignment: The Wash, UK. *Earth Surface Processes and Landforms , www.interscience.wiley.com*.

Sympatec GmbH. (2004). *QICPIC Operating Instructions*. Sympatec GmbH.

Thomas, S., & Ridd, P. V. (2004). Review of methods to measure short time scale sediment accumulation. *Marine Geology , 207*, pp. 95-114.

Tolhurst, T. J., Black, K. S., Paterson, D. M., Mitchener, H. J., Termaat, G. R., & Shayler, S. A. (2000). A comparison and measurement standardisation of four in situ devices for determining the erosion shear stress of intertidal sediments. *Continental Shelf Research , 20*, pp. 1397-1418.

Tolhurst, T. J., Black, K. S., Shayler, S. A., Mather, S., Black, I., Baker, K., et al. (1999). Measuring the in situ Erosion Shear Stress of Intertidal Sediments with the Cohesive Strength Meter (CSM). *Estuarine, Coastal and Shelf Science , 49*, pp. 281-294.

Tolhurst, T. J., Riethmuller, R., & Paterson, D. M. (2000). In situ versus laboratory analysis of sediment stability from intertidal mudflats. *Continental Shelf Research , 20*, pp. 1317-1334.

Townend, I. (2008a). Breach design for managed realignment sites. *Proceedings of the Institution of Civil Engineers: Maritime Engineering* (MA1), pp. 9-21.

Townend, I. (2008b). Hypsometry of estuaries, creeks and breached sea wall sites. *Proceedings of the Institution of Civil Engineers: Maritime Engineering* (MA1), pp. 23-32.

Townend, I., & Pethick, J. (2002). Estuarine flooding and managed retreat. *Philosophical Transactions of the Royal Society of London , 360*, pp. 1477-1495.

Townend, I., & Whitehead, P. (2003). A preliminary net sediment budget for the Humber Estuary. *The Science of the Total Environment , 314-316*, pp. 755-767.

Uncles, R. J. (2002). Estuarine Physical Processes Research: Some Recent Studies and Progress. *Estuarine, Coastal and Shelf Science , 55*, pp. 829-856.

van Ledden, M., van Kesteren, W. G., & Winterwerp, J. C. (2004). A conceptual framework for the erosion behaviour of sand-mud mixtures. *Continental Shelf Science , 24*, pp. 1-11.

Wang, Y. H. (2003). The intertidal erosion rate of cohesive sediment: a case study from Long Island Sound. *Estuarine, Coastal and Shelf Science , 56*, pp. 891-896.

Watts, C. W., Tolhurst, T. J., Black, K. S., & Whitmore, A. P. (2003). In situ measurements of erosion shear stress and geotechnical shear strength of the intertidal sediments of the experimental managed realignment scheme at Tollesbury, Essex, UK. *Estuarine, Coastal and Shelf Science , 58*, pp. 611-620.

Widdows, J., & Brinsley, M. (2002). Impact of biotic and abiotic processes on sediment dynamics and the consequences to the structure and functioning of the intertidal zone. *Journal of Sea Research , 48*, pp. 143-156.

Widdows, J., Brown, S., Brinsley, M. D., Salkeld, P. N., & Elliott, M. (2000). Temporal changes in intertidal sediment erodibility: influence of biological and climatic factors. *Continental Shelf Research , 20*, pp. 1275-1289.

Williams, B. P., & Orr, M. K. (2002). Physical Evolution of Restored Breached Levee Salt Marshes in the San Francisco Bay Estuary. *Restoration Ecology , 10* (3), pp. 527-542.

Winn, P. (2004). *Humber Estuary (United Kingdom).* EUROSION Case Study.

Wolters, M., Garbutt, A., & Bakker, J. P. (2005). Salt-marsh restoration: evaluating the success of de-embankments in nrth-west Europe. *Biological Conservation , 123*, pp. 249-268.

Wood, R., & Widdows, J. (2002). A model of sediment transport over an intertidal transect, comparing the influences of biological and physical factors. *Limnology and Oceanography , 47* (3), pp. 848-855.

Wood, R., & Widdows, J. (2003). Modelling intertidal sediment transport for nutrient change and climat change scenarios. *The Science of the Total Environment , 314-316*, pp. 637-649.

Wren, D. G., Barkdoll, B. D., Kuhnle, R. A., & Derrow, R. W. (2000). FIELD TECHNIQUES FOR SUSPENDED-SEDIMENT MEASUREMENT. *Journal of Hydraulic Engineering , 126* (2), pp. 99-104.

Wu, Y., Falconer, R. A., & Uncles, R. J. (1998). Modelling of Water Flows and Cohesive Sediment Fluxes in the Humber Estuary, UK. *Marine Pollution Bulletin , 37* (3-7), pp. 182-189.

Yorkshire Futures Regional Intelligence Network. (2002). *Warming up the Region Yorkshire and Humber Climate Change Impact Scoping Study.* Yorkshire Forward and Yorkshire and Humber Assembly.

Appendices

Appendix 1: Vegetation species at each sampling station

Vegetation species across the NW sector on PHS from EA monitoring data.

Site	Main Species: 2004	Main Species: 2005	Main Species: 2006	Main Species: 2007
1.1			*A. maritima, 5% Spartina anglica*	*A. tripolium, 5% P. maritima, S. anglica*
1.2			*A. maritima, < 5% S. anglica*	*A. tripolium, S. anglica, 5% S. maritima*
1.3	*Atriplex portulacoides*	SITE DESTROYED AND NOT RELOCATED		
1.4	*A. portulacoides*	*A. prostrata*	*A. maritima, Elytrigia atherica, Spergularia marina*	*A. tripolium, A. maritima, E. atherica, Parapholis strigosa, P. distans, P. maritima, S. marina*
2.1				*5% S. anglica*
4.1			*< 5% S. anglica*	*S. anglica*
4.4			*S. anglica*	*S. anglica*
4.5				*S. anglica*
4.6				*S. europaea*

Vegetation species across the SE sector on PHS from EA monitoring data.

Site	Main Species: 2004	Main Species: 2005	Main Species: 2006	Main Species: 2007
5.1			*Aster tripolium, A. prostrata*	*A. tripolium, < 5% P. maritima*
5.2			*A. tripolium*	*A. tripolium*
5.3	*Atriplex prostrata*	*A. prostrata*	*A. tripolium, A. maritima, 5% Suaeda maritima*	*A. tripolium, < 5% A. maritima, S. maritima*
5.4	*< 5% A. Prostrata < 5% Elymus repens*	*A. maritima, E. atherica*	*A. tripolium, A. maritima, S. marina*	*A. tripolium, 5% A. maritima, S. marina*
6.1	*A. prostrata*	*A. prostrata*	*A. tripolium, A. maritima, Puccinellia distans, S. marina*	*A. tripolium, P. distans, 5% S. marina*
6.2	*E. repens, < 5% A. prostrata*	*A. tripolium, A. maritima, E.*	*A. tripolium, A. maritima, E.*	*A. tripolium, P. distans, 5% S.*

		atherica	*atherica, P. distans, S. marina*	*marina*
6.3	*E. repens*	5% *A. maritima, E. repens*	*A. maritima, E. repens*	*E. repens*
6.4	*E. repens*	*A. tripolium, A. maritima, E. repens*	*A. tripolium,* 5% *A. maritima, E. atherica, E. repens,* 5% *F. rubra*	5% *Agrostis stolonifera, A. tripolium, E. atherica, E. repens, F. rubra*
7.1		5% *P. maritima*	< 5% *A. maritima, P. maritima, Salicornia europaea*	5% *A. tripolium, Glaux maritima, P. maritima, S. europaea*
7.2	5% *A. prostrata*	*A. maritima, S. media*	5% *A. tripolium, A. maritima, P. maritima, S. europaea, Spergularia media,* 5%, *S. maritima*	*A. tripolium,* < 5% *Plantago maritima, P. maritima*
7.3	*A. prostrata*	*A. prostrata*	*A. tripolium, A. maritima, P. maritima, S. media*	*A. tripolium, P. maritima, S. media*
7.4	*E. repens*	*A. maritima,* < 5% *F. rubra*	< 5% *A. tripolium, A. maritima,* < 5% *E. repens, F. rubra,* < 5% *P. distans, S. media*	*A. tripolium, E. atherica, F. rubra,* 5% *P. distans, P. maritima,* 5% *S. marina*
8.1		< 5% *A. tripolium,* 5% *A. maritima, P. maritima, S. media*	*P. maritima, S. europaea, S. anglica*	*A. tripolium, P. maritima,* < 5% *S. europaea, S. anglica*
8.2			< 5% *P. maritima,* 5% *S. europaea*	*P. maritima, S. europaea*
8.3	5% *Puccinellia maritima*	5% *A. maritima, P. maritima*	*A. maritima, P. maritima, S. europaea*	*A. tripolium, P. maritima, S. maritima*
8.4		*A. tripolium,* < 5% *P. maritima*	< 5% *A. tripolium,* < 5% *A. maritima, P. maritima, S. europaea*	*A. tripolium, P. maritima, S. maritima*

Appendix 2: Photos of sampling stations

Sampling station 1a

Sampling station 1b

Sampling station 1c

Sampling station 1d

Sampling station 2a

Sampling station 2b

Sampling station 2c

Sampling station 2d

Sampling station 3a

Sampling station 3c

Sampling station 3d

Sampling station 4a

Sampling station 4b

Sampling station 4c

Sampling station 4d

Sampling station 4e

Sampling station 5a

Sampling station 5b

Sampling station 5c

Sampling station 5d

Sampling station 5e

Sampling station 6a

Sampling station 6b

Sampling station 6c

Sampling station 7a

Sampling station 7b

Sampling station 7c

Sampling station 7d

Sampling station 8a

Sampling station 8b

Appendix 3: Full accretion/ erosion data

Station	Distance to level in mm- 160306				Erosion/ Accretion (mm)			
1a	1000	1000	1000	1000	0	0	0	0
1b	1000	1000	1000	1000	0	0	0	0
1c	1000	1000	1000	1000	0	0	0	0
1d	1000	1000	1000	1000	0	0	0	0
2a	1012	1015	1000	1025	-12	-15	0	-25
2b	1000	1000	1000	1000	0	0	0	0
2c	1000	1000	1000	1000	0	0	0	0
2d	1000	995	995	1000	0	5	5	0
3a	1000	1000	1000	1000	0	0	0	0
3b	995	1000	998	995	5	0	2	5
3c	1000	1000	1000	1000	0	0	0	0
3d	985	990	1002	1000	15	10	-2	0
4a								
4b								
4c								
4d	974	989	1010	1014	26	11	-10	-14
4e	1015	992	1006	1004	-15	8	-6	-4
5a								
5b								
5c								
5d								
5e	1015	1004	1002	1004	-15	-4	-2	-4
6a								
6b								
6c	1007	1007	1008	995	-7	-7	-8	5
7a								
7b								
7c								
7d								
8a								
8b								

Station	Distance to level in mm- 270406				Erosion/ Accretion (mm)			
1a								
1b								
1c								
1d								
2a								
2b								
2c								
2d								
3a								
3b								
3c								
3d								
4a	972	991	990	974	28	9	10	26
4b	961	965	971	969	39	35	29	31
4c	in pool							
4d	961	980	1009	1005	13	9	1	9
4e	950	971	990	980	65	21	16	24
5a	962	967	963	968	38	33	37	32
5b	974	975	974	977	26	25	26	23
5c	971	967	973	974	29	33	27	26
5d	947	955	935	940	53	45	65	60
5e	1024	1000	1000	1012	-9	4	2	-8
6a	930	947	924	900	70	53	76	100
6b	944	930	947	960	56	70	53	40
6c	949	950	961	951	58	57	47	44
7a	968	969	957	956	32	31	43	44
7b	934	956	945	952	66	44	55	48
7c	995	973	965	991	5	27	35	9
7d	962	969	985	978	38	31	15	22
8a	989	976	950	933	11	24	50	67
8b	inaccessible							

Station	Distance to level in mm- 220506				Erosion/ Accretion (mm)			
1a	993	995	1001	995	7	5	-1	5
1b	993	997	995	1000	7	3	5	0
1c	984	995	995	1000	16	5	5	0
1d	988	990	1000	991	12	10	0	9
2a	1024	1026	1008	1035	-12	-11	-8	-10
2b	994	1000	998	1004	6	0	2	-4
2c	1007	1010	998	1003	-7	-10	2	-3
2d	996	996	990	1000	4	-1	5	0
3a	995	991	988	989	5	9	12	11
3b	990	991	995	990	5	9	3	5
3c	993	993	991	999	7	7	9	1
3d	984	981	995	996	1	9	7	4
4a	976	984	985	970	-4	7	5	4
4b	970	978	975	979	-9	-13	-4	-10
4c								
4d	981	971	1004	1014	-20	9	5	-9
4e	998	971	986	993	-48	0	4	-13
5a	965	970	965	975	-3	-3	-2	-7
5b	974	980	979	978	0	-5	-5	-1
5c	982	979	984	980	-11	-12	-11	-6
5d	935	935	919	920	12	20	16	20
5e	1026	1003	995	1018	-2	-3	5	-6
6a	931	934	926	893	-1	13	-2	7
6b	945	940	945	960	-1	-10	2	0
6c	954	952	951	944	-5	-2	10	7
7a	965	969	960	957	3	0	-3	-1
7b	955	950	941	954	-21	6	4	-2
7c	1002	973	969	992	-7	0	-4	-1
7d	960	973	989	989	2	-4	-4	-11
8a	984	978	947	931	5	-2	3	2
8b	inaccessible							

Station	Distance to level in mm- 130606				Erosion/ Accretion (mm)			
1a	986	987	993	994	7	8	8	1
1b	990	994	994	1002	3	3	1	-2
1c	991	1000	967	1007	-7	-5	28	-7
1d	995	995	1002	996	-7	-5	-2	-5
2a	stakes destroyed							
2b	1004	1007	1005	1007	-10	-7	-7	-3
2c	1019	1021	1000	1008	-12	-11	-2	-5
2d	1007	1007	1003	1009	-11	-11	-13	-9
3a	stakes destroyed							
3b	990	994	996	992	0	-3	-1	-2
3c	990	995	991	999	3	-2	0	0
3d	984	981	995	995	0	0	0	1
4a	986	994	995	981	-10	-10	-10	-11
4b	974	983	980	984	-4	-5	-5	-5
4c	in pool							
4d	987	975	1005	1009	-6	-4	-1	5
4e	1000	970	985	990	-2	1	1	3
5a	970	971	973	971	-5	-1	-8	4
5b	985	987	989	989	-11	-7	-10	-11
5c	985	985	986	985	-3	-6	-2	-5
5d	928	929	910	911	7	6	9	9
5e	1035	1009	1010	1031	-9	-6	-15	-13
6a	934	941	929	900	-3	-7	-3	-7
6b	950	940	950	960	-5	0	-5	0
6c	955	951	954	949	-1	1	-3	-5
7a	972	969	969	965	-7	0	-9	-8
7b	962	955	942	959	-7	-5	-1	-5
7c	1004	980	975	1008	-2	-7	-6	-16
7d	966	980	995	986	-6	-7	-6	3
8a	982	977	950	935	2	1	-3	-4
8b	970	963	960	969	30	37	40	31

Station	Distance to level in mm- 100706				Erosion/ Accretion (mm)			
1a	1002	1004	1004	1003	-16	-17	-11	-9
1b	997	998	998	1002	-7	-4	-4	0
1c	1004	1009	980	1007	-13	-9	-13	0
1d	1003	1005	1009	1003	-8	-10	-7	-7
2a	1030	1036	1006	1042	-30	-36	-6	-42
2b	1012	1014	1006	1011	-8	-7	-1	-4
2c	1024	1025	1008	1019	-5	-4	-8	-11
2d	1011	1009	1009	1009	-4	-2	-6	0
3a	988	991	993	986	12	9	7	14
3b	992	994	995	993	-2	0	1	-1
3c	994	995	994	1000	-4	0	-3	-1
3d	983	981	999	996	1	0	-4	-1
4a	989	994	1002	988	-3	0	-7	-7
4b	980	991	989	987	-6	-8	-9	-3
4c	934	932	942	938	66	68	58	62
4d	984	972	997	1009	3	3	8	0
4e	995	971	986	987	5	-1	-1	3
5a	978	979	975	978	-8	-8	-2	-7
5b	988	993	994	992	-3	-6	-5	-3
5c	986	986	984	984	-1	-1	2	1
5d	925	926	910	909	3	3	0	2
5e	1037	1026	1028	1030	-2	-17	-18	1
6a	934	943	929	900	0	-2	0	0
6b	946	945	955	964	4	-5	-5	-4
6c	921	949	950	944	34	2	4	5
7a	974	975	975	970	-2	-6	-6	-5
7b	963	959	939	957	-1	-4	3	2
7c	1003	976	979	1008	1	4	-4	0
7d	972	985	1002	995	-6	-5	-7	-9
8a	990	979	953	938	-8	-2	-3	-3
8b	970	963	955	970	0	0	5	-1

230

Station	Distance to level in mm- 100806				Erosion/ Accretion (mm)			
1a	993	999	997	996	9	5	7	7
1b	995	996	996	1002	2	2	2	0
1c	993	1002	967	1004	11	7	13	3
1d	993	999	1010	1006	10	6	-1	-3
2a	poles bent							
2b	1000	1002	1001	1003	12	12	5	8
2c	1012	1015	1004	1005	12	10	4	14
2d	1006	1003	998	996	5	6	11	13
3a	1001	1004	1001	1000	-13	-13	-8	-14
3b	974	986	978	968	18	8	17	25
3c	993	995	995	995	1	0	-1	5
3d	985	982	997	996	-2	-1	2	0
4a	991	994	1003	991	-2	0	-1	-3
4b	975	988	989	987	5	3	0	0
4c	in pool							
4d	976	965	1003	1011	8	7	-6	-2
4e	992	967	983	988	3	4	3	-1
5a	977	981	968	980	1	-2	7	-2
5b	985	995	988	986	3	-2	6	6
5c	985	985	985	983	1	1	-1	1
5d	920	920	902	895	5	6	8	14
5e	1054	1041	1045	1037	-17	-15	-17	-7
6a	928	937	928	900	6	6	1	0
6b	948	941	953	963	-2	4	2	1
6c	940	947	947	936	-19	2	3	8
7a	979	979	977	950	-5	-4	-2	20
7b	957	950	940	955	6	9	-1	2
7c	1009	981	987	1002	-6	-5	-8	6
7d	977	986	1002	1000	-5	-1	0	-5
8a	poles bent							
8b	965	960	952	960	5	3	3	10

Station	Distance to level in mm- 120906				Erosion/ Accretion (mm)			
1a	993	995	998	995	0	4	-1	1
1b	994	993	994	1000	1	3	2	2
1c	996	1001	994	1004	-3	1	-27	0
1d	1000	1000	1007	1004	-7	-1	3	2
2a	poles bent							
2b	987	1001	991	998	13	1	10	5
2c	1012	1011	996	1005	0	4	8	0
2d	1001	993	993	993	5	10	5	3
3a	1000	1000	994	992	1	4	7	8
3b	982	977	973	968	-8	9	5	0
3c	994	993	989	990	-1	2	6	5
3d	982	982	997	995	3	0	0	1
4a	979	983	988	975	12	11	15	16
4b	946	965	966	962	29	23	23	25
4c	937	934	946	935	-3	-2	-4	3
4d	981	970	1000	1005	-5	-5	3	6
4e	995	957	980	1004	-3	10	3	-16
5a	950	955	950	962	27	26	18	18
5b	969	984	982	989	16	11	6	-3
5c	981	977	974	964	4	8	11	19
5d	914	920	899	896	6	0	3	-1
5e	1056	1045	1050	1047	-2	-4	-5	-10
6a	910	910	903	878	18	27	25	22
6b	920	910	925	935	28	31	28	28
6c	916	925	920	907	24	22	27	29
7a	950	955	953	920	29	24	24	30
7b	940	935	920	933	17	15	20	22
7c	1000	977	968	990	9	4	19	12
7d	966	969	992	987	11	17	10	13
8a	poles bent							
8b	945	946	937	943	20	14	15	17

Station	Distance to level in mm- 191006				Erosion/ Accretion (mm)			
1a	988	994	996	993	5	1	2	2
1b	993	994	993	997	1	-1	1	3
1c	988	1004	966	1004	8	-3	28	0
1d	1001	995	1001	1001	-1	5	6	3
2a	poles bent							
2b	1000	1002	1000	1001	-13	-1	-9	-3
2c	1011	1008	997	1002	1	3	-1	3
2d	1000	997	996	997	1	-4	-3	-4
3a	1010	1006	993	1003	-10	-6	1	-11
3b	977	979	972	963	5	-2	1	5
3c	991	990	991	985	3	3	-2	5
3d	985	976	992	992	-3	6	5	3
4a	977	980	990	974	2	3	-2	1
4b	950	964	970	964	-4	1	-4	-2
4c	910	908	919	926	27	26	27	9
4d	990	980	1002	1017	-9	-10	-2	-12
4e	1001	960	982	1025	-6	-3	-2	-21
5a	949	946	950	965	1	9	0	-3
5b	968	977	982	989	1	7	0	0
5c	980	971	961	959	1	6	13	5
5d	903	909	891	885	11	11	8	11
5e	1061	1056	1048	1055	-5	-11	2	-8
6a	901	899	890	870	9	11	13	8
6b	900	887	901	912	20	23	24	23
6c	891	885	875	865	25	40	45	42
7a	942	946	948	917	8	9	5	3
7b	935	927	916	928	5	8	4	5
7c	990	970	965	990	10	7	3	0
7d	962	970	988	980	4	-1	4	7
8a	poles bent							
8b	949	941	930	939	-4	5	7	4

Station	Distance to level in mm- 201106				Erosion/ Accretion (mm)			
1a	990	989	991	990	-2	5	5	3
1b	991	990	993	996	2	4	0	1
1c	989	1000	982	1001	-1	4	-16	3
1d	995	990	1005	1002	6	5	-4	-1
2a	poles bent							
2b	1000	1003	999	1001	0	-1	1	0
2c	1010	1011	1000	1001	1	-3	-3	1
2d	998	999	995	999	2	-2	1	-2
3a	1010	1011	1003	1006	0	-5	-10	-3
3b	974	971	969	960	3	8	3	3
3c	982	984	985	982	9	6	6	3
3d	974	973	988	990	11	3	4	2
4a	979	981	989	977	-2	-1	1	-3
4b	943	954	960	956	7	10	10	8
4c	916	907	927	916	-6	1	-8	10
4d	991	976	1003	1021	-1	4	-1	-4
4e	990	956	976	1034	11	4	6	-9
5a	955	946	937	959	-6	0	13	6
5b	956	965	973	985	12	12	9	4
5c	971	969	959	952	9	2	2	7
5d	898	902	888	871	5	7	3	14
5e	1054	1050	1047	1049	7	6	1	6
6a	882	875	870	860	19	24	20	10
6b	870	862	875	890	30	25	26	22
6c	857	837	830	813	34	48	45	52
7a	940	946	937	909	2	0	11	8
7b	930	924	914	925	5	3	2	3
7c	982	959	960	981	8	11	5	9
7d	955	965	981	971	7	5	7	9
8a	poles bent							
8b	937	939	923	928	12	2	7	11

Station	Distance to level in mm- 181206				Erosion/ Accretion (mm)			
1a	981	984	985	983	9	5	6	7
1b	985	987	988	994	6	3	5	2
1c	991	997	981	999	-2	3	1	2
1d	999	994	998	999	-4	-4	7	3
2a	poles bent							
2b	995	996	994	997	5	7	5	4
2c	1011	1009	1001	999	-1	2	-1	2
2d	998	1001	992	995	0	-2	3	4
3a	1007	1005	998	1005	3	6	5	1
3b	970	966	965	955	4	5	4	5
3c	979	3 stakes removed			3			
3d	972	966	984	985	2	7	4	5
4a	975	977	983	975	4	4	6	2
4b	950	953	965	965	-7	1	-5	-9
4c	892	892	902	898	24	15	25	18
4d	990	968	995	1016	1	8	8	5
4e	982	953	971	1015	8	3	5	19
5a	955	955	949	954	0	-9	-12	5
5b	951	968	975	985	5	-3	-2	0
5c	970	967	961	947	1	2	-2	5
5d	871	872	853	847	27	30	35	24
5e	1045	1036	1039	1044	9	14	8	5
6a	872	861	860	850	10	14	10	10
6b	855	844	862	875	15	18	13	15
6c	816	810	783	772	41	27	47	41
7a	944	941	941	908	-4	5	-4	1
7b	930	919	906	923	0	5	8	2
7c	976	954	954	976	6	5	6	5
7d	945	965	975	971	10	0	6	0
8a	poles bent							
8b	938	940	920	923	-1	-1	3	5

Station	Distance to level in mm- 220107				Erosion/ Accretion (mm)			
1a	968	977	974	974	13	7	11	9
1b	982	983	985	986	3	4	3	8
1c	985	991	955	994	6	6	26	5
1d	995	990	1007	998	4	4	-9	1
2a	poles removed							
2b	989	1001	995	998	6	-5	-1	-1
2c	1008	1004	995	998	3	5	6	1
2d	994	994	990	994	4	7	2	1
3a	1007	1012	1005	1008	0	-7	-7	-3
3b	965	965	964	952	5	1	1	3
3c	972	3 stakes gone			7			
3d	968	966	981	979	4	0	3	6
4a	966	970	975	965	9	7	8	10
4b	941	945	960	955	9	8	5	10
4c	865	866	878	874	27	26	24	24
4d	989	973	995	1025	1	-5	0	-9
4e	975	960	961	1001	7	-7	10	14
5a	945	950	952	956	10	5	-3	-2
5b	955	969	977	992	-4	-1	-2	-7
5c	971	968	960	944	-1	-1	1	3
5d	853	853	834	834	18	19	19	13
5e	1st 2 poles wonky		1032	1046			7	-2
6a	866	862	854	845	6	-1	6	5
6b	846	838	848	861	9	6	14	14
6c	788	780	757	747	28	30	26	25
7a	934	937	937	904	10	4	4	4
7b	925	911	902	918	5	8	4	5
7c	971	944	947	965	5	10	7	11
7d	945	963	972	965	0	2	3	6
8a	poles removed							
8b	944	931	914	909	-6	9	6	14

Station	Distance to level in mm- 210207				Erosion/ Accretion (mm)			
1a	968	977	972	973	0	0	2	1
1b	977	977	979	982	5	6	6	4
1c	980	987	968	988	5	4	-13	6
1d	995	992	997	995	0	-2	10	3
2a	1030	1037	1005	1038	-30	-37	-5	-38
2b	990	995	995	994	-1	6	0	4
2c	1008	1003	991	998	0	1	4	0
2d	997	993	992	994	-3	1	-2	0
3a	996	993	995	989	11	19	10	19
3b	964	957	956	941	1	8	8	11
3c	967	965	963	962	5	19	22	20
3d	966	959	974	973	2	7	7	6
4a	957	960	963	955	9	10	12	10
4b	935	928	945	945	6	17	15	10
4c	860	860	860	860	5	6	18	14
4d	983	971	995	1015	6	2	0	10
4e	975	956	960	995	0	4	1	6
5a	940	937	942	946	5	13	10	10
5b	955	965	975	989	0	4	2	3
5c	976	971	955	932	-5	-3	5	12
5d	851	850	829	825	2	3	5	9
5e	1020	1014	1024	1038	25	22	8	8
6a	845	830	831	830	21	32	23	15
6b	831	833	834	845	15	5	14	16
6c	765	763	751	728	23	17	6	19
7a	920	922	928	895	14	15	9	9
7b	908	901	890	905	17	10	12	13
7c	965	942	943	967	6	2	4	-2
7d	940	958	975	965	5	5	-3	0
8a	985	964	948	933	15	36	52	67
8b	927	924	888	877	17	7	26	32

Station	Distance to level in mm- 160407				Erosion/ Accretion (mm)			
1a	971	968	975	970	-3	9	-3	3
1b	972	979	975	980	5	-2	4	2
1c	984	987	941	989	-4	0	27	-1
1d	991	984	991	988	4	8	6	7
2a	1030	1048	1018	1042	0	-11	-13	-4
2b	995	1001	1002	1003	-5	-6	-7	-9
2c	1011	1007	997	1001	-3	-4	-6	-3
2d	1002	1001	995	993	-5	-8	-3	1
3a	997	1001	1003	996	-1	-8	-8	-7
3b	poles gone							
3c	964	963	960	961	3	2	3	1
3d	960	955	970	972	6	4	4	1
4a	942	945	953	944	15	15	10	11
4b	912	918	931	925	23	10	14	20
4c	840	841	844	825	20	19	16	35
4d	972	966	987	993	11	5	8	22
4e	961	953	951	952	14	3	9	43
5a	920	926	928	932	20	11	14	14
5b	941	955	972	990	14	10	3	-1
5c	969	954	935	915	7	17	20	17
5d	835	835	813	806	16	15	16	19
5e	1007	1010	1017	1023	13	4	7	15
6a	829	819	814	808	16	11	17	22
6b	814	807	817	830	17	26	17	15
6c	730	725	706	690	35	38	45	38
7a	905	909	910	880	15	13	18	15
7b	895	885	873	890	13	16	17	15
7c	955	935	931	954	10	7	12	13
7d	928	943	956	955	12	15	19	10
8a	963	952	917	909	22	12	31	24
8b	921	906	875	815	6	18	13	62

Station	Distance to level in mm- 170507				Erosion/ Accretion (mm)			
1a	968	974	974	974	3	-6	1	-4
1b	979	977	978	979	-7	2	-3	1
1c	978	981	956	991	6	6	-15	-2
1d	987	981	990	990	4	3	1	-2
2a	1027	1060	1023	1055	3	-12	-5	-13
2b	994	998	998	998	1	3	4	5
2c	1008	1002	989	996	3	5	8	5
2d	994	996	988	990	8	5	7	3
3a	995	1004	1008	1008	2	-3	-5	-12
3b	poles removed							
3c	963	963	956	955	1	0	4	6
3d	958	953	970	972	2	2	0	0
4a	936	940	945	942	6	5	8	2
4b	905	912	916	917	7	6	15	8
4c	830	825	842	827	10	16	2	-2
4d	965	957	976	956	7	9	11	37
4e	958	951	952	967	3	2	-1	-15
5a	921	925	926	934	-1	1	2	-2
5b	938	960	974	994	3	-5	-2	-4
5c	970	955	935	912	-1	-1	0	3
5d	822	827	801	797	13	8	12	9
5e	991	1015	997	1010	16	-5	20	13
6a	817	810	806	800	12	9	8	8
6b	806	797	810	818	8	10	7	12
6c	718	718	697	682	12	7	9	8
7a	904	905	901	863	1	4	9	17
7b	885	876	861	876	10	9	12	14
7c	950	931	924	950	5	4	7	4
7d	925	940	957	950	3	3	-1	5
8a	959	947	924	912	4	5	-7	-3
8b	911	917	865	815	10	-11	10	0

Station	Distance to level in mm- 110607				Erosion/ Accretion (mm)			
1a	972	978	976	977	-4	-4	-2	-3
1b	984	985	982	987	-5	-8	-4	-8
1c	982	989	965	992	-4	-8	-9	-1
1d	995	984	992	991	-8	-3	-2	-1
2a	1040	1065	1031	1054	-13	-5	-8	1
2b	998	1000	997	1001	-4	-2	1	-3
2c	1011	1002	997	1005	-3	0	-8	-9
2d	998	998	992	992	-4	-2	-4	-2
3a	997	1012	1022	1006	-2	-8	-14	2
3b	poles removed							
3c	965	958	956	959	-2	5	0	-4
3d	962	954	970	971	-4	-1	0	1
4a	938	942	943	937	-2	-2	2	5
4b	907	903	915	915	-2	9	1	2
4c	820	816	827	811	10	9	15	16
4d	963	951	972	954	2	6	4	2
4e	953	952	949	966	5	-1	3	1
5a	916	921	925	931	5	4	1	3
5b	938	960	975	995	0	0	-1	-1
5c	968	953	932	907	2	2	3	5
5d	815	814	787	785	7	13	14	12
5e	989	1030	998	1010	2	-15	-1	0
6a	813	803	803	796	4	7	3	4
6b	800	792	803	815	6	5	7	3
6c	711	710	689	675	7	8	8	7
7a	901	905	902	870	3	0	-1	-7
7b	883	875	865	883	2	1	-4	-7
7c	949	931	926	949	1	0	-2	1
7d	927	943	955	951	-2	-3	2	-1
8a	955	944	924	904	4	3	0	8
8b	912	911	865	811	-1	6	0	4

Station	Distance to level in mm- 110707				Erosion/ Accretion (mm)			
1a	973	979	978	979	-1	-1	-2	-2
1b	986	987	985	990	-2	-2	-3	-3
1c	982	989	965	994	0	0	0	-2
1d	994	983	991	991	1	1	1	0
2a	1055	1069	1030	1060	-15	-4	1	-6
2b	987	993	993	995	11	7	4	6
2c	1002	1004	990	995	9	-2	7	10
2d	991	993	987	985	7	5	5	7
3a	1020	1031	1025	1019	-23	-19	-3	-13
3b	poles removed							
3c	972	962	957	962	-7	-4	-1	-3
3d	964	959	968	974	-2	-5	2	-3
4a	940	943	946	942	-2	-1	-3	-5
4b	902	906	915	912	5	-3	0	3
4c	805	801	808	801	15	15	19	10
4d	960	956	976	962	3	-5	-4	-8
4e	955	958	960	968	-2	-6	-11	-2
5a	928	937	937	941	-12	-16	-12	-10
5b	947	971	990	1010	-9	-11	-15	-15
5c	971	959	941	917	-3	-6	-9	-10
5d	805	807	787	771	10	7	0	14
5e	996	1032	1008	1011	-7	-2	-10	-1
6a	820	810	809	804	-7	-7	-6	-8
6b	801	793	804	813	-1	-1	-1	2
6c	707	706	682	674	4	4	7	1
7a	904	906	903	870	-3	-1	-1	0
7b	886	875	865	882	-3	0	0	1
7c	952	935	935	951	-3	-4	-9	-2
7d	925	940	965	953	2	3	-10	-2
8a	955	952	926	909	0	-8	-2	-5
8b	927	933	882	824	-15	-22	-17	-13

Station	Distance to level in mm- 140807				Erosion/ Accretion (mm)			
1a	982	981	981	974	-9	-2	-3	5
1b	975	971	974	977	11	16	11	13
1c	982	984	984	986	0	5	-19	8
1d	986	984	987	989	8	-1	4	2
2a	1076	1086	1039	1074	-21	-17	-9	-14
2b	991	997	991	994	-4	-4	2	1
2c	1004	1003	984	993	-2	1	6	2
2d	988	985	983	984	3	8	4	1
3a	1013	3rd pole bent		1020	7			-1
3b	poles removed							
3c	968	965	962	965	4	-3	-5	-3
3d	957	956	974	975	7	3	-6	-1
4a	940	943	945	942	0	0	1	0
4b	893	896	906	909	9	10	9	3
4c	790	795	796	791	15	6	12	10
4d	962	959	974	963	-2	-3	2	-1
4e	951	962	965	961	4	-4	-5	7
5a	931	943	943	940	-3	-6	-6	1
5b	954	978	994	1017	-7	-7	-4	-7
5c	969	966	939	922	2	-7	2	-5
5d	803	801	775	768	2	6	12	3
5e	995	1044	1011	1011	1	-12	-3	0
6a	815	811	802	799	5	-1	7	5
6b	790	781	794	802	11	12	10	11
6c	688	694	671	664	19	12	11	10
7a	901	910	902	875	3	-4	1	-5
7b	875	872	862	881	11	3	3	1
7c	945	930	922	945	7	5	13	6
7d	926	941	955	951	-1	-1	10	2
8a	957	947	926	911	-2	5	0	-2
8b	926	933	889	827	1	0	-7	-3

Station	Distance to level in mm- 190907				Erosion/ Accretion (mm)			
1a	973	978	983	970	9	3	-2	4
1b	972	975	975	979	3	-4	-1	-2
1c	977	991	961	997	5	-7	23	-11
1d	991	983	995	999	-5	1	-8	-10
2a	wonky							
2b	986	991	983	995	5	6	8	-1
2c	1006	1004	990	1006	-2	-1	-6	-13
2d	1003	998	987	988	-15	-13	-4	-4
3a	1006				7			
3b	poles removed							
3c	968	960	956	952	0	5	6	13
3d	960	950	970	970	-3	6	4	5
4a	938	936	948	940	2	7	-3	2
4b	890	896	906	908	3	0	0	1
4c	787	778	792	774	3	17	4	17
4d	958	950	972	950	4	9	2	13
4e	937	947	930	920	14	15	35	41
5a	925	936	940	940	6	7	3	0
5b	942	971	988	1011	12	7	6	6
5c	971	955	930	909	-2	11	9	13
5d	795	795	770	760	8	6	5	8
5e	1002	1055	1026	1055	-7	-11	-15	-44
6a	802	798	791	784	13	13	11	15
6b	777	768	784	795	13	13	10	7
6c	681	681	660	660	7	13	11	4
7a	902	902	901	871	-1	8	1	4
7b	873	866	851	871	2	6	11	10
7c	942	927	928	942	3	3	-6	3
7d	930	945	955	950	-4	-4	0	1
8a	950	948	922	906	7	-1	4	5
8b	915	932	891	821	11	1	-2	6

Appendix 4: Suspended particulate matter data

SPM for 23/05/2006

Time (BST)	SSC gl^{-1}	SPM mgl^{-1}	Mean water depth (m)
13:35	0.1776	178	0.11
14:05	0.2533	253	0.53
14:35	0.4688	469	0.93
15:05	0.4703	470	1.13
15:35	0.2683	268	1.28
16:05	0.2457	246	1.18
16:35	0.1791	179	0.93
17:05	0.1401	140	0.53
17:30	0.2373	237	0.12

SPM for 19/07/2006

Time (BST)	SSC gl^{-1}	SPM mgl^{-1}	Mean water depth (m)
11:40	0.1056	106	0.28
12:10	0.2576	258	0.68
12:40	0.2708	271	0.98
13:13	0.1704	170	1.13
13:40	0.1167	117	1.18
14:13	0.1519	152	0.93
14:40	0.2628	263	0.68
15:10	0.2835	284	0.38

SPM for 16/08/2006

Time (BST)	SSC gl^{-1}	SPM mgl^{-1}	Mean water depth (m)
09:50	0.0664	66	0.12
10:20	0.1157	116	0.68
10:50	0.3560	356	1.08
11:20	0.1227	123	1.38
11:50	0.0483	48	1.48
12:20	0.0919	92	1.48
12:50	0.0536	54	1.18
13:20	0.0670	67	0.88
13:50	0.1671	167	0.38

SPM for 11/09/2006

Time (BST)	SSC gl^{-1}	SPM mgl^{-1}	Mean water depth (m)
07:00	0.5000	500	0.58
07:30	0.6469	647	1.38
08:00	0.5953	595	2.08
08:30	0.2600	260	2.58
09:00	0.6071	607	2.78
09:30	0.1562	156	2.78
10:00	0.2670	267	2.38
10:30	0.1958	196	1.78
11:00	0.4571	457	1.08
11:30	0.5958	596	0.28

SPM for 11/05/2007

Time (BST)	SSC gl^{-1}	SPM mgl^{-1}	Mean water depth (m)
11:40	0.090	90	0.00
12:00	0.077	77	0.060
12:20	0.073	73	0.190
12:40	0.088	88	0.380
13:00	0.099	99	0.480
13:20	0.092	92	0.480
13:40	0.062	62	0.480
14:00	0.057	57	0.480
14:20	0.050	50	0.380
14:40	0.061	61	0.190
15:00	0.082	82	0.115

SPM for 14/09/2007

Time (BST)	SSC gl^{-1}	SPM mgl^{-1}	Mean water depth (m)
06:30	0.21	215	0.48
07:00	0.31	312	1.08
07:30	0.45	455	1.58
08:00	0.17	173	1.88
08:30	0.18	184	1.98
09:00	0.30	300	1.78
09:30	0.22	222	1.48
10:00	0.13	135	0.88
10:30	0.17	170	0.38

Appendix 5: Full tidal flux data

Tidal flux data for 23/05/2006

Time (BST)	SSC gl^{-1}	SSC gm^3	Total vol flow (m^{3}s^{-1})	SSC gs^{-1}
13:20	0.1776	178	0.08	13
13:25	0.1776	178	0.23	40
13:30	0.1776	178	0.44	78
13:35	0.1776	178	1.41	251
13:40	0.19	190	4.26	810
13:45	0.2	200	7.83	1566
13:50	0.215	215	10.38	2231
13:55	0.228	228	12.30	2804
14:00	0.24	240	18.63	4471
14:05	0.2533	253	25.53	6468
14:10	0.0285	29	30.16	860
14:15	0.32	320	35.20	11265
14:20	0.36	360	40.78	14682
14:25	0.39	390	46.63	18187
14:30	0.43	430	46.43	19965
14:35	0.4688	469	50.39	23625
14:40	0.4688	469	55.94	26223
14:45	0.4688	469	61.49	28826
14:50	0.4688	469	60.31	28273
14:55	0.4703	470	54.96	25849
15:00	0.4703	470	56.08	26376
15:05	0.4703	470	56.76	26698
15:10	0.4350	435	53.18	23134
15:15	0.4000	400	49.72	19886
15:20	0.4200	420	40.10	16843
15:25	0.3350	335	28.15	9430
15:30	0.3000	300	9.95	2984
15:35	0.2683	268	11.41	3061
15:40	0.3000	300	16.92	5077
TOTAL			886	349978
15:45	0.3300	330	22.55	7441
15:50	0.3550	355	28.89	10258
15:55	0.3350	335	39.57	13255
16:00	0.4100	410	46.20	18941
16:05	0.4367	437	47.11	20572
16:10	0.3900	390	46.32	18065
16:15	0.3500	350	46.96	16434
16:20	0.3050	305	47.93	14618
16:25	0.2600	260	47.22	12277
16:30	0.2200	220	47.20	10384

Time				
16:35	0.1791	179	47.61	8528
16:40	0.1700	170	47.46	8068
16:45	0.1650	165	45.75	7549
16:50	0.1600	160	42.08	6733
16:55	0.1500	150	40.34	6051
17:00	0.0145	15	38.85	563
17:05	0.1401	140	36.85	5162
17:10	0.1600	160	30.30	4848
17:15	0.1800	180	27.91	5023
17:20	0.2000	200	20.61	4121
17:25	0.2200	220	15.18	3340
17:30	0.2373	237	10.50	2491
17:35	0.2373	237	8.41	1997
17:40	0.2373	237	1.21	288
17:45	0.2373	237	0.63	150
17:50	0.2373	237	0.32	75
TOTAL			834	207233

Tidal flux data for 19/07/2006

Time (BST)	SSC gl^{-1}	SSC gm^3	Total vol flow (m^3s^{-1})	SSC gs^{-1}
11:10	0.1056075	106	0.08	8
11:15	0.1056075	106	0.23	24
11:20	0.1056	106	0.44	47
11:25	0.1056075	106	1.41	149
11:30	0.1056075	106	4.18	442
11:35	0.1056075	106	7.84	828
11:40	0.1056075	106	13.75	1452
11:45	0.13	130	15.06	1958
11:50	0.1570	157	21.02	3301
11:55	0.18	180	28.74	5173
12:00	0.208	208	31.00	6448
12:05	0.23	230	35.13	8080
12:10	0.257554	258	43.74	11265
12:15	0.26	260	46.63	12125
12:20	0.2630	263	46.48	12225
12:25	0.265	265	50.37	13347
12:30	0.268	268	55.76	14944
12:35	0.269	269	61.22	16469
12:40	0.2708434	281	54.10	15193
12:45	0.257	267	56	14883
12:50	0.24	250	57.87	14467
12:55	0.2350	245	50.64	12406
13:00	0.21	220	47.16	10375

Time				
13:05	0.195	205	39.75	8148
13:10	0.1704057	180	40.12	7239
13:15	0.165	175	28.18	4931
13:20	0.157	167	9.91	1655
13:25	0.1470	147	11.31	1662
13:30	0.138	138	10.85	1498
TOTAL		5502	869	200742
13:35	0.127	127	22.51	2858
13:40	0.1167048	117	28.82	3363
13:45	0.122	122	39.55	4825
13:50	0.128	128	46.16	5909
13:55	0.1350	135	47.10	6359
14:00	0.139	139	46.29	6434
14:05	0.145	145	46.92	6803
14:10	0.1518692	152	47.89	7273
14:15	0.16	160	47.21	7554
14:20	0.18	180	50.24	9042
14:25	0.2000	200	50.80	10159
14:30	0.221	221	47.55	10508
14:35	0.242	242	50.81	12296
14:40	0.2627907	263	47.21	12406
14:45	0.267	227	46.56	10569
14:50	0.27	230	45.24	10406
14:55	0.274	234	32.56	7619
15:00	0.278	238	32.22	7668
15:05	0.28	240	26.11	6265
15:10	0.2835267	244	20.84	5074
15:15	0.287	244	15.37	3744
15:20	0.287	244	10.62	2586
15:25	0.287	244	3.40	829
15:30	0.287	244	1.21	296
15:35	0.287	244	0.63	154
15:40	0.287	244	0.32	77
15:45	0.287	244	0.06	15
TOTAL		5448	854	161092

Tidal flux data for 16/08/2006

Time (BST)	SSC gl^{-1}	SSC gm^3	Total vol flow (m^{3}s^{-1})	SSC gs^{-1}
09:35	0.0420	42	0.04	2
09:40	0.0500	50	0.16	8
09:45	0.0590	59	0.56	33
09:50	0.0664	66	1.23	82
09:55	0.0760	76	5.70	433

10:00	0.0850	85	8.07	686
10:05	0.0910	91	23.35	2125
10:10	0.1000	100	31.77	3177
10:15	0.1090	109	29.25	3188
10:20	0.1157	116	36.00	4166
10:25	0.156	156	42.82	6680
10:30	0.198	198	56.10	11108
10:35	0.238	238	60.13	14311
10:40	0.276	276	60.09	16586
10:45	0.318	318	65.17	20725
10:50	0.3560	356	69.68	24808
10:55	0.319	319	68.94	21992
11:00	0.279	279	71.21	19867
11:05	0.24	240	75.75	18181
11:10	0.2	200	77.54	15509
11:15	0.161	161	74.87	12054
11:20	0.1227	123	75.97	9324
11:25	0.11	110	53.49	5884
11:30	0.099	99	44.03	4359
11:35	0.085	85	33.90	2881
11:40	0.071	71	25.46	1807
11:45	0.06	60	17.42	1045
11:50	0.0483	48	8.73	422
11:55	0.056	56	5.51	309
12:00	0.063	63	15.81	996
TOTAL		4250	1139	222746
12:05	0.07	70	26.97	1888
12:10	0.078	78	45.51	3550
12:15	0.085	85	51.10	4343
12:20	0.0919	92	62.62	5758
12:25	0.086	86	69.25	5956
12:30	0.079	79	67.43	5327
12:35	0.072	72	75.07	5405
12:40	0.067	67	78.88	5285
12:45	0.06	60	74.19	4451
12:50	0.0536	54	75.47	4045
12:55	0.057	57	73.75	4204
13:00	0.059	59	68.82	4060
13:05	0.06	60	58.06	3484
13:10	0.062	62	57.68	3576
13:15	0.065	65	52.92	3440
13:20	0.0670	67	52.13	3491
13:25	0.084	84	45.08	3787
13:30	0.1	100	42.88	4288
13:35	0.128	128	43.26	5538
13:40	0.134	134	26.16	3506

Time				
13:45	0.15	150	25.92	3888
13:50	0.1671	167	25.07	4190
13:55	0.185	185	12.71	2351
14:00	0.2	200	6.54	1308
14:05	0.2	200	3	646
14:10	0.2	200	1.09	218
14:15	0.2	200	0.34	68
14:20	0.2	200	0.06	12
TOTAL		3061	1222	98061

Tidal flux data for 11/09/2006

Time (BST)	SSC gl^{-1}	SSC gm^3	Total vol flow (m^{3}s^{-1})	SSC gs^{-1}
06:35	0.500	500	0.12	61
06:40	0.500	500	0.46	230
06:45	0.500	500	2.03	1014
06:50	0.500	500	3.84	1922
06:55	0.500	500	15.61	7803
07:00	0.500	500	17.39	8697
07:05	0.520	520	29.85	15522
07:10	0.560	560	43.58	24402
07:15	0.580	580	57.69	33460
07:20	0.600	600	71.09	42652
07:25	0.630	630	100.96	63607
07:30	0.647	647	113.20	73229
07:35	0.640	640	129.21	82693
07:40	0.630	630	133.74	84255
07:45	0.620	620	140.14	86886
07:50	0.610	610	156.21	95286
07:55	0.600	600	165.55	99329
08:00	0.595	595	163.55	97359
08:05	0.530	530	170.02	90109
08:10	0.480	480	177.95	85417
08:15	0.430	430	195.89	84231
08:20	0.380	380	198.14	75295
08:25	0.320	320	198.70	63583
08:30	0.260	260	188.62	49033
08:35	0.320	320	162.92	52134
08:40	0.380	380	130.05	49417
08:45	0.440	440	115.40	50774
08:50	0.500	500	82.71	41357
08:55	0.550	550	72.17	39696
09:00	0.607	607	42.56	25839
09:05	0.520	520	31.67	16468

09:10	0.450	450	13.98	6293
09:15	0.380	380	39.37	14960
TOTAL			3164.36	1563012.74
09:20	0.300	300	65.88	19765
09:25	0.230	230	101.95	23448
09:30	0.156	156	124.53	19453
09:35	0.280	280	154.33	43211
09:40	0.200	200	173.74	34748
09:45	0.220	220	167.04	36749
09:50	0.240	240	179.75	43140
09:55	0.250	250	200.43	50107
10:00	0.267	267	202.18	53980
10:05	0.260	260	189.17	49184
10:10	0.250	250	180.73	45183
10:15	0.240	240	172.30	41352
10:20	0.230	230	167.29	38478
10:25	0.220	220	158.68	34910
10:30	0.196	196	136.57	26737
10:35	0.250	250	121.93	30482
10:40	0.290	290	109.53	31764
10:45	0.340	340	107.86	36672
10:50	0.380	380	104.35	39654
10:55	0.420	420	89.62	37638
11:00	0.457	457	85.19	38940
11:05	0.480	480	90.81	43589
11:10	0.515	515	60.17	30986
11:15	0.530	530	45.14	23924
11:20	0.570	570	35.09	20001
11:25	0.580	580	22.25	12906
11:30	0.596	596	9.14	5448
11:35	0.596	596	6.06	3611
11:40	0.596	596	3.05	1815
11:45	0.596	596	0.67	401
11:50	0.596	596	0.06	34
TOTAL			3265	918310

Tidal flux data for 11/05/2007

Time (BST)	SSC gl^{-1}	SSC gm^3	Total vol flow (m^{3}s^{-1})	SSC gs^{-1}
11:40	0.090	90	0.09	8
11:45	0.0869	87	0.27	24
11:50	0.0838	84	0.43	36
11:55	0.0802	80	0.88	71
12:00	0.077	77	1.47	114

12:05	0.0760	76	4.57	347
12:10	0.0750	75	10.05	754
12:15	0.0740	74	10.80	799
12:20	0.073	73	10.81	789
12:25	0.0768	77	11.48	882
12:30	0.0805	81	13.13	1057
12:35	0.0844	84	15.83	1336
12:40	0.088	88	18.53	1631
12:45	0.0909	91	18.72	1702
12:50	0.0938	94	18.72	1756
12:55	0.0964	96	26.58	2563
13:00	0.099	99	26.52	2625
13:05	0.0972	97	24.08	2341
13:10	0.0955	96	15.82	1511
13:15	0.0937	94	9.48	888
13:20	0.092	92	6.29	578
13:25	0.0846	85	5.77	489
13:30	0.0770	77	2.59	200
TOTAL		1966	253	22500
13:35	0.0656	66	8	496
13:40	0.0620	62	10.27	636
13:45	0.061	61	19.03	1157
13:50	0.0595	60	25.73	1531
13:55	0.0582	58	25.10	1461
14:00	0.0570	57	27.59	1573
14:05	0.055	55	23.55	1300
14:10	0.0535	54	20.97	1122
14:15	0.0517	52	20.66	1068
14:20	0.0500	50	18.91	946
14:25	0.053	53	15.22	803
14:30	0.0555	56	11.62	645
14:35	0.0582	58	10.06	586
14:40	0.0610	61	6.94	423
14:45	0.066	66	7.80	515
14:50	0.0712	71	6.54	466
14:55	0.0767	77	6.08	467
15:00	0.0820	82	3.17	260
15:05	0.082	82	1	116
15:10	0.082	82	0.45	37
15:15	0.082	82	0.26	22
15:20	0.082	82	0.09	7
TOTAL		1425	269	15634

Tidal flux data for the 14/09/2007

Time (BST)	SSC gl^{-1}	SSC gm^3	Total vol flow (m^{3}s^{-1})	SSC gs^{-1}
06:00	0.21	215	0.04	9
06:05	0.21	215	0.14	31
06:10	0.21	215	0.52	112
06:15	0.21	215	1.75	377
06:20	0.21	215	9.65	2072
06:25	0.21	215	10.99	2360
06:30	0.21	215	20.56	4418
06:35	0.23	232	31.84	7388
06:40	0.249	249	41.54	10343
06:45	0.265	265	50.64	13419
06:50	0.28	280	74.27	20797
06:55	0.298	298	82.46	24572
07:00	0.31	312	93.39	29181
07:05	0.34	339	101.66	34462
07:10	0.361	361	122.89	44362
07:15	0.384	384	123.82	47549
07:20	0.409	409	125.52	51336
07:25	0.432	432	125.45	54192
07:30	0.45	455	125.14	56889
07:35	0.42	420	126.96	53324
07:40	0.362	362	121.86	44114
07:45	0.315	315	116.37	36656
07:50	0.269	269	85.76	23069
07:55	0.221	221	80.17	17718
08:00	0.17	173	65.57	11353
08:05	0.17	174	57.08	9932
08:10	0.178	178	54.04	9619
08:15	0.18	180	40.15	7227
08:20	0.181	181	15.07	2728
08:25	0.181	181	9.56	1730
08:30	0.18	184	27.39	5038
TOTAL			1942.25	626377.81
08:35	0.20	203	46.67	9473
08:40	0.223	223	79.29	17683
08:45	0.243	243	77.25	18773
08:50	0.262	262	83.67	21922
08:55	0.28	280	116.06	32498
09:00	0.30	300	117.76	35329
09:05	0.29	288	109.06	31409
09:10	0.275	275	122.59	33713
09:15	0.26	260	133.29	34655
09:20	0.258	258	119.73	30889

09:25	0.235	235	115.91	27239
09:30	0.22	222	114.24	25369
09:35	0.21	208	112.93	23489
09:40	0.193	193	92.24	17803
09:45	0.178	178	78.54	13980
09:50	0.164	164	77.96	12785
09:55	0.15	150	73.27	10990
10:00	0.13	135	63.32	8535
10:05	0.14	140	64.77	9068
10:10	0.148	148	51.55	7629
10:15	0.152	152	45.89	6975
10:20	0.16	160	48.87	7820
10:25	0.165	165	26.78	4419
10:30	0.17	170	19.42	3307
10:35	0.17	170	7.33	1248
10:40	0.17	170	3.33	566
10:45	0.17	170	1.08	184
10:50	0.17	170	0.34	57
10:55	0.17	170	0.06	10
TOTAL			2003	447819

Appendix 6: Bulk density data

Summer wet and dry bulk density

	Summer wet bulk density		Summer dry bulk density	
Site	Mean	SD	Mean	SD
1	1.60	0.13	1.21	0.09
2	1.66	0.18	1.14	0.12
3	1.87	0.10	1.39	0.07
4	1.67	0.14	1.21	0.11
5	1.57	0.08	0.96	0.05
6	1.83	0.18	1.32	0.13
7	1.65	0.05	0.90	0.03
8	1.64	0.05	1.09	0.05
9	1.78	0.13	1.26	0.10
10	1.76	0.07	1.28	0.07
11	1.61	0.09	1.08	0.06
12	1.60	0.14	0.94	0.09
13	1.75	0.07	1.17	0.05
14	1.61	0.04	1.13	0.03
15	1.67	0.19	1.15	0.14
16	1.51	0.07	0.95	0.05
17	1.59	0.09	1.08	0.06
18	1.62	0.15	1.05	0.09
19	1.61	0.01	1.06	0.03
20	1.65	0.01	1.18	0.02
21	1.68	0.04	1.18	0.03
22	1.57	0.02	1.15	0.02
23	1.47	0.20	0.91	0.06
24	1.66	0.04	1.14	0.02
25	2.08	0.14	1.53	0.09
26	1.52	0.06	0.93	0.05
27	1.71	0.09	1.17	0.08
28	1.77	0.10	1.25	0.07
29	1.78	0.15	1.27	0.10
30	1.77	0.02	1.22	0.02
31	1.56	0.03	0.95	0.03
32	1.56	0.11	0.96	0.08
33	1.65	0.14	1.04	0.13
34	1.40	0.04	0.78	0.03
35	1.88	0.08	1.37	0.06

Winter wet and dry bulk density

Site	Winter wet bulk density		Winter dry bulk density	
	Mean	SD	Mean	SD
1	1.67	0.19	0.77	0.11
2	1.67	0.15	0.72	0.07
3	1.88	0.09	1.08	0.06
4	1.60	0.14	0.69	0.11
5	1.73	0.04	0.67	0.03
6	1.73	0.06	0.83	0.04
7	1.66	0.05	0.75	0.05
8	1.82	0.21	1.05	0.17
9	1.63	0.14	0.85	0.09
10	1.73	0.03	0.86	0.02
11	1.68	0.07	0.82	0.03
12	1.46	0.20	0.67	0.10
13	1.87	0.05	1.12	0.02
14	2.09	0.20	1.36	0.14
15	1.74	0.07	0.97	0.06
16	1.74	0.05	0.89	0.03
17	1.75	0.05	1.03	0.04
18	1.85	0.05	1.07	0.03
19	1.84	0.24	0.97	0.08
20	1.68	0.14	0.96	0.10
21	1.79	0.13	0.94	0.07
22	2.27	0.13	1.65	0.10
23	2.11	0.15	1.38	0.08
24	1.79	0.11	1.14	0.07
25	1.83	0.28	1.13	0.14
26	1.79	0.16	1.10	0.19
27	1.52	0.20	0.85	0.16
28	1.88	0.09	1.09	0.04
29	1.70	0.09	0.81	0.05
30	1.50	0.09	0.66	0.05
31	1.50	0.10	0.74	0.11
32	1.69	0.15	0.94	0.12
33	1.73	0.11	1.01	0.08
34	1.87	0.13	1.23	0.09
35	1.74	0.06	1.08	0.05

Overall mean wet and dry bulk density

Site	Mean wet bulk density	Mean SD	Mean dry bulk density	Mean SD
1	1.64	0.16	0.99	0.10
2	1.66	0.17	0.93	0.09
3	1.88	0.10	1.23	0.07
4	1.64	0.14	0.95	0.11
5	1.65	0.06	0.81	0.04
6	1.78	0.12	1.08	0.08
7	1.66	0.05	0.82	0.04
8	1.73	0.13	1.07	0.11
9	1.70	0.14	1.05	0.10
10	1.75	0.05	1.07	0.04
11	1.64	0.08	0.95	0.05
12	1.53	0.17	0.81	0.09
13	1.81	0.06	1.14	0.03
14	1.85	0.12	1.25	0.09
15	1.71	0.13	1.06	0.10
16	1.62	0.06	0.92	0.04
17	1.67	0.07	1.05	0.05
18	1.73	0.10	1.06	0.06
19	1.73	0.13	1.01	0.06
20	1.66	0.07	1.07	0.06
21	1.73	0.09	1.06	0.05
22	1.92	0.08	1.40	0.06
23	1.79	0.17	1.15	0.07
24	1.73	0.08	1.14	0.05
25	1.95	0.21	1.33	0.11
26	1.66	0.11	1.01	0.12
27	1.62	0.14	1.01	0.12
28	1.83	0.09	1.17	0.05
29	1.74	0.12	1.04	0.07
30	1.64	0.05	0.94	0.03
31	1.53	0.06	0.85	0.07
32	1.63	0.13	0.95	0.10
33	1.69	0.13	1.02	0.10
34	1.63	0.09	1.01	0.06
35	1.81	0.07	1.22	0.05

257

Appendix 7: Moisture content data

Full moisture content data for summer, winter and overall mean.

Site	Mean moisture content (%) summer	SD	Mean moisture content (%) winter	SD	Overall mean moisture content (%)	SD
1	24.83	0.61	53.76	1.40	39.29	1.01
2	31.06	0.67	57.16	0.87	44.11	0.77
3	25.84	0.35	42.68	1.72	34.26	1.04
4	27.90	0.20	57.38	3.87	42.64	2.03
5	39.01	0.05	61.40	1.05	50.20	0.55
6	27.86	0.35	51.76	0.63	39.81	0.49
7	45.67	0.47	54.81	1.77	50.24	1.12
8	33.47	0.89	42.70	3.29	38.09	2.09
9	29.17	0.70	47.95	1.10	38.56	0.90
10	27.74	1.13	50.54	0.49	39.14	0.81
11	32.57	0.02	51.22	0.49	41.89	0.26
12	41.43	0.30	54.05	1.14	47.74	0.72
13	33.09	0.71	40.45	0.77	36.77	0.74
14	29.92	1.73	34.68	1.17	32.30	1.45
15	31.08	0.51	44.36	1.20	37.72	0.85
16	36.99	2.10	48.96	0.17	42.97	1.14
17	32.12	0.31	41.21	0.66	36.67	0.48
18	35.12	1.58	42.38	0.53	38.75	1.06
19	34.07	2.03	47.32	2.41	40.69	2.22
20	28.12	1.40	42.88	2.33	35.50	1.87
21	29.75	0.62	47.22	0.41	38.48	0.52
22	26.76	1.28	27.42	1.34	27.09	1.31
23	37.44	8.16	34.43	0.66	35.94	4.41
24	31.44	1.20	36.24	0.12	33.84	0.66
25	26.48	0.86	38.19	2.07	32.33	1.46
26	39.07	1.26	38.87	4.69	38.97	2.97
27	31.80	1.50	44.38	3.58	38.09	2.54
28	29.59	0.68	41.91	1.13	35.75	0.91
29	28.64	0.38	52.52	1.08	40.58	0.73
30	30.97	0.30	55.95	0.87	43.46	0.59
31	38.85	0.50	50.67	4.55	44.76	2.52
32	38.62	0.83	44.36	2.19	41.49	1.51
33	36.96	2.26	41.86	1.68	39.41	1.97
34	43.95	2.40	33.91	0.14	38.93	1.27
35	27.19	0.70	38.03	1.34	32.61	1.02

Appendix 8: Full grain size data

Summer grain size data

Summer	Sand 2000-63 μm	SD	Silt 63-2 μm	SD	Clay <2 μm	SD
2	0.69	0.89	67.98	1.29	31.33	0.24
3	1.07	1.52	66.63	2.66	32.31	0.55
4	0.36	0.53	71.27	0.62	28.38	0.45
5	0.16	3.65	57.37	1.55	42.47	0.30
6	0.40	0.13	66.93	0.82	32.60	0.29
7	1.96	1.13	67.87	0.34	30.17	0.39
9	3.33	0.81	63.00	0.40	33.67	0.14
10	0.33	1.29	66.33	0.85	33.33	0.41
13	2.32	1.09	71.86	2.08	25.82	0.18
14	19.49	0.77	58.66	0.42	21.85	0.28
16	13.43	1.42	63.01	0.64	23.56	0.19
17	3.62	0.61	71.00	1.25	25.38	0.56
21	19.34	0.67	61.45	0.94	19.21	0.32
22	21.67	0.86	62.07	1.40	16.25	0.36
23	1.41	1.62	71.44	1.16	27.16	0.43
24	5.17	0.81	72.02	0.79	22.81	0.17
25	21.74	2.18	55.07	0.71	23.19	0.36
27	8.76	0.36	68.03	3.00	23.21	0.78
28	3.93	1.16	74.55	0.89	21.52	0.24
29	0.85	0.93	69.25	2.21	29.90	0.51
30	0.59	1.50	70.81	0.88	28.60	0.49
31	1.41	0.55	66.35	2.10	32.24	0.53
32	2.74	0.68	65.19	1.16	32.07	0.48
33	3.23	1.43	70.29	1.03	26.48	0.32
34	2.75	0.84	69.88	0.83	27.37	0.38
35	5.80	1.91	66.25	1.34	27.94	0.31

Winter grain size data

Winter	Sand 2000-63 μm	SD	Silt 63-2 μm	SD	Clay <2 μm	SD
2	1.43	1.20	68.91	1.10	29.66	0.36
3	1.62	1.11	69.75	0.69	28.63	0.19
4	0.75	0.73	70.68	0.73	28.57	0.20
5	4.60	2.45	69.70	1.12	25.70	0.37
6	2.39	0.95	72.35	2.07	25.25	0.46
7	8.40	0.28	67.59	0.45	24.01	0.18
9	8.53	0.18	65.72	0.77	25.74	0.36
10	1.25	1.38	65.69	0.72	33.06	0.14
13	19.94	0.76	62.77	1.07	17.29	0.23
14	30.46	0.19	54.19	0.87	15.35	0.43
16	23.77	0.59	54.61	0.62	21.62	0.51
17	11.14	0.93	68.33	2.31	20.53	0.66
21	31.58	0.57	54.21	0.62	14.21	0.31
22	57.22	0.72	34.09	0.47	8.69	0.44
23	50.33	0.52	38.88	1.05	10.79	0.25
24	25.24	0.86	53.16	1.13	21.60	0.41
25	22.92	0.60	61.83	1.25	15.25	0.59
27	20.17	0.33	62.49	0.77	17.34	0.23
28	12.71	1.08	65.92	0.82	21.38	0.31
29	0.93	0.40	75.87	1.27	23.20	0.43
30	0.86	1.15	66.76	0.68	32.38	0.16
31	8.31	0.35	67.07	0.80	24.63	0.39
32	14.16	0.73	66.45	5.15	19.39	1.52
33	15.77	1.03	64.91	0.49	19.31	0.25
34	13.24	0.56	64.38	1.01	22.38	0.27
35	21.15	1.30	60.56	0.44	18.29	0.11

Overall mean grain size data

Mean	Sand 2000-63 μm	SD	Silt 63-2 μm	SD	Clay <2 μm	SD
2	1.06	1.04	68.44	1.20	30.50	0.30
3	1.35	1.31	68.19	1.67	30.47	0.37
4	0.55	0.63	70.97	0.68	28.48	0.32
5	2.38	3.05	63.54	1.34	34.08	0.34
6	1.40	0.54	69.64	1.44	28.93	0.38
7	5.18	0.71	67.73	0.39	27.09	0.29
9	5.93	0.49	64.36	0.59	29.71	0.25
10	0.79	1.34	66.01	0.79	33.20	0.28
13	11.13	0.93	67.32	1.58	21.55	0.20
14	24.98	0.48	56.42	0.65	18.60	0.35
16	18.60	1.01	58.81	0.63	22.59	0.35
17	7.38	0.77	69.67	1.78	22.95	0.61
21	25.46	0.62	57.83	0.78	16.71	0.32
22	39.45	0.79	48.08	0.93	12.47	0.40
23	25.87	1.07	55.16	1.10	18.97	0.34
24	15.21	0.83	62.59	0.96	22.20	0.29
25	22.33	1.39	58.45	0.98	19.22	0.47
27	14.47	0.35	65.26	1.89	20.27	0.51
28	8.32	1.12	70.24	0.86	21.45	0.28
29	0.89	0.66	72.56	1.74	26.55	0.47
30	0.72	1.32	68.79	0.78	30.49	0.32
31	4.86	0.45	66.71	1.45	28.43	0.46
32	8.45	0.71	65.82	3.16	25.73	1.00
33	9.50	1.23	67.60	0.76	22.90	0.28
34	8.00	0.70	67.13	0.92	24.88	0.32
35	13.48	1.60	63.41	0.89	23.12	0.21

Appendix 9: Full organic content data

Full organic content data for summer, winter and the overall mean

Sample	Summer organic content (%)	SD	Winter organic content (%)	SD	Mean organic content (%)	SD
1	16.58	0.07	13.82	0.08	15.20	0.07
2	16.21	0.08	13.85	0.06	15.03	0.07
3	16.39	0.09	13.89	0.15	15.14	0.12
4	16.00	0.26	14.20	0.06	15.10	0.16
5	18.02	0.24	12.67	0.58	15.34	0.41
6	16.67	0.06	13.83	0.06	15.25	0.06
7	15.70	0.27	12.69	0.08	14.20	0.18
8	16.19	0.10	13.21	0.09	14.70	0.10
9	13.63	0.06	12.00	0.17	12.81	0.12
10	15.47	0.06	14.02	0.07	14.74	0.06
11	16.28	0.07	13.73	0.07	15.00	0.07
12	15.73	0.15	13.57	0.06	14.65	0.11
13	16.51	0.11	11.95	0.08	14.23	0.10
14	12.66	0.05	9.58	0.07	11.12	0.06
15	13.93	0.15	10.25	0.05	12.09	0.10
16	13.24	0.05	11.41	0.09	12.32	0.07
17	14.44	0.06	11.54	0.05	12.99	0.05
18	13.39	0.19	12.15	0.08	12.77	0.14
19	13.30	0.09	10.80	0.10	12.05	0.09
20	13.35	0.09	9.64	0.05	11.49	0.07
21	12.44	0.05	9.58	0.07	11.01	0.06
22	10.33	0.06	7.39	0.08	8.86	0.07
23	14.92	0.03	6.77	0.13	10.85	0.08
24	13.92	0.17	9.21	0.05	11.56	0.11
25	10.58	0.07	9.68	0.07	10.13	0.07
26	13.61	0.09	9.23	0.07	11.42	0.08
27	12.59	0.09	9.84	0.05	11.21	0.07
28	11.90	0.09	10.27	0.06	11.09	0.07
29	15.62	0.07	13.52	0.07	14.57	0.07
30	15.97	0.08	16.13	0.06	16.05	0.07
31	15.65	0.05	12.79	0.06	14.22	0.05
32	16.25	0.06	11.64	0.05	13.95	0.05
33	14.33	0.06	10.94	0.20	12.63	0.13
34	14.89	0.08	11.14	0.06	13.01	0.07
35	10.06	0.04	10.52	0.07	10.29	0.05